MIT
SEA
GRANT
PROGRAM

REPORT
on
FUNDAMENTAL RESEARCH ON UNDERWATER WELDING

by
Alan J. Brown
Russell T. Brown
Chon-Liang Tsai
and
Koichi Masubuchi

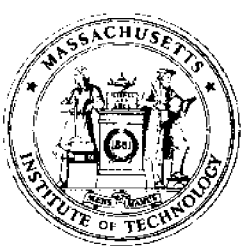

Massachusetts Institute of Technology

Cambridge, Massachusetts 02139

Report No. MITSG 74-29
September 30, 1974

REPORT

on

FUNDAMENTAL RESEARCH ON UNDERWATER WELDING

by

Alan J. Brown
Russell T. Brown
Chon-Liang Tsai
and
Koichi Masubuchi

Report No. MITSG 74-29

Index No. 74-329-Nfo

MASSACHUSETTS INSTITUTE OF TECHNOLOGY
CAMBRIDGE, MASS. 02139

SEA GRANT PROGRAM

ADMINISTRATIVE STATEMENT

This report summarizes the three-year program at the Massachusetts Institute of Technology to conduct fundamental research on underwater welding. The program includes experimental and analytical investigations as well as compilation of technical information on underwater welding.

During the three-year period, the interest and enthusiasm in the ocean engineering and welding industries have increased significantly. Therefore, the timeliness of this publication should prove very useful to the industry in developing new and improved underwater welding techniques that are needed for expanding ocean engineering activities.

Funds for this research effort came in part from the Welding Research Council, a group of Japanese companies in shipbuilding and heavy industry, the NOAA Office of Sea Grant through grant numbers 2-35150 and NG-43-72, and the Massachusetts Institute of Technology.

Ira Dyer
Director

August 1974

ROOM 1-211

(617) 253-7041

ACKNOWLEDGEMENT

The authors acknowledge the contributions by Lt. M. B. Meloney, USN, and Lt. S. L. Renneker, USCG.

Experiments were conducted in the Boston Naval Shipyard; Naval School, Diving and Salvage at the Washington Navy Yard; and the Welding Laboratories at M.I.T. Authors are grateful to a number of persons involved in the experiments, especially Mr. Julius C. Ritter (Boston Naval Shipyard), LCDR A. C. Esau (Commanding Officer, Naval School, Diving and Salvage), and Mr. A. J. Zona (M.I.T.).

The authors also wish to thank Miss Maureen A. Gallagher, who typed and proofread the final report.

The research project and this final report have been accomplished as an element of the M.I.T. Sea Grant Program. Project support funds were provided by the Welding Research Council; a group of companies including Ishikawajima-Harima Heavy Industries, Kawasaki Heavy Industries, Hitachi Shipbuilding and Engineering, Mitsubishi Heavy Industries, Mitsui Shipbuilding and Engineering, Nippon Kokan, Nippon Steel, Sasebo Heavy Industries, Kobe Works, and Sumitomo Heavy Industries; by the NOAA Office of Sea Grant No. NG-43-72; and by the Massachusetts Institute of Technology.

Encouragement and consultation were also given by several U. S. companies, including Airco Welding Products, Arcair, Chicago Bridge and Iron, Hobert Brothers, and HydroTech International.

ABSTRACT

This is the final report of a three-year program which was initiated on July 1, 1971. The objective of the program was to conduct fundamental research on underwater welding and cutting. The study includes the following phases:

Phase 1: Survey of fundamental information on underwater welding and cutting

Phase 2: A study of heat flow during underwater welding

Phase 3: Mechanisms of metal transfer in underwater arc welding

Phase 4: Effects of water environment on metallurgical structures and properties of welds

Phase 5: Development of improved underwater welding methods

The report presents results generated in this research program in the following order:

Part I: Project Summary

Part II: Welding Process Development

Part III: Present Technical and Fundamental Understanding of Underwater Welding Processes

Part IV: Heat Transfer and Bubble Dynamics

Part V: The General Concepts of Underwater Welding Metallurgy, Microstructure, and Metal Transfer

Part VI: Experimentation and Results in Metallurgy, Microstructure, and Metal Transfer

Part VII: Recommendations for Future Experimental Investigations and Developments of Underwater Welding

Appendix A: Underwater Welding of Low-Carbon and High-Strength (HY-80) Steel, preprint of a paper

Appendix B: Underwater Welding of HY-80 Steel, a summary of a thesis

TABLE OF CONTENTS

Page

PART THREE - PRESENT TECHNICAL AND FUNDAMENTAL UNDERSTANDING OF UNDERWATER WELDING PROCESSES

PART FOUR - HEAT TRANSFER AND BUBBLE DYNAMICS

PART ONE

PROJECT SUMMARY

Contents

1.0 INTRODUCTION

There has been an increasing national and international interest in ocean engineering. Structural design, materials, and welding fabrication represent important areas of ocean engineering, as do underwater welding and cutting. However, present techniques for underwater welding and cutting are far from complete, and they have limited applications such as salvaging. There is a strong need for developing reliable techniques for underwater welding and cutting.

A portion of the welding industry has recognized the importance of this subject and has made some effort to develop new techniques for welding and cutting. The problem, however, is an almost complete lack of fundamental information on underwater welding and cutting. No systematic study has been reported on the fundamentals of what occurs during underwater welding and cutting. It is very important for the ocean engineering and welding industries to generate fundamental information on underwater welding and cutting. Such information should be useful for further development of improved joining and cutting techniques.

The objective of this study is to conduct fundamental research on underwater welding and cutting. However, we consider this study as a necessary step toward developing improved underwater fabrication techniques. Although the primary objective of this study is to better understand mechanisms of underwater welding, efforts have been made to generate information which could lead to improved welding processes.

1.1 M.I.T.'s INITIAL EFFORTS ON UNDERWATER WELDING

This section summarizes briefly M.I.T.'s initial efforts on research on underwater welding which forms the basis of this research.

In 1970, Professor Koichi Masubuchi published a textbook entitled Materials for Ocean Engineering which contains as its appendix, a state-of-the-art report on underwater welding and cutting.[1] This textbook was prepared under a program supported by the National Sea Grant Office. This appendix was condensed from a comprehensive report prepared by Battelle Memorial Institute in 1968 for the Naval Ship Systems Command.[2] This report describes various underwater welding and cutting processes.

This textbook drew the attention of some students. Two theses were prepared, under the supervision of Professor Masubuchi, during the 1970/71 academic year. Lt. James A. Staub of the U.S. Navy, who received a Master's degree in June, 1971, wrote a thesis which deals with computer analysis of heat flow during underwater welding.[3] The initial analytical model developed by Staub assumes that water keeps contact with the metal surface. It was later found, however, that analytically-determined cooling rates are greater than those shown by experimental data. In other words, an actual weld cools more slowly than the initial analytical model predicted.

Mr. Alan J. Brown, who received a Bachelor's degree in June, 1971, studied the underwater welding arc by use of high-speed cinematography.[4] He studied how an underwater welding arc is surrounded by bubbles created by the intense heat of the arc. It explains why experimentally-determined cooling rates are slower than the analytical values. Due to the bubbles near the arc, the metal near the arc does not maintain a direct contact with surrounding water.

A paper was presented at the 1972 Offshore Technology Conference summarizing the studies by Staub and Brown.[5]

1.2 PROGRESS OF THIS RESEARCH PROGRAM

This three-year research program was initiated on July 1, 1971. The program covers the following phases:

Phase 1: Survey of fundamental information on underwater welding and cutting

Phase 2: A study of heat flow during underwater welding

Phase 3: Mechanisms of metal transfer in underwater arc welding

Phase 4: Effects of water environment on metallurgical structures and properties of welds

Phase 5: Development of new, improved underwater welding methods

The program was carried out as originally proposed.*

Phase 1 was studied primarily by Mr. Russell T. Brown, of which results are given in Parts II and III of this report. Part II discusses the state-of-the-art of current welding processes---what processes have been developed and used. Part III, on the other hand, discusses present technical and fundamental understanding of underwater welding processes---how much we know about these processes.

Phase 2 was studied primarily by Mr. Alan J. Brown and the results are included in Part IV. Part IV was prepared by Mr. C. L. Tsai who summarized Brown's thesis. Mr. Tsai has recommended a new approach to improve the accuracy of the heat flow analysis.

Phases 3 and 4 were studied primarily by Mr. R. T. Brown, of which results are discussed in Parts V and VI. Part V presents the general concepts of underwater welding metallurgy, microstructure, and metal transfer. Part VI presents experiments

---

* In February, 1973, an interim report was prepared covering the work performed from July 1, 1971 through December 31, 1972.[6] The interim report discusses Phases 1 and 2.

and results in metallurgy, microstructure, and metal transfer.

Studies also were conducted by Lt. M. B. Meloney and Lt. S. L. Renneker on welding of low-carbon steel and high-strength (HY-80) steel. Since Lt. Meloney and Lt. Renneker were supported by the U.S. Navy and U.S. Coast Guard, respectively, and only small portions of the funds were spent on these studies, their results are summarized in Appendixes A and B.

Although the Phase 1 survey originally intended to cover both underwater welding and cutting, no new article has been found on underwater cutting which is worthy of being included in the state-of-the-art report. Consequently, Parts II and III cover underwater welding only.

During the entire course of this research program, various ideas were generated for improving underwater welding methods. They are described in various portions of this report. At the end of the program in Phase 5, some efforts were made to improve underwater welding methods and procedures, of which results are described in Part VII. The efforts will be continued in the program entitled, "Development of New, Improved Techniques for Underwater Welding and Cutting," which will be initiated on July 1, 1974.

1.3 RESEARCH SUMMARY

1.31 Part II: Welding Process Developments

Part II is concerned with the overall development that has taken place in underwater welding techniques. This section is included to provide basic knowledge on underwater welding to readers who are not familiar with the subject. Part II covers the following processes:

(1) Basic welding processes
(2) Current state-of-the-art of underwater welding processes
(3) Shielded metal-arc underwater welding
(4) Shrouded metal-arc underwater welding

(5) Shielded gas metal-arc underwater welding processes
(6) Plasma arc underwater welding
(7) Movable chamber underwater welding
(8) Dry chamber underwater welding techniques

Included also is a short history of research, development, and application of underwater welding by industry.

1.32 Part III: Present Technical and Fundamental Understanding of Underwater Welding Processes

This section discusses "technical aspects of underwater welding." It emphasizes what we know about various technical problems related to underwater welding.

Subjects covered include:

(1) The underwater arc bubble phenomena
(2) The underwater welding arc and associated metal transfer
(3) The underwater heat transfer and temperature histories
(4) Effects of pressure on underwater welding
(5) Underwater welding polarity
(6) Electrode waterproofing
(7) Underwater electrode coating turbidity
(8) Underwater GMA research
(9) Correlations between experimental work and actual weld properties
(10) Actual weld geometrical, microstructural, and mechanical properties

In discussing the above subjects, results obtained in this M.I.T. research are integrated with results obtained by other investigators.

It is worth mentioning that most of the articles referred to in Part III are very new. The distribution of years of publication of the 54 articles referred to is as follows:

1973	6
1972	5
1971	11
1970	4
1969	4
1968	3
1967	2
1966	2
1965	2
1962	5
1961	2
1960	1
1930 - 1959	7
TOTAL	54

Twenty-two out of 54 articles were published during the last three years. Thirty articles were published since 1968 when the Battelle report[2] was prepared.

Regarding the countries where these articles were published, they are from:

USA	27
USSR	19
Japan	5
England	3

These statistics may simply mean that we have a good access to publications from these countries.* However, it may also indicate that major current technical activities in underwater welding are taking place in these countries. In

* This literature survey was conducted to find out what is already known on underwater welding so that M.I.T. studies in later phases can be directed intelligently by avoiding possible duplications and making use of information which has been generated already. No special effort was made to cover as many articles as possible published in various countries.

view of the fact that most of the 54 articles were published very recently, it is quite possible that a number of research activities were initiated rather recently in various countries, including Holland, Germany, France, and Norway, but they have not yet been published or made easily accessible to people in the U.S.A.

The above statistics indicate that there is a sudden surge in the world technical community in the interest in underwater welding. It is noticed that there has been a significant rise in the technical level of articles published. Many articles published recently are much more technical than old articles which tended to simply describe processes and applications. Efforts are apparently being made in various parts of the world to generate technical information useful for the development of new, improved underwater welding processes. These statistical results show that the funding by the National Sea Grant Office of this M.I.T. research is not only appropriate, but also, timely.

1.33 Part IV: Heat Transfer and Bubble Dynamics

Compared to arc welding in an ordinary atmosphere, arc welding underwater involves the following phenomena:

1. Due to the quenching effect of water, a weldment cools rapidly, resulting in a hard and brittle weld.
2. Bubbles are formed due to the intense heat of the welding arc and the weld metal may become very porous.
3. Hydrogen in the bubbles and the surrounding water may cause hydrogen-induced cracking.

The Phase 2 study was aimed at investigating the first subject: heat flow during welding. Mechanisms of bubble formation also were studied, because the presence of bubbles has profound effects on heat flow. The presence of bubbles

also has effects on mechanisms of metal transfer in arc welding underwater (Phase 3).

Part IV summarizes the experimental investigation of underwater welding bubble phenomena and heat transfer. Based on the investigations of the arc bubble dynamics and experimental determination of the size of the weld metal puddle, a computer model of the heat transfer processes occurring in underwater welding was prepared and tested against actual thermocouple data. Ideally, a three-dimensional transient model is desired. However, the model developed for the study was a quasi-static two-dimensional weld of the plate survace. Results of correlations between theoretical model prediction and actual thermocouple measurements were fairly good, but not completely satisfactory. Based on the results, a new approach to modeling involving a two-dimensional model of a longitudinal cross-section of a welded joint is recommended and discussed. This section develops in the following way:

(1) The underwater arc bubble dynamics determined by experimentation.

(2) The development of the 2-D surface computer model incorporating the bubble phenomenon and surface heat losses due to boiling and convection.

(3) The experimental procedures used in determining the weld puddle boundaries and measuring the temperature histories with thermocouples.

(4) Recommendations and discussion involving an alternate modeling scheme involving the plate thickness.

1.34 Part V: The General Concepts of Underwater Welding Metallurgy, Microstructure, and Metal Transfer

This part presents the general principles and conceptual framework of welding metallurgy and microstructure. This part is included to provide fundamental knowledge of welding metallurgy to readers who are not familiar to welding. Basic air welding results and phenomena are presented and modified or interpreted to

apply to the peculiar conditions of underwater welding. The basic concepts are developed in the following order:

(1) Temperature histories in underwater welding. Differences in cooling rate characterize the differences between air welds and underwater welds.

(2) Basic metallurgy and microstructure of underwater welds.

(3) Microhardness in underwater welding.

(4) Potential underwater defects--quenching-induced and hydrogen-induced.

1.35 Part VI: Experimentation and Results in Metallurgy, Microstructure, and Metal Transfer

Part VI details the original experimentation and investigation that were conducted on the metallurgy and microstructure of underwater shielded metal-arc welding.

(1) The discussion begins with some general considerations concerning underwater welding research explaining the reasoning behind choosing a comparative study between air and underwater welds.

(2) The discussion then proceeds with the identification of the relevant welding process parameters, which are found to be:

a. welding current
b. welding speed
c. electrode size and type
d. polarity
e. air or underwater environment

(3) Descriptions of the equipment and the procedure used

to obtain the data and also the method of analyses are presented. A short discussion of safety follows.

(4) The bulk of material relates to the analysis and documentation of the information obtained in this study. The types of data included are:

a. welding current and voltage recordings for all welds
b. welded bead appearance and regularity
c. geometrical measurements and comparisons
d. microhardness profiles and comparisons
e. microstructural studies of the weld heat-affected zone
f. general observations and remarks on assorted details not included in a previous division

1.36 Part VII: Recommendations for Further Experimental Investigations and Developments in Underwater Welding

This report summarizes a program of experimental and analytical investigations and information compilation involving three years work at M.I.T. During the same three year period, the interest and enthusiasm in the industry in underwater welding technologies have increased significantly. In many respects, underwater welding technologies are in a critically important period of development. This section of the report discusses what needs to be done at M.I.T. and elsewhere in order to bring about an orderly development of underwater welding technologies. The following subjects are covered:

(1) Future experimentation
(2) Possibilities for future developments
(3) Future efforts at M.I.T.

1.37 Appendix A: Underwater Welding of Low-Carbon and High-Strength (HY-80) Steel

The thesis study by Lt. M. B. Meloney was conducted to supplement Phase 4. The study covered two subjects:

a. Multipass welding of low-carbon steel
b. A feasibility study of underwater welding of HY-80, a quenched-and-tempered steel with a minimum yield strength of 80,000 psi.

Shielded metal-arc process was used for welding these metals.

Since the main efforts in Phase 4 were aimed at developing fundamental information on underwater welding, the efforts by Lt. Meloney were directed at developing practical information.

An experimental study was made of mechanical properties (tensile strength, elongation, impact properties, etc.) of multipass underwater weldments of low-carbon steel

A study also was made into the feasibility of welding HY-80 steel underwater. HY-80 steel has been widely-used for the construction of submarine hulls and other marine structures. There must be a need for emergency repairs of underwater structures in HY-80.

A literature survey revealed no published record of any experimental or theoretical work done on underwater welding of any high-strength steel. Verbal conversations with some engineers at the Department of the Navy indicated that no study has been made on underwater welding of HY-80 steel. In fact, the consensus of opinion was that a high-strength quenched-and-tempered steel such as HY-80 could not be satisfactorily welded underwater. The major reason appears to be sensitivity of HY-80 steel to hydrogen embrittlement. Even in air welding, delayed cracking due to hydrogen often occurs, especially when a weld is made with electrodes which have

absorbed moisture. When a weld is made underwater, hydrogen which exists in water would cause cracking.

However, no one, to the best of our knowledge, has ever tried to weld HY-80 steel underwater. We are fully aware that high-quality welds in HY-80 steel would not be obtained in underwater wet welding. We felt that it is worthwhile to find out whether it is possible to perform emergency underwater repair or temporary welding for salvaging operations.

Lap and tee joints were fabricated underwater (using tap water for most tests) and tests were conducted to determine joint strength, ductility, and overall weld quality. We were pleasantly surprised by the experimental results. It was found that welds in fairly good perperties could be obtained in the HY-80 steel.

1.38 Appendix B: Underwater Welding of HY-80 Steel

The initial study by Lt. M. B. Meloney was expanded by Lt. S. L. Renneker.

The objective of the thesis study by Renneker was two-fold:

(1) To extend the previous laboratory work to evaluate the ability to fabricate acceptable underwater welded HY-80 steel joints, under working conditions, within the guidelines of the U. S. Navy governing underwater welding operations.

(2) To investigate the occurrence of the hydrogen embrittlement phenomena in the underwater welded HY-80 steel joints.

A series of working dives were conducted by Lt. Renneker using the facility at the Naval School of Diving and Salvage, Washington Navy Yard, Washington, D.C. Welds in various positions were made in fresh water, at a depth of twelve feet by a diver wearing a Navy Standard MKV hard hat diving system.

The results of the microscopic investigation, microhardness tests, and mechanical bend tests have indicated a capability to fabricate acceptable underwater welded HY-80 steel joints, under the working conditions, which do not suffer from the hydrogen embrittlement phenomena. This capability is found to exist for water environment temperatures of 25°C (77°F) and below, providing the water is clear and the welder-diver is able to use the multipass welding technique.

1.4 PERSONNEL

The research program was conducted under the supervision of Professor Koichi Masubuchi. He was assisted by three graduate students, Messrs. Alan J. Brown, Russell T. Brown, and Chon-Liang Tsai. He was also assisted by two naval officer graduate students, Lt. Michael B. Meloney, U.S. Navy, and Lt. Stanley L. Renneker, U.S. Coast Guard. The services of these two officers were made available at no cost to this research contract.

1.5 PUBLICATIONS

Four theses were prepared as follows:

1. A. J. Brown, "Mechanisms of Heat Transfer During Underwater Welding," for Master of Science in Ocean Engineering, June, 1973.

2. M. B. Meloney, "The Properties of Underwater Welded Mild Steel and High-Strength Steel Joints," for Ocean Engineer and M.S. in Naval Architecture and Marine Engineering, June, 1973.

3. R. T. Brown, "Current Underwater Welding Technologies," for M.S. in Ocean Engineering, May, 1974.

4. S. L. Renneker, "An Investigation of Underwater Welded HY-80 Steel," for Ocean Engineer and M.S. in Naval Architecture and Marine Engineering, June, 1974.

1.52 Technical Papers

The following two papers were presented:

5. K. Masubuchi and M. B. Meloney, "Underwater Welding of Low-Carbon and High-Strength (HY-80) Steel," OTC 1951, Offshore Technology Conference, Houston, Texas, May, 1974.

6. A. J. Brown, R. T. Brown and K. Masubuchi, "Fundamental Research on Underwater Welding," a paper presented at the 1974 Annual Meeting of the American Welding Society, Houston, Texas, May, 1974.

1.53 Other Publications

M.I.T. researchers were asked to prepare the following paper:

8. T. Brown and K. Masubuchi, "Latest Developments in Underwater Welding Technologies," Underwater Journal, October, 1973, pp. 202-212.

An arrangement has been made to prepare an interpretive report on underwater welding. The report will be published by the Welding Research Council as a WRC Bulletin.

Also, an interim report was prepared in February, 1973 which covered the work performed from July 1, 1971 through December 31, 1972.(6)

References

(1) Masubuchi, K., Materials for Ocean Engineering, M.I.T. Press, May, 1970.

(2) Vagi, J. J., Mishler, H. W., and Randall, M. D., "Underwater Cutting and Welding State-of-the-Art," a report to the Naval Ship Systems Command from Battelle Memorial Institute Columbus Laboratories, 1968.

(3) Staub, J. A., "Temperature Distribution in Thin Plates Welded Underwater," Naval Engineer's Thesis, M.I.T., 1971.

(4) Brown, A. J., "Methods of Research in Underwater Welding," B.S. Thesis, M.I.T., 1971.

(5) Brown, A., Staub, J. A., and Masubuchi, K., "Fundamental Study of Underwater Welding," Paper No. OTC 1621, 1972 Offshore Technology Conference, Houston, Texas.

(6) Brown, A. J., Brown, R. T., and Masubuchi, K., "Interim Report on Fundamental Research on Underwater Welding," Department of Ocean Engineering, M.I.T., February 15, 1973.

PART TWO

WELDING PROCESS DEVELOPMENT

Contents

2.0 INTRODUCTION

This opening section is concerned with the overall development that has taken place in underwater welding technologies. This material will give the reader an introductory familiarity with the basic welding techniques and capabilities in underwater situations. The following subjects are included:

(1) Basic Welding Processes - Shielded Metal-Arc Welding
Gas Metal-Arc Welding

(2) Current State-of-the-Art of Underwater Welding Processes: A short comparison of their techniques and applications

(3) Shielded Metal-Arc Underwater Welding

(4) Shrouded Metal-Arc Underwater Welding

(5) Shielded Gas Metal-Arc Underwater Welding Processes

(6) Plasma Arc Underwater Welding

(7) Movable Chamber Underwater Welding

(8) Dry Chamber Underwater Welding Techniques

This general material is directed towards those with a general curiosity about underwater welding and thus does not present the basic technical data needed to support all statements and conclusions.

2.1 BASIC WELDING PROCESSES, JOINTS, AND TECHNIQUES

Most discussion of underwater welding assumes a basic familiarity with welding processes and techniques. Since it is possible that the reader is approaching underwater welding from an ocean-oriented, rather than a welding-oriented background, a few simple concepts are presented to aid in the comprehension of the remainder of this report.

There are currently only two basic welding processes being used in underwater applications. The simplest process is

shielded metal-arc welding. This involves a rod of metal, called the welding electrode, which has been coated with some flux material. The flux coating will:

(1) form a protective coating over the weld bead as it solidifies,

(2) shield the burning arc from the ambient water atmosphere by producing a gaseous bubble around the burning arc,

(3) promote electrical conductivity across the arc and hence, increasethe arc stability.

An electric arc is established between the workpiece and the welding electrode. The arc melts the electrode and the metal is deposited as weld metal. Figure 2-1A shows a sketch of the shielded metal-arc process. A slightly different, and more complex process is also used in some underwater welding applications. This process is basically a thin wire gas metal-arc (GMA) process. Instead of a large rod electrode, a continually advancing thin wire provides the weld metal. Rather than a solid flux coating around the electrode, a shielding gas is pumped around the bare wire or the wire is cored and contains the flux material internally. This process involves more complicated control mechanisms to always feed the proper amount of wire into the weld region and also maintain the proper current and voltage drop across the arc gap. Figure 2-1B shows a sketch of a GMA process.

The polarity of the process is determined by whether the electrode is positive (the anode), or negative (the cathode). Straight polarity is when the electrode is negative (cathode) and the workpiece is positive (anode). Reverse polarity is when the electrode is positive (anode) and the workpiece is negative (cathode). The polarity of a welding arc will change the characteristics of the arc and will result in slightly different weld bead shape, Figure 2-2.

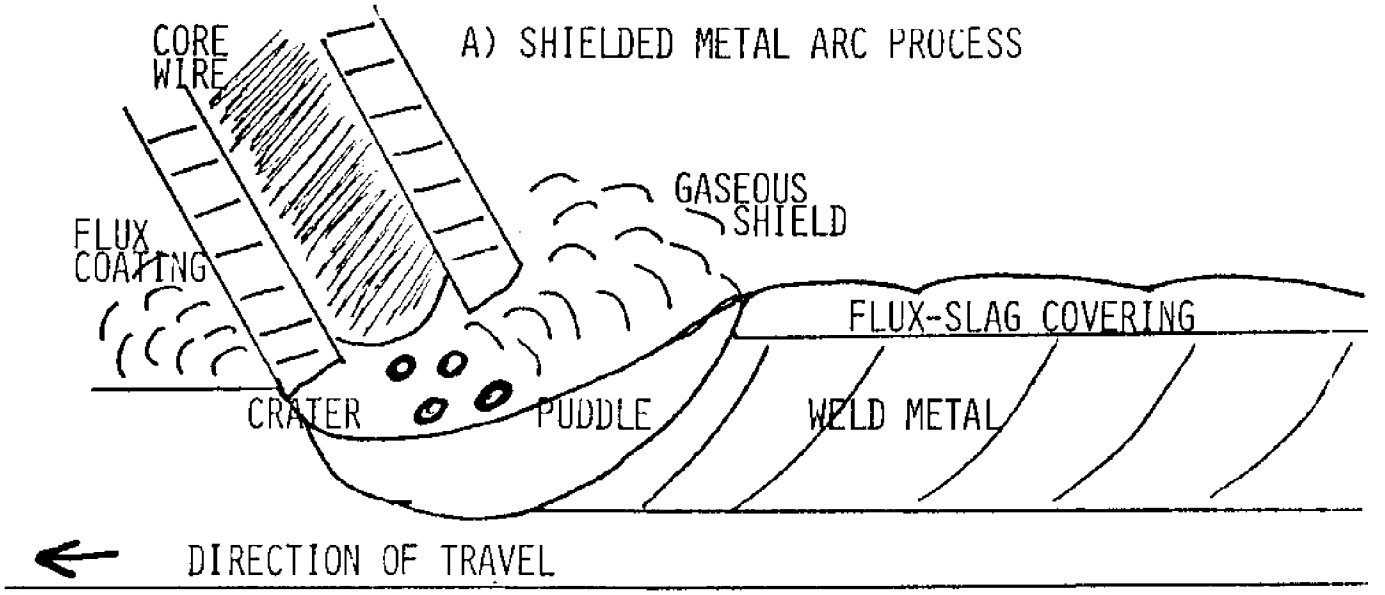

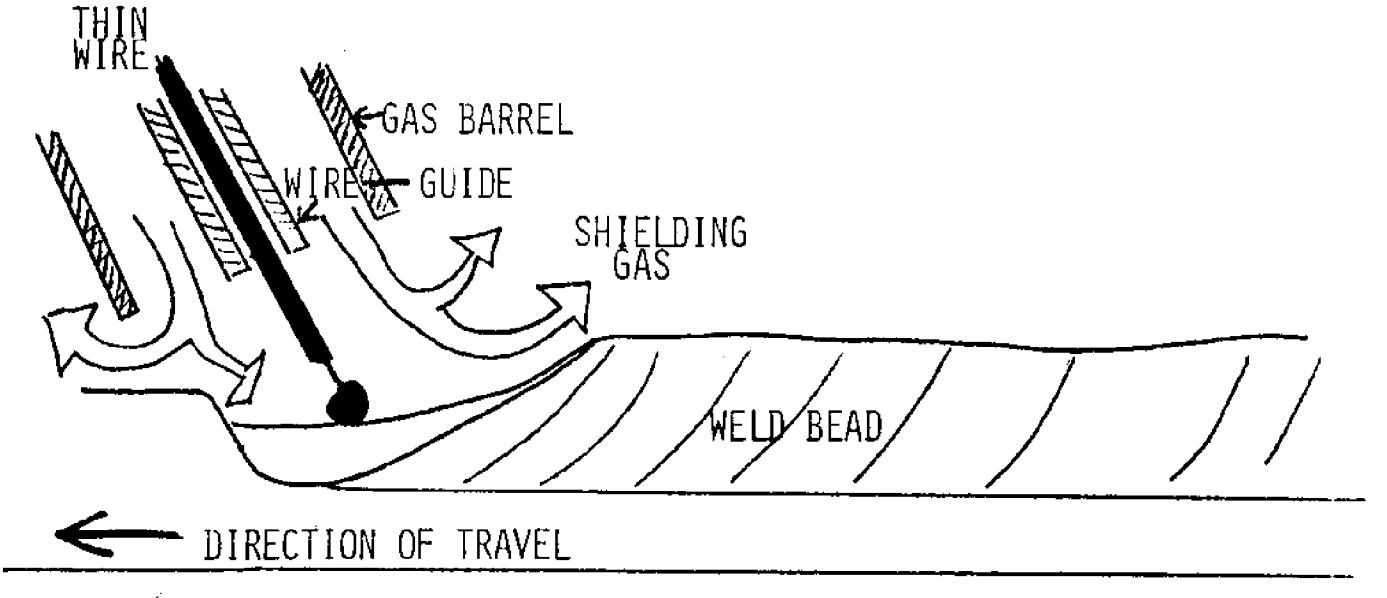

FIGURE 2-1

BASIC UNDERWATER WELDING PROCESSES

FIGURE 2-2

EFFECTS OF ELECTRODE POLARITY ON WELD BEAD SHAPE

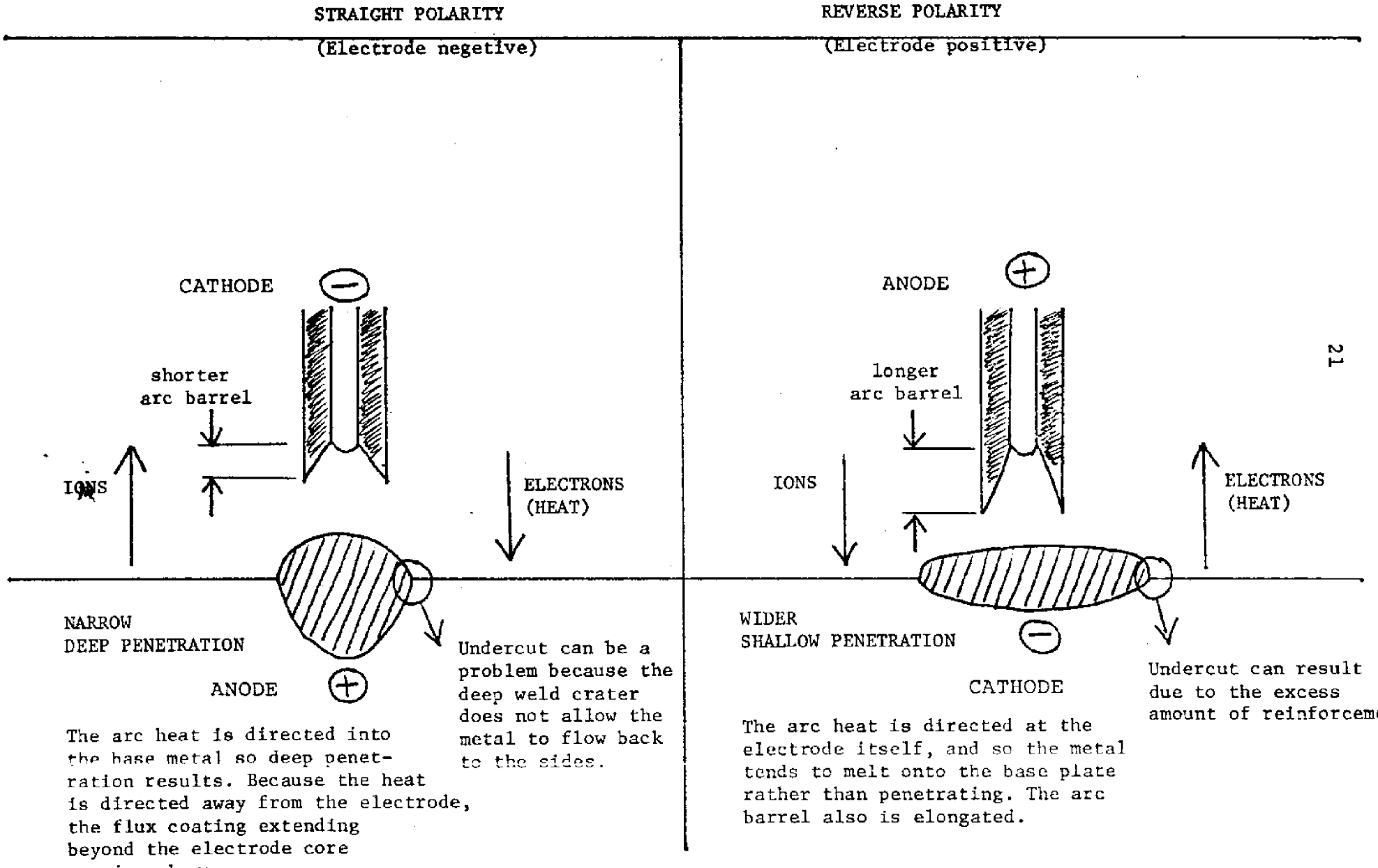

It is very important to have a constant arc gap between the electrode and the weld puddle to give a constant voltage and current so that a uniform penetration depth will result. Too long an arc gap will result in a high amount of heat dissipation and excessive spatter.

Welds can be made in all positions. Welding on the floor of a room is downhand welding. Welding up or down the corner of a room is vertical welding. Welding on the ceiling is overhead welding. And, welding horizontally across a wall is horizontal welding. The base plate is the piece of metal being welded. The weld bead is the resulting welded seam of metal composed of both parent metal from the base plate and filler metal from the melted electrode.

Many different kinds of joints can be welded. Bead-on-plate welds are those that are simply laid down onto a single base plate without joining plates together. Bead-on-plate welds are used exclusively in this research. Figure 2-3 shows some other common joint configurations. How well these plates match up the way they are supposed to is called joint fit-up. Fit-up can be a serious probelm in underwater welding situations. No welding process can make up for poor joint design or fit-up. Fit-up involves both cleaning the base plates and positioning the two plates to provide the proper spacing and overlap. In underwater welding situations, weld joints are normally lap, tee, or strap welds. Butt welds are especially hard to fit up.

To produce a weld, the welder touches the arc to the base plate to cause an arc to ignite. He then quickly pulls the welding electrode back to the proper arc length (approximately the same as the electrode diameter) and slowly moves the electrode along the weld joint. The weld puddle advances as the electrode melts, and as the weld pool solidifies, the weld is completed.

FIGURE 2-3

COMMON WELD JOINT CONFIGURATION TYPES

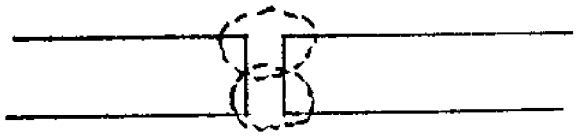

BUTT WELD JOINT WITH SPACING

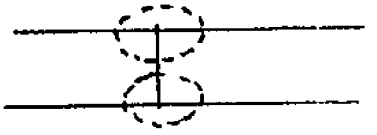

BUTT WELD JOINT WITHOUT SPACING

SINGLE "V" WELD JOINT

DOUBLE "V" WELD JOINT

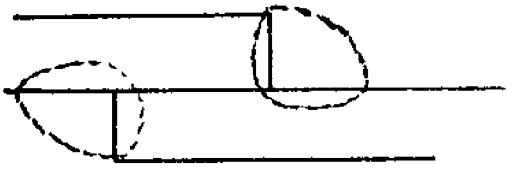

LAP JOINT

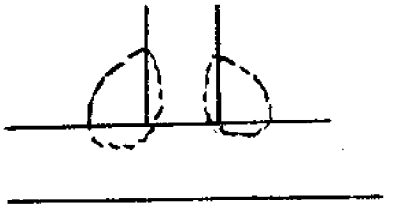

TEE JOINT

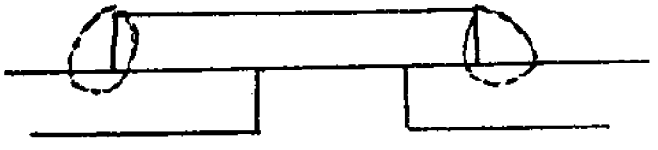

SINGLE STRAP WELD JOINT

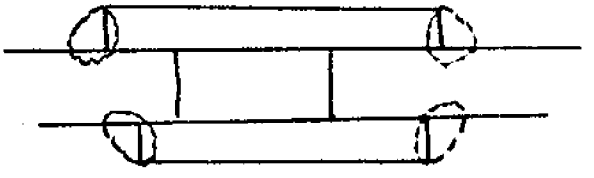

DOUBLE STRAP WELD JOINT

BEAD ON PLATE WELD (EXPERIMENTAL ONLY)

Optimum weld appearance and quality is obtained only for a narrow range of arc voltage, welding current, and travel speed. A low current will produce too small a weld puddle and the metal will pile up in ripples unevenly. A high current will cause excessive melting and produce a wide bead. A rapid travel speed will result in a narrow bead with very pointed ripples. Too slow a travel speed will result in the weld metal piling up, forming almost straight ripples. It is due to this narrow range of welding variables which produce ideal weld beads that welding becomes involved. The basic operation of welding is simple. But, in order to achieve the desired results, much investigation is needed into the effects of changing these welding variables.

2.2 STATE-OF-THE-ART OF CURRENT WELDING PROCESSES

During the past few years, as a result of increased activity in the construction of offshore structures, there has been considerable interest in the development of underwater welding technologies. For many years, underwater welding has been avoided except in special salvage situations or during temporary repair operations.[7,15,68] Seldom have underwater welds been thought of as permanent. However, during the past few years, there has been much renewed interest and considerable activity in the area of developing and improving underwater welding technologies to a point where they might serve as a reliable underwater fabrication process. It will soon be impossible to completely prefabricate structures above water due to the growing size and complexity of these objects.[62] Underwater fabrication will then be required. However, it must be remembered that performing any task underwater is more expensive and more difficult than doing the same thing above water. Thus, whenever possible, the job

should be completed in the air.

Welding requires good visibility of the work area and a considerable amount of time. Both of these are precious commodities in an underwater situation. The lack of visibility causes problems not only during the welding itself when it prevents good positioning or control of the weld bead, but it also places a severe handicap on the diver as he maneuvers and positions his equipment. This disorientation makes every necessary movement slow and awkward. These poor operating conditions require more elaborate safety procedures which in turn require more time. Because of the severe demands imposed on the diver to allow for adequate decompression procedures, bottom time, especially at any but the most shallow depths, is limited and very expensive.[56] Saturation diving techniques are being used more regularly in conjuction with underwater welding operations.[19] Diver life support problems are being solved by increasingly sophisticated breathing mixtures, equipment, operational procedures, and monitoring equipment.[70] The actual welding of a joint becomes only a small portion of a successful underwater welding operation. That which started out as a simple task of improving the metallurgical microstructure of welds produced in a water environment has become in recent years one of the most complex and challenging underwater tasks to be attempted by the ocean engineering industry.

2.21 Basic Processes

Table 2-1 summarizes various underwater welding processes which are either being used or have been well-developed. Figures 2-1 through 2-6 explain these processes. All of these processes are arc welding processes.*

Underwater welds can be produced using an arc directly in the surrounding water or by protecting it in an evacuated chamber surrounding the area of the joint to be welded. These alternate methods are called wet welding if no surrounding chamber is employed, or dry welding if a surrounding enclosure is used. The major reason for using a chamber is to isolate the welded region from the severe quenching action of the water. Other advantages are achieved inculding increased visibility, improved positioning of the weld bead, decreased susceptibility to hydrogen embrittlement, and improved working conditions, enabling the welder to maintain improved stability. There are some increased safety hazards from the explosive gases often evolved during welding or used in the chamber atmosphere. There is also the increased complexity of life support systems, monitoring equipment, transfer vehicles to transport the welder to the chamber, and increased construction and development costs of the welding chamber itself. These factors result in an extremely expensive operation which appears prohibitive except in cases when the chamber can be standardized and used repeatedly under similar circumstances such as in pipeline welding operations.[20,55,56,69,70]

A major advantage of wet welding is its simplicity and ability to be used in many different positions to produce

---

* Other welding processes also can be used underwater. For example, a study was conducted at M.I.T. on the feasibility of exothermic welding of a stud to a plate. A paper entitled, "Underwater Application of Exothermic Welding" was presented by K. Masubuchi and A. H. Anderssen before the 1973 Offshore Technology Conference, Houston, Texas (OTC 1910).

FIGURE 2-4

UNDERWATER WET WELDING PROCESSES

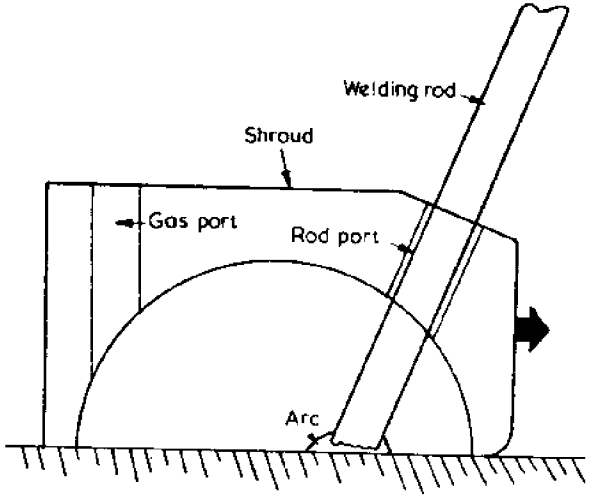

A) SHROUDED METAL ARC

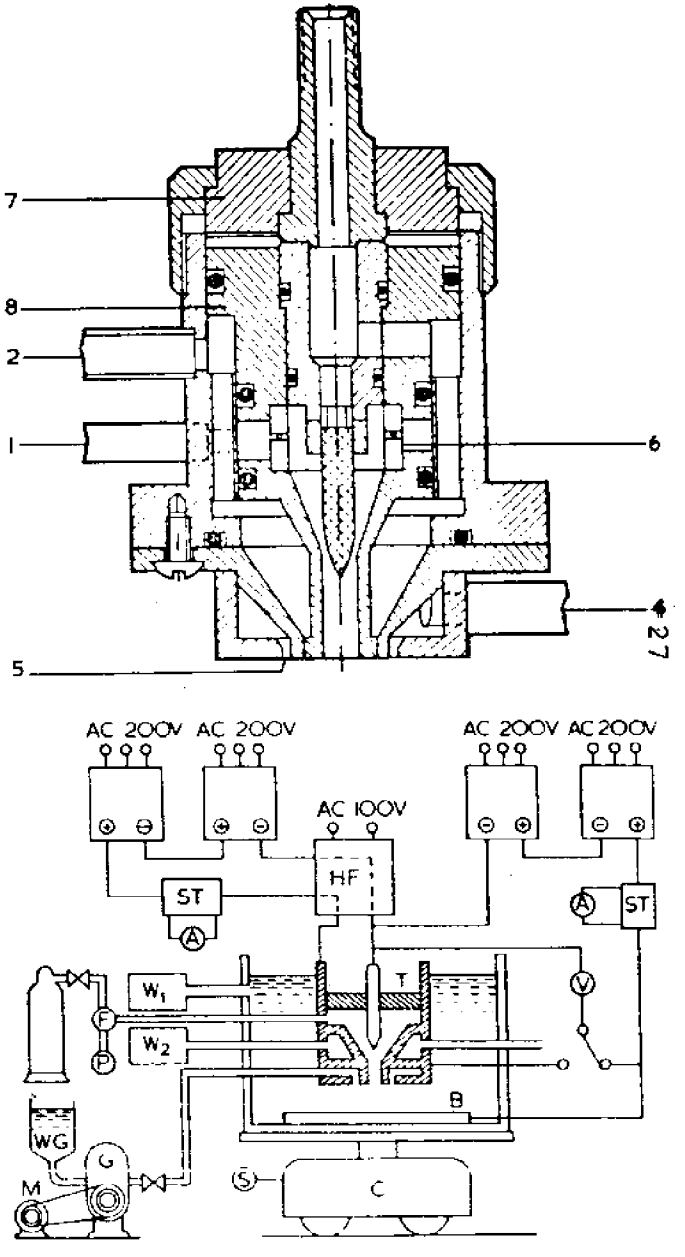

B) PLASMA ARC SCHEMATIC

TABLE 2-1

SUMMARY OF UNDERWATER WELDING PROCESSES

Process	APPLICATIONS	Limitations
I WET WELDING TECHNIQUES		
A. Shielded Metal-Arc	Complex lap, tee or butt welds. Very maneuverable. Single or multipass.	Visibility-positioning, diver stability, rapid cooling, hydrogen, discontinuities from changing electrodes.
B. Shrouded Metal-Arc	Fairly uniform joints. Single-pass. Fair maneuverability.	Visibility-positioning, diver stability, non-uniform joints, hydrogen, cooling rate. Discontinuities from changing electrode.
C. Plasma Arc	Butt, lap, tee joints. Very good weld bead shape and penetration. (Experimental stage only).	Slow speed, visibility-positioning, moderate complexity of equipment, rapid cooling, diver stability.
D. Gas Metal-Arc (continuous wire electrode)	Butt, tee, lap joints. Moderate maneuverability. Multipass. Superior quality to metal arc.	Visibility-positioning, maintenance, complexity hydrogen (without shielding), rapid cooling, diver stability.
II DRY WELDING TECHNIQUES		
E. Movable Chamber	Uniform joint design. Butt and fillet joints, pipelines possible. Multipass. Very high quality.	Visibility-positioning, diver stability, complex equip. maintenance (need wide area adjacent to joint for chamber)
F. Fixed Chamber (complete enclosure) Gas Tungsten-Arc Process	Pipelines, simple enclosable structures. Very high quality.	Expense, complexity of chamber & equip., explosion. Elaborate support crews.

FIGURE 2-5

UNDERWATER DRY WELDING PROCESSES
FIXED CHAMBER METHOD

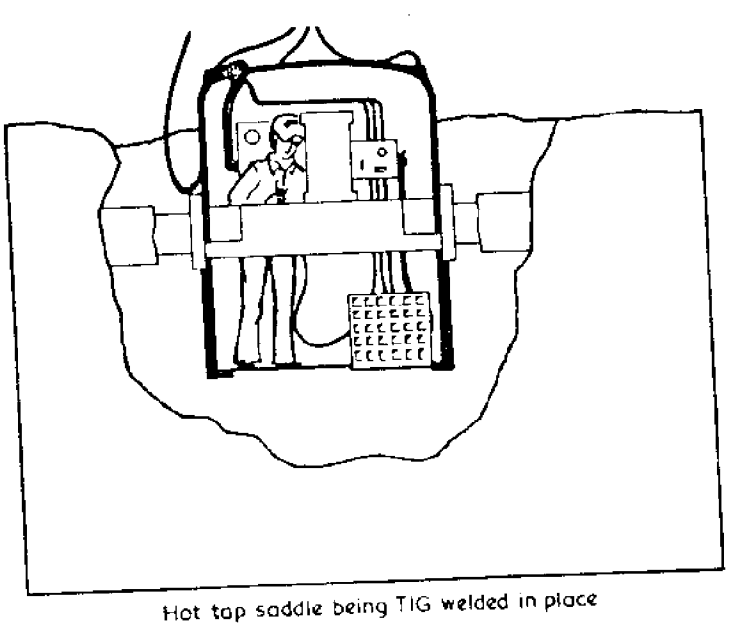

Hot tap saddle being TIG welded in place

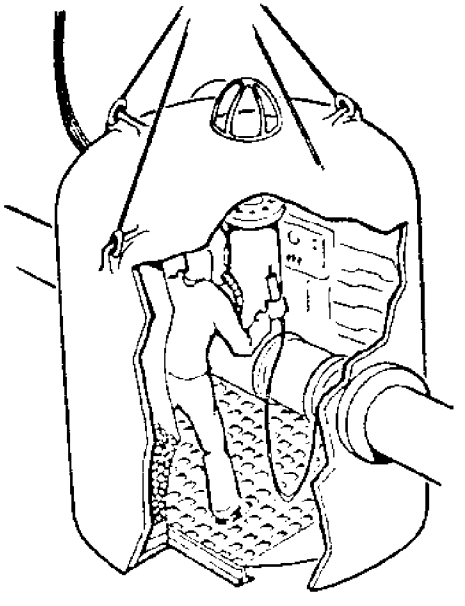

Hot tap chamber

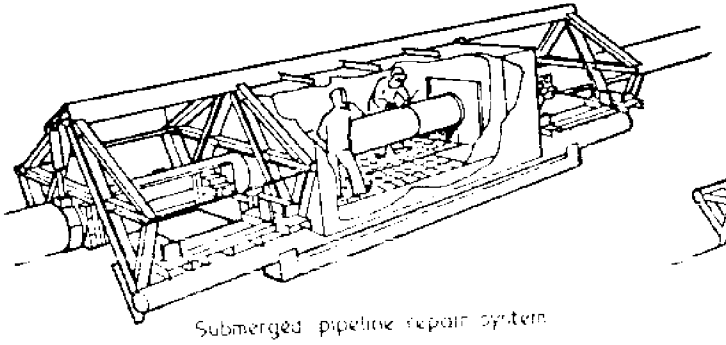

Submerged pipeline repair system

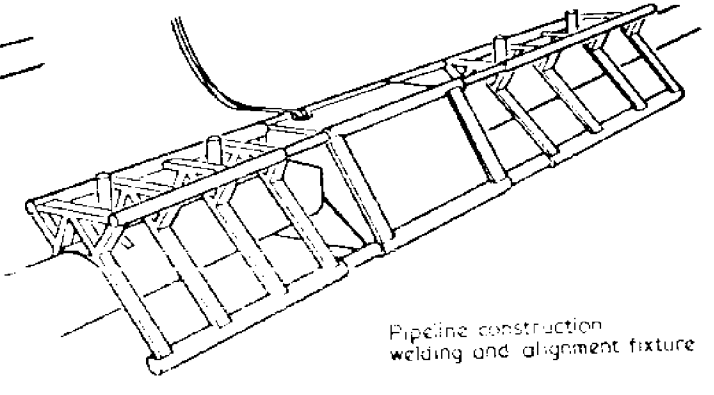

Pipeline construction
welding and alignment fixture

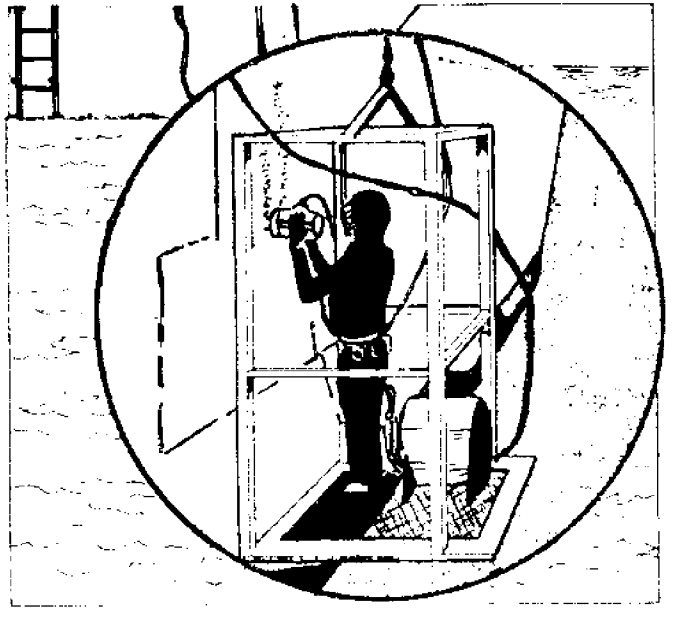

OPERATIONAL VIEW

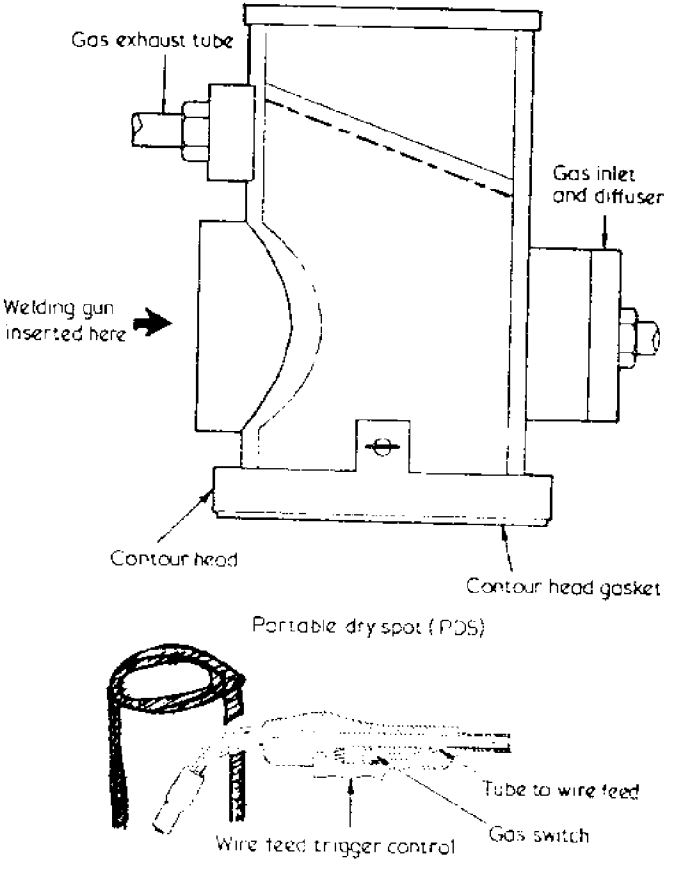

"DRY SPOT" DESIGN

FIGURE 2-6

UNDERWATER DRY WELDING PROCESSES
MOVABLE CHAMBER - "DRY SPOT" - TECHNIQUE

unusual and complex joints.[22] Visibility and positional stability remain major problems. But, the original objections to underwater welding of increased brittleness and problems with hydrogen embrittlement remain unsolved. During the past few years, various combinations and modifications of both wet and dry welding concepts have been used by both researchers and commercial operators. These include the basic shielded metal-arc wet welding and the basic chamber welding with the welder and the joint enclosed in an evacuated chamber. Wet welding using a continuous wire feed welding apparatus both with and without shielding gas and with solid or flux cored wire has been tried.[7,43,58] Plasma arc welding has also been tested using argon shielding, and also, without shielding.[23] Various combinations of wet and dry welding processes have also been attempted.

SubOcean (formerly HydroTech) has developed a GMA process for underwater welding that is enclosed in a small chamber which contains the weld area and is held by the diver-welder.[51] A smaller chamber called a shroud has been used in conjunction with the ordinary stick electrode welding to produce a small gaseous bubble around the critical weld puddle region.[63] Most of these variations have been developed during the last few years and are evidence that work in underwater welding is proceeding at an accelerating rate. The following sections contain more complete descriptions of each of these welding process technologies.

2.22 Shielded Metal-Arc Underwater Welding

Electrodes with a flux covering have been the most widely used welding process in underwater welding operations. The technique has been referred to as touch or drag welding because the electrode is dragged along the workpiece without the welder holding an arc gap. The arc burns in a cavity formed inside the flux covering which has been designed to

burn slower than the metal barrel of the electrode. A constant arc is thus maintained even in very poor visibility conditions. The diver exerts a downward pressure on the electrode to keep the flux chipping and burning away to provide a constant arc barrel length. The electrode is held in a nearly vertical position with a 60-80° leading angle.[35] The electrode coating most often used for this welding technique contains iron powder. A waterproofing is added to the electrode to keep the covering from disintegrating underwater. Everything from wax to paint has been used with varying degrees of success. The ease with which the touch method gives sound underwater welds should be emphasized in light of the often poor welding conditions, and the fact that divers are often unskilled welders.

Because of the poor visibility often encountered in underwater welding, it is most desirable to weld with some sort of guide for the electrode. For this reason, tee joints and lap joints are often selected when using stick electrode welding. Until recently, underwater stick electrode welds were predominantly single pass. This avoided the problems of cleaning the weld bead in preparation for another pass. However, Chicago Bridge and Iron Company has in the past several years done quite exhaustive underwater welding jobs using multipass welding.[22] They are using welders who are trained to be divers, rather than the more common case of divers who take a short welding course. This allows a more usual manual electrode welding technique (non-drag) to be used, as well as their own specially developed electrodes. They have produced multipass welds with a quality which is often better than the Navy's estimates of 80% tensile and 50% ductility.[67] They have been able to weld metal with a carbon equivalent number of .60 without underbead cracking by using austenitic electrodes.

2.23 Shrouded Metal-Arc Underwater Welding

Because of the extremely steep temperature gradients in underwater welding, even the iron powder touch welding technique does not eliminate weld degradation, especially its brittle properties. The drastic quenching continues to produce bainite and martensite formations at the fusion line, fine grain size in the heat-affected zone, slag entrapment and porosity, and the possibility of hydrogen embrittlement. A shroud is a small device used to displace the water from the immediate vicinity of the weld pool. The gas evolved from the arc is used to displace the water so that no external shielding gas is required. This helps keep equipment to a minimum and still provides some advantage from the small air pocket covering the welding puddle. The gas atmosphere contains a large amount of hydrogen and does not reduce the problems of hydrogen embrittlement. A shroud does help slow down the cooling rates and so enables welds with less martensite and thus, more ductility to be produced. The mechanical properties of such welded joints are found to be intermediate between air welding and unshrouded underwater welding quality.[62] The actual operation, the size of the shroud is critical. The size of the shroud must be compatible with the amount of gas formation at the arc. Too much gas will tend to bounce the shroud off the workpiece. Too little gas will be ineffective in displacing the water under the shroud. The most practical design for a shroud will therefore include a controllable venting system to allow an equilibrium between the gas formed at the arc and the gas flow under the shroud which is necessary to keep it free from water without bouncing it off the workpiece. Silva[63] met with some success using a 1-1/2" hemispherical shroud. The shroud seemed to eliminate undercut and produced a better bead shape. The decreased cooling rates were indicated by welds with less hardness and with less martensite observed

in the microstructure. This type of imaginative device may well prove to be an asset in attempting to upgrade the quality of underwater stick electrode welding processes.

2.24 Shielded Gas Metal-Arc Underwater Welding Processes

Although most underwater welding has historically been performed using the shielded metal-arc process, a growing amount of work is being done with thin wire GMA processes. The process has been used both in the "wet" ambient water environment and also in conjunction with either portable, hand-held chambers or with large hyperbaric enclosures. When the welding arc is not exposed to the ambient water, it is called "dry welding."

Underwater semi-automatic GMA equipment was first developed in the U.S.S.R. in the late 1950's. The equipment was successfully used with and without CO_2 shielding to a depth of 200 ft.[60]

Beginning in 1968, Ocean Systems Incorporated and Linde Division of Union Carbide developed a prototype shielded inert gas metal-arc (SIGMA) wet welding apparatus consisting of a pressurized submersible wire feeder, a torch, and related controls. Numerous problems were encountered and the system was not further developed. Reading and Bates Company developed similar equipment, but neither prototype system has been reported out in the literature.[7]

The wet GMA welding process is more complex than the shielded metal-arc process because a consumable electrode is fed continuously from a spool through the welding gun by means of a wire feed mechanism that automatically maintains a stable welding arc length. This arc length regulation accomplishes the same task as the drag welding technique for shielded metal-arc welding and provides for underwater situations of poor visibility. The metal transfer in GMA welding is either globular, axial spray, or rotating spray. DCRP is

usually used because DCSP seems to produce a more erratic arc action and less weld bead penetration. However, this makes the electrode gun and equipment susceptible to galvanic corrosion because it is the anode (+) with respect to the workpiece. This tradeoff seems regrettable but necessary. Increased pressure seems to result in increased arc power which induces uncontrollably large and fluid weld puddles. For this reason, it is desirable to develop controls for underwater GMA machines which make wire feed and current independent variables.[56] There is disagreement as to whether or not a shielding gas should actually be employed. Some gas must be used in the welding feeder mechanisms to prevent flooding. More research is needed to determine what gas mixture, if any, should be used. It is also possible that thin wire flux cored wires might be successfully employed underwater. The filler wires used in Russia and the U.S. have contained .09 -.12% Carbon, .45 -.95% Silicon, 1.0 - 2.0% Mn. Apparently, no filler wire or flux core has been developed specifically for underwater use. In the U.S., no GMA welding apparatus is used for actual wet welding. Companies contracting for dry pipeline welding may use specially modified GMA feeders, guns, or controls. No published data, however, exist for these systems, and they are not a true wet welding system.

The power supply and gas supply equipment usually remain topside, while only the wire feeder mechanism and the welder gun are submerged. This follows a basic rule of underwater work which is to put everything you can above water and take only the minimum in equipment and supply cables below!

The major disadvantage of this underwater welding scheme is that it involves much complex equipment which is especially prone to failure and resulting high maintenance when used underwater. However, in view of its improved results, this

increased complexity may be an acceptable tradeoff where the superior quality is a critical factor.

2.25 Plasma Arc Underwater Welding

Workers in Japan have developed an underwater plasma arc welding process.[23,24] The process produces the best results when water glass shielding is used. The plasma arc is a constricted flow of partially ionized gas through an electric arc. The constricted arc nozzle produces greater arc stability and a high concentration of power. These are both found to be advantageous in underwater welding resulting in a very reliable arc producing an exceptionally even weld bead, and also, very good weld shape due to the high penetration of the arc. The disadvantages of such a process are its speed, which is very slow compared to stick electrode welding, and its complexity, which is a disadvantage in underwater operations. The shielding technique employed in the process results in substantially slower cooling rates and thus, produces superior weld quality. Doublepass welds were found to be superior in ductility to singlepass welds, thus lending more evidence to support multipass underwater welding recommendations. This process is still in an early development stage, but appears to have possible application to at least some underwater welding.

2.26 Movable Chamber Underwater Welding

This process involves a small diver-held chamber which contains a gas metal-arc welding apparatus, and is filled with shielding gas at a pressure sufficient to exclude the surrounding water. The welder operates the apparatus by guiding the hand-held chamber along the desired weld seam and manipulating the GMA welding tip as in normal air operation. The small chamber is made of clear plastic to reduce its interference with normal welding methods. Removable contour heads and gaskets are attached to the open end of the portable

dry spot chamber to allow the chamber to be used on a variety of odd-shaped joint contours. The welding gun penetrates the welding chamber through a flexible rubber collar, allowing the welding tip to be manipulated independently of the chamber. Operation of the apparatus, thus, will require both hands of the operator and necessitates firm footing and support while the welding is being performed. The chamber has an adjustable exhaust tube. This is adjustable to allow gas to escape from the chamber without blowing the chamber away from a tight contact with the welding surfaces. A high-intensity light in the chamber illuminates the work area prior to the striking of the arc. The shielding gas that expels from the welding gun tip and is normally used as the only shielding atmosphere, is now used only to stabilize the flow of gas around the weld puddle, and produce a drying effect for any remaining moisture.

The wire feed unit is located separately from the chamber in a pressurized steel casing. This unit is placed as close to the chamber as possible to minimize the danger of mechanical fouling of the welding wire. All controls for the apparatus except the on-off control are located on the surface. The welder operates the on-off switch himself.

The movable chamber process is successful in allowing underwater welds to be completed without direct contact with the surrounding water until the weld metal is cooled enough to prevent significant hardening of the HAZ. The mechanical properties are therefore excellent. Using GMA as the basic process, the technique achieves air quality welds. The disadvantages of the process lie elsewhere, as in its practical limitations of maneuverability and flexibility. Any underwater task which involves both the operator's hands is subject to difficulty. Underwater work is similar to work in a weightless environment. In addition, diving suits and safety equipment add encumberances to any underwater job.

In spite of the fact that the movable chamber is constructed out of clear plastics, the operator has a difficult time maintaining a complete view of the workpiece. Due to the size of the chamber (approximately 4" in diameter), the joint design may not be the same as conventional air welding work. Some ingenuity may be required to design joints which both perform structurally, and also allow room for the movable chamber.

Extremely complex weld joints are also less suited for movable chamber welding. However, this technique has been employed on all positions of welding. As in all underwater welding procedures, proper joint alignment and fit-up are critical to obtaining the best welded joint properties. Applications include the repair of tubular offshore structural members, dock pilings, ship hull damage (saving dry dock expenses), offshore pipelines, and other repair, maintenance or construction situations involving ocean engineering structures.

2.27 Dry Chamber Underwater Welding Techniques

Dry chamber welding involves a sealed chamber completely enclosing a portion of the pipeline or underwater structure to be welded. The water is displaced by some mixture of pressurized gases. This artificially-induced environment solves the major difficulties of underwater welding by reducing the cooling rate to normal air welding rates and excluding much of the hydrogen that would normally be present if the welding were performed directly in the water. The hydrogen is not completely removed because the humidity of these chambers is extremely high. The gas mixture to be used must not be explosive, and yet, should be able to sustain life for short periods of time in case of diver life support system malfunction. A helium-oxygen mixture with an oxygen partial pressure of 6-8 psi has been found suitable.[20] The welders

breathe through a separate system of gases more suitable for sustaining life. This mixture will change with different job depths. Because of the welding heat, the chamber is often at an elevated temperature of 90-95°F and combined with the high humidity, working conditions remain far from ideal inside these chambers. However, problems with visibility and positional stability are solved using these chambers. Because the chamber atmosphere is not free from gases which cause weld defects, a separate shielding gas must be used for the welding arc. The most practical applications of this process has been to pipeline welding where the chamber shape is simple and also reusable. In spite of the process' high specialization to enclosable weld joints, it remains an extremely expensive technique. But, in several applications where code-quality welds are a necessity, this type of underwater welding may be well worth the cost. It will continue to be an extremely useful underwater fabrication tool, especially as more standardized construction jobs are attempted underwater.[20]

Several applications of chamber methods are in operation today. Pipeline repairs, tie-ins, and planned construction operations are all areas that can use chamber welding applications. The alternative to underwater welding involves making the repair or tie-in on a barge at the surface. This operation is extremely hazardous to the pipeline, inducing buckling, stresses, and possible failure of the pipeline. Thus, the prospect of completing the job underwater, below the dynamic surface wind, wave, current, and tide forces is inviting. The first-generation underwater welding chamber was an inverted cup chamber called the Underwater Hot Tap Chamber. It was first used in 1967 to complete a 6" to 10" "hot tap" and later was used to repair a 4' section of 8" oxygen pipe used in a river crossing. The depth of the "hot tap" was 110 feet. The chamber had an independent breathing system, a power

supply control and a gas feed control for the shielding gas. The Submerged Pipeline Repair System was a similar welding chamber. It also was equipped with a hydraulic pipe aligning system. It had a triangular tube truss with a rectangular welding chamber. In addition to the ordinary controls, it had hydraulic controls for the alignment equipment, and a buoyancy control for the "set down" on the pipe. It is used to replace short sections of pipe in one "set down" or to repair longer sections of pipe (up to 900') with two "set downs."

The second generation chambers evolved as a refinement of the pipe repair and alignment capabilities of the Submerged Pipeline Repair System. They are designed to join two large sections of pipe during the laying of new pipeline, either using the offshore bottom pull, or barge methods. Third generation chambers are equipped with fine positioning and aligning capabilities, so that they are able to join two large sections of pipe without a short section of pipe called the "pup joint." In all of these pipe joining chambers, the operation involves airlifting a hole around the pipe, lowering and positioning the chamber around the pipes and dewatering the chamber. Then, the welders and their life-support and welding equipment are lowered and the welding and fit-up operations are completed. The weld is X-ray tested and also hydrostatically tested. Finally, it is coated to prevent corrosion and the chamber is removed.

Any welding process that might be selected for underwater chamber welding would have to operate satisfactorily at high pressures and also be used in all positions of welding. High deposition rates of metal would also be ideal. The shielding gas would have to be controllable. Gas metal-arc and gas tungsten-arc have been the two processes used by various people. GMA has almost four times the metal feed

rate as does GTA. But, GTA has better control. Both give high quality welds. It was found that the voltage increased with pressure which caused an increase in the total arc energy which in turn resulted in a larger, more fluid weld puddle. With GMA, control of this large weld puddle became difficult, and so GTA was selected (Lynch and Pilia, 1969). During the 110' "hot tap" operation, a constant current DC machine was used at 150-180 DCSP. Argon shielding was employed at 200 cfh. The voltage was 12v for the root pass and 16-18v for the remainder of the weld. If GMA is selected as the welding process, an inductance control is recommended to control the fluidity of the puddle (Robinson, 1967). Controls should be provided to be able to change the voltage and current with increasing depth. When using GMA, there can be a real problem of corrosion of the feed wire. It should be dept in a sealed container of some sort. Code quality welds have been obtained using both GMA and GTA processes. GMA does produce much better ductility than does GTA. But, GMA is simply more difficult to control at high pressures. For this reason, GTA is often selected.

2.3 A SHORT HISTORY OF THE RESEARCH, DEVELOPMENT, AND APPLICATION OF UNDERWATER WELDING BY INDUSTRY

An interesting way to trace the growing interest and importance of underwater welding is to document the research and development efforts by industry and briefly sketch the case histories of the commercial applications.during the past several years. Without doubt, the recent, almost explosive expansion of the offshore oil industry has given the incentive and investment motivation which has stimulated this development in the United States. This may explain the simultaneous initiation of several R&D efforts in the late 1960's.

Development of underwater welding in any kind of a formal research setting began in the late 1950's with some work in Russia leading to the development of underwater, wet GMA welding (Shlyamin, 1971). They reported satisfactory welds at 200 feet. Work in the United States did not begin, however, until the late 1960's. In 1966, Ocean Systems Incorporated (OSI) together with the Linde Division of Union Carbide began R&D efforts towards a dry habitat, GTA, underwater welding process. They initially developed a "Hot Tap Chamber" and completed a 6"Ø tie in to a 10"Ø existing line at 100 feet in the Gulf of Mexico for Humble Pipe Line Company. The weld was hydrostatically tested and X-rayed and found satisfactory. This job was completed in September of 1967. In October, 1967, OSI performed a welded repair of a 4"Ø line tie into a 16"Ø in 58 feet of water for Transcontinental Gas Pipe Line Corporation. The joint was cut out, rewelded, and X-ray inspected in a dry habitat. Later that same year, in October of 1967, OSI completed a pipeline repair under the Raritan River near Keasbey, New Jersey for the Linde Division of Union Carbide. An 8"Ø oxygen pipeline had been damaged by a dredge. The damaged section was cut out and a short pup joint was welded into the pipeline.

In May of 1967, the Sanford Marine Services and Westinghouse Ocean Research and Engineering Center began "Project 600" which was primarily a saturation diving system test program. However, as part of the work assignment at 600 feet, they attempted SMA welding. Problems with the flux coating terminated the tests, but this does show the developing trend of interest. During this same time period, Reading and Bates Offshore Drilling Company pursued the development of a dry habitat and the associated GMA welding apparatus. Repairs to a corrosion-damaged platform were completed satisfactorily, although no further efforts are reported, apparently because of equipment difficulty.

Ocean Systems Incorporated continued their activity. In 1968, they briefly experimented with wet GMA welding apparatus. But this option was apparently abandonned in favor of the dry habitat methods. In May of 1968, they completed two riser repairs in the Gulf of Mexico for Tennessee Gas Pipeline Company. During 1968, HydroTech of Houston, Texas began preliminary R&D with what is now called the Portable Dry Spot (PDS) technique. This movable, minihabitat employed a specially sealed GMA underwater apparatus. Commercial applications of this and a similar process called HydroBox did not commence until late in 1972.

In 1969, OSI had developed a Submerged Pipeline Repair System by which two pipe ends could be aligned and welded within a dry habitat. They used the system to add 900 feet of 12" pipeline to an existing line in the Gulf of Mexico in 80 feet of water. The habitat and pipeline restraint trusswork frame is 25' long, 10' wide, and 8' tall. The company's development tests continued at 300 feet and a 600-foot depth capability was predicted.

Early in 1970, Chicago Bridge and Iron Company began research and development for an in-house underwater repair capability. They began working with wet SMA welding techniques. Also, that year, a U.S. patent was granted for an underwater welding process that involved a composite welding rod that was hollow and through which some shielding gas was to be pumped. The process was patented from Japan, and no further mention of this process has been found. During the last part of 1969, with completion in 1970, there was a major underwater habitat weld project by OSI. They joined two 24"Ø pipeline sections which linked an offshore platform with the shore in the Bass Strait, Australia, for Esso Standard Oil and Santa Fe International. The pipeline joining took place in 220-feet of water using the Submerged Pipeline Repair System. Saturation diving techniques were employed

to complete the pipe fit-up and weld which was X-rayed and met API 1104 Code criteria. The joint was coated with epoxy. Perhaps one of the reasons that this technique is not used more regularly is the high cost associated with the habitat, saturation diving techniques, and assorted surface support systems. These factors are estimated to have resulted in a price tag of nearly one million dollars for the underwater pipeline weld in the Bass Strait.

In January of 1970, Canadian Diving Services Ltd. (Now DIV CAN Oceaneering) repaired the damaged hull of a semi-submersible platform for Shell Canada Ltd. with a 1/2" patch plate. They wet-welded the patch using an SMA welding technique which they call "overhead" that involves a weaving and preheating stroke movement of the electrode. In August of 1970, Chicago Bridge and Iron completed their first commercial application of wet SMA welding for the S&W Construction Company. Retaining pilings on a Memphis, Tennessee dock were repaired by welding an extensive number of 1/2" plates over damaged piling sections. A problem with high carbon content in the pilings was solved by using austenitic electrodes. Visibility was very limited.

In June of 1971, SubSea International Inc. designed and built a pipeline alignment and habitat system similar to that earlier developed by OSI. Their habitat incorporated a "dry to dry" transfer of the welder from a submerged diving bell to the habitat by a direct mating procedure. The alignment rig was 29' long and 15' wide. It can accomodate a 56" pipeline, and the two ends can be out of alignment by 32°. Also this month, CBI completed the underwater repair of a 14"Ø strut on an offshore platform for Humble Oil and Refining Company at a depth of 63 feet.

In January of 1972, HydroTech patented its Portable Dry Spot GMA process. Meanwhile, CBI was employed by the Port of Houston to repair holes in dock pilings caused by corrosion

damage. A total of 1400 feet of 1/2" vertical fillet welds and 400' of 1/2" horizontal fillet welds were completed. The welds had a tensile strength of 18 to 28 thousand pounds per inch. The visibility was 3-4" but underwater TV inspection was accomplished by using a water displacement tube flushed with fresh water. In March, CBI replaced a 20"Ø and a 22"Ø pipeline for the Dow Chemical Company in 0-10 feet of water in the Barge Canal, Freeport, Texas. Backup rings were employed to allow butt welds to be completed. In May in the Gulf of Mexico, CBI repaired a "k" joint using a 6' double-sleeve and gusset plates for Humble Oil and Refining Company in 52 feet of water. In July, CBI replaced the value operator adapter on a 20'Ø value in 52 feet of water for the Tennessee Gas Pipeline Company. In August of 1972 in the Gulf of Mexico for Humble Oil, CBI completed extensive repairs to a platform damaged during the driving of a pile. Several horizontal braces and struts and two "k" joints were replaced or repaired and reinforced. The depth varied from 32 feet to 165 feet and saturation diving techniques were used for the 165' repairs. At the completion of the structural repairs, 5 anodes were reinstalled by welding. In September, HydroTech began its first commercial job in a joint effort with the British Oxygen Company called SubOcean Services (SOS). They welded high pressure blocks on a 16"Ø riser in the Gulf of Mexico for the Transcontinental Pipeline Company in 112 feet of water. The weld was performed using the HydroBox technique of enclosing the weld joint in a plastic box and evacuating the area with an inert gas. A GMA welding process is then employed with the welder in the wet and inserting the welding gun from below the evacuated box towards the weld joint. The welds were hydrostatically tested at 1600 psi. In October, CBI was again underwater welding for Dubai Petroleum to replace a "T" stiffener on two underwater storage tanks in 137 feet of water. The year, 1972,

was indeed an active one for underwater welding developers.

During 1973, there was also much activity in underwater welding. Both Chicago Bridge and Iron Company and SubOcean Services were busy completing several jobs each in the Gulf of Mexico, the Arabian Gulf, the North Sea, and other places. During February, CBI repaired another dock for the Exxon Company in Baytown, Texas. Repair sections were fillet welded in a 2" visibility situation. In March, CBI was in the Arabian gulf repairing a crack by back gouging and welding from both sides of a 42"Ø header pipe at a depth of 130 feet. While working on the inside of the pipe for the Dubai Petroleum Company, an airlift was used to displace the water and give the effect of a habitat to increase the visibility during the welding operation. Then in April, two 700 lb. anode replacements were welded into place at 157 feet.

SubOcean Services completed two jobs during April of 1973. They replaced three 3"Ø riser for the Atlantic Richfield Company in 15 feet of water. These welds were satisfactorily hydrostatic tested at 4700 psi. Later this month, they repaired a 4' crack in a 14'Ø pontoon on Santa Fe Drilling rig "Blue Water #2" in 14 feet of water. In May, SOS was in the North Sea to replace two 14"Ø horizontal braces in 20 feet of water for Phillips Petroleum Company. In June, SOS completed three separate welding jobs. They replaced four 6"Ø risers in 15 feet of water for Shell Oil Company which were hydrostatically tested at 1500 psi in the Gulf of Mexico. They similarly replaced two 2"Ø risers in 10 feet of water for Shell in the Gulf of Mexico. Next, they completed the repair of a 12"Ø horizontal brace in a platform "A" for POGO (United Gas-Penzoil) in 30 feet of water. CBI was also busy during June replacing and reinforcing crushed and ruptured 18"Ø and 24"Ø struts in 96 and 145 feet of water. Split sleeves were fabricated and

welded together underwater to make the repairs. The production platform in the Gulf of Mexico belongs to the Exxon Company. During July, SOS was again busy. For Shell Oil in the Gulf of Mexico, three 6"Ø risers were replaced, ultrasonic, hydrostatic, and X-ray tested in 15 feet of water. A 20"Ø diagonal brace was repaired at 30' on a platform for P060. And one 3"Ø riser and seven 4"Ø risers were replaced and tested satisfactorily for Shell Oil Company in the Gulf of Mexico. SOS replaced one 3"Ø riser and replaced a section of a 3"Ø flowline for Atlantic Richfield during September. During October, SOS replaced one more 6" riser in 15 feet of water for Shell Oil. Also busy during October, CBI was working under extremely poor visibility and current situations in the Atchafalya River near Morgan City, Louisiana, replacing a river pipeline crossing for the Wanda Petroleum Company. The damaged section of pipe was cut out and flanges were fitted to the two good ends. A template was then fitted as the replacement. The permanent pipe section was fabricated from the template. Meanwhile, a temporary habitat was constructed to give better visibility while the flanges were welded underwater in the dry habitat using SMA. Then, the replacement section was bolted securely at the flange ends and the pipe recovered.

Beginning in October of 1973, and continuing through July of 1974, CBI underwater welders were employed continuously repairing an extensively damaged production platform in 200 feet of water in the Gulf of Mexico. Working with Oceaneering International Inc., tubular members and corroded HAZ areas of welds are being repaired by patching, back-gouging, and rewelding. Underwater TV is being used to document the damage and inspect and verify the repairs. This situation portrays the serious need for underwater welding repair and maintenance and the fact that all of CBI welders are being used on this one job outlines the need for further expansion of underwater welding capacility. Finishing an active year, SOS completed the repair of a 17" long

groove which had become worn into a 48"Ø x60 steel oil loading pipe. The groove was filled and patched to prevent further wear. The job was done for Shell B.P. in Nigeria at a depth of 90 feet. SOS also completed the repair of a 3"Ø riser for the Atlantic Richfield in the Gulf of Mexico in 35 feet of water and the replacement of three risers in 20 feet of water for Shell Oil Company. That brings the underwater welding commercial activity up to 1974.

These industrial efforts have been paralleled by basic research by several working organizations throughout the world. Plotting the course of events involving underwater welding in this way, it is not difficult to foresee an expanding future for underwater welding technologies. Responding to such activity, the American Welding Society Committee on Marine Construction has recently formed a subcommittee on underwater welding. Mr. C. E. Grubbs of Chicago Bridge and Iron Company is the acting chairman at this time and several other men from industry, universities and the Navy are beginning thoughts on developing standard codes for underwater welding procedures and qualifications for diver-welders. Underwater welding for repair and construction of underwater structures must develop concurrently with other expansions in the offshore industries.

PART THREE

PRESENT TECHNICAL AND FUNDAMENTAL UNDERSTANDING OF UNDERWATER WELDING PROCESSES

Contents

3.0 INTRODUCTION

Experimental investigations of underwater welding have produced data that has not adequately been collected and sorted and presented in a unified manner. This section of the report will attempt to do this. Description of the welding processes appears in Section II and a discussion of the basic metallurgy is included in Section IV. This section will concentrate on the remaining areas of underwater welding information, including:

(1) The underwater arc bubble phenomena
(2) The underwater welding arc and associated metal transfer
(3) The underwater heat transfer and temperature histories
(4) Effects of pressure on underwater welding
(5) Underwater welding polarity
(6) Electrode waterproofing
(7) Underwater electrode coating turbidity
(8) Underwater GMA research
(9) Correlations between experimental work and actual weld properties
(10) Actual weld geometrical, microstructural, and mechanical properties

3.1 UNDERWATER WELDING BUBBLE DYNAMICS

The arc bubble is one of the peculiar phenomena which distinguish underwater welding from air welding. The heat of the welding arc dissociates water molecules into hydrogen and oxygen, and the oxygen is consumed in the combustion of the electrode coating material which results in the formation of CO, CO_2, and various mineral salts. The bubbles appear brownish in tint as they rise to the surface, although the pulsating bubble around the welding arc appears blue, suggesting that spontaneous burning of a portion of the dissociated hydrogen may be occurring.[64] The bubble is oscillating

continuously between a small bubble barely covering the arc column and a larger bubble that eventually breaks away from the weld puddle and floats towards the surface. Only a portion of the bubble breaks away, leaving a nucleus bubble with a diameter of .25 -.35 inches (6-9mm).[14] The arc heat and the combustion of the coating material produces gas at a constant rate, but the bubble size oscillations are governed by the buoyancy and surface tension forces and these will not result in anything except this process of bubble growth, breakaway, growth, breakaway...etc. The oscillations of the bubble growth and breaking occur at a rate of 15 bubbles per second in six inches of water.[13] Effects of depth on the bubble dynamics are not reported. Brown (1972) reports that the maximum bubble size, before breakaway is 10-15mm (.4 -.6 inches). Madatov (1965) reports that the maximum bubble size is 16-22mm. The minimum bubble size immediately after breakaway is 6-9mm as reported by both Madatov and Brown. Madatov (1965) reports the frequency to be 10 bubbles per second. He reports the life history of the arc bubble to be .06 seconds of growth, .006 seconds for breakaway, and .03 seconds for contraction.

The total volume of gas being evolved is reported by different investigators to vary according to the electrode type used, but to be invariant with welding conditions. Brown (1972) reports E6013 to generate 40cc/sec. Silva (1971) reports a rate of 50cc/sec. for E6027 and 60cc/sec. for the E7024 electrode. Madatov (1965) reports rates of 33cc/sec. and 100cc/sec. for the two electrodes he employed.

Thus, while various electrode coverings produce more or less gas, the gas rates are constant at a constant depth, even with changes in voltage or current. This implies that the dissociation of water is directly related to the arc temperature which is a function only of the depth. It is postulated that gas rates increase with depth for a given

electrode (Silva, 1971), although no actual pressure tests have been run. The bubble velocity after breakaway has been determined (Silva, 1971) to be 2.3 ft/sec. Madatov (1965) reports a bubble velocity of 200cm/sec. (6.5 ft/sec.). This discrepancy is unexplained, but does not appear critical to the underwater welding process.

Madatov reports that these bubble size fluctuations result in pressure changes on the arc column which change the arc column density and result in small oscillations in the voltage and current of the arc. This effect was not observed in the present investigations, possibly because this effect is more predominant at greater depths and pressures.

It appears that the small bubble that is maintained around the arc column is the phenomena which allows the arc to function normally underwater. If this bubble were to become unstable and lose contact with the arc column, the underwater welding arc would change drastically and might be in danger of being interrupted.

A major portion of the bubble results from dissociation of the water by the extreme heat of the arc. This produces a large amount of hydrogen and oxygen. Most of the oxygen reacts quickly with the combustible elements of the electrode coating to produce CO and CO_2. A small portion of the gas consists of metal vapor, and various mineral salts from the electrode covering. On a percentage basis, the gas is 62-82% H_2, 11-24% CO, 4-6% CO_2, and the remaining 3% is N_2 and metallic and mineral salt vapors (Silva, 1971).

These gaseous products of combustion of the weld metal, the parent metal, the components of the electrode flux covering, and of dissociation of water, as well as the water vapor continuously interact within the bubble environment. And, the atmospheric components vary both with time and with location in the bubble. The degree of dissociation of water

vapor is maximum at the interior of the bubble nearest the extreme temperatures of the arc and decreases radially towards the bubble-water interface.[36]

The high hydrogen content in the atmosphere is perhaps the most critical component. This produces, during the mechanism of metal transfer from the electrode tip to the weld puddle, an extreme danger of possible hydration and saturation with hydrogen.

This gaseous, dynamic atmosphere reacts with the molten metal as it is transferred a ross the medium from the electrode tip to the weld pool. Burn-off of certain of the constituents, especially the reducing agents, manganese and silicon, occurs and is dependent of the concentration of the individual metal components in the electrode, and in the electrode covering used. The burn-off process is not as affected by current and voltage in the underwater process as it is in open air welds (Madatov, 1972). Burn-off appears to be directly dependent on the dwell time in the bubble of the metal being transferred.

So, a measure of the degree to which metallurgical reactions are taking place is the reaction rate in the bubble atmosphere. This rate will increase with depth (pressure). It is a function of the weight per time and volume of drops per time and the frequency of drop formation and the lifetime of the drop from electrode tip to puddle (Madatov, 1972). This reaction rate is formulated after the method of Potap'evskii for open air welds.

$$C_{\eta} = \frac{\eta v T_d \rho}{w \rho_o}$$

η = drops/unit time

w = weight/unit time (grams)

ρ = excess pressure of arc

ρ_o = atmospheric pressure

v = volume of drop at the puddle

T_d = lifetime of the drop from formation to puddle

Table 3-1 gives some tabulated results of this parameter C_η for various welding conditions. The effect of the metal transfer mechanisms on the coefficient of reactivity can be clearly seen. This is empirical data, as the relationships between the metal transfer and the bubble atmosphere reactions are not known. It is still useful for comparing two welding processes and achieving an understanding at least of their relative rates of bubble atmosphere reactions. The welding atmosphere of an underwater weld will be dependent on the electrode coating material and the mechanism of dissociation producing high concentrations of hydrogen. These considerations will become more important for low alloy high-strength steels, which are particularly susceptible to arc atmosphere contaminants.

3.2 THE UNDERWATER WELDING ARC AND ASSOCIATED METAL TRANSFER

An electric welding arc of any type is fairly complicated and has not been adequately investigated or explained. Several general statements as to the forces acting on the arc or on the coinciding metal transfer have been offered by various authors. A short review of these basic arc principles is presented to assure a clear understanding of the specific remarks and observations concerning underwater welding arcs which are to follow.

3.21 General Electric Arc Characteristics

The basic structure of an electric arc such as that used in underwater welding appears schematically in Figure 3-1. The welding electrode and the workpiece act as the two electrodes. The electrode connected to the positive side of the power supply is called the anode, and the electrode connected to the negative side is called the cathode. Figure 2-2 illustrates the difference between straight polarity and

TABLE 3-1

RATE OF METALLURGICAL REACTIONS IN VARIOUS METHODS OF UNDERWATER WELDING

Characteristics of Metal Transfer	Thin Wire Without CO_2, salt	Thin Wire Without CO_2, salt	Thin Wire Without CO_2, fresh	Thin Wire Without CO_2, fresh	Thin Wire With CO_2, fresh	EPS-52 Covered Electrode
Number of drops transferred in 1 second	12	12.2	9.7	16	23	44
Lifetime of drops, second	.1700	.121	.132	.1305	.0575	.0254
Average Weight of one drop, gram	.1670	.1100	.0804	.0804	.1100	.1100
Volume of one drop, mm^3	21.4	14.1	10.3	10.3	14.1	14.1
Coefficient of reactivity of the process, C_η	21.8	15.5	16.92	16.77	7.37	3.26
Voltage of Arc	39	42	36	40	39	39(SP)
Arc Current	240	250	250	250	240	240

Notes: (1) Drop Transfer Throughout
(2) Lifetime of drop has largest apparent effect.

Reference (Madatov, 1972)

FIGURE 3-1

STRUCTURE OF AN ELECTRIC ARC

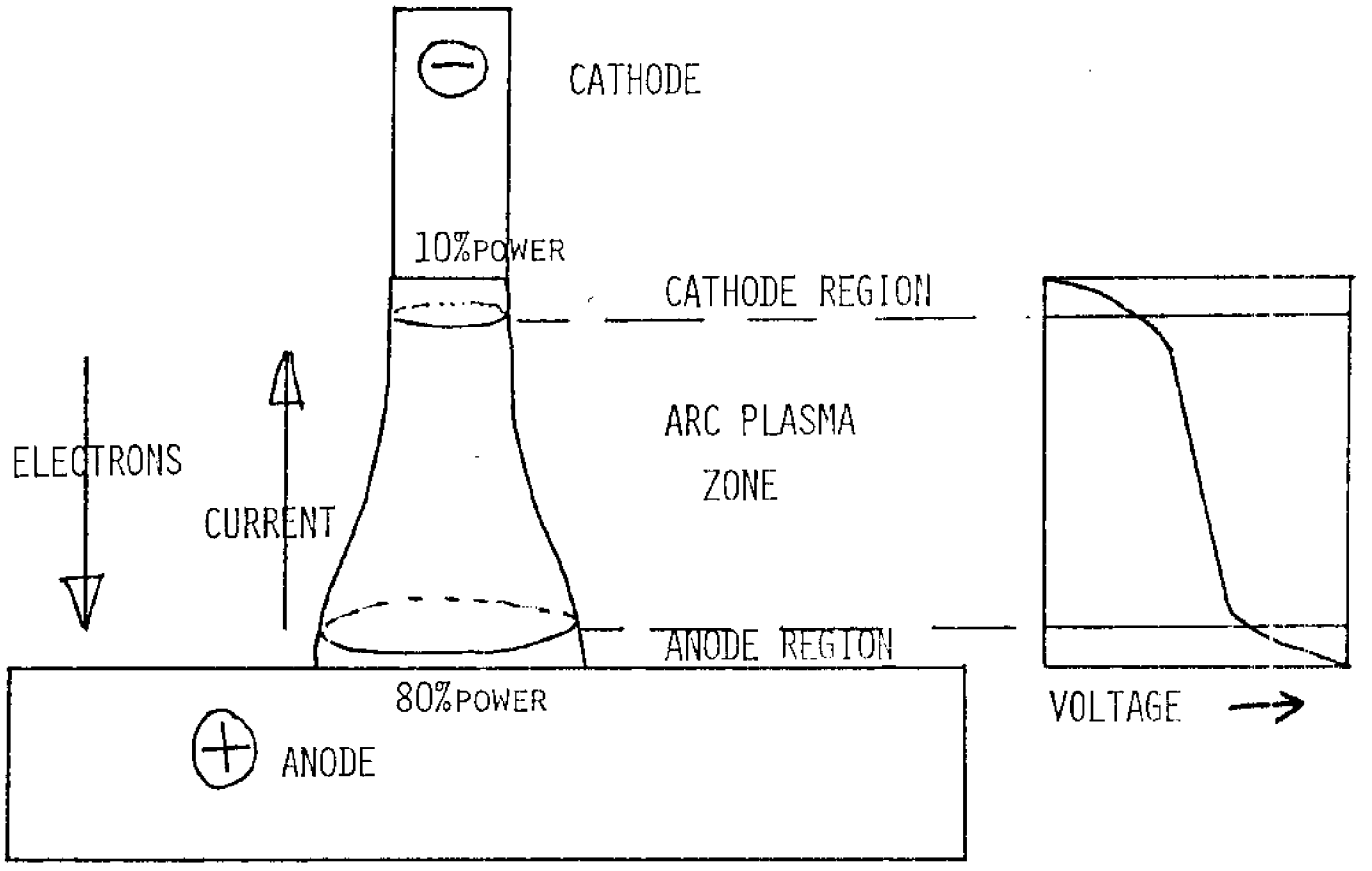

(STRAIGHT POLARITY)

FIGURE 3-2

A) MOVING ARC CHARACTERISTICS

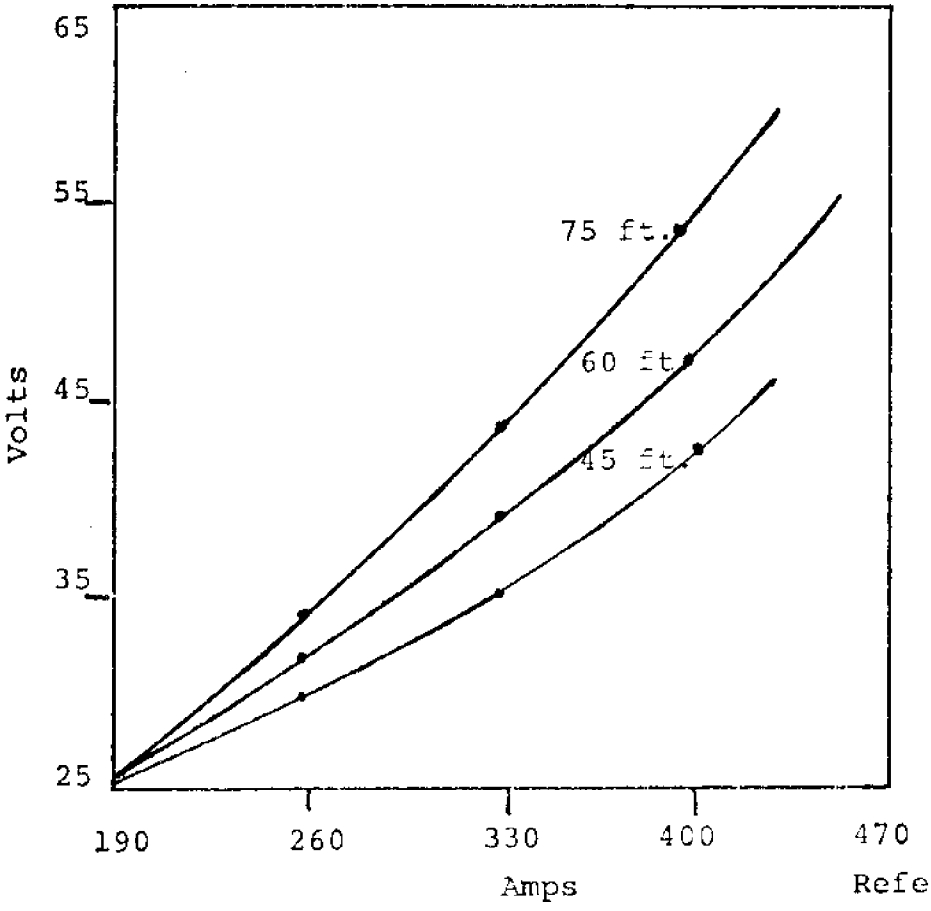

Rising Characteristic

Reference (Avilov, 1960)

B) MOVING ARC VS. STATIONARY ARC

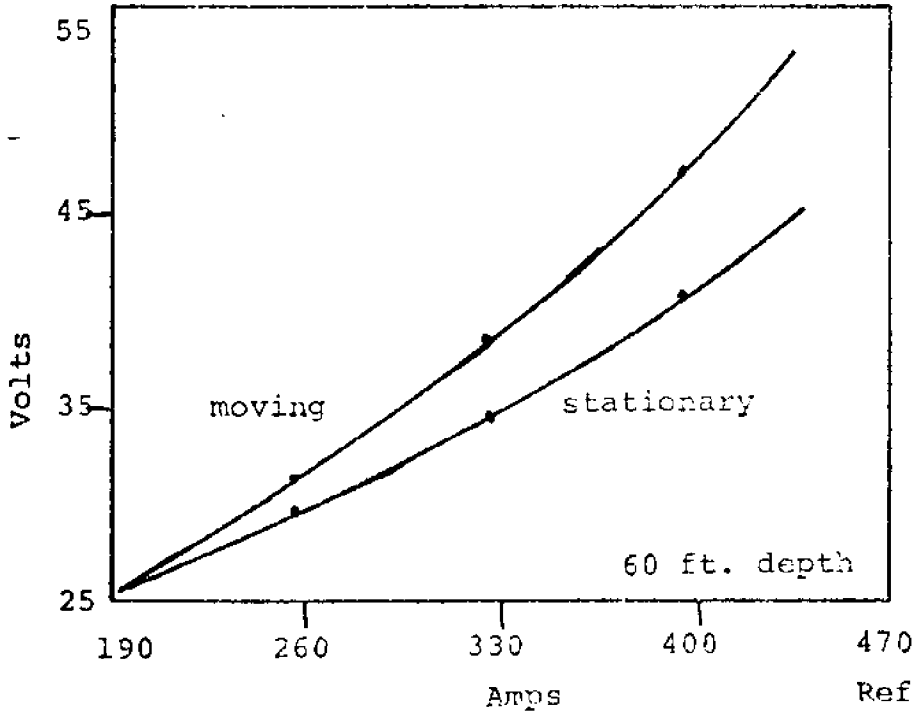

Reference (Avilov, 1960)

reverse polarity. Straight polarity exists when the welding rod is connected to the negative side so that it is the cathode. Although the current flows from the anode (+) to the cathode (-), the electrons are actually flowing in the other direction. As will be discussed later, the impingement of the electron stream on the anode (+) causes it to receive 80% of the heat energy. This differential heating between the anode (+) and cathode (-) produces the major difference in straight and reverse polarity welding conditions.

Returning to the arc column structure, Figure 3-1, it is divided into three regions: (1) the anode region; (2) the arc plasma zone, and; (3) the cathode region. There are very steep potential drops in the anode and cathode regions. This reflects the high heat loss in both due to the melting of the two electrodes. The temperatures of the anode and cathode regions are much less than the plasma zone and thermal equilibrium does not exist. The anode and cathode zones are very short (10^{-1}- 10^{-4}mm) compared to the entire arc length (2-3mm). The arc plasma zone is a thermal plasma in which most of the water and gas molecules are decomposed into atoms and further into ions (+) and electrons. In the arc plasma, the ions and electrons move in a rapid and disorderly manner, with a low drift velocity compared to the thermal velocities (temperature). The electrons drift toward the anode (+) and the ions toward the cathode (-). This drift velocity is the result of electromagnetic forces constricting the arc. The velocity is proportional to the current. Figure 3-2 shows the directions of drift during straight and reverse polarity.

The shape of the arc will correspond to the minimum potential drop. Cathode and anode spots form to minimize the heat loss to the electrodes. The cathode arc spot wanders around on the electrode in response to the ease of emitting electrons at particular locations.

3.22 Underwater Welding Arcs

Underwater welding arcs are acted on by two basic mechanisms of compression or constriction.

(1) The high hydrogen content of the bubble atmosphere as well as the surrounding cooling effects of the water cause the arc column to cool below the normal air values and results in a higher current density in underwater arcs.

(2) An additional effect occurs in straight polarity welding (electrode -, cathode) when the cathode spot is geometrically constricted, preventing the free expansion of the cathode spot. These compression phenomena explain why the voltage-current curves are concave, or rising in underwater welding, Figure 3-2.[4]

Understanding the arc processes involves knowing the shape and size of the welding arc. Madatov (1966) investigated the geometry of underwater arcs for both metal-arc and CO_2 thin wire welding. The basic shape found using a technique of X-ray cinematography was a cylinder for metal-arc welding and a truncated cone with its base on the work for thin wire welding. The diameter of the arc is related to the current using an expression by T. I. Avilov (1960) of

$$D = A\sqrt{I} \quad \text{where } A = 0.11 \text{ as found by Madatov (1966).}$$

Table 3-2 shows how the arc diameter increases with current.

As the arc is moved along a weld, energy is being lost even more rapidly due to increased convective cooling of the arc. This produces a steeper gradient in the volt-amp curve than in the case of a stationary arc (Figure 3-2b. With some form of shielding, this volt-amp curve is generally lower. This may be due to the fact that the shielding partially prevents the water column from constricting the arc column

TABLE 3-2

TEMPERATURE OF ARC COLUMN AT DIFFERENT CURRENTS AND DEPTHS

Welding Conditions			Temperature of arc column, °K	
Depth m	Current amp	Effective Diameter of Arc Column cm	Thin Wire Electrode	Rod Electrode
10	100	.202	8400*	9300
10	200	.205	9200*	10200
10	300	.210	9750	10700
10	400	.260	10150	11100
10	500	.317	10650	11500
20	300	----	10000	11000
40	300	----	10300	11300
60	300	----	10400	11500
80	300	----	10600	11700
100	300	----	10800	11800

*Note: Calculations based on assumption that arc column is a cylinder
ARC LENGTH 2mm
Rod electrode air arc temperature is $6000^{\circ}K$ Reference (Madatov, 1966)

(Hasui, et al., 1972). These processes are both dependent on the arc length. The longer the arc, the more cooling by the water and by the effect of hydrogen cooling or deionization. A longer arc will give a higher voltage and a lower current.

From these relationships of current to voltage and arc length, the arc field intensity can be determined (Avilov, 1960). This is given by the ratio between voltage increase and the arc length increase. Field Intensity,

$E = \frac{dV}{dL}$ (Figure 3-3) shows this relationship.

The field strength is seen to increase with the welding current. This distinguishes underwater welding from open air welding. This is explained by the effect of the various compressions of the arc column causing the cross-sectional area increase of the arc to lag behind the welding current increase, producing a current density or field intensity increase. Avilov (1960) found current densities in underwater arc columns of 280 amp/sq. cm. which for his welding conditions, were five to ten times the current density of an equivalent arc in open air conditions. This may help to explain the fact that to maintain the same arc conditions, the current will have to be increased by 10% per atmosphere (33 ft. of water) of additional pressure (Silva, 1971).

The higher current density of underwater arcs produces higher arc temperatures. Direct measurement of the interior arc temperatures is difficult. Madatov (1966) computed the theoretical temperatures using the Stefan-Boltzman Law, realizing that the arc was not a perfect black body. Radiation occurs off the sides of the arc and the absorption coefficient was assumed to be the same as an arc burning in the air ($\alpha = .6$) then:

FIGURE 3-3

FIELD STRENGTH INTENSITY

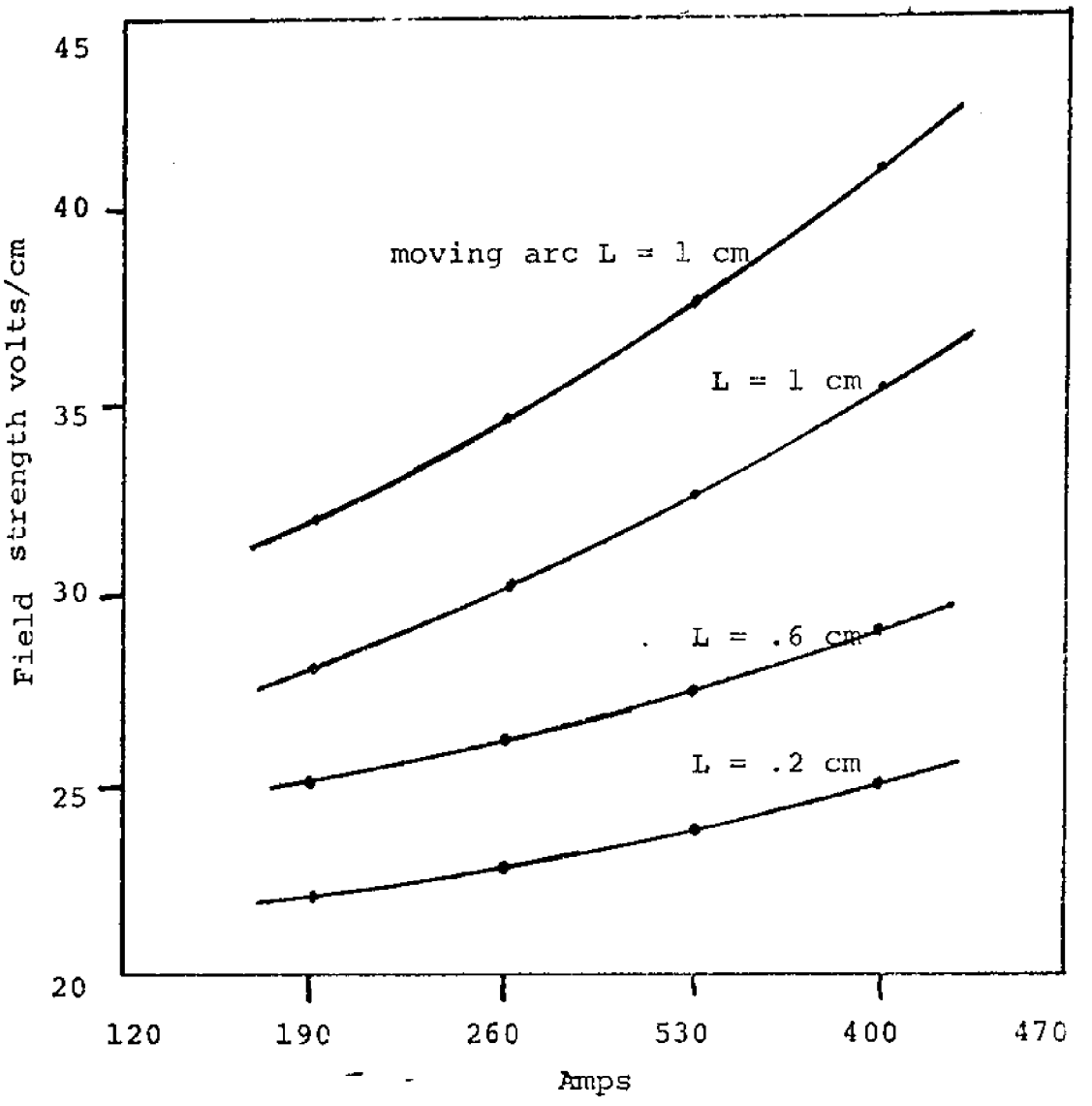

Note: Hydrostatic "lag" effect is greater with longer arc.

Reference (Avilov, 1960)

$$T^4 = \frac{E\ \ell ac}{\alpha \tau F}$$

E = radiating power of arc and arc column

ℓac = arc length

α = coefficient of absorption

τ = Stefan-Boltzman constant

This was related to a formula involving a factor that takes into consideration the welding conditions, and another factor that considers the welding depth or pressure. Then, the temperatures of the arcs for these two parameters appear in Table 3-2:

$$T = C\xi^4 \sqrt{I}$$

The ionization potential is found to be (Madatov, 1966) 12.0-12.4 volts for thin wire and 13-14 volts for stick electrodes, suggesting the case of high hydrogen content in the arc bubble atmosphere (13.6v). These levels of potential also suggest the possibility of CO_2 (14.3v), CO (14.1v) and some N_2 (14.5v).

A stability factor is defined by Madatov (1962) as the maximum current divided by the minimum current:

$$\frac{I\ max}{I\ min} = S$$

For ordinary metal-arc underwater welding with D.C., the stability factor was 1.61. For values near one, the arc is considered stable. For values >>1, the arc is considered unstable. One cause of fluctuations in the voltage and current occuring every .3 seconds or less has been attributed to the thick coating collapsing during the arc welding (Silva, 1971). Different electrodes produce different levels of stability. Silva (1971) found E7024 more stable than E6027, while E6013 was unstable due to the thin coating it has. It also appears that in salt water, the metal-arc will

become more stable due to the salt ions serving as charge carriers (Silva, 1971). This is evident in the change in sound of the arc from an erratic effervescence in freshwater to a smooth gurgling in salt water.

Finally, it is mentioned that depending on the quality of equipment used, there can be quite a current leakage in saltwater. This can have quite an effect on changing what actually happens at the arc compared to what is thought to happen, based on the power source meters. Silva (1971) found it could be as high as 65-110 amps at the open circuit voltage of 83-99 volts.

3.23 Metal Transfer

There are three basic modes of metal transfer in welding arcs. The first is globular or drop transfer, where the metal is transferred in large drops that travel slowly to the workpiece. Spray transfer is where the metal is transferred in many fine particles that travel at a higher rate. The third is short circuit transfer, where direct metal-to-metal contact and transfer occur. These modes may sometimes occur in combination, or during a welding process that mode may undergo a transformation from one to another as the welding parameters are changed.

Theoretically, in metal-arc welding, such a transition should occur with changing pressure. The metal transfer might be expected to change from the spray mode to the globular mode as the underwater welding depth increased (Silva, 1971). However, in practice, using the touch method of underwater welding with covered metal-arc electrodes, the normal metal transfer is small droplets except when an occasional large drop forms and short circuits the arc (Madatov, 1972). Silva (1971) also found that, even at shallow depths, metal-arc welding underwater involves the globular rather than the spray mode of metal transfer. The present investigation found that the frequency of the drop transfer is 80-100 drops per second.

Madatov (1972) has done some investigation of metal-arc and thin wire underwater welding metal transfer. In thin wire welding, the drop does not transfer immediately to the weld puddle, but may have a dwell time in the bubble surrounding the arc that is equal to or greater than the time taken to form the drop on the electrode. This slow drop transfer is in conjunction with occasional short circuiting. An interesting observation is that without CO_2 shielding gas, the drops formed may be hollow at the time of formation and as they drop to the weld puddle, they interact with the bubble atmosphere and become more solid, thereby decreasing in volume. Shielded metal-arc drops transferred at a rate of 44 per second. The time of formation and the time in the arc bubble atmosphere were about the same. Table 3-1 summarizes the data collected by Madatov concerning metal transfer.

The constricted arc produces a high arc core temperature in spite of the cooling effect of the hydrogen present in the bubble atmosphere. Thus, whereas the welding arc between two iron electrodes in air may have a temperature of between 5000°K and 6000°K, underwater the same arc may burn at a temperature of 7000°K and 9000°K for depths of under 10 meters (Madatov, 1970).

Table 3-2 shows the effect of welding current and welding process on the arc core temperature. This increased temperature produces fast melting rates of the metal at the weld electrode and at the weld pool which tends to produce a very large fluid puddle that would be difficult to control except that in welding underwater, the quenching property of the water seems to minimize or compensate for this effect by rapidly solidifying the weld puddle.

In general, the welding arc of an underwater welding process and the metal transfer from that underwater arc appear to be very similar to the normal air welding arc and meta-

transfer. However, once the metal begins to solidify in the weld puddle and cool down, extreme differences between air welding and underwater welding are encountered.

3.3 UNDERWATER HEAT TRANSFER AND TEMPERATURE HISTORIES

The temperature history of an underwater welded joint remains a very complex and difficult characteristic to determine or predict. The two major factors which will contribute to its determination are the nature of the heat source, which depends on the welding arc, the type of metal transfer, the welding efficiency, and the nature of the heat flow in the joint, which depends on the thermal properties of the metal, the plate thickness, the welding speed, and the quenching effect of water.

3.31 Heat Input

A measure of the theoretical heat from a welding arc is the theoretical heat per inch of weld. This can be computed as:

$$\text{Heat Input} = \frac{\text{Voltage x Current x 60}}{\text{Speed (inches/minute)}} \quad \left[\frac{\text{Joules}}{\text{inch}}\right]$$

However, due to uncontrollable heat losses from the welding arc, the actual heat that reaches the weld is some percentage of this heat input. This factor is called the welding efficiency. It is not known precisely the value of this factor in underwater welding.

Heat output of arc x efficiency = Heat input to workpiece

3.32 Heat Flow

Whatever this final heat input to the workpiece turns out to be, it will determine the amount of melting and pene-

tration of the weld bead. The second portion of the critical heat transfer process involves the heat flow away from the weld zone. This heat flow process will determine both the time that the region stays at its maximum temperature and the cooling rate from this temperature. Both these characteristics are critical in the determination of the final weld microstructure.

For surface heat sources moving at a steady rate along a homogeneous joint, there will be a quasi-steady temperature distribution set up. The isothermal or constant temperature lines represent the potential for heat flow. By measuring the temperature profiles, an approximation of the direction of heat flow (which will be perpendicular to isothermal lines) can be determined.

There is a differential equation referred to as the hea equation which completely describes this quasi-static temperature distribution surrounding a welded region. However, the boundary conditions are very complicated, and in some cases unknown, which makes an exact solution equally complex and unsoluable. For this reason, several types of approximations have been used to simplify the solutions to the heat equation. The three-dimensional heat equation may be written as:

$$\frac{\partial^2 T}{\partial x^2} + \frac{\partial^2 T}{\partial y^2} + \frac{\partial^2 T}{\partial z^2} - \frac{1}{\alpha}\frac{\partial T}{\partial t} = 0$$

where, T = temperature

α = thermal diffusivity

Approximating the welding arc as a point source and the welded joint as a continuous semi-infinite plate, the solution has been found to be:[73]

$$T = \frac{q}{2\pi kr} e^{-v(r-x)/2\alpha}$$

where, v = velocity

k = thermal conductivity

q = heat input rate

$r^2 = x^2 + y^2 + z^2$

This solution is used when very thick plates are involved. However, the underwater welding arc is a spread or diffuse heat source, and cannot be properly thought of as a surface point source. Another approximation has been to consider the arc in 2-D cases.[57] In this approximation, the plate is considered to be thin, and the source is thought to extend down throughout the thickness of the plate. The solution to this approximation is found to be in terms of Bessel functions:[57]

$$T = \frac{q'}{2\pi k} e^{-vx/2\alpha} K_o\left(\frac{vr}{2\alpha}\right)$$

$$r^2 = x^2 + y^2$$

This solution is found for ordinary arc welding in air to give reasonably good qualitative results, especially for regions outside the weld pool region. Away from the weld puddle, the arc may appear as a point or line source; however, convection currents within the liquid weld metal greatly reduces the predicted temperature gradients. And this further affects the actual temperature profile in the critical HAZ immediately adjacent to the weld puddle.

For these reasons, it seems that a semi-empirical approach to underwater arc welding ought to be employed cooperatively with a mathematical approach. Various attempts have been made at this.[14] Because the weld bead boundary

remains as a permanent record of the maximum extent of the melting temperature isotherm, some work has been directed at using the welded bead width to estimate the heat input to a weld (Lancaster, 1965). The heat input is postulated to be some function of the welding speed, width of the final weld, and the thermal diffusivity as:

$$\text{Heat input } q \approx f\,\frac{(\text{welding speed})(\text{weld width})}{(\text{thermal diffusivity})}$$

2D $\quad q/w = 8kT_m\left(\frac{1}{5} + \frac{vd}{4\alpha}\right)$ $\qquad$ (Thin plates)

3D $\quad q = \pi dkT_m\left(1 + \frac{4}{5}\,\frac{vd}{4\alpha}\right)$ $\qquad$ (Thick plates)→underwater

w = plate thickness

d = width of weld

Thus, for a given width of desired weld, you need a minimum heat input to the weld region. Once the heat has been introduced into the weld puddle, it will flow out causing different cooling curves for regions at differing distances from the fusion line. The theoretical cooling curves can be found using the same approximations of a point source or a line source to be:

For a point source: $\frac{dT}{dt} = \frac{-vT}{r}\left[\frac{x}{r} - \frac{vr}{2\alpha}\left(1 - \frac{x}{r}\right)\right]$ (thick plate)

For a line source: $\frac{dT}{dt} = \frac{-v^2T}{2\alpha}\left[\frac{x/r\ K_1(vr/2\alpha)}{K_o(vr/2\alpha)} - 1\right]$ (thin plate)

$K_1(z)$ is the modified Bessell function of the second kind of order unity

For simplicity, consider a point along the central axis of the weld at the weld pool boundary where $r = x = x_1$ and $T = T_m$, the melting temperature. Then, in the case of 3-D flow:

$$\frac{dT}{dt} = \frac{-2\pi k T_m^2}{(q/v)}$$

Figure 3-4 shows these curves for a point along the central axis at the pool boundary (where $T = T_m$). It can be seen that qualitatively, both of these approximations make sense in that they predict the cooling rate will increase with increasing travel speed or with a smaller weld pool. The approximate models can also give an estimate of the complete thermal cycle of a region. As the distance from the welding arc increases, the peak temperature is lower and it also lags behind the source in time.

The liquid region is a small area directly around the source where heat transfer takes place via a complicated complicated combination of convection, conduction, melting, and fusion. A numerical method for predicting the temperature distribution in thin plates using not a point source, but the liquid weld pool as the interior boundary condition was developed at the University of Wisconsin and adapted to underwater welding at M.I.T.[14,53,66]

Keeping track of all the energy emitted by the welding arc is a difficult problem, which has not been completely solved, even for the simplest of arcs. It now seems apparent that spread heat or a pre-heating, post-heating effect takes place even in an underwater environment. The nature of this heat distribution is yet to be solved (Brown, et al., 1972).

The increased heat losses underwater are from boiling and radiation around the weld puddle, and increased conduction through the base plate. Boiling is a complex heat transfer phenomena and is usually divided into several distinct regimes

FIGURE 3-4

THEORETICAL COOLING RATE AT THE REAR OF THE WELD POOL

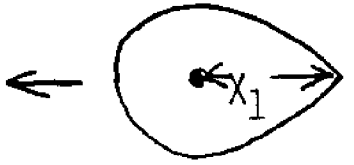

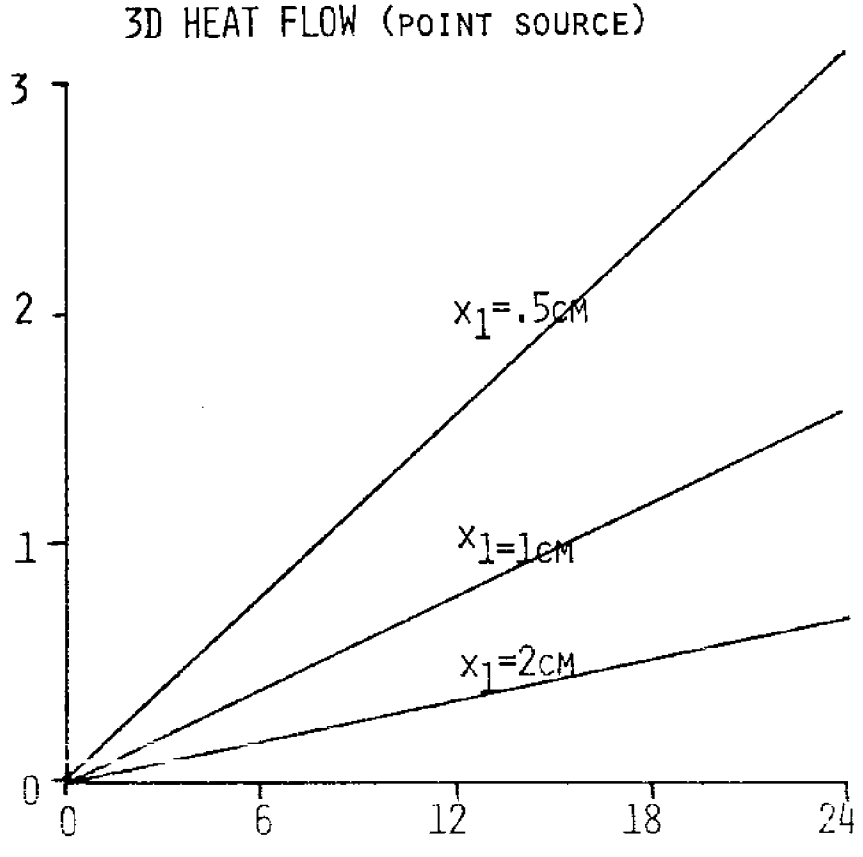

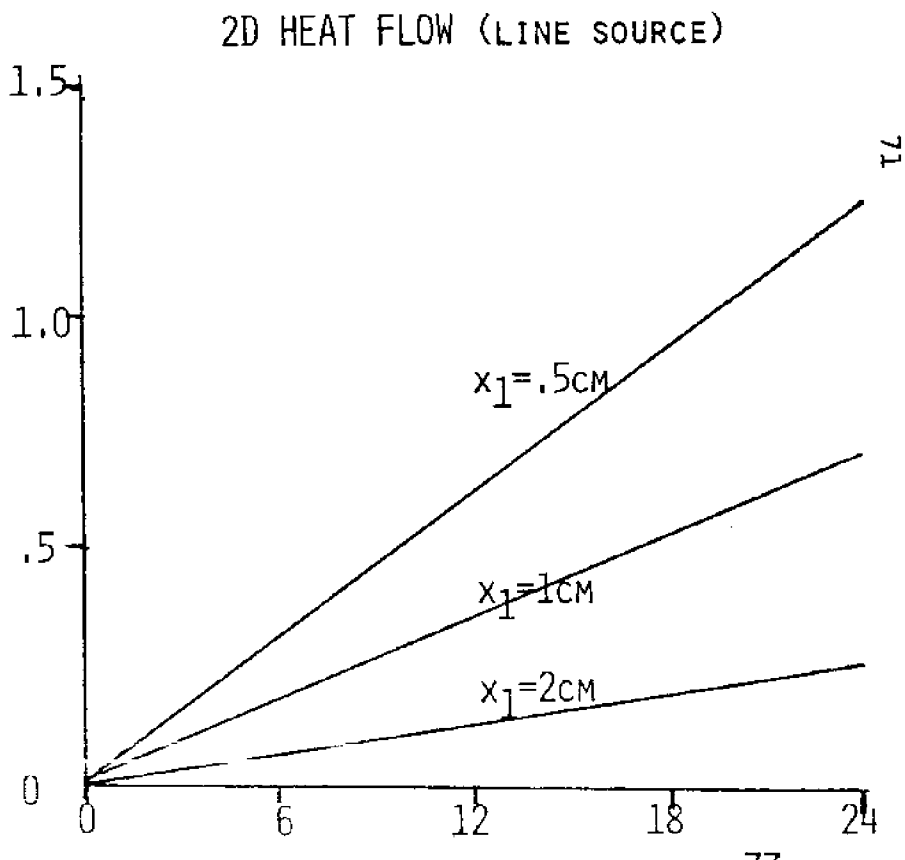

(24IN/MIN=1CM/SEC)

LANCASTER (1965)[73]

or modes, including nucleation boiling, transition boiling, and stable film boiling. But, the areas involved are so small that no one mode of boiling can be established without both interfering and being interfered with. Finally, the large perturbations resulting from the arc bubble phenomena of a continuously pulsating bubble destroys any stable film boiling mechanism on the top of the plate. The other problem with this model is that the heat transfer is three-dimensional and the bottom of the plate is undergoing significantly different heat transfer. Boiling there may well be film boiling as the bubbles are trapped against the plate, or it may simply involve increased heat conduction and convection from the plate into the water.

Based on these formal modelling approximations, several general principles are arrived at which contribute to an understanding of the role that heat transfer and cooling rates play in underwater welding metallurgy. The higher the initial heat input, the slower will be the cooling rate. Cooling rates are slower in the regions further from the weld bead. The heat input will be proportional to the current and inversely proportional to the welding speed. These various cooling rates will thus produce a weld microstructure that changes as the distance from the welded bead increases. Results of semi-empirical attempts to duplicate the temperature histories of underwater welding by Brown (1972) are shown in Figure 3-5.

3.4 EFFECTS OF PRESSURE ON UNDERWATER WELDING

A major difference of underwater welding affecting the welding process may be the increased pressure. This hydrostatic pressure causes a constriction of the arc column. In addition to this hydrostatic pressure effect, there are two other forces on an underwater arc. One is the cooling effect

FIGURE 3-5

TEMPERATURE HISTORY CURVES
(TYPICAL SHAPES)

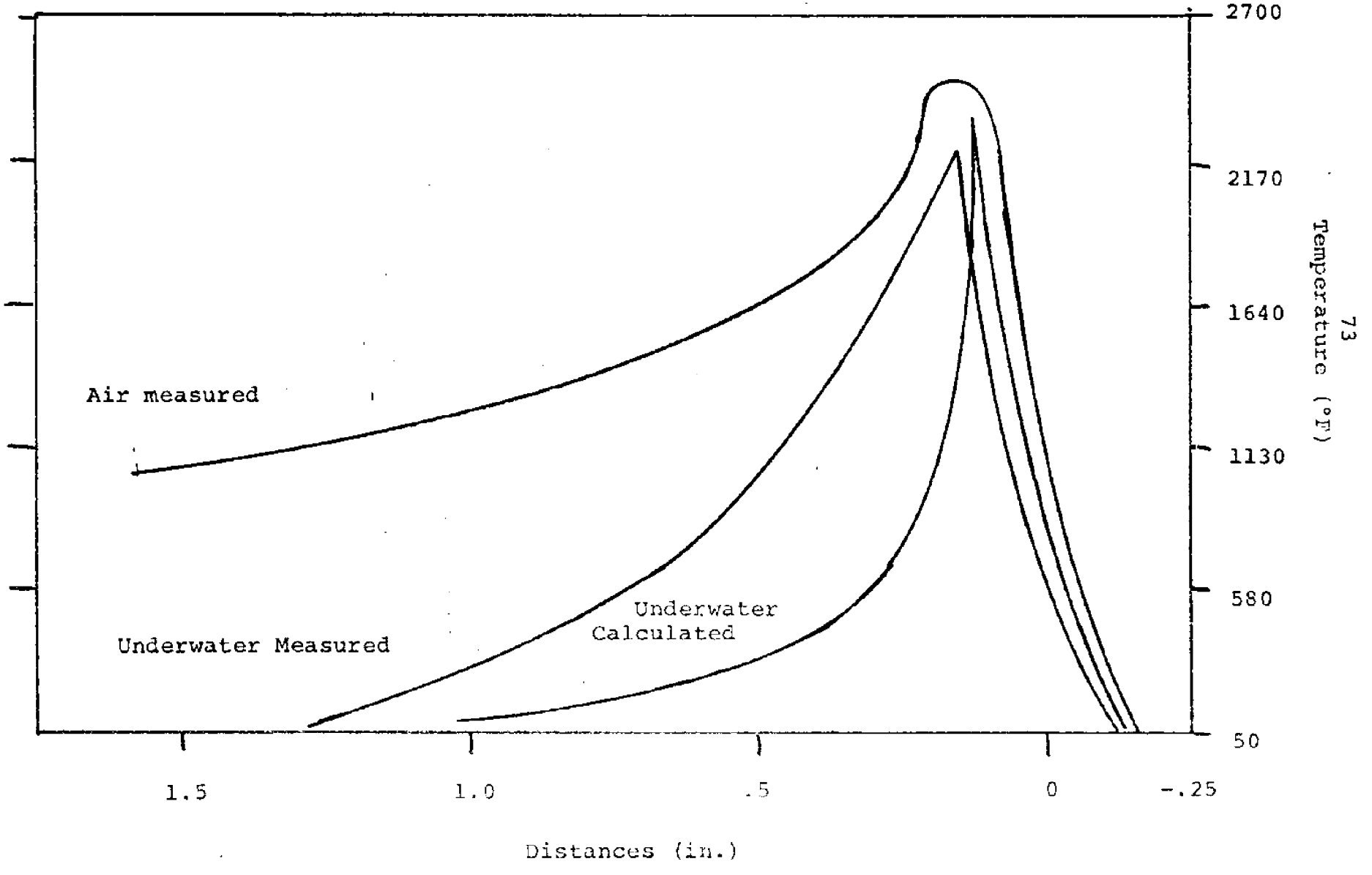

of the high hydrogen content bubble surrounding the arc which further constricts the arc. The other effect is the constriction of the cathode spot caused by the geometric shape of the electrode tip. These compression phemonema explain why the volt-amp curves for underwater welding are concave or rising.[38] The arc length is important because the larger the arc length, the more cooling by hydrogen and the more constriction by the water pressure are possible. The greater the depth, the greater also will be the water pressure effect. These pressure effects cause the current density of an underwater arc to increase with welding current. To help compensate for these factors, the welding current should be increased by 10% per atmosphere of additional pressure to maintain similar arc conditions.[5]

Madatov (1969) reported that the depth may affect the weld bead shape of underwater welds. For shielded metal-arc welds, the penetration is found to increase, and the bead also widens out to reduce the penetration shape factor, (W/P), from 5 to 3. At great depths, he found that the current was limited to 180-240 amps due to the concentration of heat (current density) from the hydrostatic pressure. Due to the increasing current density, the arc may become more steady. The power expended by the arc goes up by 40% between 1 and 2 atmospheres.

Billy (1971) investigating underwater GMA reported that high pressures may produce a reversion to large globular metal transfer resulting in very poor crowned beads. Pressure seems to nullify the advantages of GMA welding by producing an uncontrollably large weld puddle.

Pilia (1967) conducted wet welding GMA tests for Ocean Systems Inc. and Linde Division and found that welds at 60 feet were peaked and thin and that penetration was more than adequate at 80-100 feet, causing burnthrough. In shielded metal-arc welding at 600 feet, the flux peeled off and

satisfactory welds were not made. DeSaw et al. (1969) found that SMA welding at depth produced a severe porosity problem. They also report that reverse polarity welds were shallower, wider, and less porous than straight polarity welds. This apparent reversing of arc characteristics with depth was not explained.

Brandon (1970) reports that from pressurized air chamber welding tests, the voltage and travel speed may become important variables at high pressures. From other chamber type experiments, the following effects were observed and may be important in underwater welding. More direct research is needed and recommended.

(1) The necessary voltage and current needed to retain the same arc characteristics and metal transfer mode increase with depth.

(2) In order to maintain the same arc length, a higher voltage is required as the arc is squeezed and cooled by the arc bubble atmosphere.

(3) The power requirements of the welding arc increase with depth.

(4) In GMA welding, the metal transfer reverts back to globular transfer at increasing pressure unless the arc voltage and current are increased correspondingly.

(5) As the pressure increases and the heat input becomes greater, the internal core temperature is higher and this causes a greater amount of metal to be transferred in the vapor state.

(6) The current density increases with increasing pressures. The longer the arc length, the greater this pressure effect will be.

The plasma forces in the arc are the dominant forces controlling the metal transfer. These depend on the depth

or pressure and thus, the metal transfer mechanism will change with depth. When the arc column becomes constricted, it will have a high current density and a high radial pressure. Plasma will tend to flow or be squeezed toward an area of the arc with a larger cross-section and thus, a smaller current density. This will draw cold has into the arc column which will tend to further constrict the arc column. This increased flow rate will then result in deeper penetration and metal transfer rate.

A force that counteracts these squeezing forces is the thermal expansion term. As the current density increases, the temperature increases causing the arc column to expand. The other forces counteracting this increasing flow rate and metal transfer are due to a reflection of the plasma jet off the workpiece, a pressure-induced squeeze effect on the bottom of the bell-shaped arc column. At a critical pressure, the counter-balancing squeeze effect will begin to retard the plasma flow rate and eventually the metal transfer will revert back to large drop transfer rather than spray or droplet transfer.

These theoretical ideas are quite vague and more information is needed. However, as the beginning of a conceptual framework for evaluating data from underwater welding arc behavior with depth, Figure 3-6 illustrates the interrelationship of these arc plasma and pressure-induced forces.

3.5 UNDERWATER WELDING POLARITY

Direct current welding is employed for safety reasons in underwater welding situations. Silva (1971) reports that after surveying nine previous underwater welding investigators concerning the preferred polarity, seven used straight polarity (electrode negative) welding because it apparently resulted in a better bead shape, less overheating of the electrodes, more

FIGURE 3-6

SCHEMATIC DEMONSTRATION OF THE EFFECTS OF DEPTH ON THE ARC CHARACTERISTICS

A) Forces acting on the top of the arc

1. Constriction due to rise in the thermal conductivity.

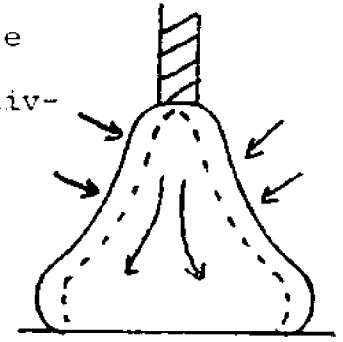

2. Constriction due to cold gases drawn past the electrode.

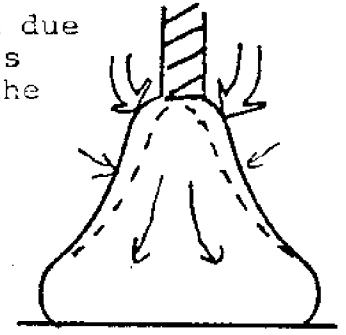

3. Expansion due to the increased temperature of the arc

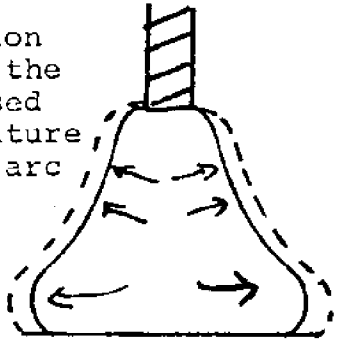

(These forces tend to accelerate metal transfer: Increased penetration)

77

B) Forces acting on the bottom of the arc

1. Constriction due to ambient pressure effects

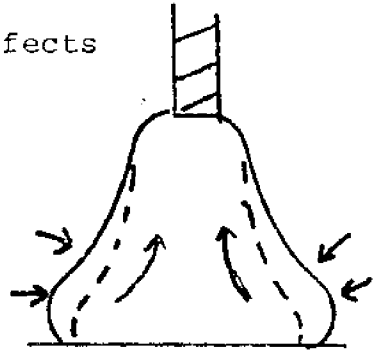

2. Turbulence and reduction of flow caused by reflection of the plasma jet

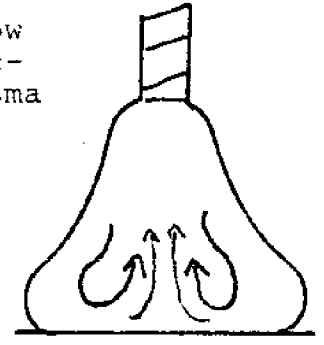

(These forces tend to resist metal transfer: Decreased penetration)

Forces (A) and (B) are in equilibrium. When (A) forces predominate, there is spray metal transfer. As forces (B) become larger, the plasma jet is decreased until drop transfer replaces spray transfer.

regular beads, less undercutting, and less spatter. However, other investigators have employed reverse polarity because this reportedly gave them easier starting and the same penetration. Welding with reverse polarity, electrode and holder positive (anode), will produce electrolytic corrosion of the welding gun. The present investigation used both polarities and distinct differences were difficult to determine.

3.51 Electrode Waterproofing

Varnish or paraffin have been the classical waterproofing agents in underwater welding stick electrodes. The purpose of the waterproofing is to keep water from penetrating the coating and changing its shielding properties as it burns. Lack of waterproofing is also reportedly the cause of increased porosity. Galerne (1969) evaluated paraffin, shellac, varnish, etc. and found that vinyl varnish worked the best. Silva (1971) reports, however, that varnish did not work well for him, blistering and causing little flaps to stall the arc. Flaps of unburned enamel similarly stalled the arc. He settled for rubbing the electrodes with a thin coating of paraffin. Others have suggested rubber cement and talcum powder, etc. It appears that a more important effect of the waterproofing coating will be to insulate the arc from the cooling water and allow the flux coating to burn off at the proper rate. Some work is being done in Holland and elsewhere on this problem of eliminating the underwater arc elongation phenomena.

3.52 Underwater Electrode Coating Turbidity

Poor visibility associated with a brown cloudy turbidity has been a major problem in practical underwater welding work. Underwater visibility is already a problem without additional turbidity from the weld itself. This has forced some welds to be made by touch, others to be made using the drag or touch method, and in more technical investigations, has motivated

investigators to use X-ray photography to view the hidden arc. This cloudiness is independent of bubble activity. A slow moving brown cloud forms at the arc and gradually spreads out through the water. In a closed test tank, the problem can be critical.

In the past, it has been thought that this cloud was a fine suspension of iron oxides. However, Silva (1971) reports that separation did not occur after using either settling tests, glass wool filter, 2-3μ pore size filter paper, sodium ion exchange columns, or centrifuges. Next, using a spectronic colorimeter, the particle size was determined to be extremely small. An iron compound was suspected as the cause of the cloud due to the nature of the welding process. The pH of the water was determined and it was found that the welding water had a pH of 7.3, slightly above the freshwater pH of 7.1. Silva (1971) has hypothesized the cause to be the formation of ferrous hydroxide, $Fe(OH)_2$, a strong base, and then the oxidization of this to hydrous ferric oxide, $Fe_2O_3 \cdot xH_2O$, which turns from a green to a reddish brown. Confirmation of this hypothesis was sought using X-ray diffraction studies, but they were inconclusive. It was determined, however, that the turbidity was not simply powdered electrode coating. The only other evidence supporting this hypothesis is the fact that adding a weak acid to a turbid sample resulted in immediate clearing of the sample.

3.6 GMA RESEARCH

An investigation of wet GMA was made at the Naval Civil Engineering Laboratory in Port Hueneme, California, in 1971 by A. F. Billy.[7,8] Travel speed was found to be the most influential variable. Increased travel speed gave a decrease in weld bead penetration, width, and size. Filler metal speed

not significantly influence the weld penetration, but increasing filler speed did increase the bead width, reinforcement, and size. All the weld beads obtained were well-shaped with width/penetration ratios varying from 2 to 3, apparently increasing with heat input. The appearance of the underwater GMA weld beads seems superior to the shielded metal-arc weld beads obtained in the present study. Some undercut was observed, but no visible porosity was present. (Argon +5% oxygen shielding gas was used). X-ray examination showed that higher filler feed rate may induce "blisters" in the weld puddle and produce internal porosity. Welds made without shielding gas were significantly more free of porosity. This result corresponds to similar conclusions from Russia.[41] Heat input is a very general parameter that averages the effect of several welding variables. But, some simple relationships were observed. Width increased dramatically from .4 to .7 inches as the heat input varied from 25 to 65 kilo-joules/inch. Penetration increased slightly from .18 to .25 inches and the reinforcement height remained constant at .15 inches. The size of the heat affected zone also increases with higher heat input.

In general, then, to obtain the optimum weld geometry, it might seem proper to use low welding currents and high travel speeds (low heat input) to produce lower W/P ratios. However, higher travel speeds seem to result in poorer appearance and soundness. Low current may also cause an unstable arc. Thus, the optimum welding variables appear to be restricted to a narrow range of values if both a stable arc and acceptable welds are to be obtained. In conclusion, the NCEL report found that:

(1) The travel speed is the most significant factor influencing all weld geometrical parameters;

(2) It is impossible to directly correlate the weld appearance with specific welding variables;

(3) Optimum weld beads can be obtained only in a narrow range of welding variables.

It is significant that the general conclusions from this study indicate the complexity of an underwater welding process. Although it may be possible to observe general trends or influences from various welding variables, it is foolish to expect simple linear correlations between welding variables such as current or welding speed and the resulting weld appearance and geometry. This is true for underwater shielded metal-arc welding as well.

3.7 CORRELATIONS BETWEEN EXPERIMENTAL WORK AND ACTUAL WELD PROPERTIES

Obtaining a sound weld in laboratory conditions is a far cry from producing acceptable underwater welds in an offshore environment considering the complexities of underwater work. Laboratory results are at best applicable only to the particular steel used at the laboratory pressure for the particular joint configurations and welding positions and parameters employed. Meloney (1973) has done some work in showing that bead-on-plate experimental techniques yield optimistic estimates of joint properties. Using mild steel 3/16" plate and E6013 - 5/32" electrodes, he showed that the properties of single pass bead-on-plate welds were higher than multipass butt welds.

Joint Type	Tensile(ksi)	%Elongation(2")	%Reduction in Area
Longitudinal Bead on Plate	62 (93% plate)	10 (40% plate)	12
Transverse Bead on Plate	62 (93% plate)	18 (74% plate)	20
Multipass Transverse Butt Weld	43 (64% plate)	7 (28% plate)	9

Even with deep penetration of 1/4" plates (up to 2/3 plate thickness), the specimen behavior during testing approaches that of the base plate rather than a butt weld joint. He found that specimens pulled longitudinally with the weld resulted in failure initiating from the region of poorest ductility, the embrittled fusion zone and weld metal. Grubbs (1971) gives joint properties for actual butt welds of mild steel using E6013 electrodes. Silva (1971) however, reports bead-on-plate results. There is real doubt as to the validity of predicting joint properties from anything less than actual joints.

Investigator	Joint Type	Tensile(ksi)	%Elongation	%Reduction in area
Grubbs (1971)	Plate	57	17	
	Butt Weld	67	7	6
	100% WM	61	8	9.5
Silva (1971)	Plate	65	32	52
	Bead on Plate	58	7	15

It is suggested that where there is interest in mechanical joint properties from underwater welding, actual underwater weld joints be made.

3.8 ACTUAL UNDERWATER WELD PROPERTIES

Ultimately, the properties of multipass underwater welded joints are the most important results coming out of welding research for use in actual industrial applications. Everything else is the proper scientific basis for explaining unsatisfactory joint properties and for modifying processes and techniques in order to obtain better weld characteristics. This section summarizes and compares the results to date of

underwater welded joints.

3.81 Underwater Weld Geometry

Madatov (1969) reports that underwater SMA welding at 200 - 300 amps with EPS-52 5mm electrodes gave a penetration of 3 - 3.5mm with a width of 12 - 14mm resulting in a W/P ratio of 3.5 - 5. He found using a GMA process with 1.2mm wire at 34 - 43 volts that the penetration was 3 - 4mm with a width of 10 - 16mm giving a W/P ratio of 2.5 - 5.

Masumoto, et al. (1971b) using a 4mm coated iron powder electrode obtained underwater welds at 150 and 180 amps. The penetration shape factors were 5 - 7. GMA welds at 120 and 210 amps gave W/P ratios of 3 - 5.5.

Hasui, et al. (1972) developed a plasma arc underwater welding process that gave reportedly excellent welds. For welding without shielding liquid underwater, the W/P ratio was 1.7 - 4.2, with shielding the ratio was 1.8 - 2.3. The plasma welding appears to give better shaped welds than either SMA or GMA processes.

Billy (1971) investigated underwater GMA welding and determined that at a voltage of 36 - 42 volts, the bead penetration was 4 - 6mm. The weld width was 10 - 17mm and the height was 2.5 - 4mm. The W/P ratio was 2.1 - 2.9, reflecting the very good penetration which was achieved.

Silva (1971) also investigated underwater SMA welding and reports penetration shape factors of 4.2 - 5.4. He claims that to maximize the underwater welds, sufficient energy was required so that the heat affected zone remained approximately the same size underwater as in air. He found that the underwater penetration did not decrease by 20 - 25% as had been previously claimed by other workers. Figure 3-7 summarizes these shape properties.

Madatov (1969) reports that for covered electrode welding,

FIGURE 3-7

UNDERWATER SHAPE PROPERTIES

INVESTIGATOR	PENETRATION	WIDTH	W/P SHAPE FACTOR	HEIGHT
MADATOV(1969) 3-3.5MM 5MM EPS-52 200-300 AMPS		12-14	3.5-5	4.5
1.2MM GMA SV-0862S	3-4	10-16	2.5-5	4
MUSUMOTO(1971B) IRON OXIDE SMA 4MM			5-7	
GMA 120-210 AMPS			3-5.5	
HASUI(1972) PLASMA ARC NO SHEILDING			1.7-4.2	
WITH SHEILDING			1.8-2.3	
BILLY(1971) 4-6 GMA 36-42 VOLTS		10-17	2.1-2.9	2.5-4
SILVA(1971) SMA 5/32" E7024 E6027 E6013			4.2-5.4	

as the current is increased, the width of the weld increases but the penetration becomes more shallow, resulting in a shape factor that approaches 5. This is not generally the case in open air welding where an increase in the welding current will result in increased penetration. Thin wire welding produces slightly deeper penetration, but the trend is the same. In this case, using reverse polarity will give better penetration. There is an optimum voltage after which penetration does not increase.

There are several extraneous factors which influence the weld shape. As salinity is increased from 0 to 41%, there is an increasing penetration and a slight width increase resulting in a shape factor change from 3.5 to 1.8. Thus, salinity has a favorable influence.

Welding cable length increase results in higher resistance with a corresponding voltage and current drop. This results in reduced penetration and width and tends to produce a "humped" bead shape. As the pressure increases, the bead penetration and width increase, but together they result in a reduced shape factor. The welding nozzle angle has an effect on the bead shape. As the angle changes from a leading to a trailing angle, the bead becomes narrower and taller with decreased penetration. It is reported that thin wire welds in the vertical position produce a concave "countersunk" shape that has very good penetration. The lead angle may affect the weld undercutting. A larger lead angle may give increased "post heating" to the weld puddle and increase the flow back into the sides of the weld crater.

3.82 Underwater Weld Microstructure

The microstructure of underwater welds can be summarized and compared in microhardness profiles. These profiles typify the degree of hardening that results in the HAZ and the extent of the hardened region.

Hasui, et al. (1972) reports that for single pass welds, the hardened zone approaches 400 VHN (200g) for a short "spiked" region of 1 - 2mm. The very hardened zone is less than .5mm in width. Multipass welding (a second pass on the opposite side of the plate) decreases the original hardened zone to a maximum hardness of 300 VHN (200g). Figure 3-8 illustrates these results. The total HAZ extended for a total of 4 - 5mm from the fusion line.

Masumoto, et al. (1971) report similar data. With a 4mm iron powder electrode at 180 amps, they report a maximum hardness of 300 Hv (1 kg) extending for less that 1mm and a partially hardened weld bead and an HAZ that extends for 4mm. GMA welds at 120 amps produced a similar hardened spike with a total HAZ width of 6mm. Figure 3-9 shows these results.

Silva (1971) also reports microhardness surveys of underwater welds. The hardened spikes that he reports are in the vicinity of 400 - 450 VHN for E7024, E6027, and E6013 - 5/32" electrodes. The width of these hardened zones was .2 -.6mm. These profiles are shown in Figure 3-10. These results show that the hardening region of an underwater weld is very limited and occurs immediately adjacent to the weld fusion line.

The one area of microstructure that is being increasingly investigated is the problem of hydrogen in the weld. Martensite together with hydrogen are associated with underbead cracking. The hydrogen dissociated from water in the bubble atmosphere diffuses into the weld puddle. Rapid quenching prevents its being able to escape. Thus, it becomes trapped in the recrystalizing metal. When it is trapped in the highly stresses martensite regions, the small hydrogen bubbles coalesce into cracks. This can be critical. This sort of an embrittlement process is dependent on the history of the metal, the amount of hydrogen, the type of material, service loading, thermal cycle, etc. Underbead cracking is not the only phenomena associated with hydrogen content. Flakes on the fracture surface,

FIGURE 3-8

HARDNESS DISTRIBUTION IN SINGLE PASS AND DOUBLE PASS METHODS

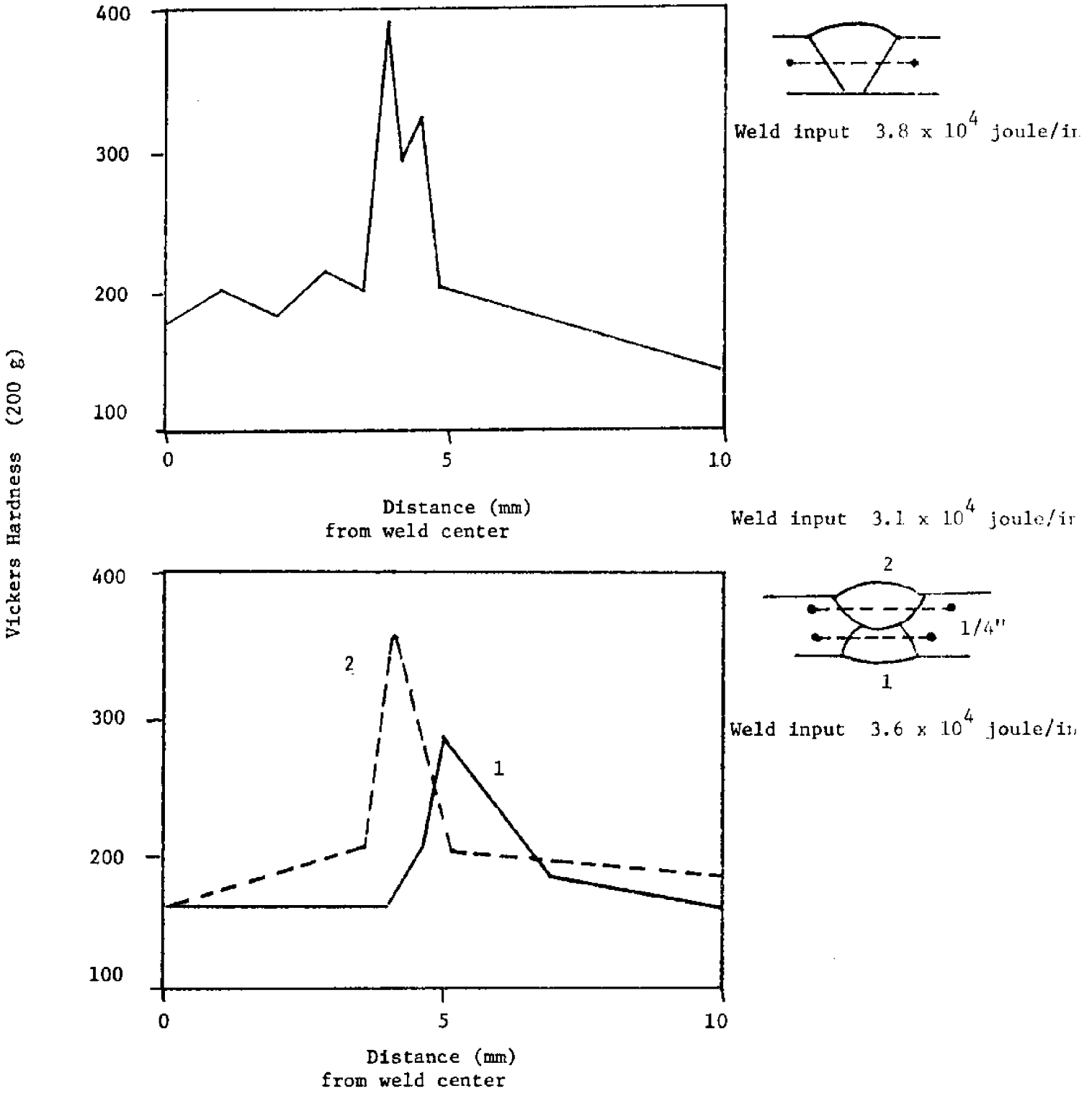

(Hasui, et al., 1972)

FIGURE 3-9

UNDERWATER MICROHARDNESS SURVEYS

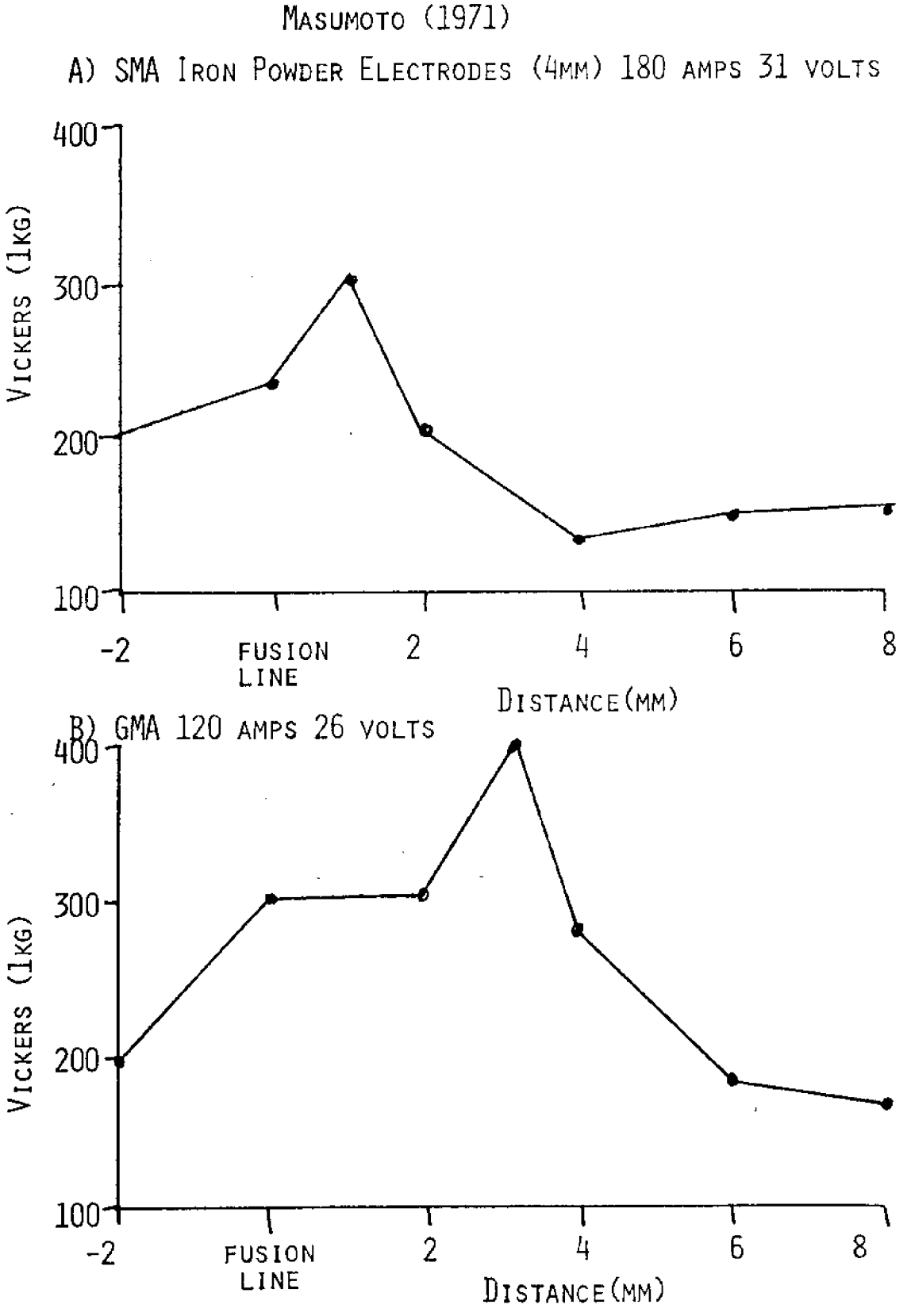

FIGURE 3-10

UNDERWATER MICROHARDNESS SURVEYS

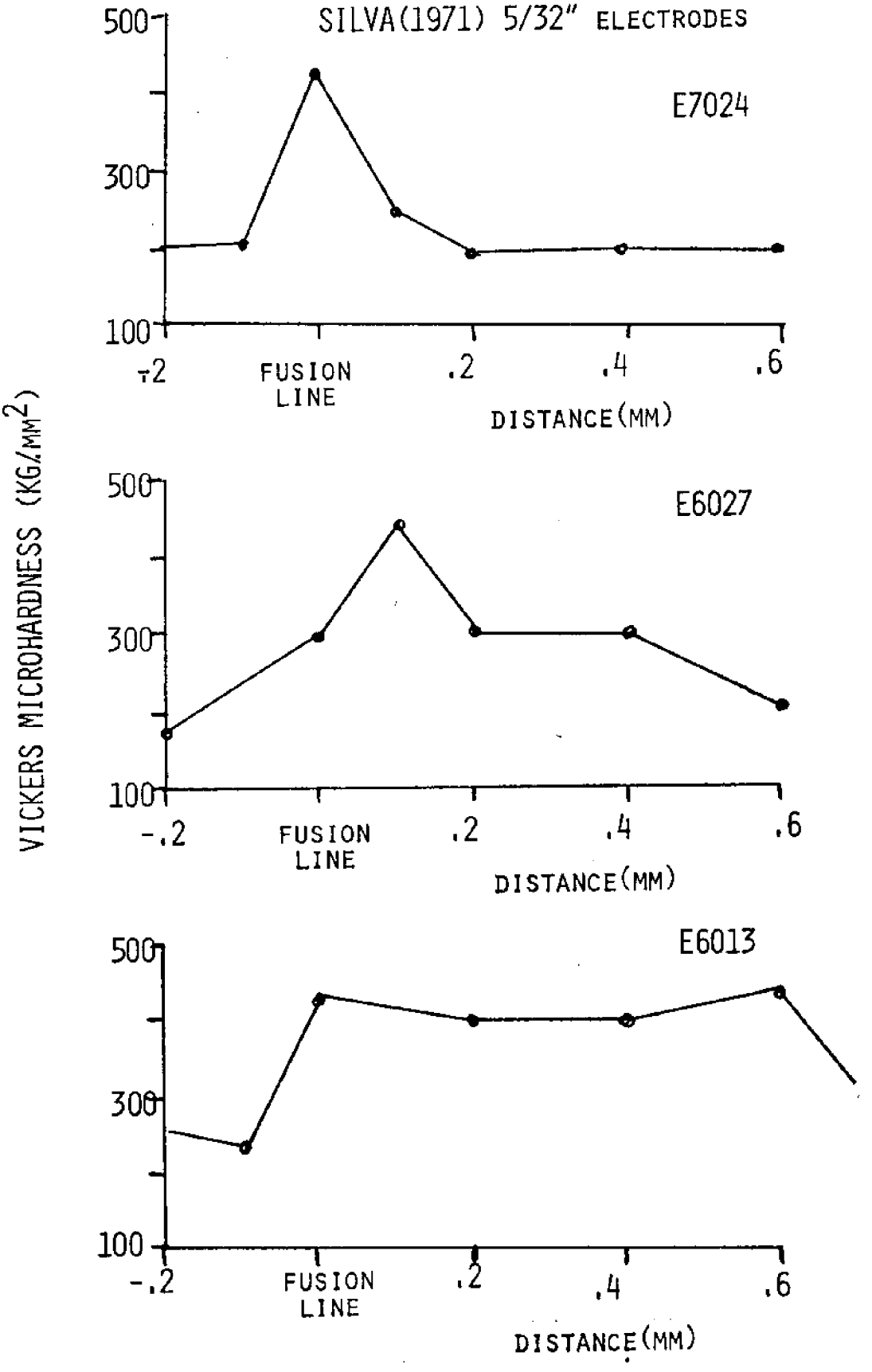

fisheyes (bright spots with cracks at the center), and delayed cracking are also attributed to hydrogen. There seems to be no simple correlation between hydrogen content and mechanical properties of the weld. Degradation of weld has been observed with less than a 3ppm hydrogen content (Silva, 1971). Generally, weld metals may contain from 1 to 50 ppm. Using neutron radiography, Silva (1971) found 3 to 4 times the hydrogen content in underwater welds as was reported in the literature. Insufficient data prevents any conclusive explanation of the effects of hydrogen in the weld metal microstructure.

3.83 Underwater Weld Mechanical Properties

Historically, it is reported that an underwater weld will result in only 80% of the tensile strength and 50% of the ductility of a similar weld made in air. This is not very encouraging. This has been slightly improved by using iron powder electrodes, thin wire welding, multipass techniques, and plasma arc welding, as well as shrouds and other protective or shielding devices or process modifications.

Standard Charpy impact testing was done by Silva (1971) on covered arc underwater and open air welds. For electrodes E7024 and E6024, the impact tests at 0°C (a good test for ocean specimens) showed 75% and 60% of an open air weld notch toughness. However, the E6027 showed less variation and is recommended as being more reliable than E7024.

Ductility in underwater welding is better using covered arc iron powder electrodes than when using a thin wire semi-automatic process. However, it is nowhere near open air quality as shown by Silva (1971), reporting only 20% ductility for covered arc welds.

Hasui, et al. (1972) reports that underwater plasma arc metallurgical tests showed that all weld metal had a joint efficiency of 100%. Ductility was much increased for water glass shielding as evidenced by the doubling of the crack

initiation angle. Two pass welding in both the unshielded and the water glass shielded processes increased the crack initiation angle by 50 - 60%. Single pass water glass shielded welds had 80% of the base metal notch toughness based on the Charpy impact test at 15°C. Double-pass shielded welds had 100% of the base metal notch toughness. Unshielded single-pass welds had only 40% notch toughness, while the double-pass welds were about the same. Here it appears that while the tempering effect of the second pass bead on the first has a positive effect, the main factor preserving a good notch toughness is the slower cooling rate initiated by the water glass shielding.

Meloney (1973) found for both mild steel and for HY-80 that the strength and especially the ductility of welded joints were reduced when welded underwater. Tables 3-3 and 3-5 summarize the data from several reports which investigated the strength, ductility, and toughness of underwater welds. These tables give an idea of the type of welds possible in underwater welding situations.

FIGURE 3-11

WELD METAL DUCTILITY
(NOTCH TOUGHNESS)

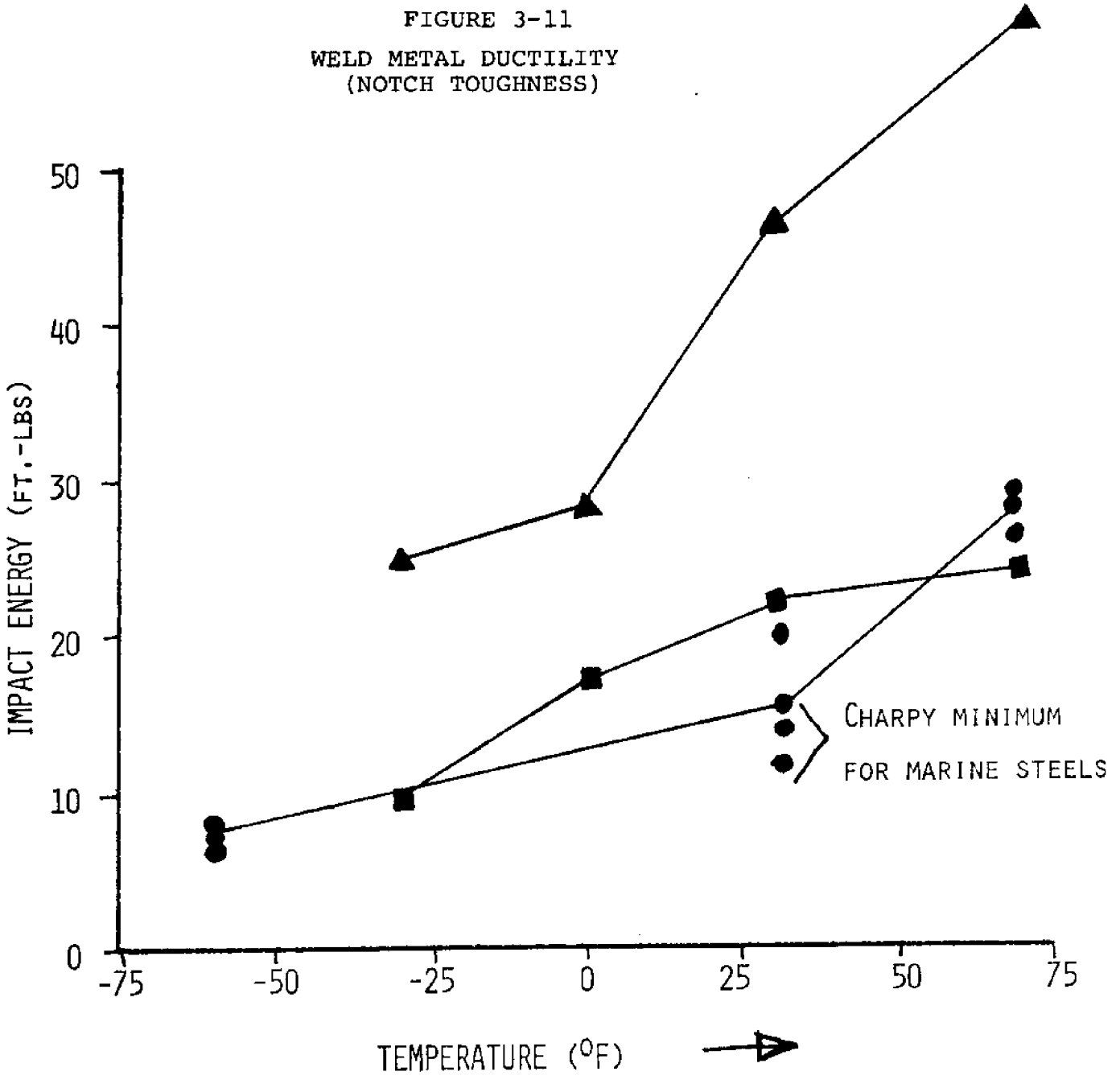

▲ AIR, MULTIPASS E6013 5/32" (GRUBBS,1971)

■ UNDERWATER, MULTIPASS E6013 5/32" (GRUBBS,1971)

● UNDERWATER, MULTIPASS E6013 5/32" (MELONEY,1973)

TABLE 3-3

MECHANICAL PROPERTIES OF UNDERWATER WELDS

SOURCE	JOINT	UTS	YIELD	ELONGATION (2 inches)	% REDUCTION IN AREA	CRACK INITIATION ANGLE
Grubbs	Multipass stick	60-67	52-57	7-8%	6-10	
Hasui	Doublepass plasma arc	50-60 kg/mm^2	45-48 kg/mm^2	23-24%		45-80
Levin and Kirkley	stick	46	42			50
	GMA (flux cored wire)	45	35			145
	Air (stick)	57	49			180
Silva	stick					
	E7024	60	48	9%	16	
	E6027	66	52	10%	13	
	E6013	57	48	7%	15	
	shroud					
	E7024	60-70	50	10-16%	17-27	
	E6027	70	70	11%	22	
	Air stick	65-70	45-50	30%	40-45	
Madatov	Iron Powder stick		38-50			70-90

TABLE 3-4

RESULTS OF SINGLE PASS AND DOUBLE PASS UNDERWATER WELDING
PLASMA ARC WELDING PROCESS

	C	Si	Mn	P	S
Plate Composition	.17	.021	.89.	.009	.022

Plate thickness: 6mm ∿ 1/4"

SAMPLE SPECIFICATIONS	% ELONGATION	CRACK INITIATION ANGLE (°)	CHARPY IMPACT VALUE AT 15°C (ft - lb)	HARDNESS VALUES (VICKERS 200 g) MAXIMUM
#1 Shielded Single Pass	22.6	46.8	32 - 44	330
#2 Shielded Double Pass	25.1	78.4	44 - 63	180 (1st), 310 (2nd)
#3 Single Pass	22.9	26.8	18 - 23	390
#4 Double Pass	24.5	52.5	15 - 18	280 (1st), 350 (2nd)
Weld Metal			49 - 52	

(Hasui, et al., 1972)

TABLE 3-5

CHICAGO BRIDGE AND IRON HARDNESS RESULTS OF UNDERWATER WELDS (1972)

		HK(30KG) BASE METAL	HAZ	WELD METAL
1) A36 3/4" Double-V joint	1st	120-130	180-380	200-210
Overhead, Lincoln E6013	2nd	130	200-320	180-200
2) A36 3/4" Double-V joint	1st	120-130	240-400	120-160
Horizontal, Lincoln E6013	2nd	130	180-390	130-180
3) A36 3/4" Double-V joint	1st	120-130	250-410	150-170
Vertical, Lincoln E6013	2nd	130	240-410	180-190
4) A36 3/4" Double-V joint	1st	130-150	190-250	160-170
Overhead, Lincoln E6013	2nd	130-150	210-400	170-180

BLANK

PART FOUR

HEAT TRANSFER AND BUBBLE DYNAMICS

Contents

4.0 INTRODUCTION

This section of the report summarizes the experimental investigations of underwater welding bubble phenomena and heat transfer. Based on the investigations of the arc bubble dynamics and experimental determination of the size of the weld metal puddle, a computer model of the heat transfer process occurring in underwater welding was prepared and tested against actual thermocouple data. Ideally, a three-dimensional transient model is desired. However, the model developed for this study was a quasi-static, two-dimensional model of the plate surface. Results of correlations between theoretical model predictions and actual thermocouple measurements were fairly good, but not completely satisfactory. Based on these results, a new approach to modelling involving a two-dimensional model of a longitudinal cross section of a welded joint is recommended and discussed. The section develops in this way:

(1) The underwater arc bubble dynamics determined by experimentation.

(2) The development of the 2-D surface computer model incorporating the bubble phenomena and surface heat losses to boiling and convection.

(3) The experimental procedures used in determining the weld puddle boundaries and in measuring the temperature histories with thermocouples.

(4) Recommendations and discussion involving an alternate modelling scheme involving the plate thickness.

4.1 NOMENCLATURE

a	film thickness
A	contact area (cm^2)
b	bubble growth rate
c_p	specific heat (Btu/lbm. °F)
E	machine voltage (volts)
e	emissivity (Btu/hr-ft^2)
G	volume flow rate (cc/sec)
H_m	total heat content
h	bubble height (cm); enthalpy
I	machine current (amps)
K_o, K_1	Bessel functions
L	plate thickness (ft)
$\dot{m}$	mass flow rate (lbm/hr)
N	lumped welding parameter
p, B, a, b	pool correlation parameters
$\dot{Q}$	energy input frim machine (Btu/hr.)
P	pressure
$\dot{q}$	heat transfer rate (Btu/ft^2-hr)
R	bubble radius (cm.)
R_o	residual volume radius (cm.)
$\bar{R}$	universal gas constant
S	finite difference grid spacing
T	plate temperature
T_o	ambient temperature
T_{sat}	water saturation temperature
T_M	plate melting temperature
T_{sub}	subcooled temperature
t	time (sec)
V	welding speed

w	time independent x coordinate
x	distance in direction parallel to weld bead
X_o	characteristic length (ft)
X_{max}, Y_{max}	maximum length and width of weld pool
w_i	volume source term (Btu/ft^3-hr)
α	thermal diffusivity (ft^2/hr)
λ	average reciprocal diffusivity (hr/ft^2); wavelength
κ	thermal conductivity (Btu/hr.ft.°F)
ρ	density (lbm/ft^3)
τ	bubble period (sec.)
σ	surface tension (lbf/ft)
σ	Stefan-Boltzmann constant (Btu/ft^{2}hr°R^4)
η	deflection of film interface (cm); welding efficiency
*	indicates non-dimensionalized variable
$\overline{\text{bar}}$	indicates average

4.2 THE UNDERWATER ARC BUBBLE DYNAMICS

During underwater SMA welding of gaseous bubble is continuously growing and departing from the tip of the electrode. A high speed motion picture study of this bubble mechanism was conducted. Experiments using E6013 and E7014 electrodes may be summed up as follows:

(1) There appears to be a gas and plasma void immediately around the arc column which is relatively stable. The arc energy is so intense here that any water in this region is immediately vaporized.

(2) Within this void hydrogen gas, steam, and various organic by-products are produced, causing a dynamic bubble to grow from it.

(3) This bubble grows and rises continuously until its radius becomes tangent to the initial void, at which time the bubble breaks away and a new bubble begins to form.

(4) It has been observed here and by Silva and Madatov (4 and 5) that varying the welding parameters (current, voltage, speed, polarity) for a given liquid environment, electrode, and depth has little effect on gas flow rate and bubble dynamics. It should be noted that the electrode coating and the salinity of the environment will affect the production of organic by-products and thereby the gas flow rate.

(5) The flow rate predicted by collection (after the gases have filtered through the liquid) does not take into consideration the steam generated at the arc. Although the steam does eventually condense, leaving only hydrogen and organic by-products, it is very active during the rapid bubble growth process and augments the apparent flow rate. By considering bubble volumes and frequencies, volume flow rates in the order of 100cc/sec. were observed

rather than the 50-60cc/sec. rate determined by collection.

(6) The shape of the bubble, especially late in its growth, may be assumed spherical.

4.3 HIGH SPEED CINEMATOGRAPHY -- EXPERIMENTATION

In order to determine the arc bubble mechanism, it was necessary to observe it closely and to slow its action down. This was done using high speed cinematography.

The method and setup is shown schematically in Figure 4-1. By welding along a line parallel to the direction of the lens it was possible to keep the camera stationary while moving the arc within its line of sight. The problems remaining to be solved were those of focus, film type, camera type, and exposure.

The first SMA run used Kodachrome II film. These pictures showed an exceedingly bright red fireball which obscured everything. The blue-green filter used in the second run did little to lessen this problem. Ektachrome film eliminated the red glare enough to tell that the subject was out of focus and too bright. Increasing the speed in run 4 improved the exposure, but did little for the focus. Up to this time, focussing was done through the lens. The depth of field was not sufficient using the 50mm lens, so a 75mm lens was tried. Finally, the subject-to-camera distance was simply measured and set on the lens. This at last resulted in a satisfactory run (Ektachrome film, HiCam camera, f2.8, 750 fps, no filter 6 ft. distance). All remaining SMA runs were made using the same settings.

Filming the shroud required only that annew exposure be found and focus be maintained. Run 4 for the shroud proved satisfactory and required one f-stop more than the SMA run.

The film results for each process provided extremely valuable information, and this method is highly recommended for any

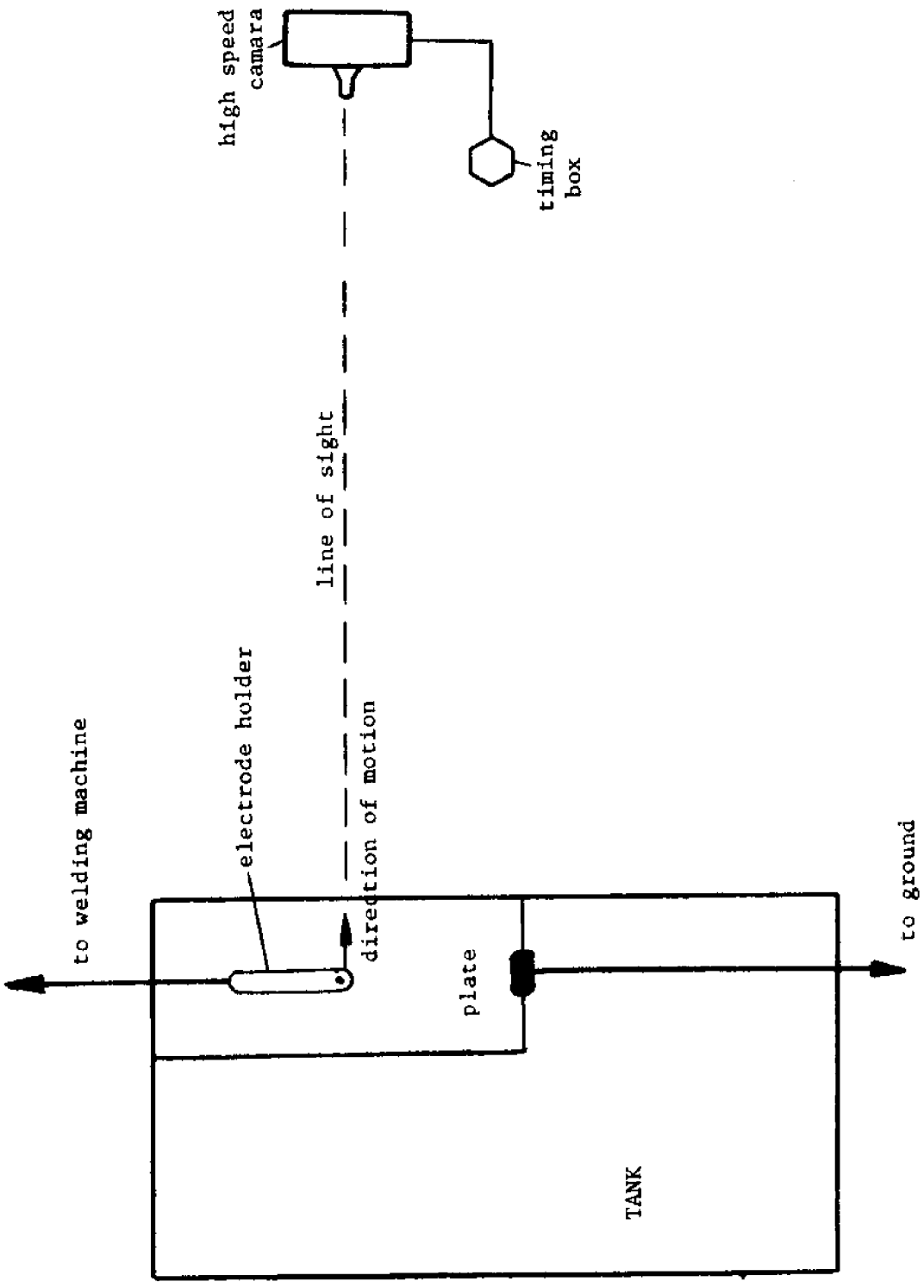

FIGURE 4-1
PHOTOGRAPHIC SETUP

future research.

4.4 ARC BUBBLE DYNAMICS MODEL

A general model is necessary to predict bubble phenomena for various electrodes and also satisfy the above observations. Davidson's (1960) model with bubble formation from an orifice was observed to have much in common with underwater welding bubble growth.

Large flow rates made it possible to neglect surface tension, leaving only the balance of buoyant and inertial forces to control the process. It was further assumed that growth begins at a point on or just above the plate and that the gas behaves ideally. The volume at any time may then be represented in terms of mass and volume flow rates:

$$\nabla = Gt = \frac{wRT}{P} \quad cm^3$$

where: ∇ = volume; G = volume flow rate; t = time; p = pressure; R = bubble radius; w = time independent x-coordinate

The apparent mass of a sphere moving perpendicular to a wall is derived in Milne-Thompson (ref. 28):

$$m = m_V + \frac{11}{16} m_L \simeq \frac{11}{16} m_L = \frac{11}{16} \rho_L \nabla$$

Equating the inertial forces to the buoyant forces yields:

$$\rho_L \nabla g = \frac{d}{dt} \left(\frac{11}{16} \rho_L \nabla \frac{dh}{dt}\right)$$

or:

$$Gtg = \frac{11}{16} \frac{d}{dt} \left(Gt \frac{dh}{dt}\right)$$

The solution of this equation yields:

$$h = \frac{8}{22} gt^2 \text{ cm} \qquad h = \text{bubble height}$$

The idealized bubble growth mechanism is shown in Figure 4-2. Break-away occurs when the bubble is tangent to the void or when its height equals its radius plus the redius of the void. Critical height, radius, and departure time may be determined graphically by plotting height and bubble radius plus void radius on the same graph and finding their intersection:

$$R = (\frac{3}{4\pi} Gt)^{1/3} \text{ cm}$$

$$h_{max} = R_{max} + R_o$$

This was done for the E6013 electrode (flow rate of 100cc/sec.) and for the E7014 electrode (flow rate of 125cc/sec.). Results are shown in Tables 4-1 and 4-2.

It can be assumed that the mass flow rate is constant for these processes and that the volume flow rate would change with pressure. Substituting new volume flow rates into the above expressions would determine bubble sizes at various depths. Unfortunately, the lack of equipment made the testing of pressure effects beyond the scope of this report.

Given this model for bubble growth, the actual contact radius and area must be determined, as they are critical to the plate heat transfer. It can be assumed that the maximum contact radius determines the region in which boiling is prevented as hot gases from the arc are periodically sweeping this entire area. Plots of contact radius vs. time are shown in Figures 4-3 and 4-4.

$$R_{contact} = (R^2 - h^2)^{1/2} \text{ cm}$$

FIGURE 4-2
IDEALIZED BUBBLE GROWTH

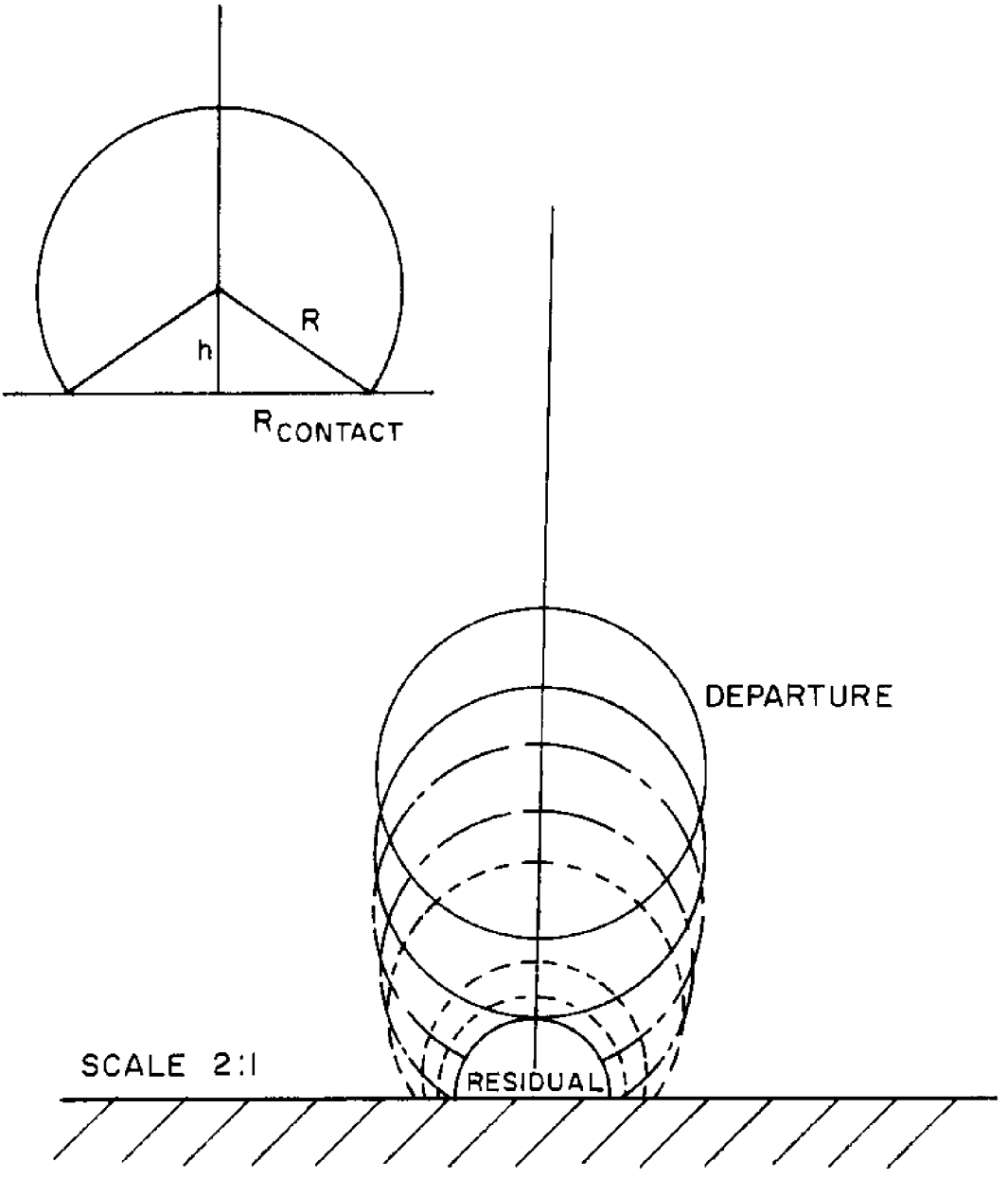

TABLE 4-1

BUBBLE GROWTH CHARACTERISTICS

(E6013)

MEASURED		CALCULATED
.075 Sec.	Period	.068 Sec.
13 Bubbles/sec.	Freq.	15 Bubbles/sec.
.5 cm.	R_o	.5 cm.
100 cc/sec	G	100 cc/sec
1.30 cm.	R_{MAX}	1.18 cm.
1.81 cm.	H_{MAX}	1.68 cm.

TABLE 4-2

BUBBLE GROWTH CHARACTERISTICS

(E7014)

MEASURED		CALCULATED
.076 Sec.	Period	.071 sec.
13 Bubbles/sec.	Freq.	14 Bubbles/sec.
.5 cm.	R_o	.5 cm.
125 cc/sec	G	125 cc/sec
1.35 cm.	R_{MAX}	1.28 cm.
1.83 cm.	H_{MAX}	1.78 cm.

FIGURE 4-3

CONTACT RADIUS VS. TIME FOR E6013 ELECTRODES

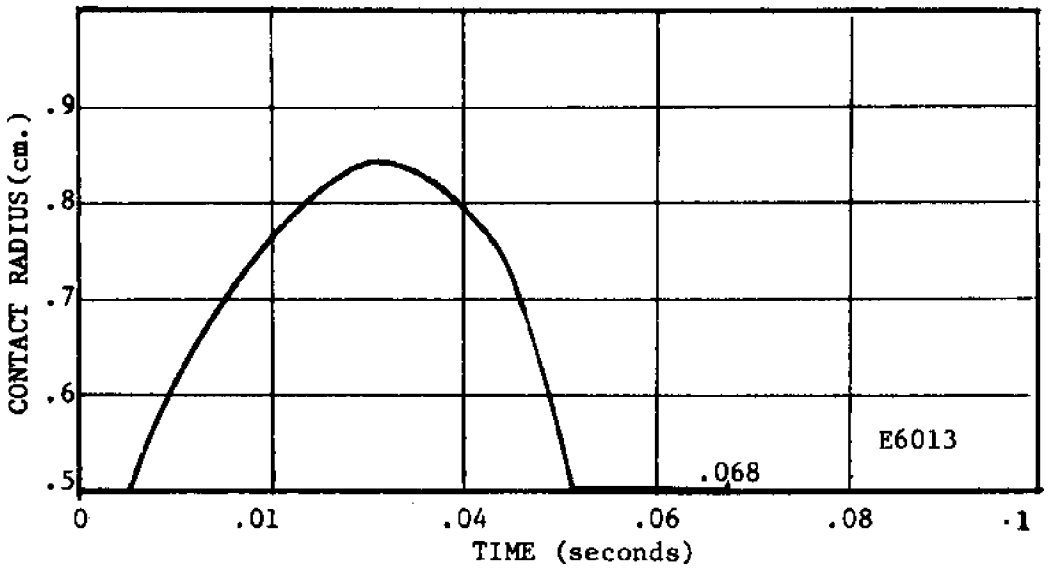

FIGURE 4-4

CONTACT RADIUS VS. TIME FOR E7014 ELECTRODES

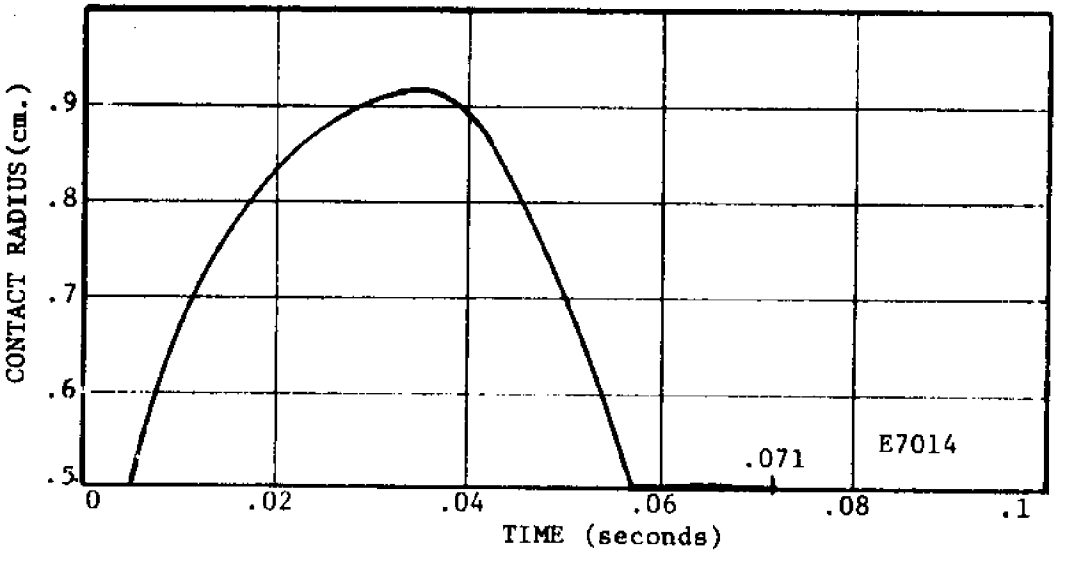

FIGURE 4-5
SHROUD OPERATION

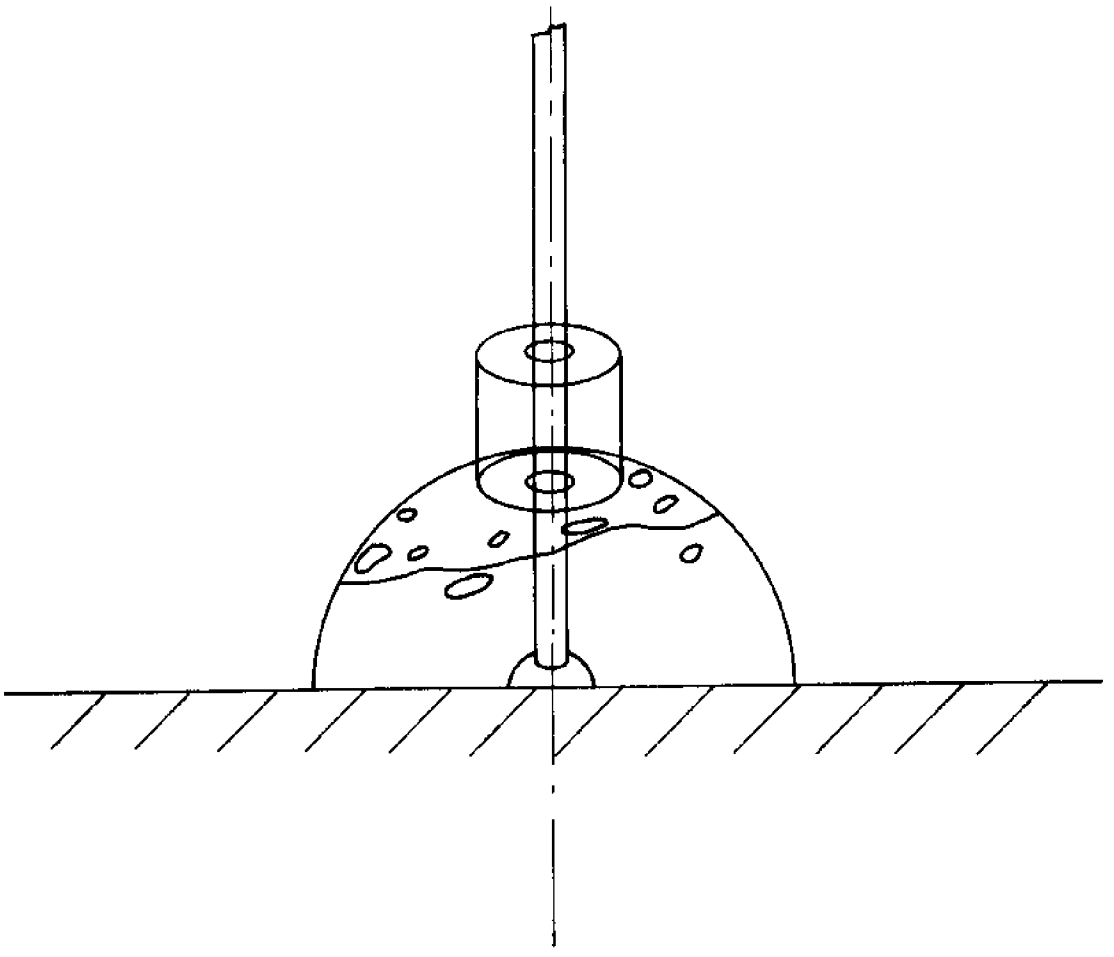

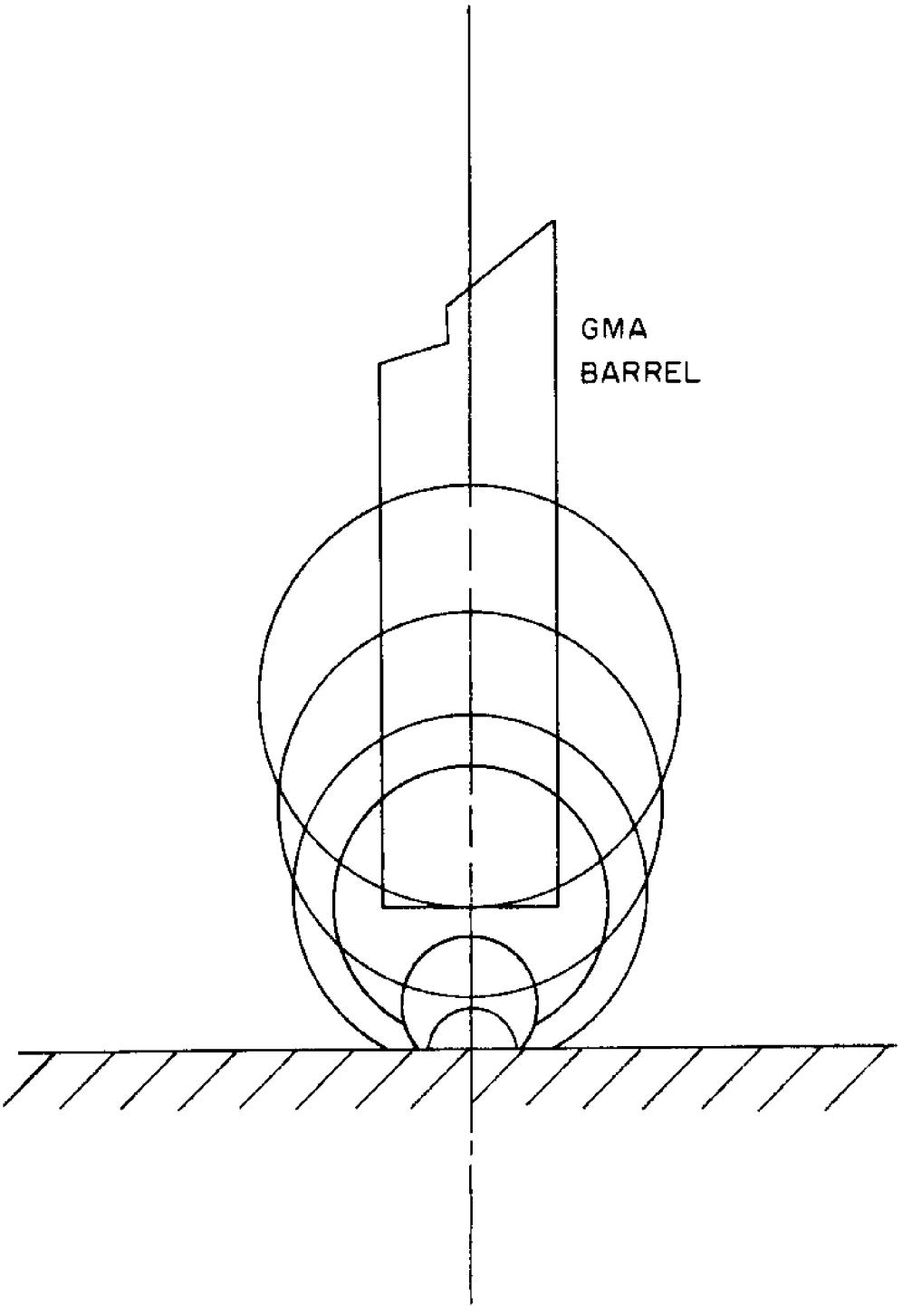

FIGURE 4-6
GMA BUBBLE DYNAMICS

The values chosen for the critical radii were .35 inch (E7014) and .32 inch (E6013).

4.41 The Shroud Model

Using high speed photography, it was immediately noticed that the acrylic shroud was not serving its purpose. The gas being produced by the arc was not sufficient to fill the shroud even with the gas escape port blocked (Figure 4-5). The failure of this shroud was attributed to its slightly larger size over that of Silva's. As this project does not encompass the development of a shroud, experiments with it were abandoned, but a vital lesson was learned. The value of this device would certainly be enhanced by an external gas source.

If the shroud were made to function properly, heat transfer within its radius would be reduced to radiation. This could be modelled by simply setting the critical radius mentioned earlier equal to the shroud radius.

4.42 Gas Metal-Arc

The gas metal arc process demonstrated a combination of bubble growth phenomena. It had been expected that the gas would impinge on the plate, creating some sort of gaseous shield, but instead the gas generated a second bubble phenomena (see Figure 4-6).

Growing from the large orifice at a volume flow rate of 50 ft^3/hr. (570cc/sec), this bubble merges with the normal arc bubble growing below. Due to the lack of organic materials aroung the GMA wire, the gas flow rate of its arc bubble was only 75cc/sec. The period predicted for both bubbles was was fairly accurate, but as the two volumes mixed and interacted, they were difficult to measure and varied significantly from ideal. The fact that the gas orifice was maintained at 1.5mm above the plate prevented the orifice bubble from intersecting the plate. Thus, all shielding came from the arc bubble. The contact radius for this bubble is plotted

in Figure 4-7. A critical radius of .27 in. (.7cm.) was chosen. The other bubble growth characteristics are summarized in Table 4-3.

Effective use of GMA underwater necessitates effective use of its shielding gas. This was not obtained in the above application. Future processes must use this gas in a more efficient manner.

5.0 INTRODUCTION TO MODELLING UNDERWATER WELDING HEAT TRANSFER

After transients have settled out, the moving arc is surrounded by a quasi-static tempera ure distribution which produces a corresponding quasi-static solid and liquid region in the plate (Figure 5-1). The liquid region is a small area directly around the source where heat transfer takes place via a complicated combination of convection, conduction, melting, and fusion. Recent work in the University of Wisconsin (Pavelec, 1968) introduced a finite difference numerical procedure for determining the temperature distribution in thin plates welded on the surface. This work has been modified at M.I.T. for use with underwater welding. The advantage of this method is that it uses the location of the melting isotherm as a boundary condition, thus overcoming problems encountered with the point source method.

To investigate the heat transfer mechanisms during underwater welding, a mathematical model has been used to simulate three proposed processes:

(1) The shielded metal-arc process (SMA)
(2) The shroud technique (Gas Trapping)
(3) The gas metal-arc process (GMA)

An empirical study on temperature distributions during underwater welding for each of these three processes has been

FIGURE 4-7

CONTACT RADIUS VS. TIME

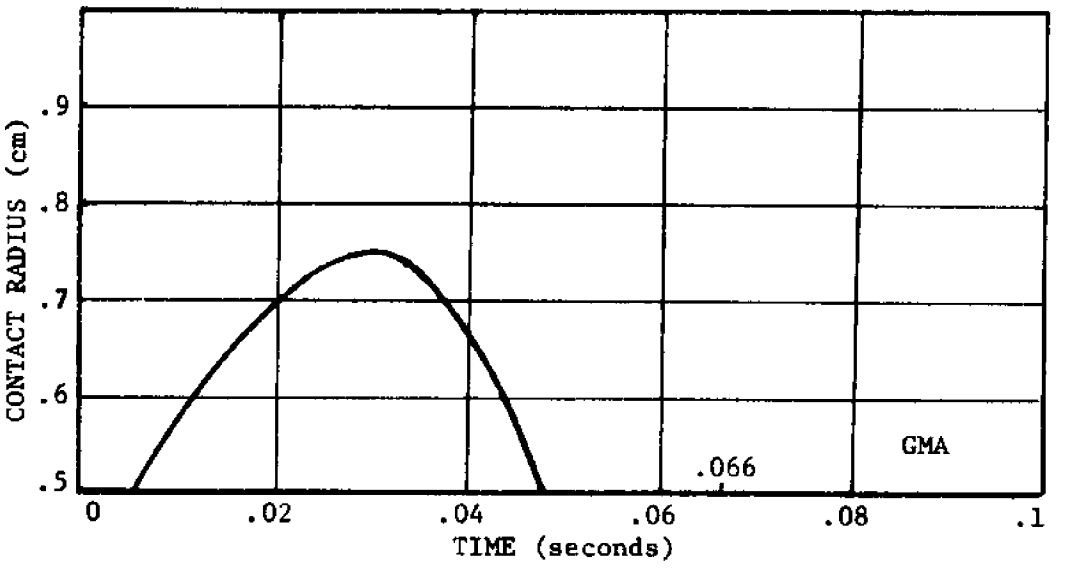

TABLE 4-3

BUBBLE GROWTH CHARACTERISTICS

(GMA - bottom)

MEASURED		CALCULATED
.070sec.	Period	.066sec.
14bubbles/sec	Freq.	15bubbles/sec
.5cm.	R_o	.5cm.
75ec/sec	G	75cc/sec.
1.5cm.	R_{max}	1.05cm.
1.5cm.	H_{max}	1.55cm.

FIGURE 5-1
QUASI-STATIC TEMPERATURE DISTRIBUTION

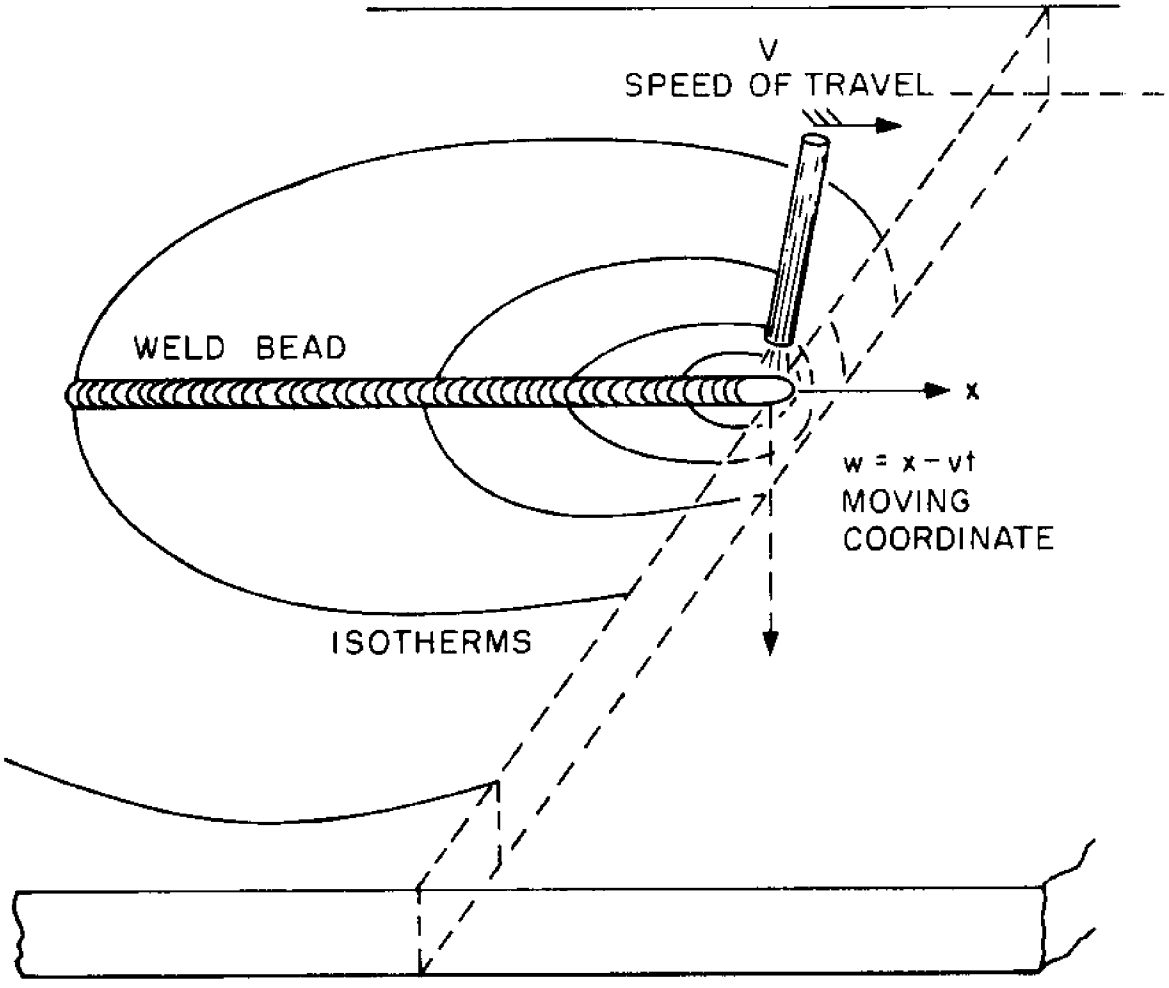

compared with the mathematical analysis to evaluate and modify the basic heat transfer mechanism models, which may then lead to an improved underwater welding process.

The predicted direction of heat flow is shown in Figure 5-2. Heat conducts downward as well as in its radial direction around the heat source region. Heat losses due tc boiling, radiation and convection on its boundaries give the rapid cooling effects during the underwater welding process. For a two-dimensional analysis, three approaches can be simulated to predict the trend of temperature distributions during underwater welding processes.

(1) The plane X-Y surface, on which a moving heat source travels toward the right. A differential temperature distribution is modelled in the X-Y plane (surface), but a lumped temperature distribution is assumed in the Z direction. In this approach, boiling, convection and radiation play a significant role in the heat transfer mechanism.

(2) The plane X-Z cross-section, longitudinal with the weld.

(3) The plane Y-Z cross-section, transverse to the weld.

In approaches (2) and (3), the conductive heat transfer becomes more prevalent. From the study of microstructure of the weldment and HAZ, is appears that the primary mechanism of cooling results from increased conduction into the baseplate rather than boiling or convection directly into the water.

In this report, the major effort of the heat transfer modelling was concentrated on the first approach. Discussion of the boiling phenomena and bubble dynamics has been treated in some depth. A final section gives some general conceptual discussions of the second and third approaches.

FIGURE 5-2

A) Direction of Heat Flow During Welding Process

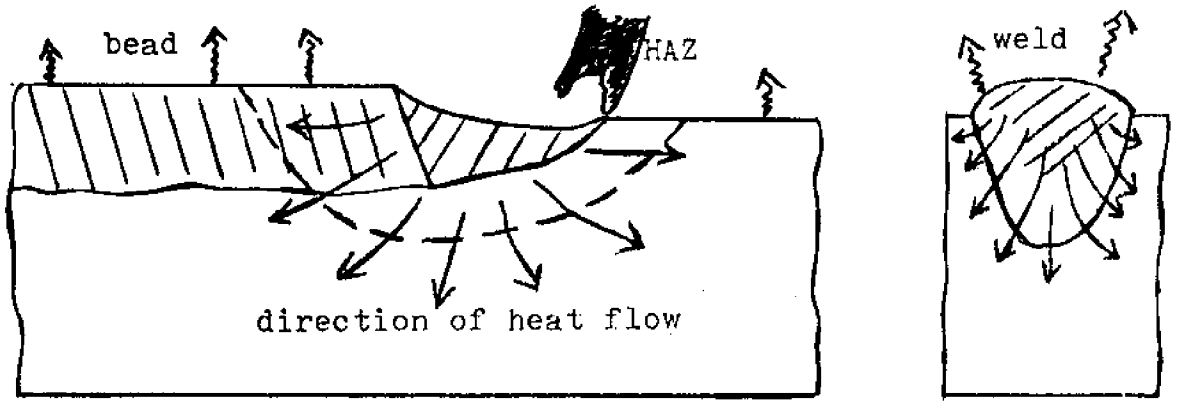

B) Welding Block

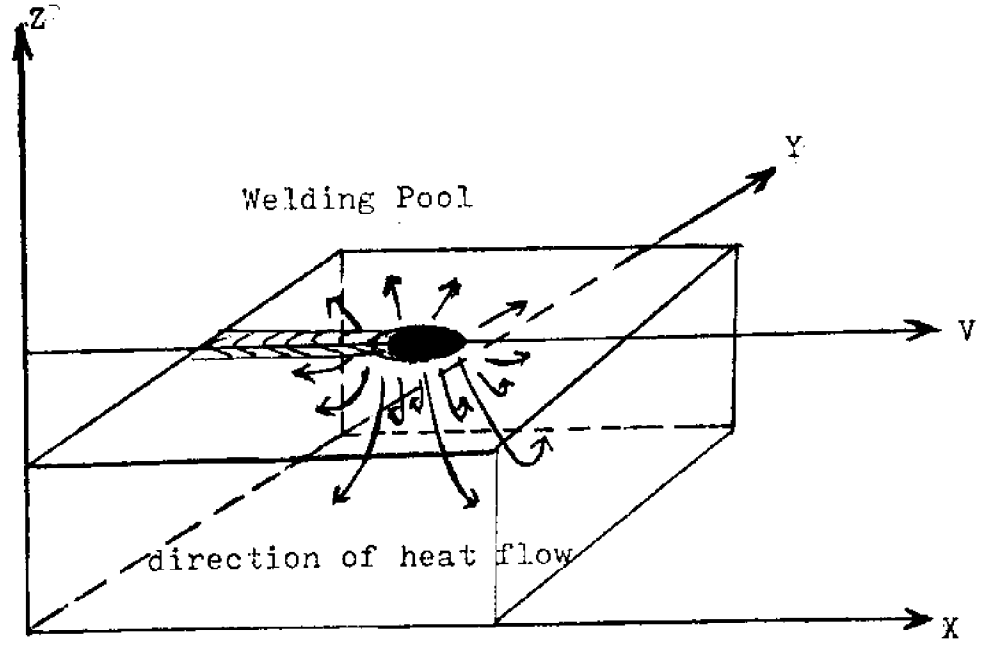

5.1 THE HEAT TRANSFER MODEL

Heat transfer during underwater welding involves a number of intricate heat flow mechanisms. An understanding of the entire welding heat flow can be obtained by integrating models of each mechanism into a single temperature predicting program and comparing results to those obtained empirically. The steps involved in such a procedure are as follows:

(1) Set up the basic differential equation describing the conduction and energy conservation in the plate.

(2) Identify and model all sources and losses of energy.

(3) Mathematically define the boundary conditions on the differential equation.

(4) Solve the differential equation numerically on the digital computer.

The general method used here follows that developed by Pavelec (1968) for GTA (gas tungsten arc) welding and later applied by Staub (1971) to underwater welding.

5.2 THE BASIC GOVERNING EQUATION

The entire analysis to be presented here is based on the energy equation in two dimensions with source terms:

$$\frac{\partial}{\partial x}\left(\kappa\frac{\partial T}{\partial x}\right) + \frac{\partial}{\partial y}\left(\kappa\frac{\partial T}{\partial y}\right) + w_i = \rho c_p \frac{\partial T}{\partial t}$$

This equation can be non-dimensionalized for a quasi-steady, time-independent situation to yield:

$$\frac{\partial^2 T^*}{\partial^2 w^{*2}} + \frac{\partial^2 T^*}{\partial y^{*2}} + \frac{\partial \log \kappa}{\partial T^*}\left[\left(\frac{\partial T^*}{\partial w^*}\right)^2 + \left(\frac{\partial T^*}{\partial y^*}\right)^2\right] + \frac{\dot{q} X_o^{\,2}}{KL(T_M - T_o)} = -\frac{V X_o}{\alpha}\left(\frac{\partial T^*}{\partial w^*}\right)$$

TABLE 5-1

Values of Physical Constants

At saturation temperature:

$\rho_L = 59.8$ lbm/ft^3

$\rho_v = .0372$ lbm/ft^3

$h_{fg} = 970.3$ Btu/lbm

$\sigma = 4.04 \times 10^{-3}$ lbf/ft

$g = 4.17 \times 10^8$ ft/hr^2

$\mu_v = .0314$ lbm/hr-ft

$Pr = 1.9$

$C_{sf} = .013$

$K_v = .0145$ Btu/hr-ft-^oF

$g_o = 4.17 \times 10^8$ lbm-ft/lbf-hr^2

$C_L = 1.005$ Btu/lbm^oR

$\mu_L = .72$ lbm/ft-hr

At ambient temperature:

$\rho_L = 62.3$ lbm/ft^3

$K_L = .327$ Btu/hr-ft^oF

$\alpha_L = 5.17 \times 10^{-3}$ ft^2/hr

$Pr_L = 6.4$

Boundary Conditions. Conduction taking place in the plane of the plate is bounded along two boundaries. The outer boundary represents conditions far from the pool origin. This boundary can be assumed to be at ambient temperature and may be represented by:

$$T^*(\pm\infty, y^*) = \frac{T_\infty - T_\infty}{T_M - T_\infty} = 0$$

$$T^*(W^*, \pm\infty) = \frac{T_\infty - T_\infty}{T_M - T_\infty} = 0$$

The inner boundary is the melting isotherm which separates the molten pool from the solid portion of the plate. It can be assumed to be at the metal's melting temperature and may be represented by:

$$T^*[f(w^*, y^*)] = \frac{T_M - T_\infty}{T_M - T_\infty} = 1$$

Predicting the location of the pool contour analytically requires the use of a temperature model, but such a model is precisely what we do not have. Point source theory predicts egg-shaped contours, quite unlike the observed tear-drop shape. For these reasons, reliance on entirely analytical methods is ruled out. Second best to an entirely analytical approach is analytical correlation of empirical data. This was done using Rosenthal's point source temperature equation:

$$T - T_o = \frac{\dot{Q}}{L} \frac{1}{2\pi\bar{K}} e^{-\bar{\lambda}Vw} K_o(\bar{\lambda}Vr)$$

By employing this equation along with certain geometric aspects of the weld pool, a lumped welding parameter was derived:

$$N^* = \frac{3.415\ EI}{2\pi\bar{\alpha}LH_m}$$

This welding parameter may be used to correlate values for maximum pool length and width (see Figure 5-3). The correlation results in expressions of the form:

$$X_{max} = AN^{*B}$$

$$B_{max} = CN^{*D}$$

The constants A, B, C, D depend on the particular process used.

The two dimensions for maximum width and length establish three points on the weld contour. From these, it is possible to determine a shape function which describes the entire contour.

5.3 INPUTS AND LOSSES OF ENERGY

Using the molten pool as the inner boundary to plate conduction makes it possible to overlook the very complicated process involved in energy transfer from the arc to the molten pool. Only energy transfer directly to and from the solid portion of the plate need be considered. This includes:

(1) Heat radiated directly from the arc to the solid portion of the plate (spread heat).

(2) Boiling heat transfer away from the plate.

(3) Radiation from the plate to the surrounding water.

(4) Heat conducted from the molten pool through the boundary to the plate.

5.31 Spread Heat

The spread heat, or energy passing directly from the arc to the plate was computed in terms of an exponential distribution extending from the tip of the electrode and diminishing out to infinity. When actually added as an energy input to

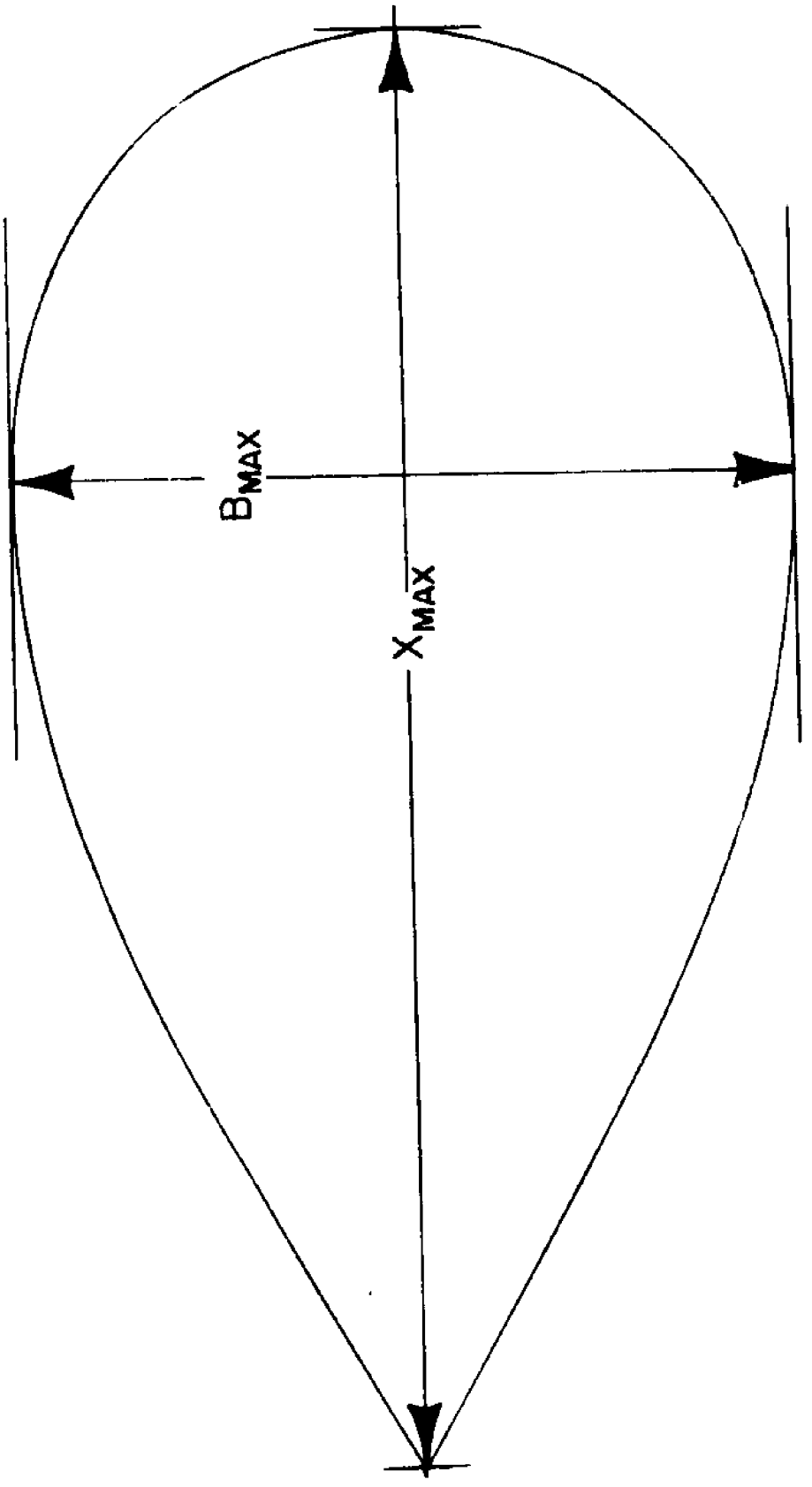

FIGURE 5-3
WELD MOLTEN POOL

FIGURE 5-4
BOUNDARY CONDITIONS

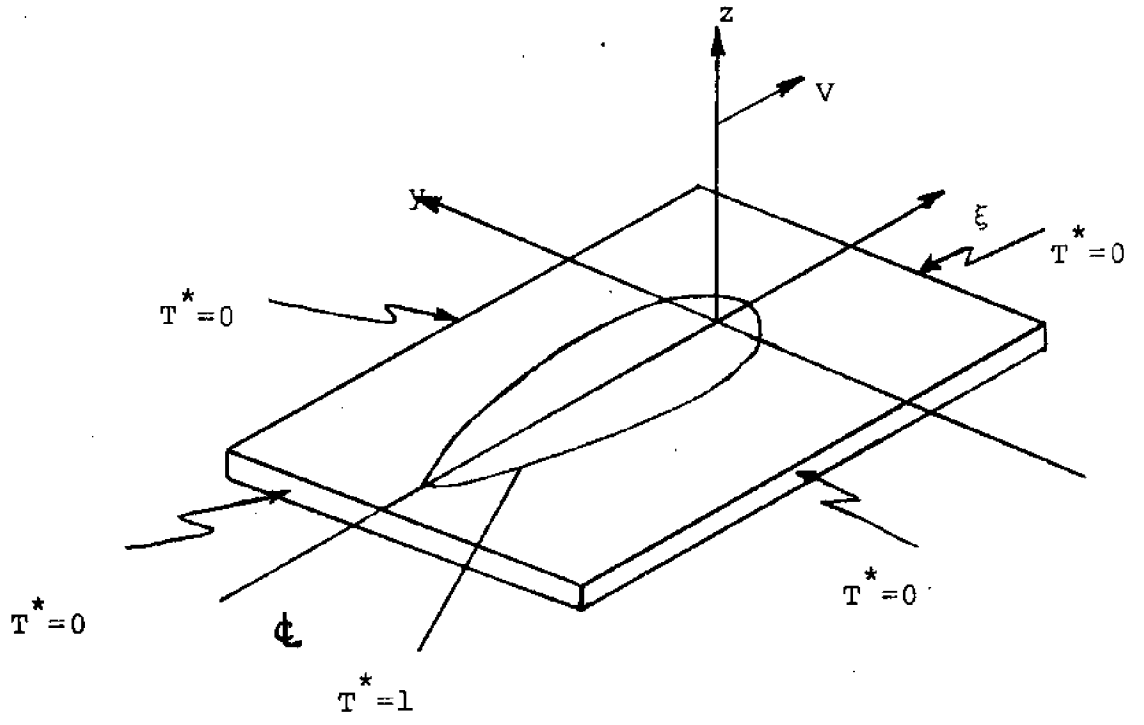

the model, two things must be recognized:

(1) By establishing the shape of the weld pool, spread heat within this region does not enter into the model.

(2) Spread heat will be significant only in the void surrounding the arc.

Therefore, spread heat is added only between these bounds. With a few simple assumptions, the following expression was derived:

$$\dot{q}_D(r) = q(o)e^{-Cr^2}$$

where q(o) and C are functions of basic welding parameters and the radius of the welding hot spot (Figure 5-5).

5.32 Boiling Heat Transfer

The greatest heat losses during underwater welding are due to boiling and radiation. Prior to boiling, the heat transfer is mainly due to convection. McAdams (29) derived the relations for top and bottom of the plate convection:

$$\frac{h_{ctop}L}{k_L} = 0.14\ (Gr_L \cdot Pr_L)^{1/3}$$

$$\frac{h_{cbot}L}{k_L} = 0.27\ (Gr_L \cdot Pr_L)^{1/4}$$

where

$$\frac{Gr_L}{L^3\ \Delta T} = \frac{g \cdot \beta_L \cdot \rho_L^2}{\mu L^2} = 4.4 \times 10^7$$

This yields for the heat transfer:

$$\dot{q}_{ctop} = 32.1\ (T-T_\infty)^{4/3}\ \frac{Btu}{ft^2\text{-}hr}$$

FIGURE 5-5

SPREAD HEAT DISTRIBUTION

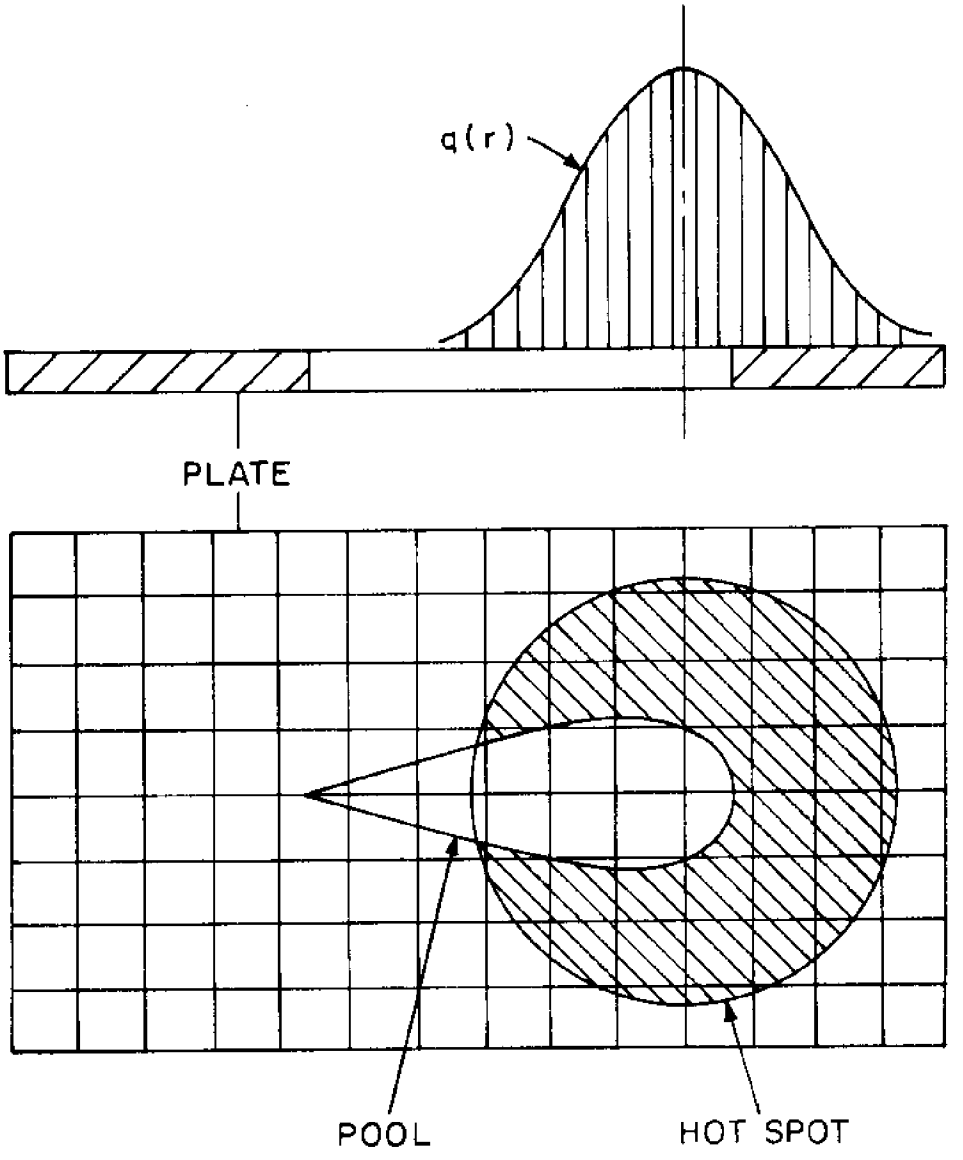

$$\dot{q}_{cbot} = 12.2\ (T-T_{\infty})^{5/4}\ \frac{Btu}{ft^2\text{-}hr}$$

At temperature above the boiling point, boiling and radiation play a much more significant role in heat losses. Three regines with distinct heat transfer mechanisms will be discussed individually in detail (Figure 5-6). Underwater welding involves extremely transient temperature distributions with steep gradient and takes place in sub-cooled water.

5.33 Nucleate Boiling Regime

When the surface temperature sufficiently exceeds the saturation temperature of the liquid, vapor bubbles may begin to nucleate on or near this surface. In a sub-ccoled liquid, these bubbles will grow and collapse under the influence of various hydrodynamic and thermodynamic forces. The heat transfer rate during this nucleate boiling is very high. A correlation proposed by Forster and Grief was evaluated and used to express this heat flow-temperature relationship:

$$\dot{q}_{nuc} = 1.663\ (T - T_{sat})^3\ \frac{Btu}{hr.\text{-}ft.^2}$$

5.34 Peak Heat Flux Regime

As the temperature continues to increase, so does the bubble population until finally these outgoing bubbles begin to jam up the flow and reduce the heat transfer. The peak heat flux and temperature were calculated on the basis of a different analysis, as neither method was entirely satisfactory and required comparison:

(1) The standard calculation proposed by Zuber for boiling in liquids at their saturation temperature yields:

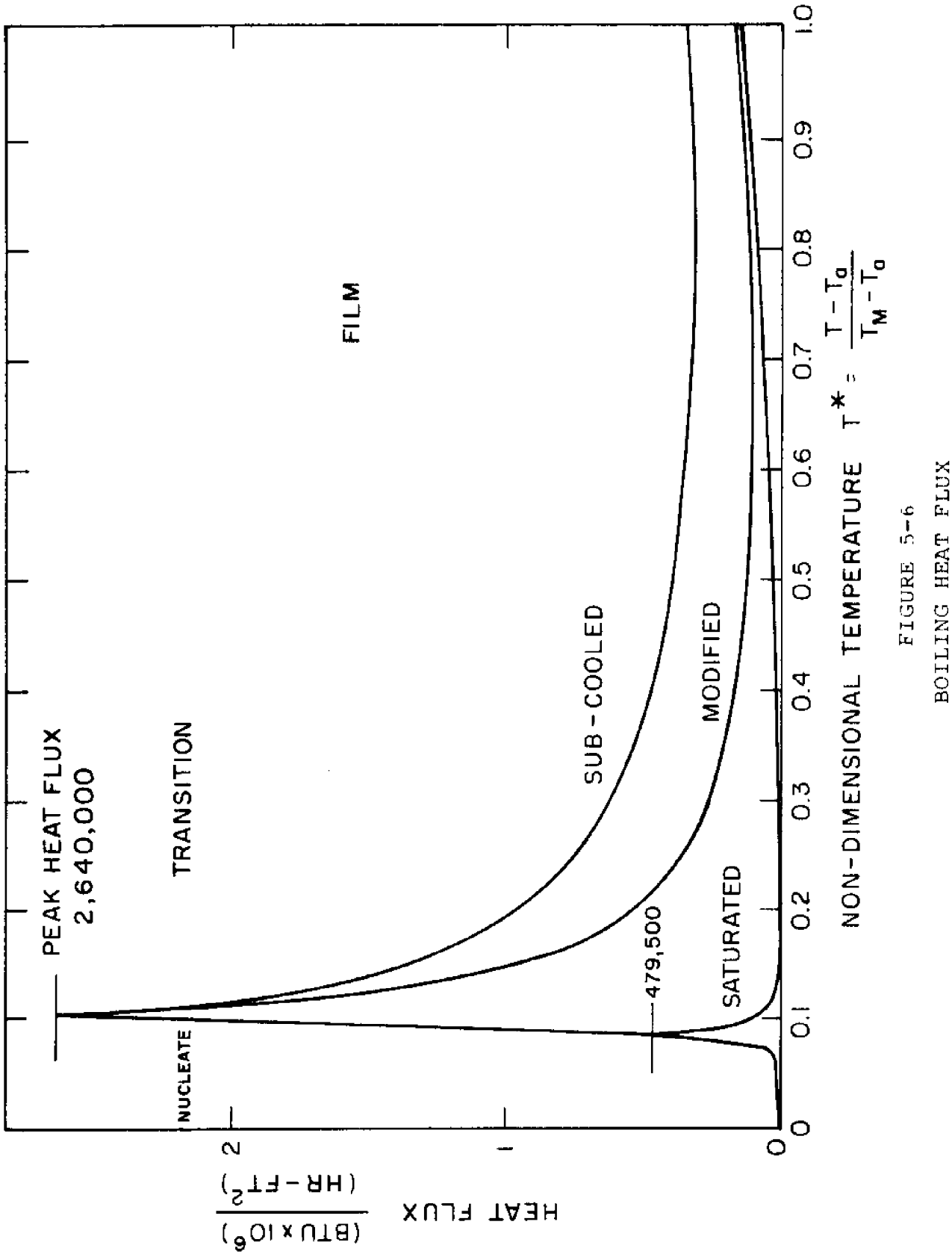

FIGURE 5-6

BOILING HEAT FLUX

$$q_{max} = 479,500 \frac{Btu}{ft.^2\text{-hr.}}$$

$$(T - T_{sat})_{max} = 66°F$$

(2) Since the boiling does not take place in a liquid at its saturation temperature, the second correlation used was chosen because it considers the degree of sub-cooling of the surrounding water. Based on this correlation, and assuming the ambient temperature to be 55°F, calculation yields:

$$q_{max} = 2,640,000 \frac{Btu}{ft.^2\text{-hr.}}$$

$$(T - T_{sat})_{max} = 116°F$$

The second of these methods proved to give the best agreement with empirical results.

5.35 Film Boiling Regime

As the temperature continues above the peak, the bubble stream becomes more and more jammed up until a minimum temperature is reached and a continuous film has formed. Film boiling on a horizontal surface facing up, and submerged in a liquid at its saturation temperature, has been considered by a number of investigators. The applicability of these theories for describing phenomena in underwater welding is again limited by the effect of a sub-cooled liquid environment. In this case, three alternative theories were considered:

(1) A purely saturated boiling model which yields:

$$(\dot{q}_{Film})_{sat} = 84 (T - T_{sat})^{.75}$$

$$(q_{min})_{sat} = 5980 \frac{Btu}{ft.^2\text{-hr.}}$$

$$(T - T_{sat})_{min} = 296°F$$

(2) A model with <u>both</u> peak and minimum heat flux modified using the previous peak heat flux correlation.

$$(\dot{q}_{min})_{mod} = 33{,}000 \frac{Btu}{ft.^2\text{-}hr.}$$

$$(T - T_{sat})_{min} = 2877°F$$

The temperature of minimum heat flux predicted by this correlation indicates that film boiling will not occur within the range of the welding model.

(3) A model using the modified peak heat flux and a minimum heat flux derived by considering sub-cooling and transient conduction.

$$(\dot{q}_{min})_{sub} = 115{,}000 \frac{Btu}{ft.^2\text{-}hr.}$$

$$(T - T_{sat})_{min} = 5700°F$$

Again, this model predicts that a stable film will not form within the range of the welding model.

Connecting the peak heat flux with the minimum heat flux is the transition regime for which a relation of the form

$$\dot{q} = M(T - T_{sat})^b$$

was assumed and the constants solved for using the two end conditions.

It is assumed that boiling heat flux from the bottom side of the plate is negligible as a completely stable vapor film is assumed to form there.

5.36 Radiation Loss

Assuming the emissivity of the plate is 0.8 and the surrounding water is 0.95, and that the energy radiates from the plate to the surrounding water through the vapor film or

bubble at saturation temperature, the normalized heat flux loss can be calculated as a function of a non-dimensional temperature.

$$\dot{q}_{rad} = 1.317 \times 10^{-9} \{[T^{*}(T_m - T_\infty) + T_\infty]^4 - T_{sat}\}$$

5.4 EXPERIMENTAL METHOD

5.41 Welding Equipment

Common to each process is the problem of a proper grounding and insulation. A direct insulated ground was connected from the welding machine to the workpiece. The workpiece was in turn insulated from the tank by setting it up on oven bricks. Welding gloves were worn and rubber mats provided to stand on.

The length of the welding electrode in SMA was quite adequate for reaching through the free surface to the plate. During use, the electrode was replaced when the holder approached the free surface. This allowed a normal surface holder and rig to be used.

The shrouded process was set up in the same manner as SMA. In order to photograph the dynamics of this process, a clear plastic shroud was used. This shroud was fashioned from a plastic dome-like cover of an old-fashioned clock. This worked very well except that the shroud's buoyancy had to be compensated for by adding additional weight. This was done by balancing a nut and bolt between the ports.

The final process, GMA, was a bit more difficult to set up. It was necessary to modify the nozzle of the semi-automatic gun so that it would extend through the free surface to the plate without having the submerge the gun. The inner contact tube was replaced with a 10-inch one, machined

from copper tubing. An eight-inch extension was brazed onto the outer barrel. This provided more than enough length to reach the plate.

5.42 Welding Conditions

It was next necessary to establish a set of welding conditions which were consistent with the desired experiments. This meant determining plate thickness, machine settings, wire feed, welding speed, etc.

Most important in these calculations was the requirement for two-dimensionality. From the heat transfer standpoint, this required as thin a plate as possible (maximum of 1/4-inch). In order to maintain a two-dimensional weld pool, combinations of welding speed and current were also limited. When the plate got too thin, burnthrough was very excessive. Considering the above 1/8-inch mild steel plate was chosen for the experiments. Welding speeds and currents were then determined by trial and error. Results for these are tabulated in Tables 5-1 and 5-2. The two electrodes (E6013 and E7014) behaved very similarly in terms of required welding speed. Straight polarity required a slightly faster speed than reverse for both electrodes. During the blow-out experiments, the 1/8-inch stock obtained ran slightly thick (.130 inch). The required welding speed was extremely sensitive to this change and had to be reduced.

TABLE 5-1

CURRENT CHARACTERISTICS FOR UNDERWATER SMA WELDING

(E6013 and E7014 Electrodes)

I (amperes)	Description
150 amps	The bead was eratic and the arc was very difficult to start
180 amps	Although starting was still difficult, the bead was smooth and the penetration sufficient. Minimum current in experimental range.
220 amps	Starting was easier and the weld bead smooth. Probably the optimum current found.
250 amps	Burnthrough became a problem and welding speed was very fast. Maximum current in experimental range.

TABLE 5-2

CURRENT AND MACHINE SETTINGS FOR UNDERWATER GMA WELDING

Machine Settings		Resulting	
Arc Length	Wire Feed	Current	Comment
5	4.8	250 amps	Minimum of possible range Bead piles up in globs due to short circuit transfer.
6	5.2	300 amps	Good welding range Moderate penetration Smooth bead
7	5.7	340 amps	
8	6.0	370 amps	Beyond this point burnthrough is uncontrollable even at fast welding speeds.

5.43 Temperature Measurements

In order to determine the accuracy of the mathematical model, it was necessary to generate a set of temperature distributions for actual welding runs. The basic steps involved in this experimentation are:

(1) Mount the thermocouples
(2) Mount the plate in the tank
(3) Attach thermocouple leads to the recorders
(4) Set up the welding system
(5) Attach voltage and current recorders
(6) Flood the tank
(7) Turn on the power
(8) Lay the weld bead and record temperature, voltage, current, and time
(9) Measure bead length and distance from centerline to each thermocouple
(10) Process and plot the data

Mounting the thermocouples was the most tedious operation and required a certain amount of trial and error. This will be discussed in detail.

Four thermocouples were mounted in each plate. Asbestos wrapped chromel-alumel thermocouple wire served as both the thermocouples and the leads. Staub's method of jamming these leads into a tight hole in the plate and then peening the pole shut was tried without success. This was probably due to a poor thermocouple junction as well as poor contact with the plate. Steps involved in the method finally chosen are as follows:

(1) Drill and counter drill 4 holes in each plate as shown in Figure 5-7.
(2) Bare about 1/2 inch on each wire, twist the ends together and insert them through the plate (Figure 5-7).
(3) Using a gas torch, melt this twisted end down until a small bead is formed.

FIGURE 5-7

THERMOCOUPLE INSTALLATION

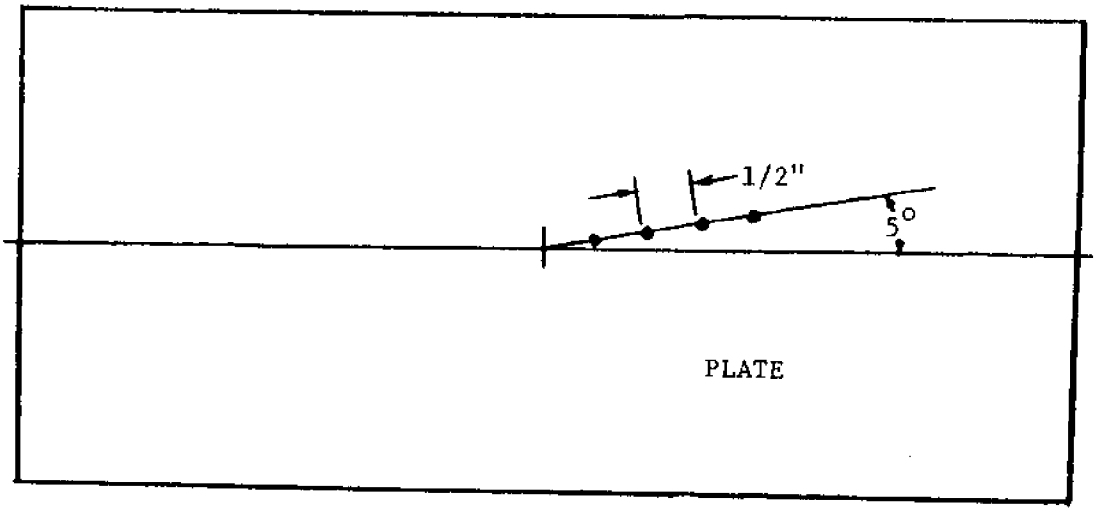

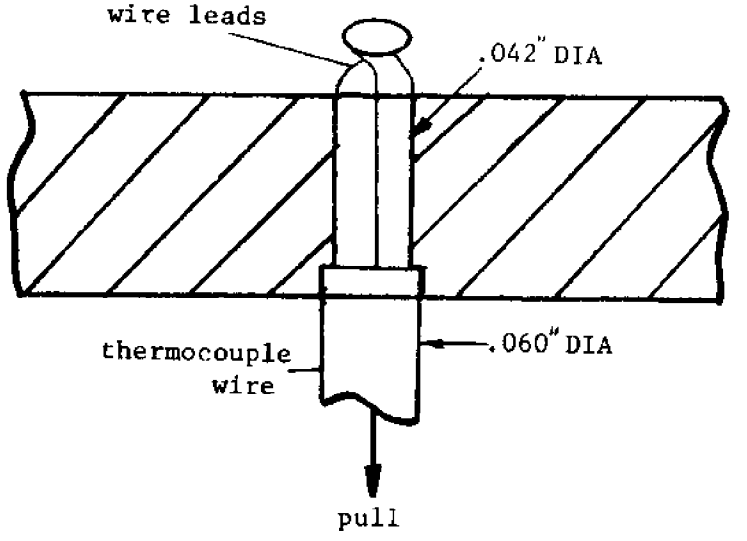

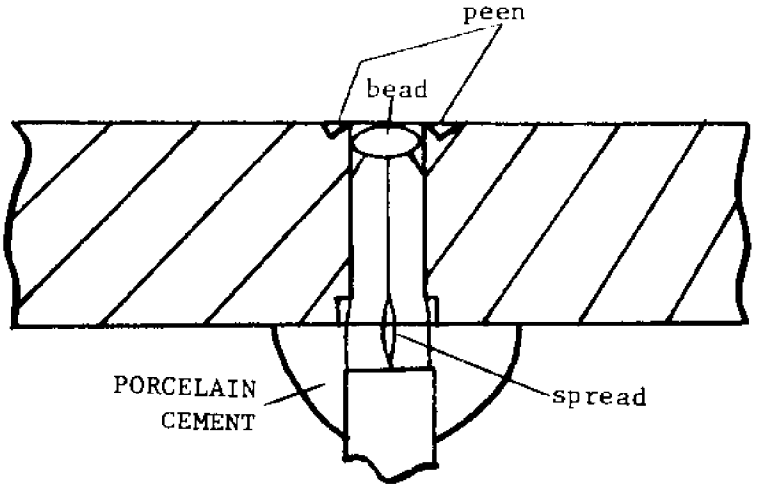

(4) Pull the bead to the plate and peen flush.

(5) Seal the underside with porcelain cement. Let dry and waterproof with mild acetic acid.

This setup insured a good junction and metal contact. Its results were quite satisfactory.

The thermocouple leads were connected, two to each of two recorders. The sensitivity settings for the recorders were 1mv/div for three channels and 2mv/div for the fourth. The fourth channel was connected to the thermocouple closest to the centerline or the weld. Current and voltage recorders were connected between the welder and the machine. They also recorded the duration of the run (see Figure 5-8).

Once the welding run had been made, the length of the weld bead as well as thermocouple distance from center were measured with a micrometer device. Using the length of the bead along with run time allowed the welding speed for the run to be calculated.

The voltage readings from the thermocouples were converted to temperatures and everything normalized for comparison to the model. The results are displayed and discussed in Section 5.6.

5.44 Molten Pool Blow-out

In order to establish the inner boundary on plate heat transfer, it was necessary to determine, for each process, the relationship between maximum pool dimensions and the lumped welding parameter. This was done by laying a bead and at some point during the welding, blowing a sharp blast of air towards the base of the electrode and molten pool, terminating the welding at this point. If aimed properly, this blast would blow the molten metal away, leaving a crater in the form of the weld puddle. These craters were measured with a micrometer and their maximum dimensions normalized and correlated.

FIGURE 5-8
THERMOCOUPLE SETUP

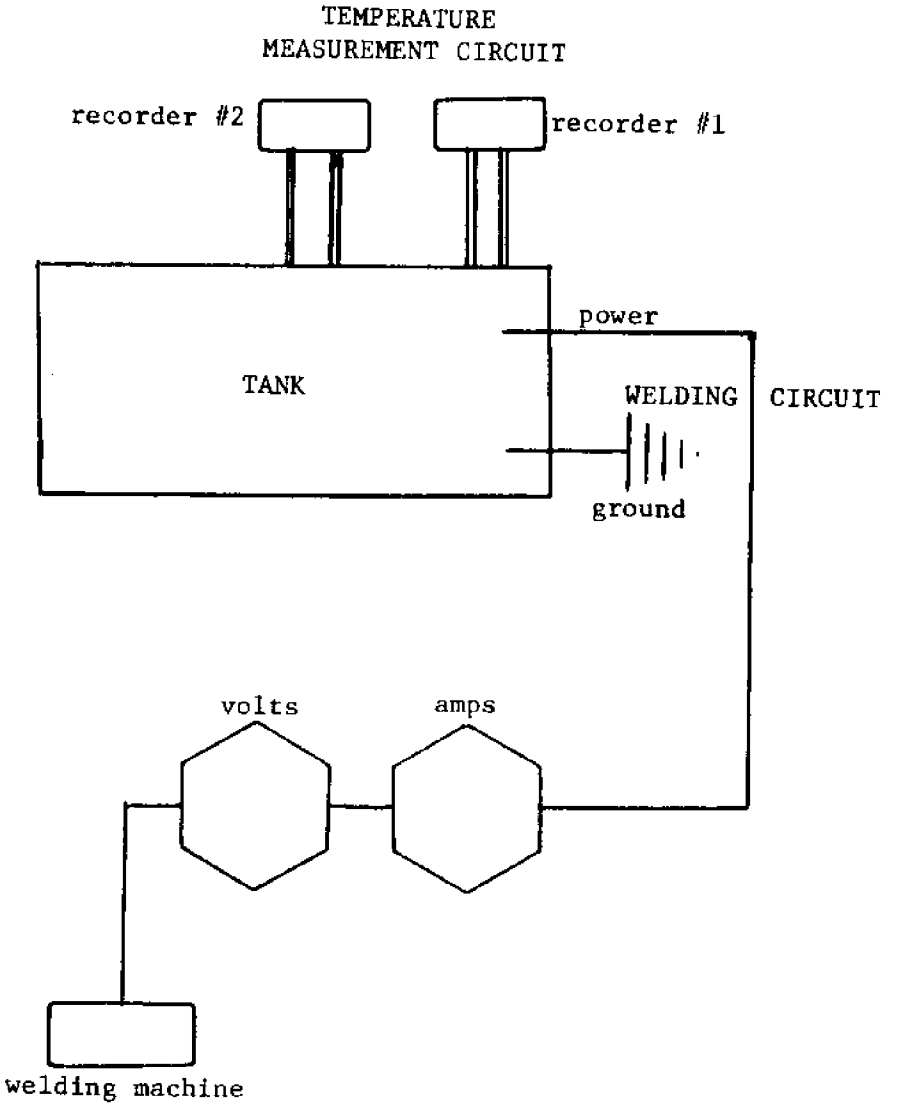

Figure 5-9 illustrates the blow-out setup for the SMA process runs. After a number of trials, it was found that the blast should be aimed at an angle of 45 degrees and pointed at the front of the teardrop towards the tail. Since the apparatus was fixed to the consuming electrode, it was necessary to blow out just as the tubing neared the plate. This timing was crucial for a successful run. About one out of three craters was satisfactory. This meant proper shape (teardrop) and two-dimensionality. The electrode was replaced after every run and the trial repeated.

The operation was much simpler for GMA as it was possible to fix the blow-out apparatus to the gun barrel and actuate it at any time. Most of the runs for this process were successful (Figure 5-10).

High speed photographs had shown that the shroud was not functioning properly, but merely sustaining normal bubble growth within the shroud. As time could not be devoted to improving the shroud, no blow-out experiments were made for it.

Collection of this data showed excellent agreement with the derived correlation.

5.5 THE COMPUTER MODEL

The purpose of this computer model is to verify the derived knowledge of various underwater welding phenomena. It is a purely two-dimensional model, and probably has little practical application beyond testing and developing this knowledge. However, evaluation of new "above the plate" phenomena as might be involved in a shroud-GMA process could hopefully be done using this model.

The program is an adaptation of Pavelec's, so changes rather than basic program organization and methods will be stresses here. The entire program is based on the heat

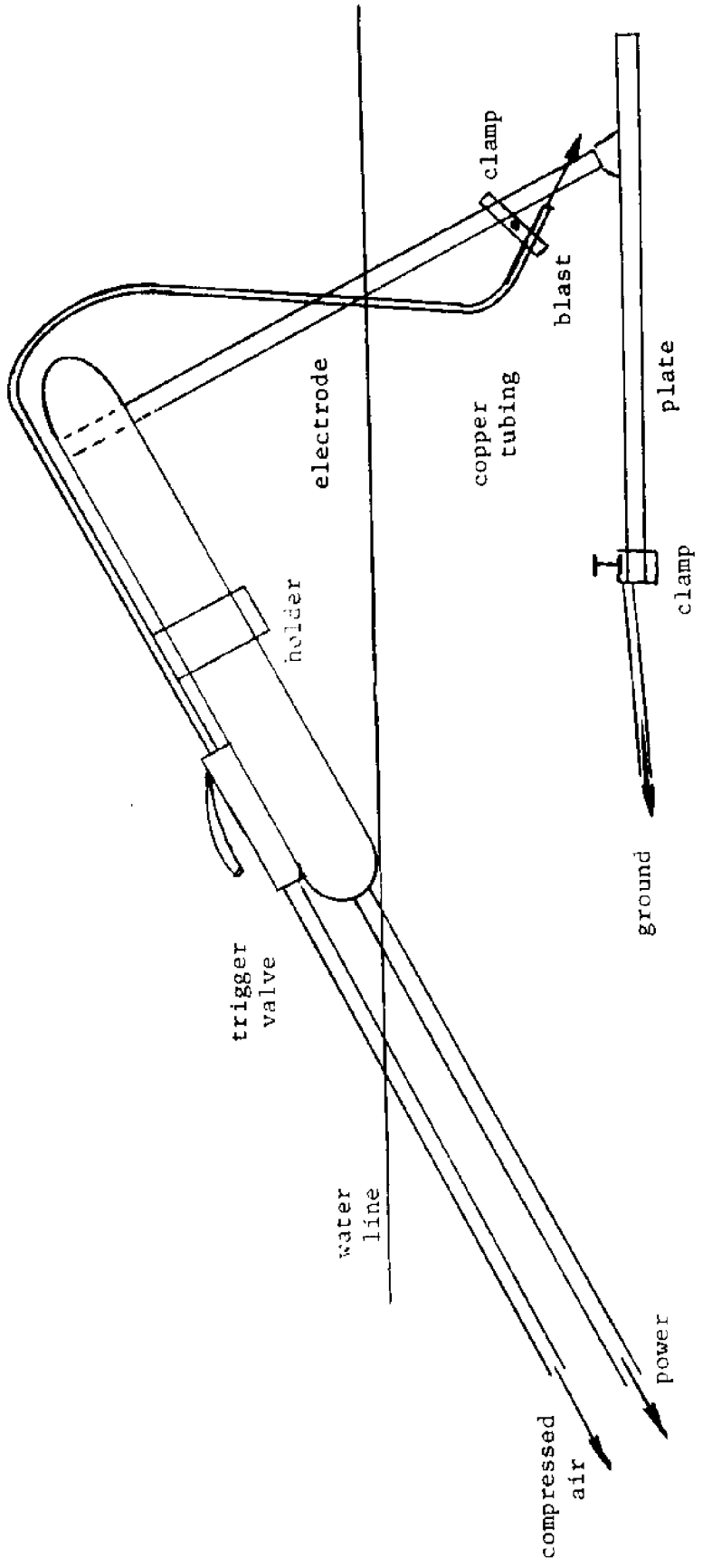

FIGURE 5-9
BLOWOUT SYSTEM - SMA

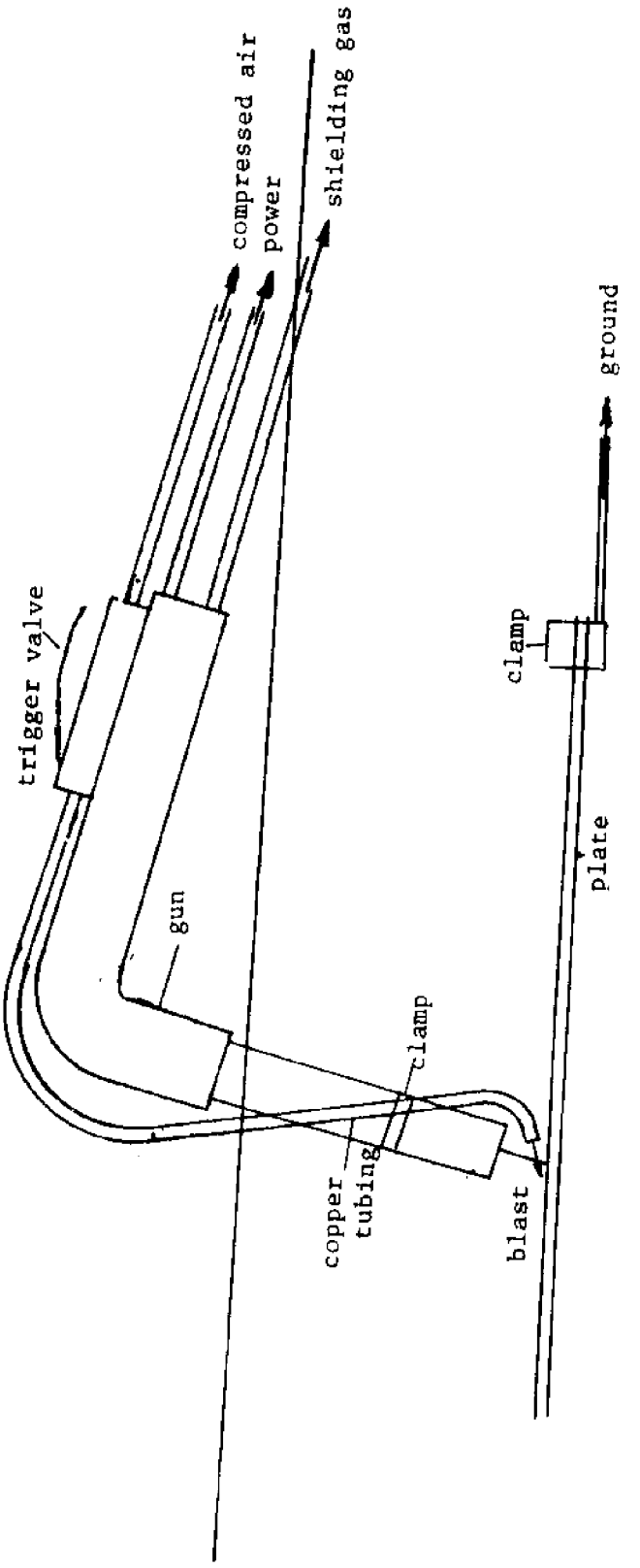

FIGURE 5-10
BLOWOUT SYSTEM - GMA

conduction equation with source terms. This equation is transformed into a finite difference equivalent which expresses the temperature at a point as a function of the surrounding temperatures in the grid and its value on the previous iteration. This equation along with the characteristic grid setup are shown in Figures 5-11 and 5-12. Solution of this equation was done using a Gauss-Sidel iterative procedure. For specifics on grid setup, origin location, and iterative procedure, see the reference on Pavelec.

5.51 Program Changes

The problems encountered and changes made in Pavelec's program included the following:

1. Boundary conditions
2. Incorporating the new boiling models
3. Accounting for bubble phenomena

Each of these will be discussed in detail.

5.52 Boundary Conditions

In order to solve the finite difference equation, it was necessary to establish inner and outer bounds on the plate conduction. Pool blow-out data was gathered and correlated. The resulting maximum dimension equations for each process were then incorporated into the computer model. To specify a specific process, its corresponding number was read in as program input:

Process number 1 - GMA
Process number 2 - 6013S
Process number 3 - 6013R
Process number 4 - 7014S
Process number 5 - 7014R

This change was straight-forward and proved satisfactory.

The external boundary conditions proved to be more difficult to specify. Pavelec's model was for dry-welding, and

FIGURE 5-11

THE FINITE DIFFERENCE EQUATION

$$
\begin{aligned}
T_{i,j}^{*n+1} = \Bigg\{ & T_{i+1,j}^{*n} \left(\frac{\alpha(T_{i,j}^{*n}) + a_{i-1,j}}{\alpha(T_{i,j}^{*n}) a_{i,j} (a_{i,j} - a_{i-1,j})} \right) + \left(\frac{\alpha(T_{i,j}^{*n}) + a_{i,j}}{\alpha(T_{i,j}^{*n}) a_{i-1,j} (a_{i,j} + a_{i-1,j})} \right) T_{i-1,j}^{*n+1} \\
& + T_{i,j+1}^{*n} \left(\frac{1}{b_{i,j}(b_{i,j} + b_{i,j-1})} \right) + T_{i,j-1}^{*n+1} \left(\frac{1}{b_{i,j-1}(b_{1,j} + b_{i,j-1})} \right) \\
& + \frac{X_o^2 \dot{q}}{KL(T_m - T_o)} + \frac{1}{2K(T_{i,j}^{*n})} \frac{dK(T_{i,j}^{*n})}{dT^*} \Bigg[\Bigg\{ \left(\frac{a_{i,j} - a_{i-1,j}}{a_{i,j} a_{i-1,j}} \right) T_{i,j}^{*n} + \left(\frac{a_{i,j} T_{i+1,j}^{*n}}{a_{i,j}(a_{i,j} + a_{i-1,j})} \right) \\
& + \left(\frac{a_{i,j} T_{i-1,j}^{*n+1}}{a_{i-1,j}(a_{i,j} + a_{i-1,j})} \right) \Bigg\}^2 + \Bigg\{ \left(\frac{b_{i,j} - b_{i,j-1}}{b_{i,j} b_{i,j-1}} T_{i,j}^{*n} \right) + \left(\frac{b_{i,j-1} T_{i,j+1}^{*n}}{b_{i,j}(b_{i,j} + b_{i,j-1})} \right) \\
& + \left(\frac{b_{i,j} T_{i,j-1}^{*n+1}}{b_{i,j-1}(b_{i,j} + b_{i,j-1})} \right) \Bigg\}^2 \Bigg] \Bigg\} \Bigg/ \frac{1}{a_{i,j} a_{i-1,j}} + \frac{1}{b_{i,j} b_{i,j-1}}
\end{aligned}
$$

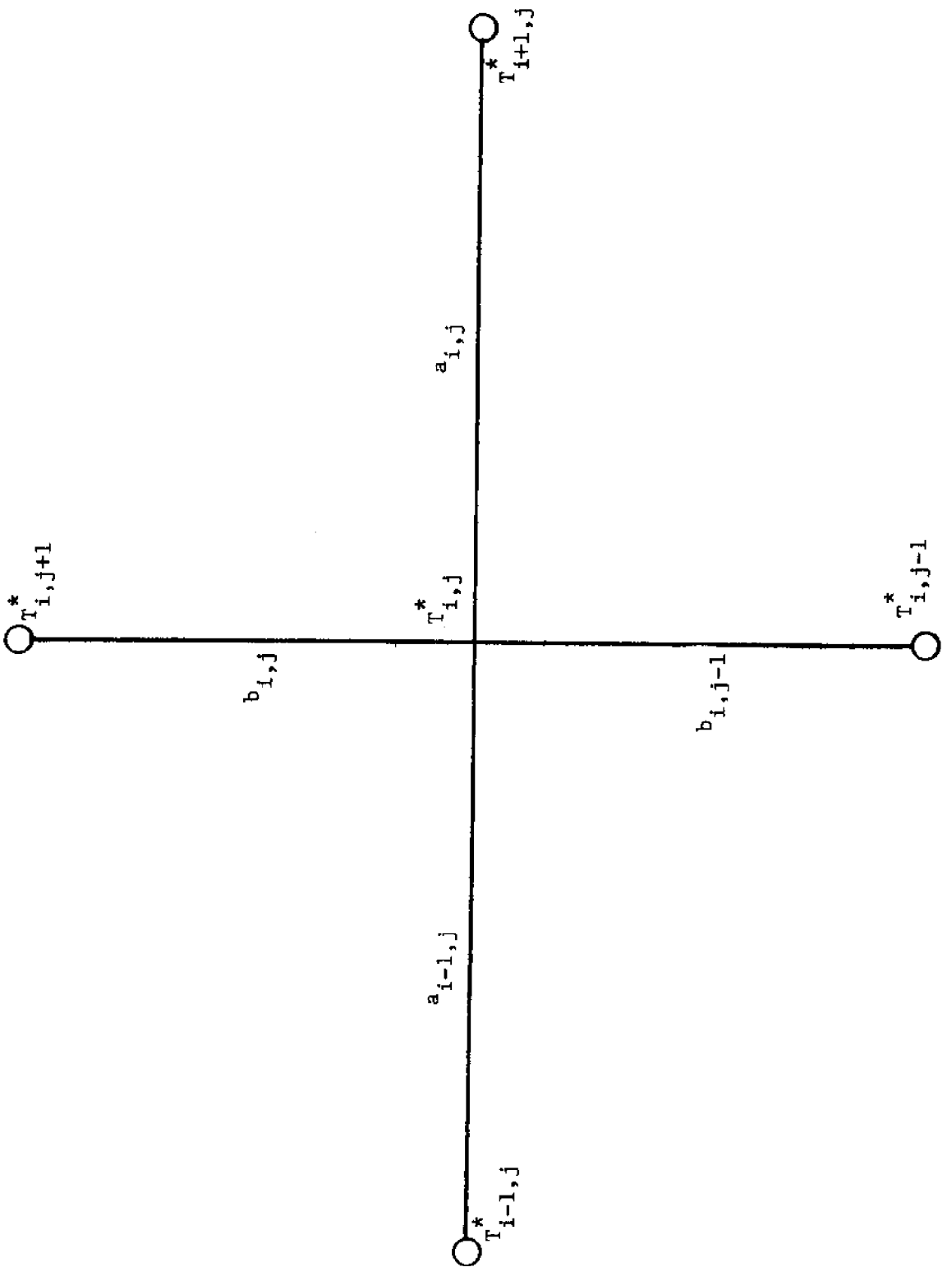

FIGURE 5-12
GRID LAYOUT

he assumed that far away from the weld the temperature distribution would converge to that derived by point source theory. This assumption is not valid underwater, so another method had to be determined. To extend the size of the computational block so that ambient temperature might be specified would have increased execution time by at least a factor of 10. Such a method had to be ruled out. The non-linear aspect of the boiling model made the development of an underwater point source theory nearly impossible.

It was observed in the experimental temperature measurements that the rapid cooling during boiling was followed by a period of relatively slow cooling, that is, all the temperature distributions were asymptotic to a temperature just above boiling ($T^* = .07$). It was further noticed that a computational block size of one inch in front of the arc, three inches in back, and one-half inch to either side was sufficient to satisfy this condition. This size was left as input, however, to allow flexibility for adapting to other processes. This external boundary model proved adequate.

5.53 The Boiling Models

Except for the dynamic bubble model, all the actual heat transfer information is incorporated into subroutine COEF. The heat transfer equation for surface welding does not change with various temperature ranges, but the numerous boiling regimes underwater required that the proper heat transfer relations be chosen for a given temperature. This was done using a series of if-statements. Furthermore, it was necessary to set boiling heat transfer within the bubble (RMAX) to zero. As the spread heat was already set to zero outside RMAX, values for boiling heat transfer were assigned only to points in this region, using the zero spread heat value as a test of location.

Three separate COEF subroutines were made, one for each of the three boiling models to be tested:

1. Sub-cooled
2. Modified
3. Saturated

The result of interchanging these is quite evident and consistent.

5.54 The Dynamic Bubble Models

A dynamic bubble model was derived for each of the processes. From this information, values for RMAX, the effective radius of the dynamic bubbles were chosen. During the temperature initialization stage of Pavelec's program, he used the radius to the origin and computed spread heat. Modifying this for underwater welding simply required that the value of this radius be compared to RMAX. Points within RMAX were assigned a spread heat value which is later used in the finite difference equation. Those points outside were assigned spread heats of zero.

5.55 Flow Chart

This section gives some general concept of the programing procedures. Brown (1972) gives more information in detail.

The structure of this flow-chart is mainly as follows:

(1) Main Program;
(2) Subroutine BESSEL;
(3) Subroutine ORIGIN; (based on the length of the pool)
(4) Subroutine PROP;
(5) Subroutine ROWPS;
(6) Subroutine COLUMN;
(7) Subroutine TYPFN;
(8) Subroutine PNTFND;
(9) Subroutine COEF;

(10) Subroutine DIFEQ;

(11) Subroutine ORBLW; (based on the length and width of the pool)

(12) Function DRAJH;

(13) Function AUTSCL.

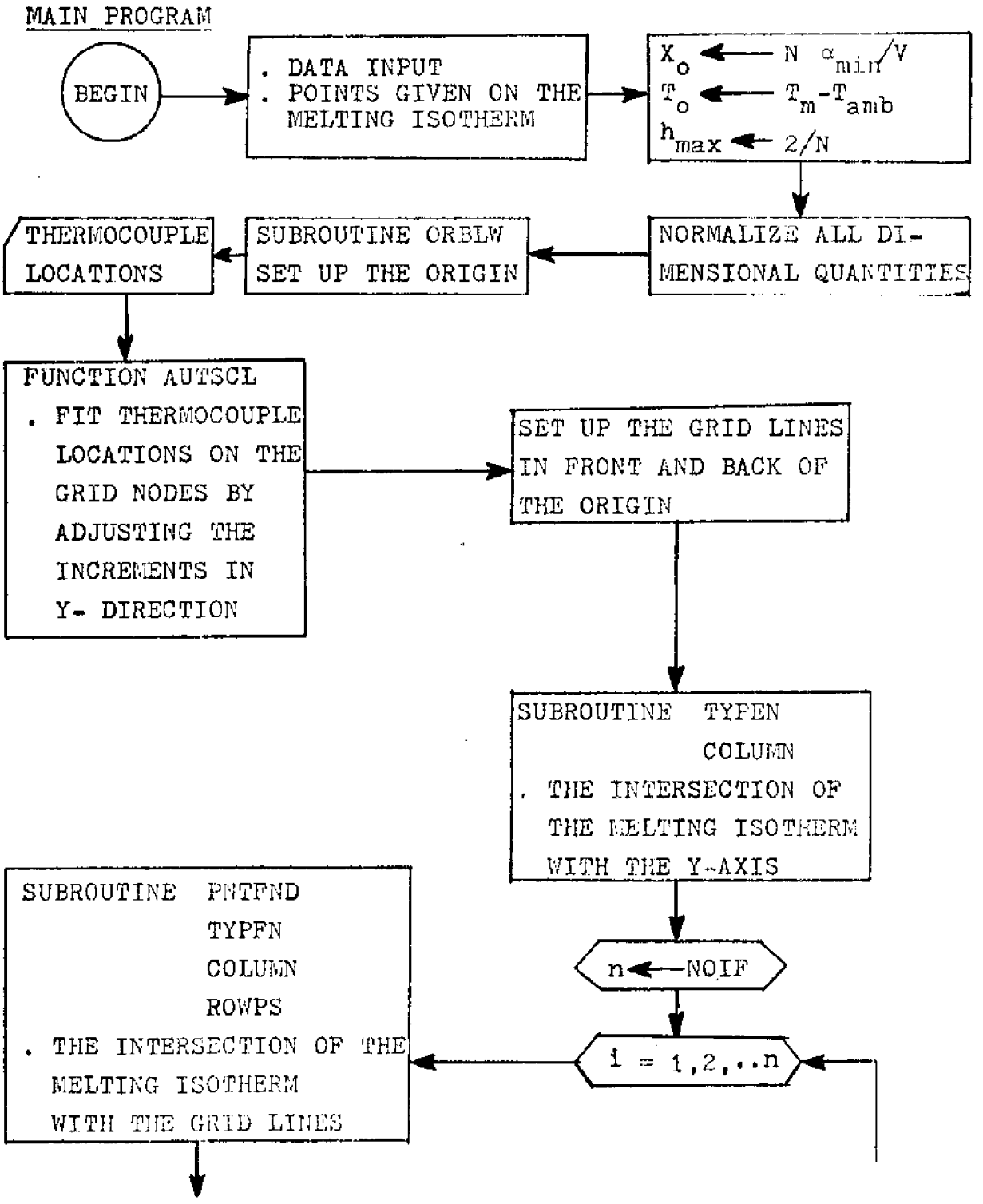

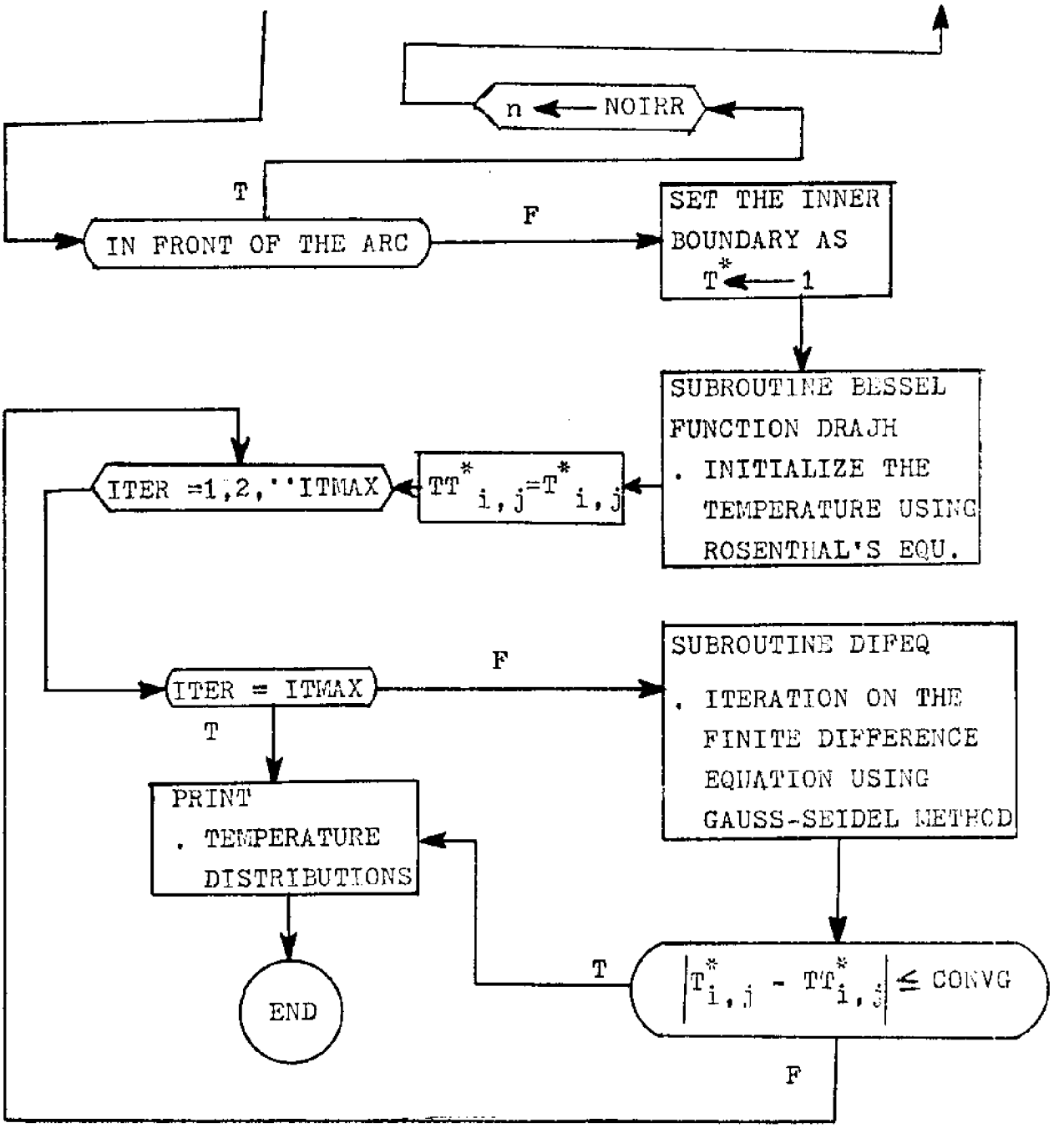

The sub-flow-chart for subroutines and the program listing can be found in Brown (1972).

5.6 RESULTS AND CONCLUSIONS

Both the calculated temperature distributions and the experimental temperature distributions for each of the three underwater welding processes have been plotted in Figures 5-13 through 5-17. Recall that the calculated temperature distributions are all stationary corresponding to the moving electrode. In other words, it is equivalent to the plate moving through the source zone which is fixed in space, and in the opposite direction of the electrode motion. The rapid cooling phenomena in front of the arc, the extremely steep temperature gradient, is due to the opposite direction of total thermal diffusion and the energy carried toward the back of the arc by the moving plate. Mathematically, the nondimensional parameter VX_o/α is the term corresponding to the left of the arc. The deviation between the tabulated temperature curve and experimental temperature curve may be caused by the mathematical inaccuracy due to the first or second order approximations and the improperly-guessed welding efficiency (0.4) employed in the calculations.

Predicted, actual, and open-air cooling curves are plotted in Figures 5-18 through 5-21, as they would appear on a cooling transformation diagram. It can be seen that the results are quite adequate, especially when compared to the cooling of an open-air weld. When used with a cooling transformation diagram, the resulting microstructure and properties could be predicted at various distances from the weld. The ability to predict metallurgical properties is extremely valuable.

The limitations of this work suggest definite guidelines for future research:

(1) All calculation and welding was done for the downhand position. Most ship repair will require vertical and overhead positions. Some means for predicting tempera-

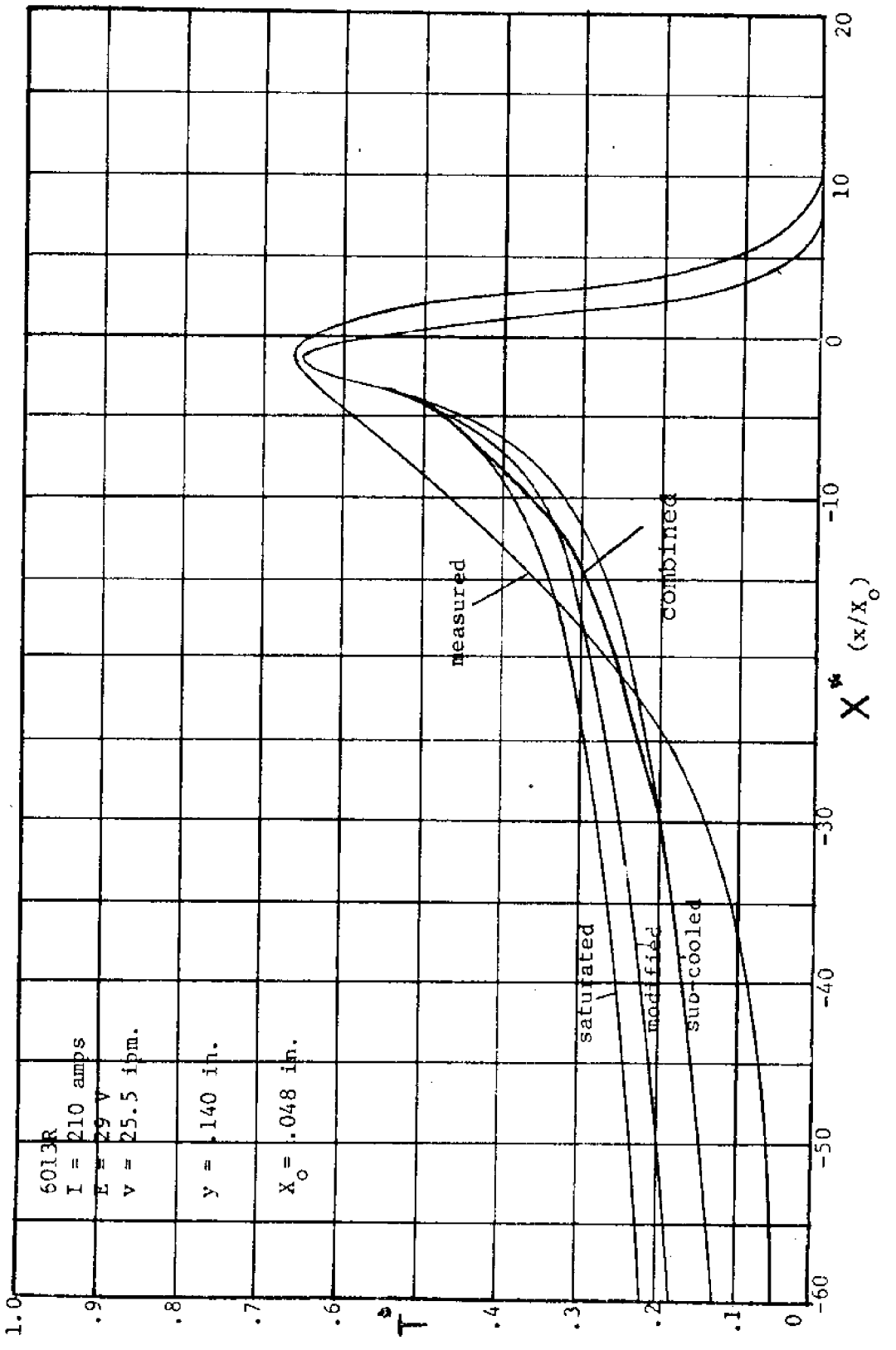

FIGURE 5-13
UNDERWATER WELDING TEMPERATURE DISTRIBUTION

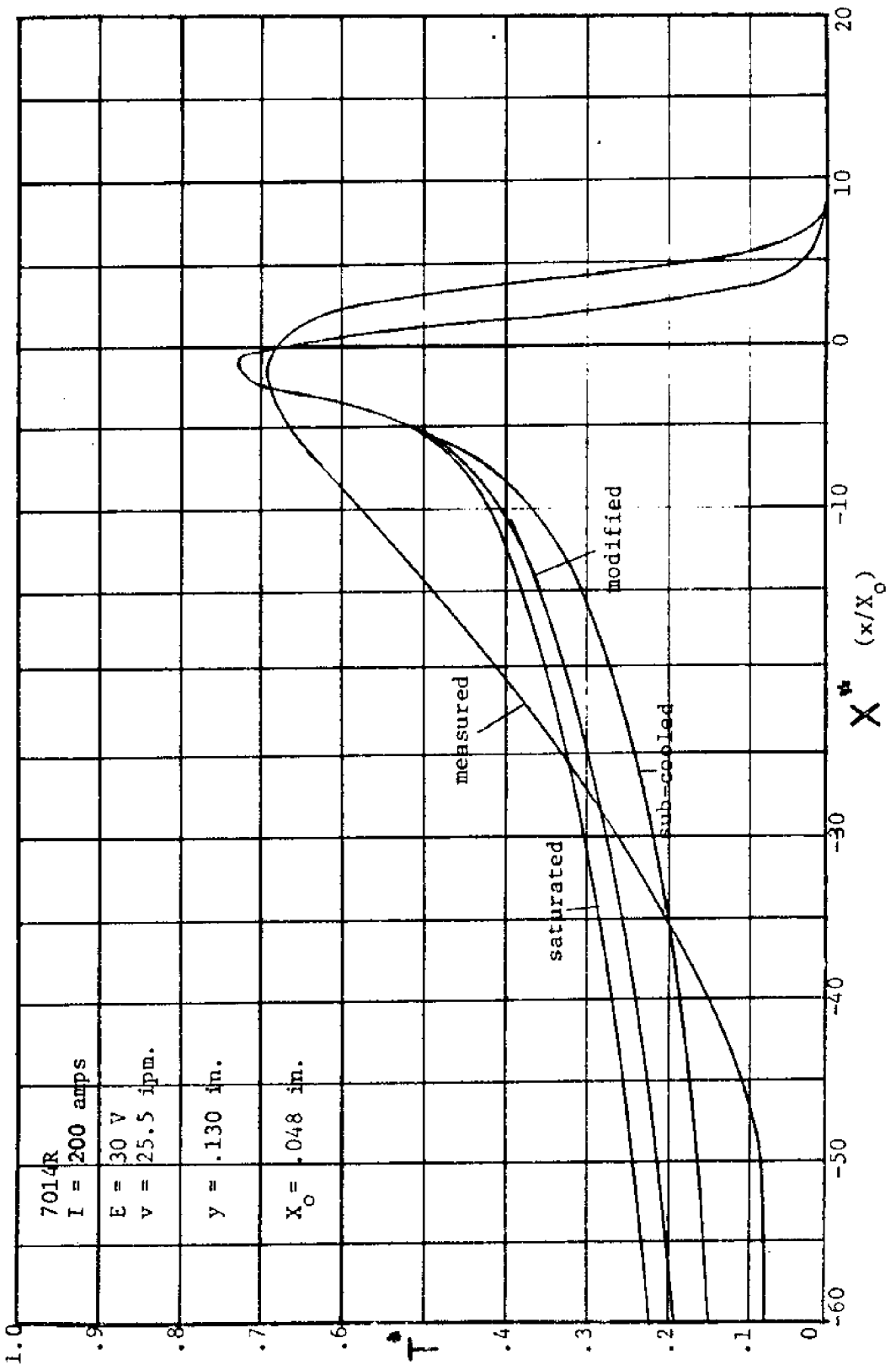

FIGURE 5-14

UNDERWATER WELDING TEMPERATURE DISTRIBUTION

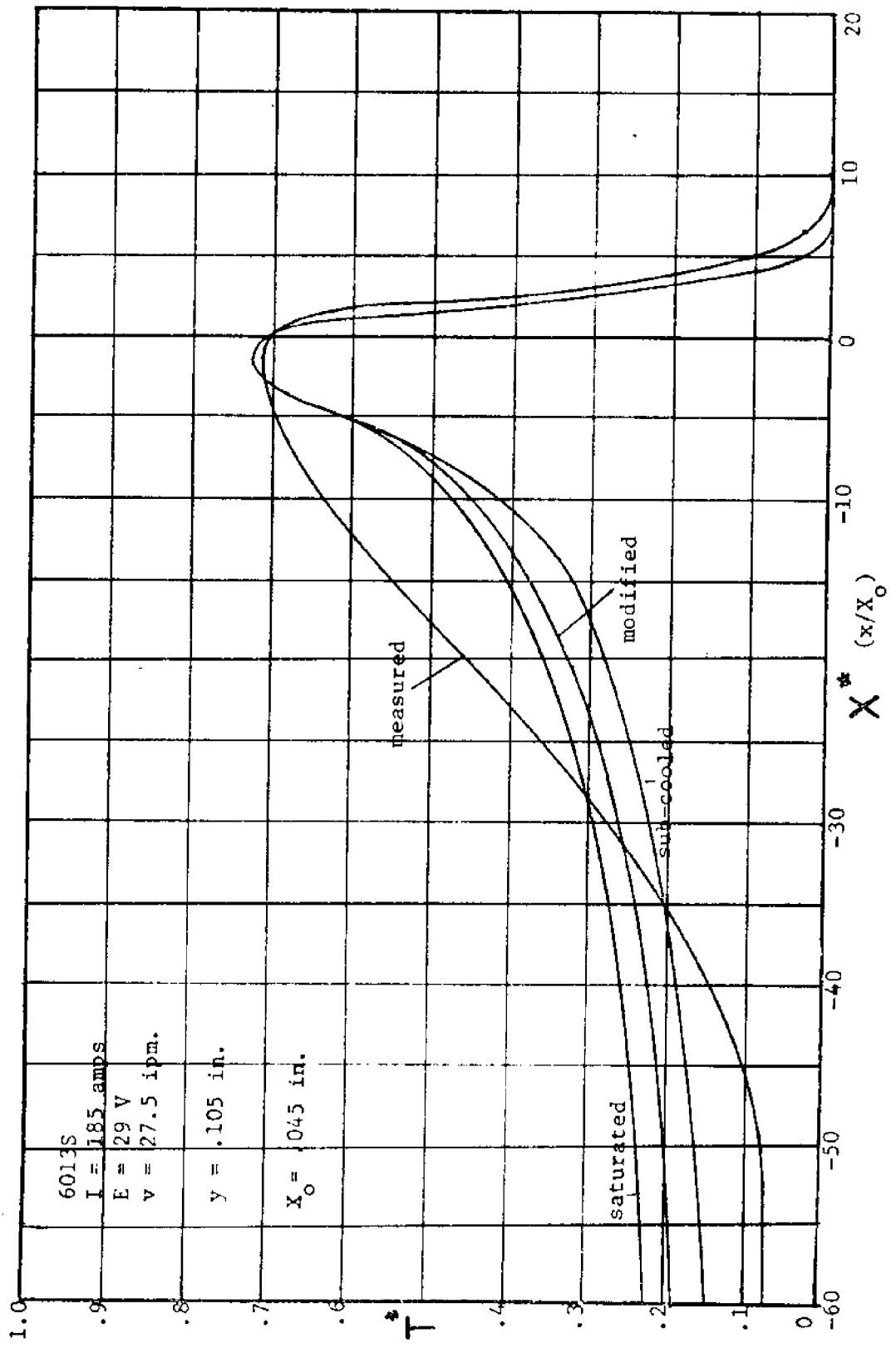

FIGURE 5-15

UNDERWATER WELDING TEMPERATURE DISTRIBUTION

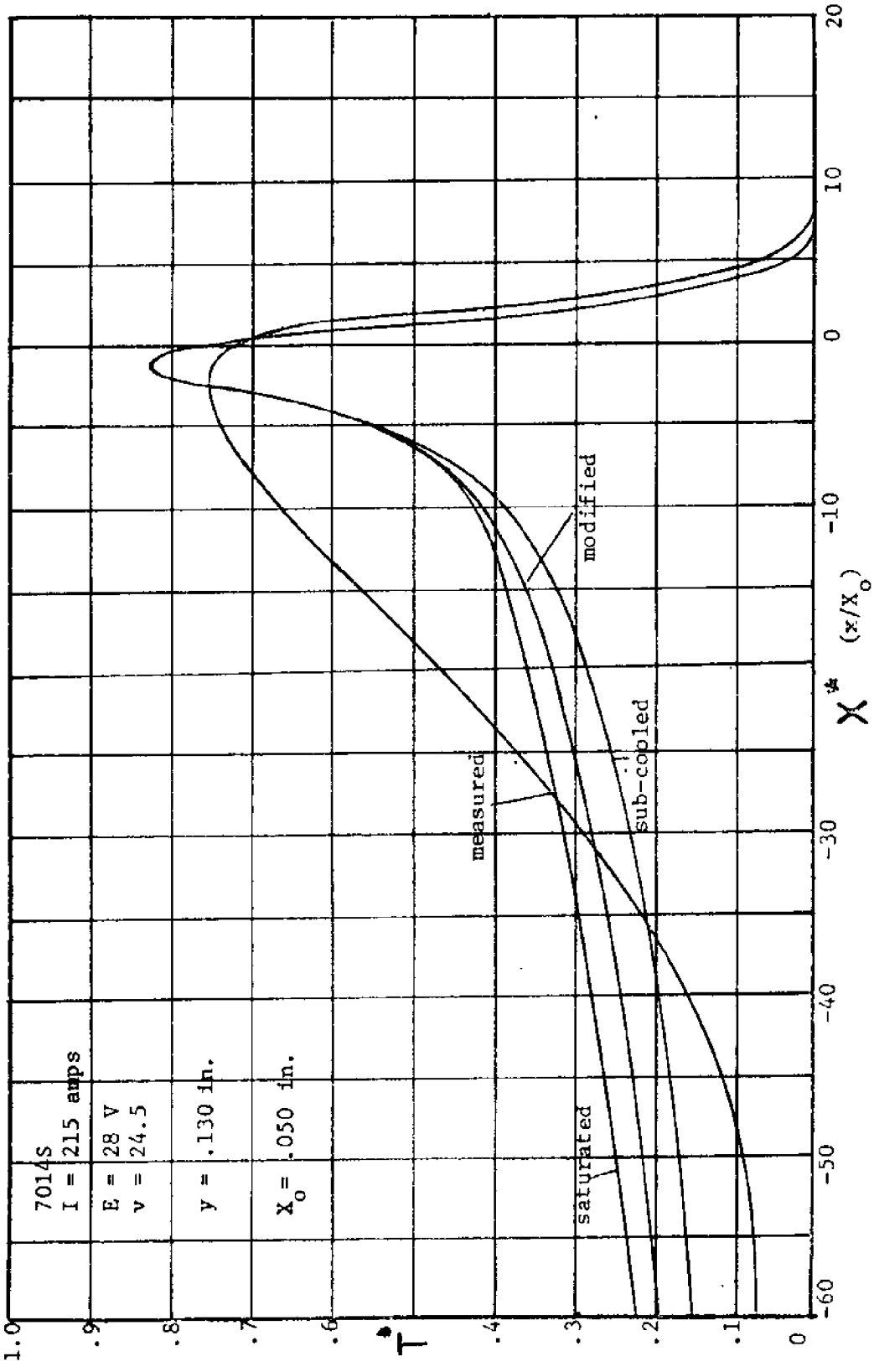

FIGURE 5-16

UNDERWATER WELDING TEMPERATURE DISTRIBUTION

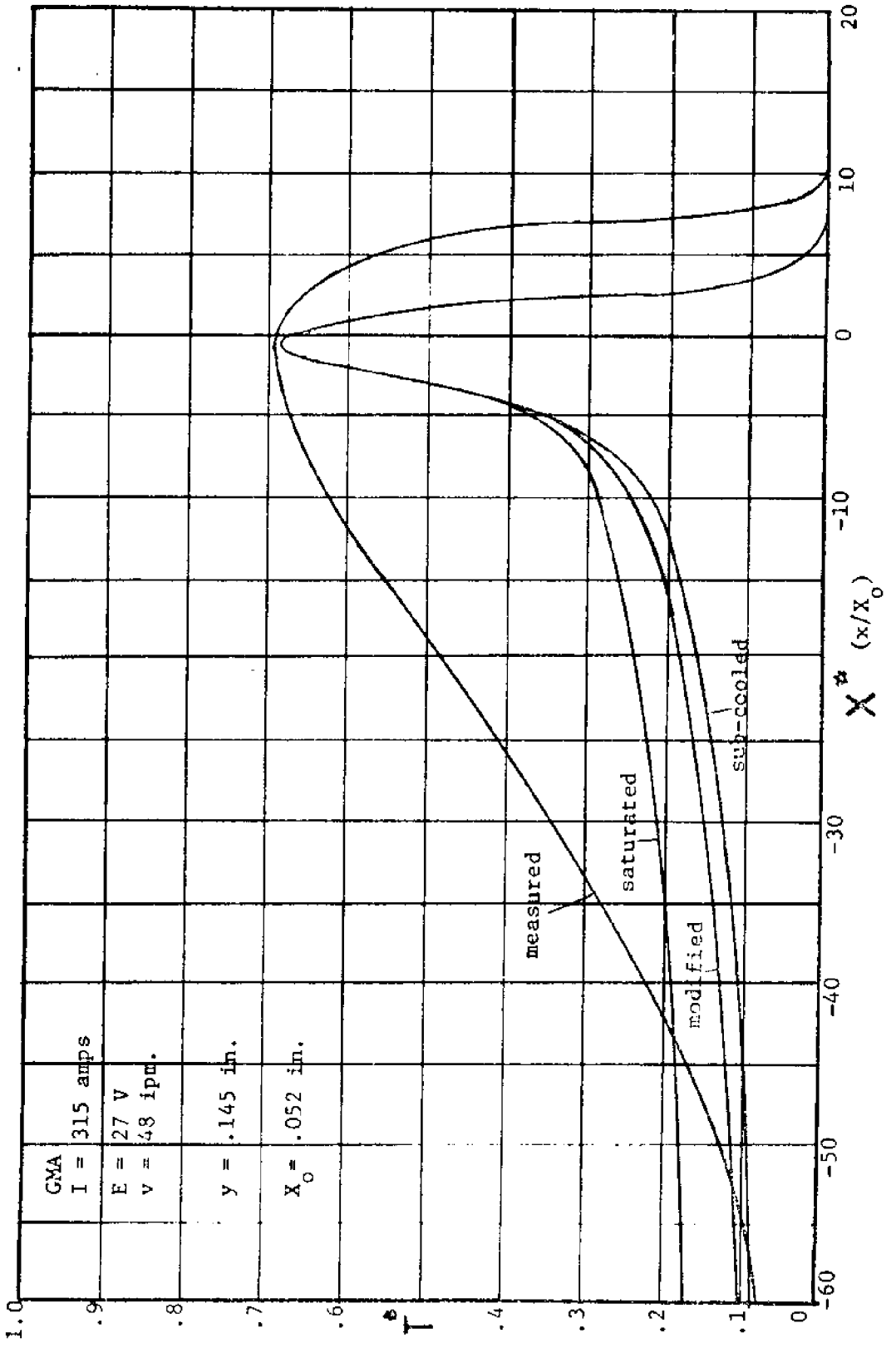

FIGURE 5-17
UNDERWATER WELDING TEMPERATURE DISTRIBUTION

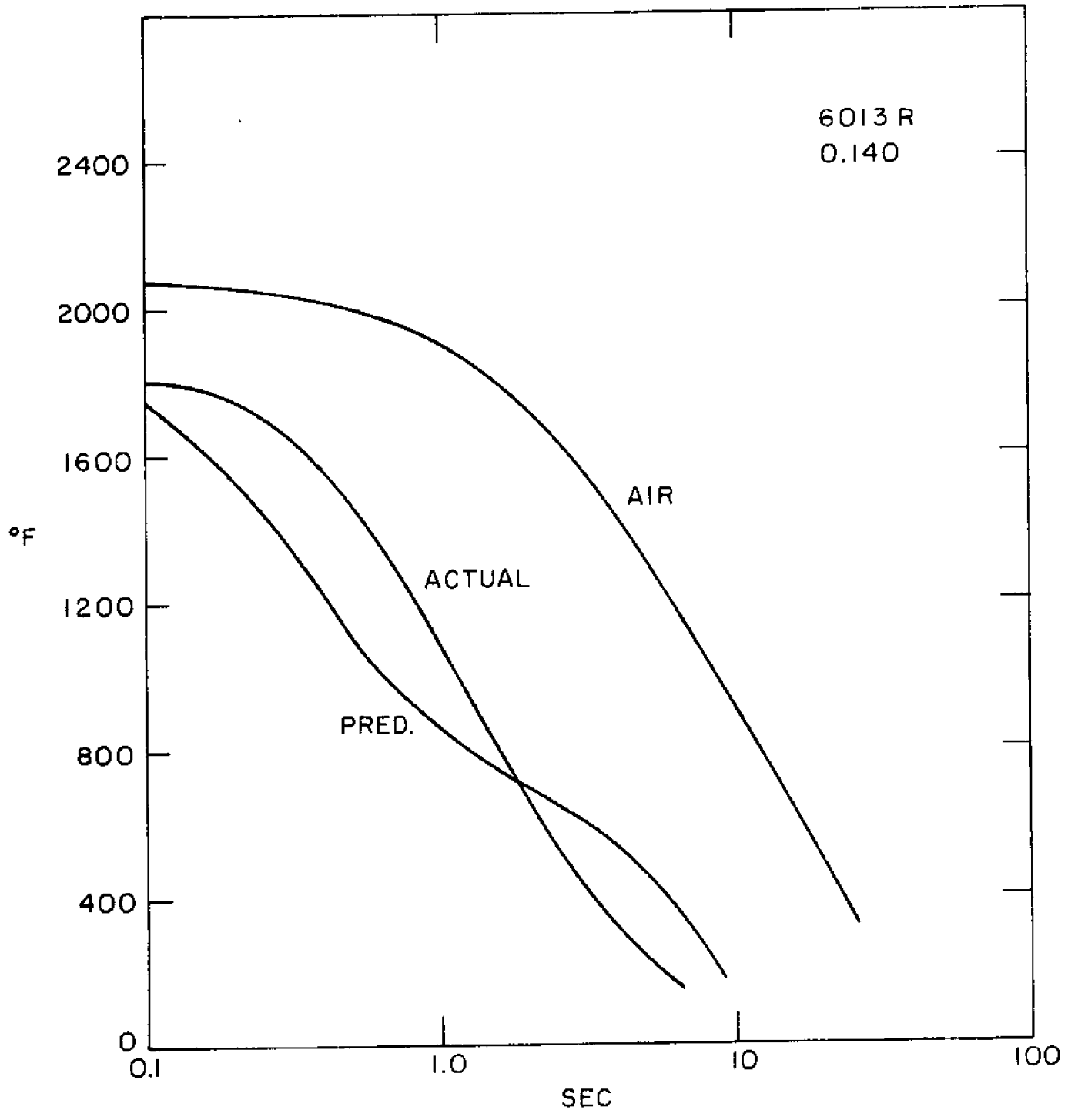

FIGURE 5-18

PREDICTED, ACTUAL, AND OPEN AIR COOLING CURVES - 6013R

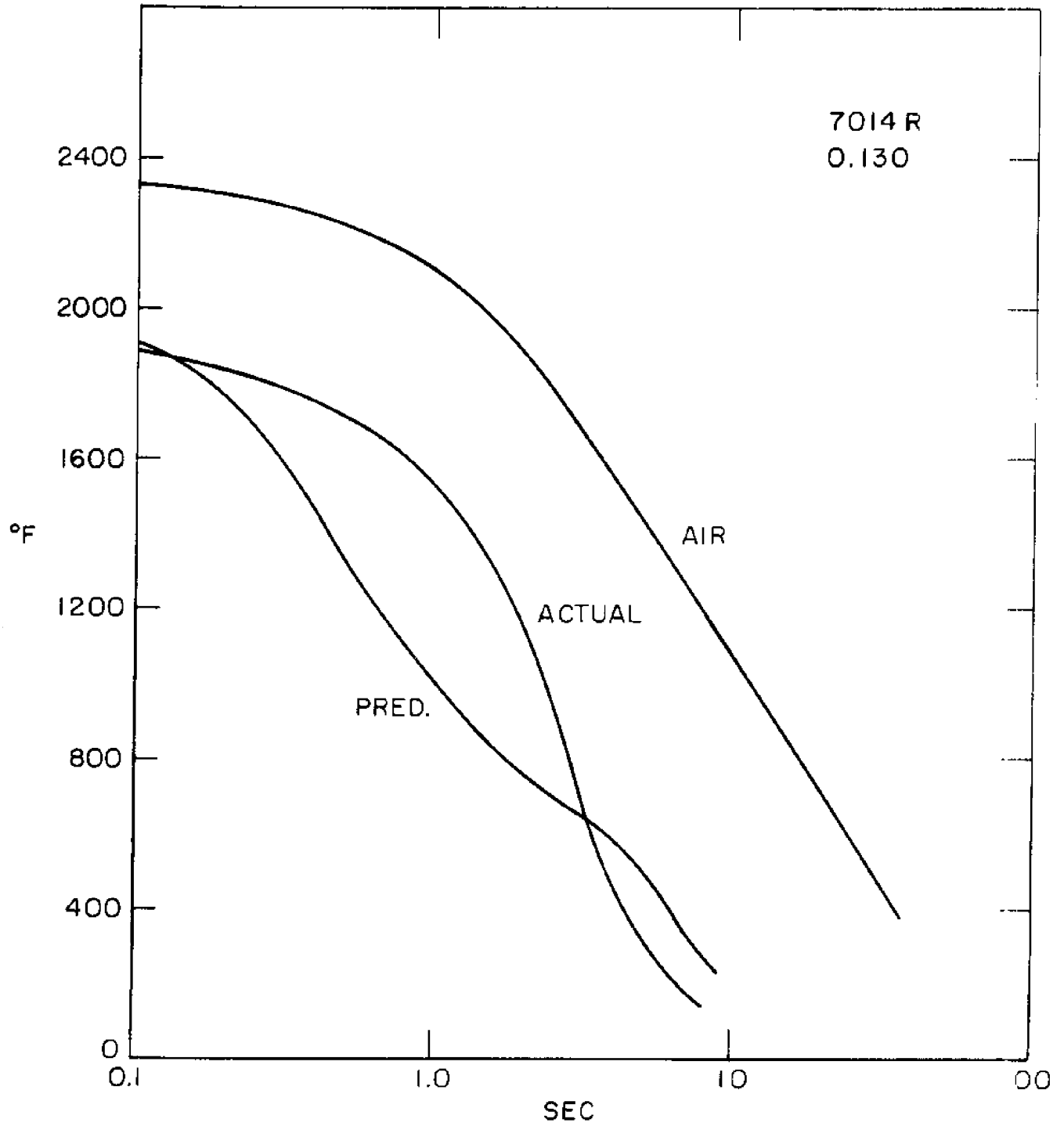

FIGURE 5-19

PREDICTED, ACTUAL AND OPEN AIR COOLING CURVES [illegible]

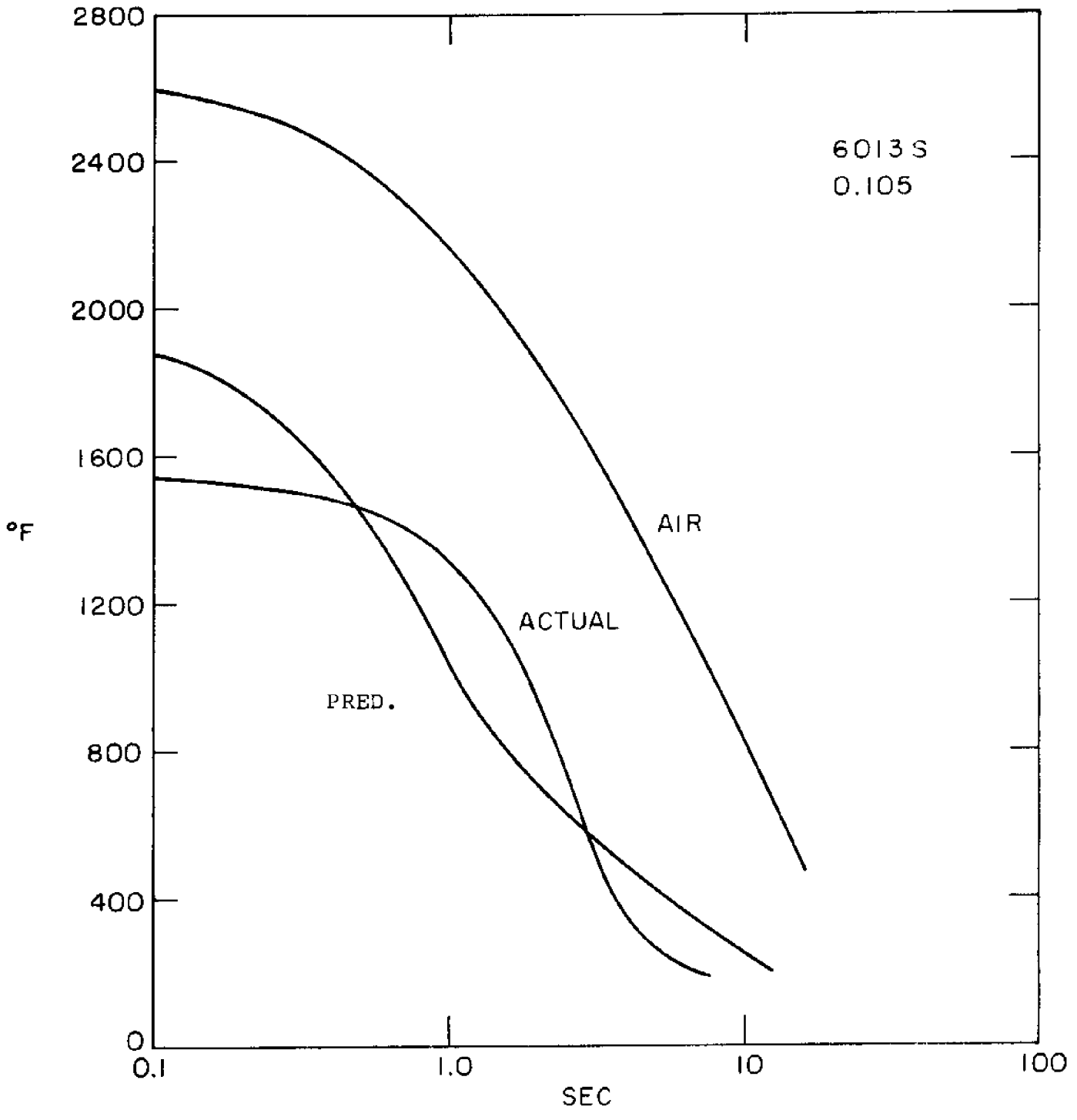

FIGURE 5-20

PREDICTED, ACTUAL, AND OPEN AIR COOLING CURVES - 6013S

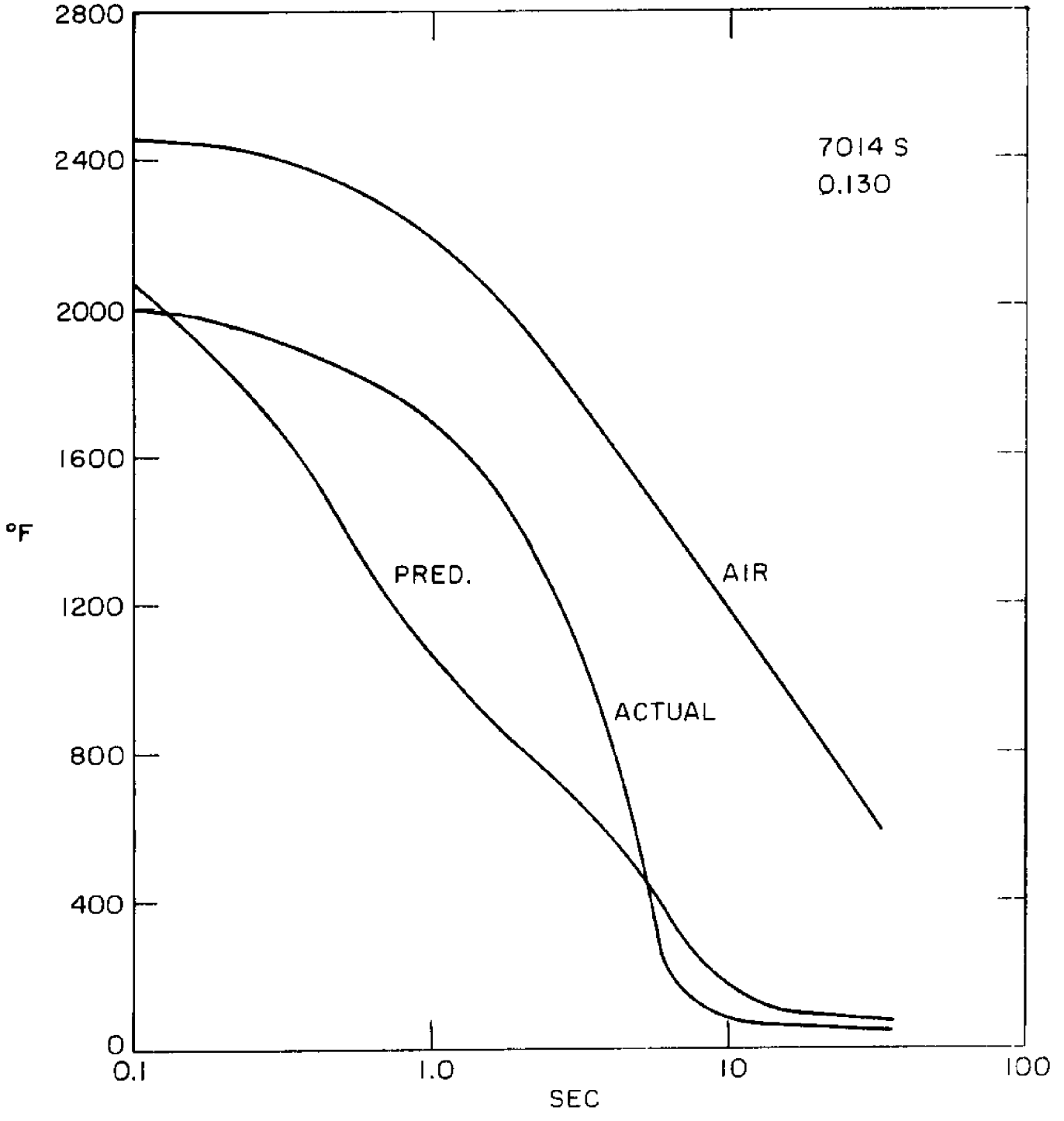

FIGURE 5-21

PREDICTED, ACTUAL, AND OPEN AIR COOLING [illegible]

tures while welding in these positions must be derived.

(2) Testing under various conditions of salinity and pressure must also be conducted.

(3) Application to thicker plates should be made.

(4) The combination of GMA and shroud welding could prove effective. Investigation is warranted.

(5) All calculation and welding was done using a single-pass technique. Other investigators have found multi-pass methods to be very efficient. Experiments should be conducted in this area.

Hopefully, this work will give useful insight and a good start to any future investigation.

Probably the most useful information uncovered in this report pertains to "above the plate" phenomena. Analysis of the various processes has pinpointed their problems and revealed a number of possible methods for overcoming these problems.

(1) The SMA process is not an effective process as is. This is due to the limited shielding offered by its dynamic bubble. Using multipass methods could increase the reliability of this process, and thus take advantage of its relatively simple and unencumbered application.

(2) The shroud process is limited by the gas production at the arc, and the sliding shroud does not provide a positive, stable barrier. A larger shroud with an external gas supply could make this a very efficient process.

(3) Probably most unexpected of all was the poor performance observed using the GMA process. The shielding gas was not impinging to the plate, but was just bubbling up ineffectively. Higher flow rates or combination with a shroud-type device could greatly improve the process.

In closing, although the inadequacy of the boiling model limited the accuracy of the predicted temperature distributions, a greater understanding of the interactions between the boiling, spread heat, and "above the plate" phenomena has been derived.

Most important, the knowledge obtained using high-speed cinematography to study "above the plate" phenomena has suggested a number of alternatives for future development.

5.7 RECOMMENDED NEW APPROACH TO TWO-DIMENSIONAL MATHEMATICAL MODEL OF UNDERWATER WELDING

Due to the complexity of three-dimensional approaches, only two-dimensional heat transfer has been considered. Selection of an appropriate two-dimensional mathematical model in order to understand overall mechanisms of heat flow can be divided into two types:

(1) The first type model predicts the heat losses due to boiling, convection, and radiation on the surface plate boundaries. The investigation of the"above the plate" phenomena is the major effort for understanding of the rapid cooling mechanisms which are directly related to the quench rate during the welding process. This has been the model described in this report.

(2) The second type model predicts the conductive heat flows in the weldment and in the base metal. This is the main flow through the HAZ, and so is responsible for the metallurgical structure change in the HAZ during the welding process. This section will discuss this alternative approach in general.

The graphical expression of the mathematical model for this approach is shown in Figure 5-22. The governing equation is the same as that discussed for the first type model. All four boundaries are subject to convection of boiling and convection

FIGURE 5-22

MATHEMATICAL MODEL FOR METALLURGICAL STRUCTURE INVESTIGATION

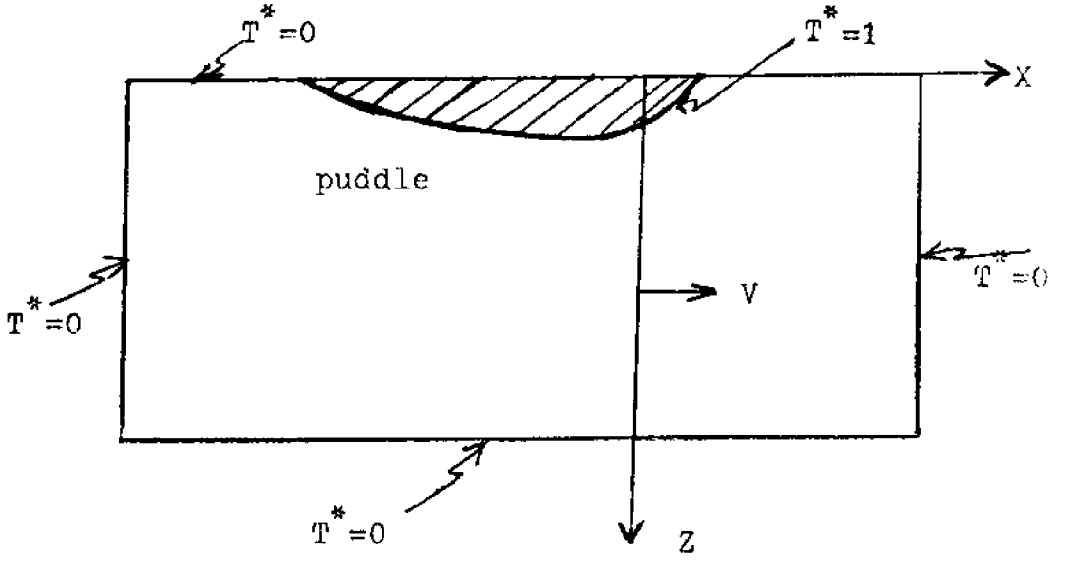

FIGURE 5-23

QUENCH RATE TRANSFORMED FROM QUASI-STEADY RESULTS

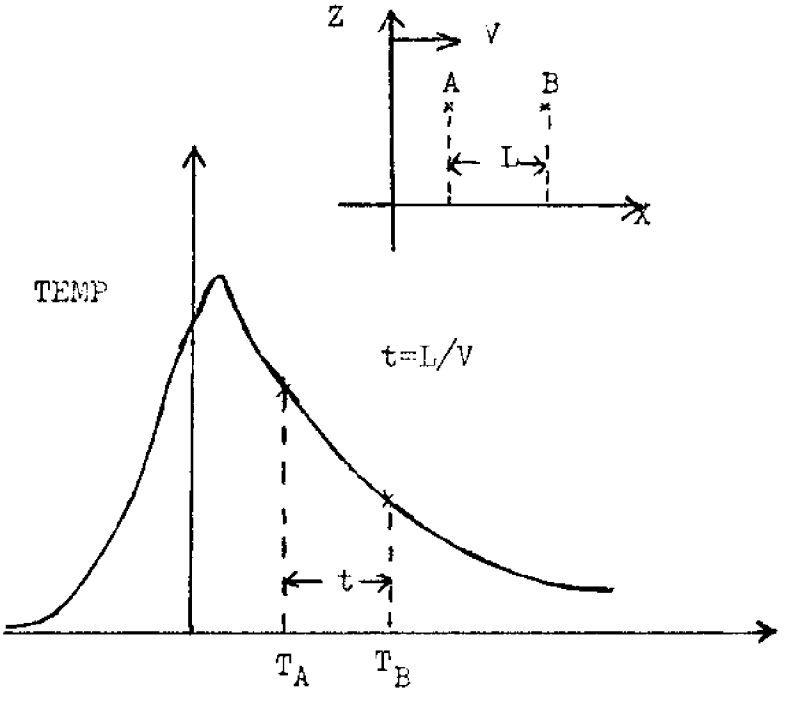

losses except the hot spot on the top surface. The determination of the melting temperature contour is again by using Rosenthal's point source temperature equation along with certain geometric aspects of the weld pool which are found by empirical measurements; the maximum length of the puddle and the depth of penetration. Heat losses on the boundaries can use the same boiling and convection model as was appropriate for the surface type model for the top and bottom of the plate. For two side-boundaries, a conductive heat flux approximation can be employed.

The entire computer model is based on the governing equation and its finite difference equivalent, which has been discussed, along with the respective boundary conditions of the new approach. Since the computer method is the same as that in the first part of the two approaches, the detailed investigation numerically is not covered in this report.

Due to the high nonlinearity of the equations, it is very difficult to simulate a transient situation. Fortunately, the rapid cooling rate can be expressed in terms of quasi-steady results with some transformation steps. For instance, the computed temperatures at two different points along the same horizontal line, T_A and T_B (Figure 5-23), can be plotted as the temperature change at one position in the base metal during a time which is the ratio of the distance between two points and the electrode speed. With the predicted temperature vs. time plots, along with CCT diagrams, it is easy to explain the metallurgical structure change in the weldment, HAZ, and the base metal during welding process.

5.8 REFERENCES - PART FOUR

1. Vagi, J. J., Mishler, Randall, "Report on Underwater Welding and Cutting--State of the Art," Battelle Memorial Institute.

2. Masubuchi, K., Materials for Ocean Engineering, M.I.T. Press, M.I.T., 1970.

3. Silva, E. A., An Investigation of Fusion Controlled Metallurgical Bonding in a Marine Environment, Ph.D., University of California at Berkeley, 1971.

4. Madatov, "U.W.W. Electrodes-Iron Powder Coatings," Welding Production, Vol. 10, No. 8, 1962.

5. Madatov, "Special Features of Underwater Touch Welding," Automatic Welding, Vol. 15, No. 9, 1962.

6. Madatov, "Energy Characteristics of the U.W.W. Arc," Welding Production, Vol. 13, No. 3, 1966.

7. Madatov, "Shape Relations for U.W.W.," Welding Production, Vol. 16, No. 3, 1969.

8. Avilov, T. I., "Electrodes for U.W. Welding and Cutting Steel," Welding Production, Vol. 3, No. 6, 1955.

9. Madatov, N. M., "The Properties of the Bubble of Steam and Gas Around the Arc in U.W.W.," Automatic Welding, Vol. 18, No. 12, 1965.

10. Silva, E. A., "Shielded Metal Arc Welding Underwater with Iron Powder Electrodes," Welding Journal, pp. 406-415, June, 1971.

11. Silva, E. A., "Gas Production and Turbidity During Underwater Shielded Metal Arc Welding with Iron Powder Electrodes," Naval Engineer's Journal, pp. 59-63, December, 1971.

12. Silva, E. A., "Welding Processes in the Deep Ocean," Naval Engineer's Journal, Vol. 80, No. 4, pp. 561-568, August, 1968.

13. Tanbakuchi, R., "Metal Temperatures During Arc Welding," Ph.D. Thesis, University of Wisconsin, 1967.

14. Pavelec, V., "Temperature Histories in Thin Steel Plate Welded with TIG," Ph.D. Thesis, University of Wisconsin, 1968.

15. Liphert, R., "Temperature Distribution in Thin Steel Plate During Gas Metal Arc Welding," Ocean Engineer Thesis, M.I.T., 1972.

16. Staub, J., "Temperature Distribution in Thin Plates Welded Underwater," Naval Engineer's Thesis, M.I.T., 1971.

17. Forster, K. E., Grief, R., "Heat Transfer to a Boiling Liquid-Mechanism and Correlations," Journal of Heat Transfer, February, 1959.

18. Rohsenow and Choi, Heat, Mass, and Momentum Transfer, Prentice-Hall, Inc., Englewood Cliffs, New Jersey, 1961.

19. Zuber, T., "The Hydrodynamic Crisis in Pool Boiling of Saturated and Sub-Cooled Liquids," International Developments in Heat Transfer, Part II, ASME, p. 230, 1961.

20. Freith, F., "Principles of Heat Transfer," International Textbook Company, 1969.

21. Jacob, M., "Heat Transfer," John Wiley and Sons, New York, 1949.

22. Lamb, H., Hydrodynamics, 6th Edition, Cambridge University Press.

23. Berensen, PL J., "Film Boiling Heat Transfer from a Horizontal Surface," Ph.D. Thesis, M.I.T., 1960.

24. Nestor, O. H., "Heat Intensity and Current Density Distribution at the Anode of High Current, Inert Gas Arcs," Physics of the Welding Arc, British Institute of Welding, 1966.

25. Rykalin, N. N., "Berechnungder Warmevorgange beim Schweissen," Veb Verlag Technik, Berlin, 1957.

26. Brown, A., "Methods of Research in Underwater Welding," B.S. Thesis, M.I.T., 1971.

27. Davidson, J. F., "Bubble Formation at an Orifice in an Inviscid Liquid," Institute of Chemical Engineers, Vol. 38, 1960.

28. Milne-Thomson, L. N., Theoretical Hydrodynamics, 3rd Edition, 1955.

29. McAdams, W., Heat Transmission, McGraw-Hill Book Co., New York, 1954.

30. Westwater, "Photographic Study of Boiling," Industruial and Engineering Chemistry, Vol. 47, 1955.

31. Greenspan, D., "Introductory Numerical Analysis of Elliptic Boundary Value Problem," Harper and Row, 1965.

BLANK

PART FIVE

THE GENERAL CONCEPTS OF UNDERWATER METALLURGY, MICROSTRUCTURE, AND METAL TRANSFER

Contents

6.0 INTRODUCTION

This portion of the report presents the general principles and conceptual framework of welding metallurgy and microstructure. Basic air welding results and phenomena are presented and modified or interpreted to apply to the peculiar conditions of underwater welding. The basic concepts are developed in the following order:

(1) Temperature histories in underwater welding. Differences in cooling rates characterize the differences between air welds and underwater welds.

(2) Basic metallurgy and microstructure of underwater welds.
The Heat Affected Zone - Grain size changes
- Crystal transformation structures

(3) Microhardness in underwater welding. What determines microhardness and how it can help analyze the cooling rates of underwater welds.

(4) Potential underwater defects - Quenching-induced
- Hydrogen-induced

6.1 TEMPERATURE HISTORIES IN UNDERWATER WELDING

Before reporting and discussing some results pertaining to solidification and microstructural transformations of a water weld, it is necessary to consider the heat transfer and flow processes which are ultimately responsible for these metallurgical structures and thus, the mechanical properties of an underwater weld. The heat affected zone is of particular interest in weld metallurgy. This area has been found to be susceptible to critical defects such as microcracking, hydrogen embrittlement, low notch toughness, and low ductility.[52] This HAZ region has reached a temperature above the eutectoid temperature (1360°F = 730°C), but below the melting point (2720°F = 1490°C), and metal in this temperature range has

FIGURE 6-1

CORRELATION OF THE MAXIMUM
TEMPERATURE WITH REGIONS IN THE HEAT AFFECTED ZONE

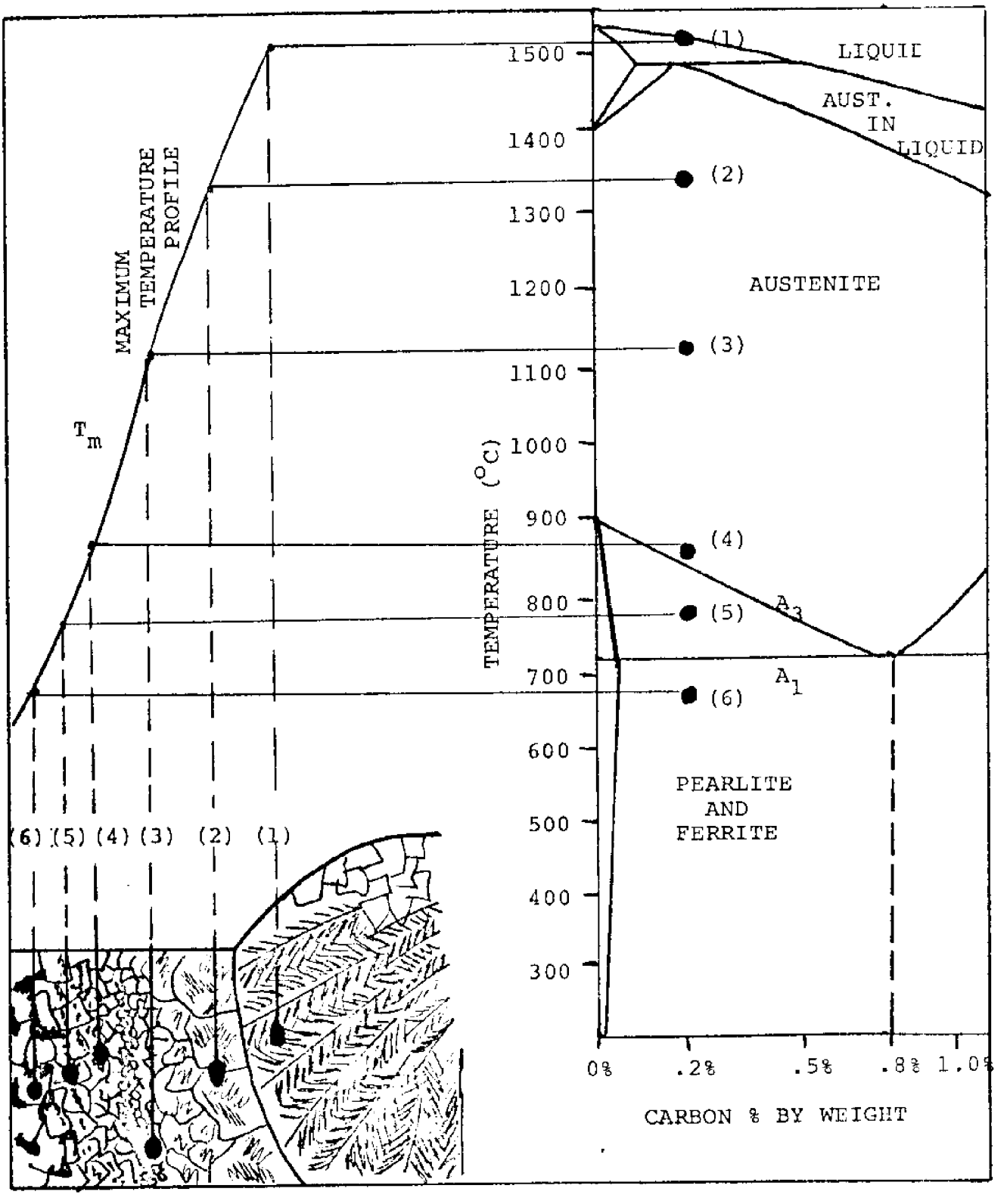

the potential for many crystal transformations depending on the subsequent cooling rate. Figure 6-1 shows the relationship between the maximum temperature reached and the location of the region in the weld HAZ.

The heat input to the workpiece will determine the amount of melting and the penetration of the weld bead. The heat flow mechanisms will affect both the time that a region stays at its maximum temperature and the cooling rates from that temperature. For surface heat sources moving at a constant rate along a continuous, even joint, a quasi-static temperature distribution will form around the arc.[12] The isothermal lines represent the potential for heat flow. Heat will flow perpendicular to these lines at a rate directly proportional to the temperature differences between the isotherms. The basic heat equation describing heat flow in the welded plate is well-known.[57] However, those portions of the boundary conditions which regulate the heat flows at the plate-water interface are unknown.[65]

For this reason, several types of approximations have been used to simplify the solution of this heat flow equation. The welding arc can be grossly modelled as a point source of heat on the surface of a semi-infinite plate. This solution predicts a surface temperature that is inversely proportional to the distance from the heat source. Because underwater conditions produce very high heat flow rates away from the weld puddle, and because the weld puddle is not a point source, the predicted temperature profiles are not very accurate for the HAZ region of the welded plate. Other workers have used a two-dimensional approximation for modelling thin plate welding. This also produces misleading results. More recently, computer techniques have been applied to this problem.[53,66] Although approximations must still be made, more involved boundary conditions can be used. The weld puddle can serve as the inner boundary for heat input. Com-

puter modelling of underwater shielded metal-arc welding has been attempted at M.I.T.[14,65] Although these analytical and numerical methods have not completely described the thermal history of underwater weld HAZ regions, several important trends, which have been confirmed experimentally, are obtained. An increase in travel speed or other factors which lower the heat input to the weld will produce a smaller weld bead and will lead to more rapid cooling rates in the HAZ. This is especially critical in water welds. Regions of the HAZ which are further from the fusion line will experience lower maximum temperatures, and the cooling rates from the lower temperatures will be slower. Figure 6-2 illustrates these basic trends and emphasizes the shorter temperature history of a water weld, the higher maximum temperatures near the weld fusion line, the faster cooling rates from the higher temperatures, and the extremely rapid cooling rates in an underwater weld near the weld fusion line. Cooling rates are illustrated by the downward sloping arrows. It has been determined that the cooling rate at 540°C (1005°F) is a critical one in determining the structural transformations that will occur.[74]

6.2 THE BASIC METALLURGY AND MICROSTRUCTURE OF UNDERWATER WELDS

A basic understanding of welding metallurgy and microstructure is necessary in order to deal with the problems associated with underwater welding. Many of the difficulties stem from the rapid quenching of the weld zone by the surrounding water environment. The microstructure present in an underwater welded joint will be a direct consequence of the composition of the base metal and welding electrode as well as the thermal history of the welded joint. The macroscopic properties of the joint, such as tensile strength, ductility, hardness, notch toughness, and fatigue strength,

FIGURE 6-2

TEMPERATURE HISTORIES OF AIR WELDS COMPARED TO THOSE OF UNDERWATER WELDS

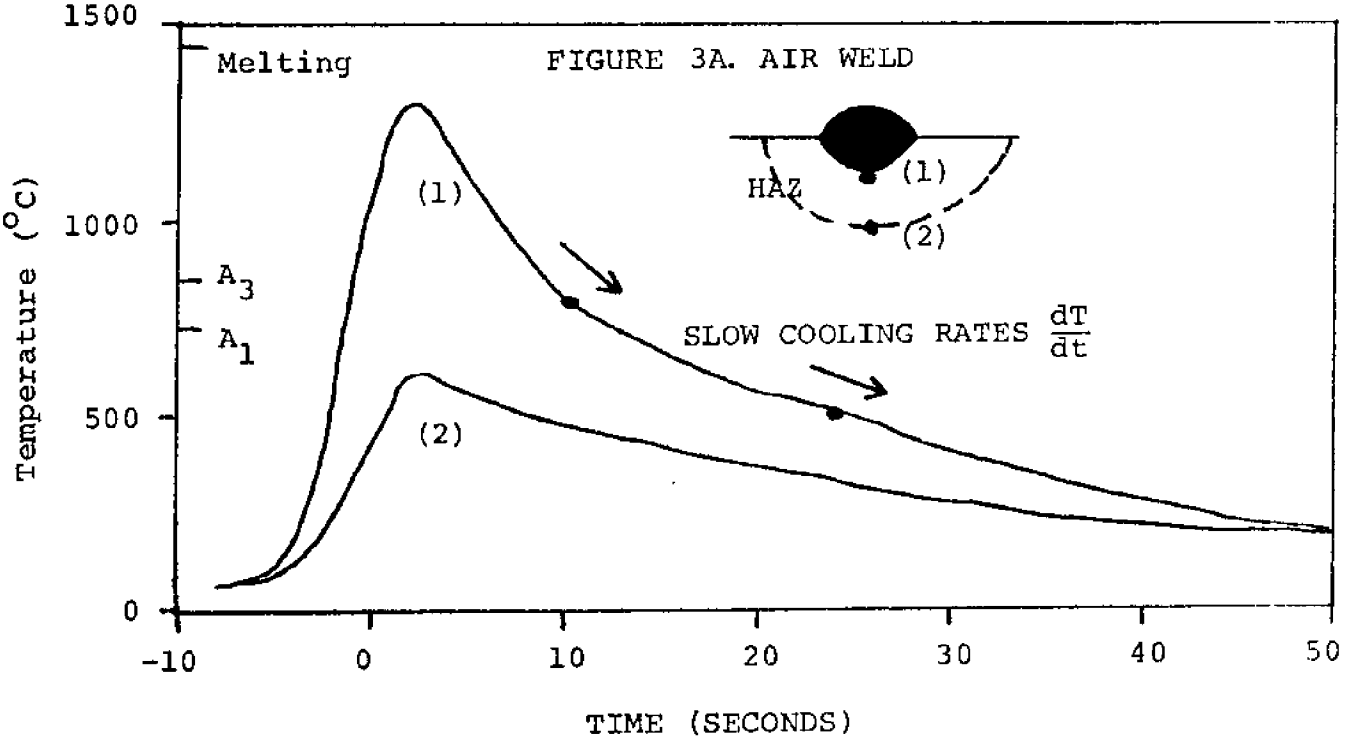

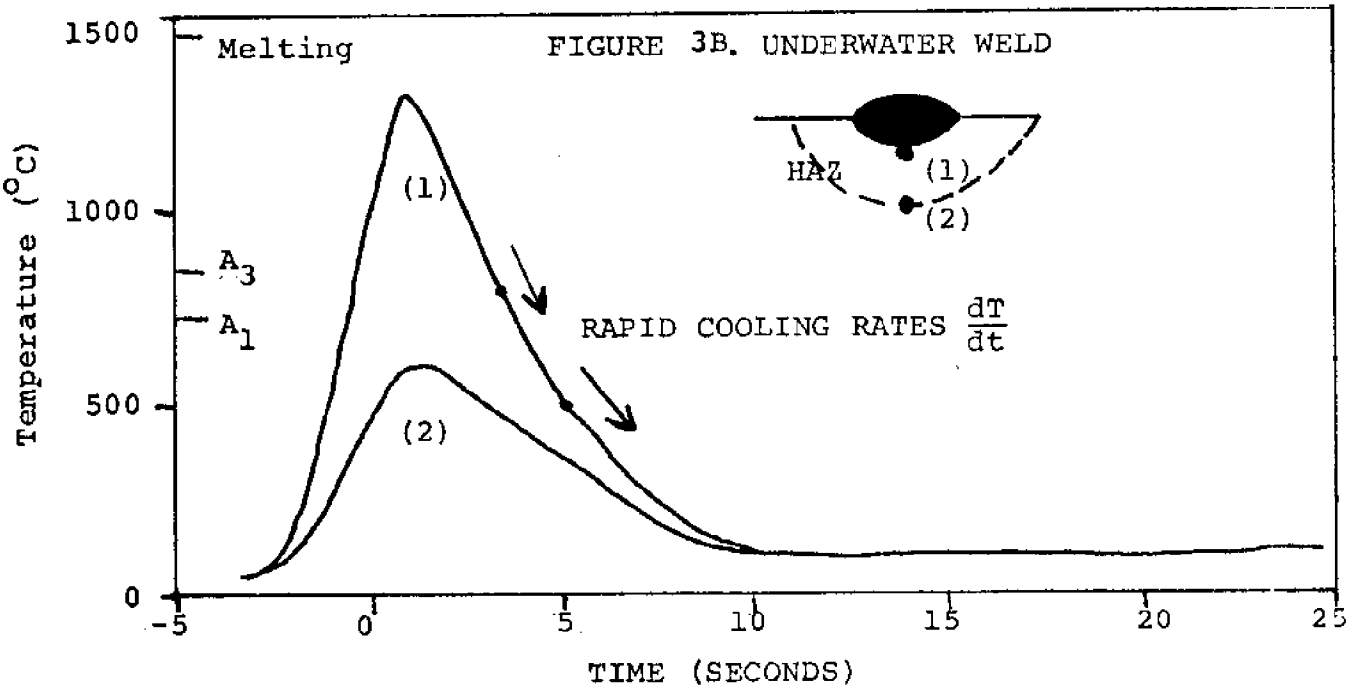

can be related directly to the microstructure. Thus, an investigation of the microstructure of underwater welds is of practical engineering interest, as well as fundamental scientific importance.

The microstructure in the vicinity of a welded joint is very complex and non-homogeneous due to varying structures which result from differing thermal histories. Basically, these different structures can be separated into three areas: weld metal; heat affected zone (HAZ), and; base metal. Figure 6-3 shows the three zones and the differences in microstructure associated with each. The heat affected zone is a very important region in the study of underwater welding because it is affected the most by the increased cooling rates.

There are two elements that influence the structure which is present in the HAZ of low-carbon underwater welds. First, due to recrystallization and growth, there is a grain size gradient across the zone. This is a result of the temperature reached and the length of time the temperature is held in any particular area. Secondly, during cooling, a microstructure transformation from austenite to some other crystal structure will occur in those regions whose maximum temperature has exceeded the low critical temperature, A_1.

The first step in analyzing the microstructure of a welded joint involves looking at the grain structure throughout the specimen. Grains are simply pockets of metal having the same lattice orientation. The size and shape of grains are dependent upon the thermal history of any particular area. For example, dendrites, because of the strong directional heat flow of solidification, grow more in one direction than any other. Therefore, long thin grains are a result of this growth pattern. However, another type of grain, the equiaxed grain, grows equally in all directions.

MICROHARDNESS AND MICROSTRUCTURE OF UNDERWATER WELD METAL, HEAT AFFECTED ZONE, AND BASE METAL

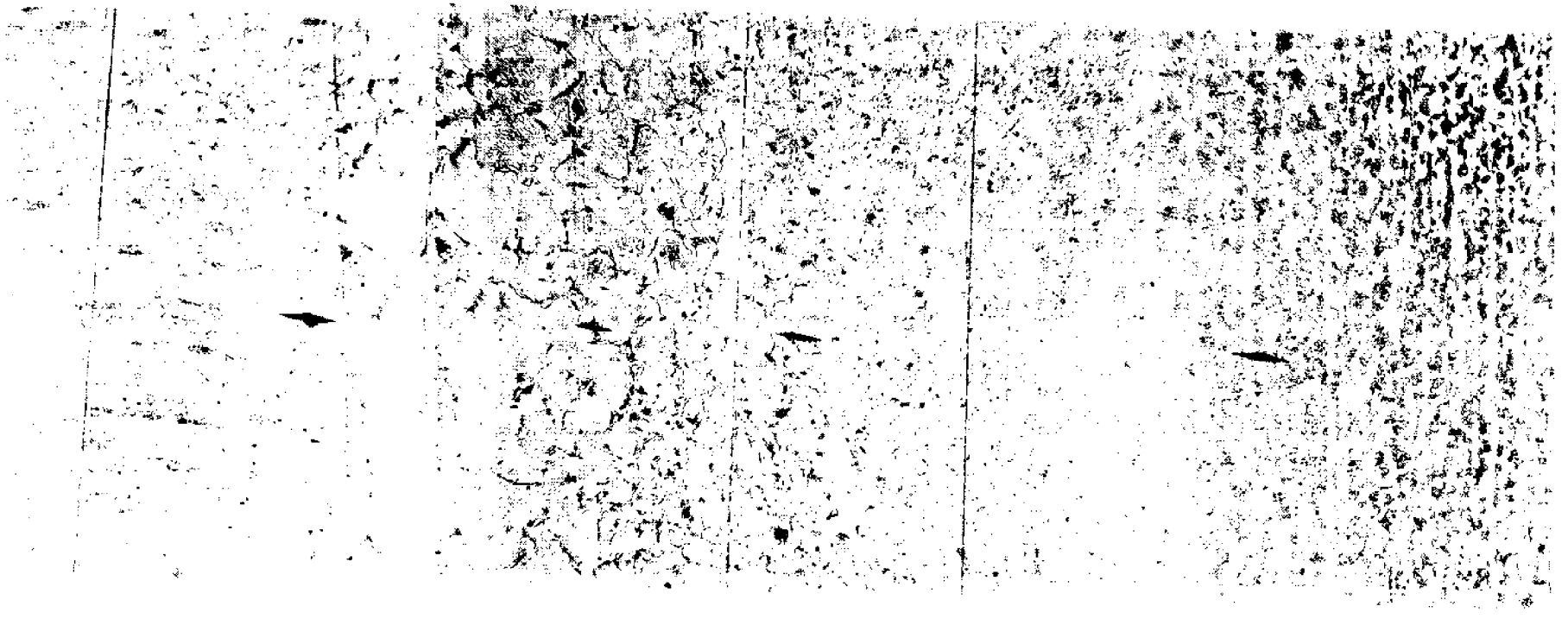

FIGURE 6-3

STRUCTURE OF THE WELD METAL, HAZ AND BASE METAL OF UNDERWATER WELD

6.21 Grain Size Changes

Recrystallization, a process involving nucleation and growth, occurs in metals at elevated temperatures. Nucleation of new grains takes place at the points of highest strain or dislocation buildup when the temperature of the metal structure reaches or exceeds the upper critical temperature (A_3). As long as the temperature is held at or above the recrystallization level, the new grains grow at the expense of others. Due to the greater number of grain boundaries in a fine-grained structure, which are collection points of impurities, dislocations, and brittle phases, smaller grains are tougher, stronger, and harder than the larger ones.

The weld zone, the first of three specific areas, has a composition resulting from the mixture of molten base metal and molten electrode material. Upon cooling, solidification occurs, resulting in formation of tree-like columnar grains called dendrites. The initial dendrites nucleate at the interface of the liquid and solid and undergo epitaxial growth in a direction opposite to the direction of heat flow. This means that the dendrites tend to grow roughly perpendicular to the weld pool boundary toward the center of the weld. Occasionally, the last portion of weld metal to solidify forms a small area of equiaxed grains in the center of the weld zone. This occurs because the area nucleates itself and solidified almost instantaneously.

Most of the HAZ has been heated above the lower critical temperature, A_1 (133°F). At this temperature, the pearlite and ferrite structure of the base metal begins a transformation to austenite, a solid solution of carbon in gamma iron. Recrystallization also begins in this regions. Proceeding from the fusion line to the unaffected base metal, the HAZ may be divided into five general areas of interest (See Figure 6-1):

(1) Immediately adjacent to the fusion line, the metal has been heated almost to the melting point. Often partial liquation of the grain boundaries occurs due to the high concentration of impurities which lower the melting point. This is extremely detrimental to the welded joint because hot cracking may occur.

(2) The temperature in this region has far exceeded the upper critical, A_3. This results in a severely overheated area allowing a maximum amount of grain growth.

(3) The next area is called the annealed region for the temperature is high enough to cause full austenization without grain growth but with some grain refinement.

(4) The temperature in this region is not high enough to cause complete austenization, but recrystallization does occur to some extent. Therefore, this area will have a very fine grain size.

(5) This area has been heated to temperatures between the upper and lower critical. Here, some recrystallization and grain refinement occur, but to a lesser extent.

(6) Temperatures in this last area, adjacent to the unaffected base metal, do not reach the lower critical temperature and therefore, no phase changes occur. However, some recovery may take place causing some softening. Softening may also be caused by spheroidization.

The size of the HAZ depends upon the welding process used. Gas welding produces a large HAZ compared with that produced by arc welding. Similarly, the HAZ corresponding to arc welding conducted in air is large compared to that conducted underwater. The metal beyond the HAZ remains unaffected by welding because the temperatures reached are not sufficient to cause any changes.

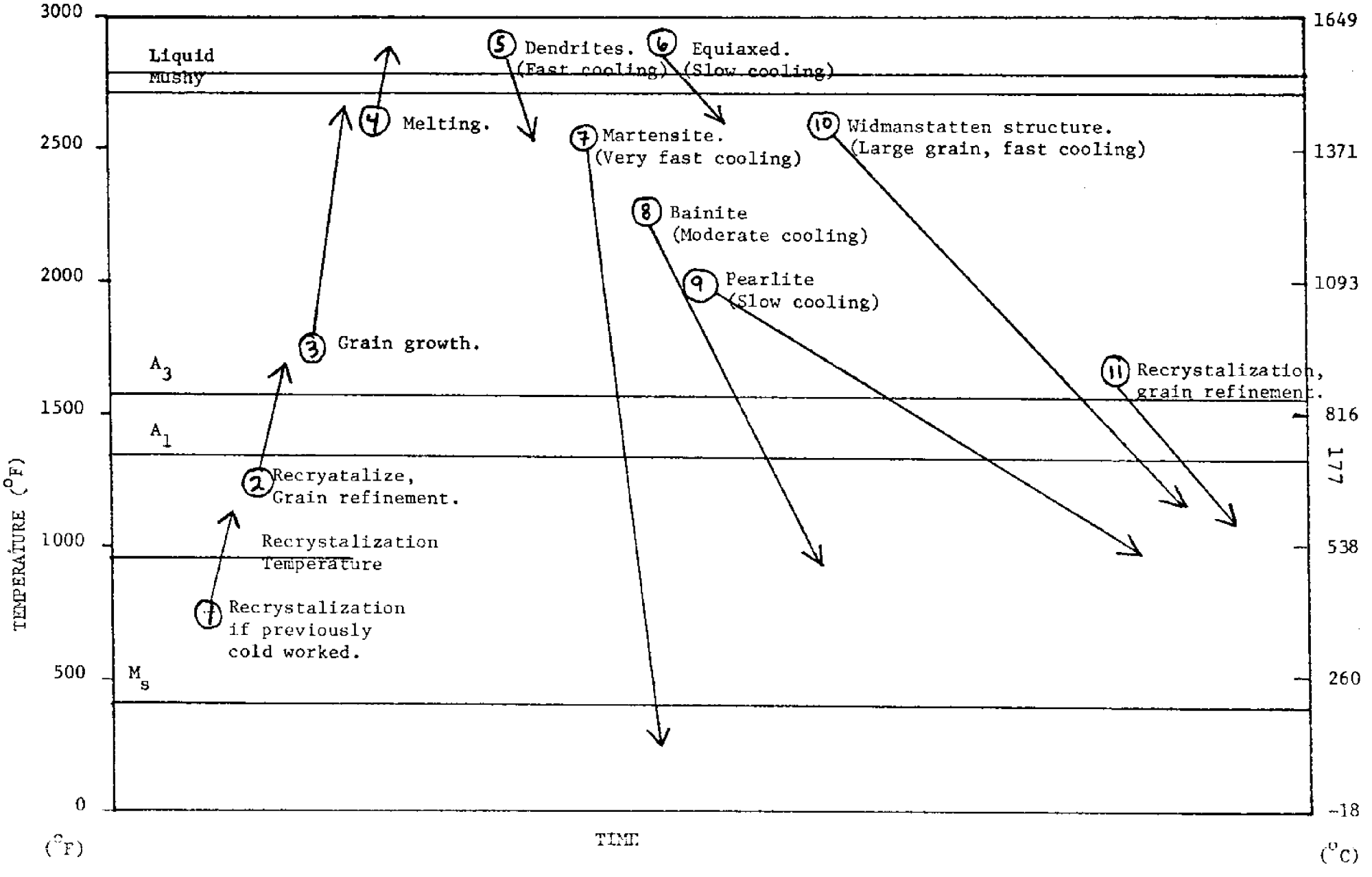

FIGURE 6-4

POSSIBLE MICROSTRUCTURAL TRANSFORMATIONS DURING WELDING

6.22 Iron Carbon Phase Transformations

As grain size is primarily a function of the maximum temperature reached, phase transformation is a result of the cooling rate. A welded joint exhibits several different phases at different point due to changes in cooling rates and the temperatures from which cooling occurs. All of the phases are a result of transformations from austenite. Austenite is a one-phase solid solution of iron and carbon containing up to 2.06% carbon. Austenite occurs at temperatures between the upper critical, A_3, and the solidus temperatures shown in the iron carbon diagram (Figure 6-1). As austenite is cooled slowly, ferrite, which dissolves only 0.008% carbon at room temperature, and cementite, Fe_3C, form in a layered structure called pearlite. The ferrite is very soft, while the cementite, being a carbide, is extremely hard and brittle. At room temperature following a slow cool, the microstructure of 1020 plain carbon steel will be 75% pure ferrite and 25% pearlite. This is calculated using the inverse lever rule and may be easily estimated by viewing the polished and etched surface with a microscope.

The transformations which can occur during heating or cooling of low-carbon (.2%C) steels are schematically illustrated in Figure 6-4. The most important transformation range is between temperatures A_1 and A_3; which is the transformation into or out of the austenite phase field. As a region of the weld cools from the austenite range, there are three possible transformations, depending on the cooling rate:

(1) Pearlite. This occurs with a relatively slow cooling rate. The austenite forms a lamellar arrangement of ferrite and cementite crystals. The transformation process is nucleation and grain growth. This is the equilibrium transformation giving a structure very similar to the original base metal.

(2) Bainite. This transformation is not a nucleation and growth process and requires a more rapid cooling rate. Several types of bainite structures are identified ranging from pearlite-like to martensite-like. It is the transformation which produces all structures intermediate between pearlite and martensite. Bainite forms when the austenite cools rapidly and temporarily traps the carbon atoms in tetragonal ferrite crystals. The carbides subsequently precipitate out on various crystallographic surfaces in a peculiar, characteristic, feathery pattern.

(3) Martensite. This transformation occurs only in rapidly quenched regions. As the crystals cool, they attempt to form ferrite, but the carbide is trapped since it does not have time to diffuse out of the lattice network. The supersaturated solution of ferrite with carbon then is distorted by shear action into tetragonal crystals which can more easily accomodate the carbon atoms. These tetragonal crystals within the ferrite (bcc) matrix is the structure called martensite. The number of tetragonal crystals, and thus, the amount of distortion in the lattice which results in the extreme hardness of martensite, depends on the carbon content of the steel.

There is another peculiar structure which can be identified in a weld microstructure. It has been given the name of its first investigator, Widmanstätten structure. This is a geometrical pattern of ferrite grains which are oriented along previous austenite grain boundaries (Figure 6-5). These ferrite grains outline new pearlite grains as the metal rapidly cools below the lower critical temperature A_1, (1335°F, 724°C). Therefore, Widmanstätten structure occurs as the result of a particular nucleation and growth pattern involving the pearlite transformation from austenite. The intermediate grains of

FIGURE 6-5

IDEALIZED REPRESENTATIONS OF MICROSTRUCTURAL CHANGES DURING WELDING

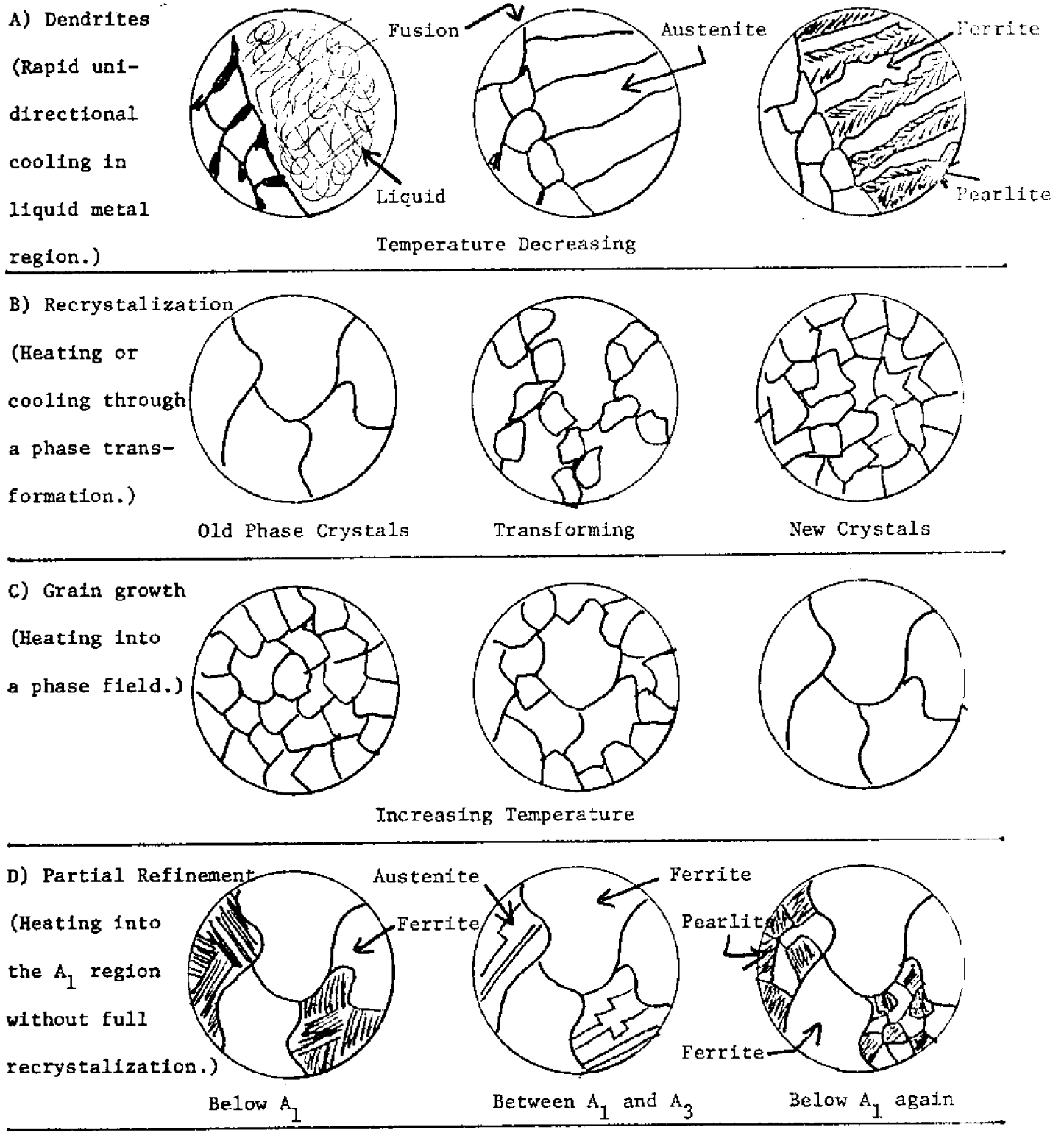

FIGURE 6-5 (Continued)

IDEALIZED REPRESENTATIONS OF MICROSTRUCTURAL CHANGES DURING WELDING

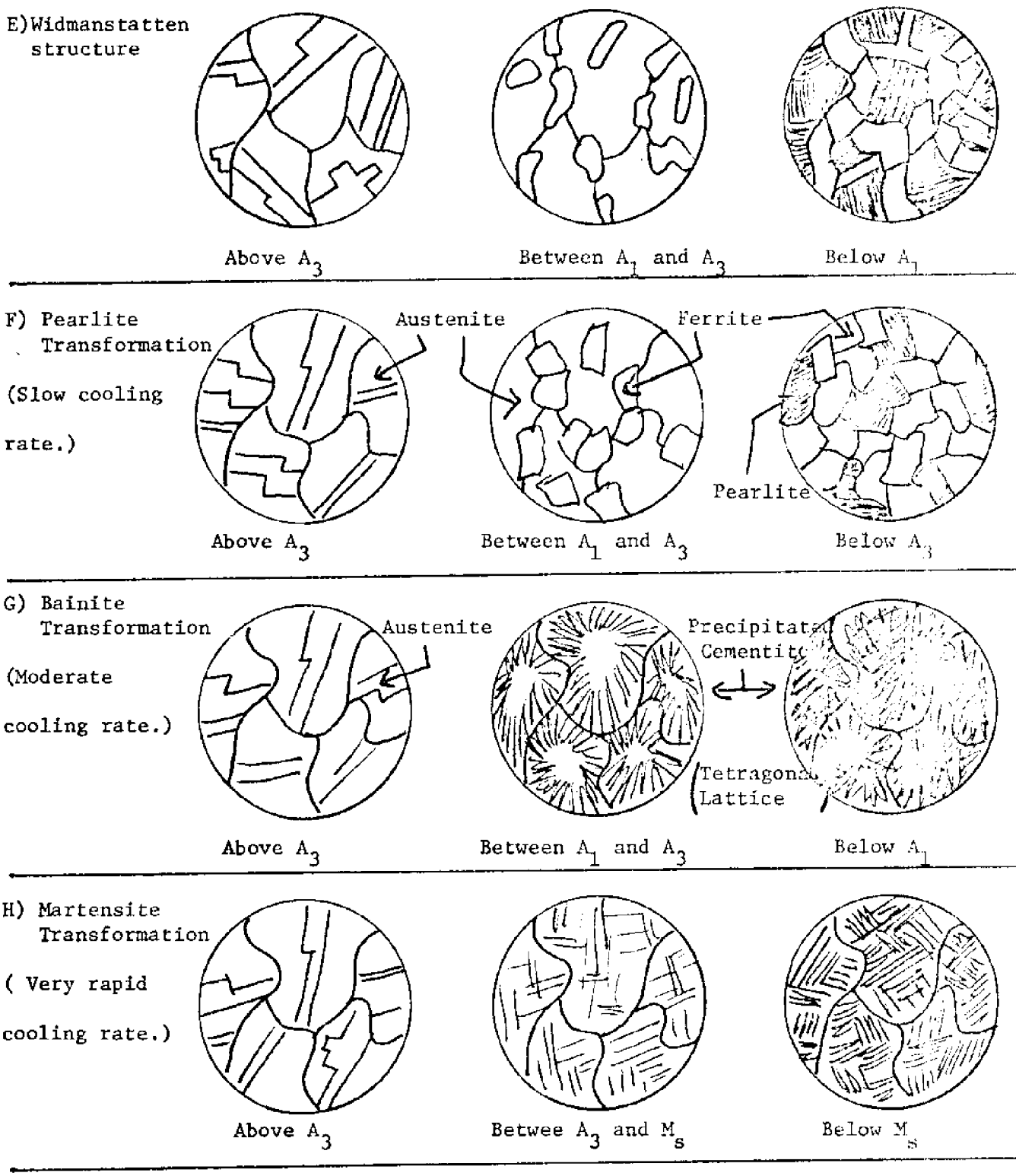

austenite must be very large to form the Widmanstätten structure, and so, only those areas in a weld HAZ which were heated almost to melting [or those areas in the weld forming large original dendrites] are able to produce this peculiar grain pattern. The large grains give this structure poor notch toughness and poor ductility. At the edge of the HAZ, a distinctive structure is observed that appears to be a partial refinement of the original pearlite grains. As the steel is heated between A_1 and A_3, the pearlite changes to austenite and begins to absorb some of the ferrite grains. When the steel is cooled, small grains of ferrite appear in each grain of austenite until A_1, the remaining austenite, changes into very small pearlite grains (Figure 6-5). If the region has been heated to below the lower critical temperature, A_1, there may be a tendency for the iron carbide in the pearlite grains to coalesce into larger particles (spheroidize). But, welding speeds are usually too fast to allow for spheroidization. These are the major changes occurring in the weld microstructure. Their formation processes are depicted by a visual representation of what is happening to the grain structures in Figure 6-5.

It is these crystal structures which can be identified in the weld HAZ and linked back to a particular thermal cycle. However, to identify a specific cooling rate with a resulting structure, experiments must be done to determine, for a particular steel, those cooling rates which are required to produce the various rate dependent transformations. This information can be plotted on charts called Isothermal Transformation Diagrams. Figure 6-6 is the isothermal transformation diagram for low-carbon steel (.2%). This diagram gives a good idea of the hardenability of the steel, but it does not accurately predict the structure for continuous cooling situations, since non-equilibrium conditions will then prevail. So, another diagram has been developed to predict the structures which result from a known constant, or continuous cooling rate.

FIGURE 6-6

RELATIONSHIP BETWEEN IT AND CCT DIAGRAMS FOR .2% C STEEL

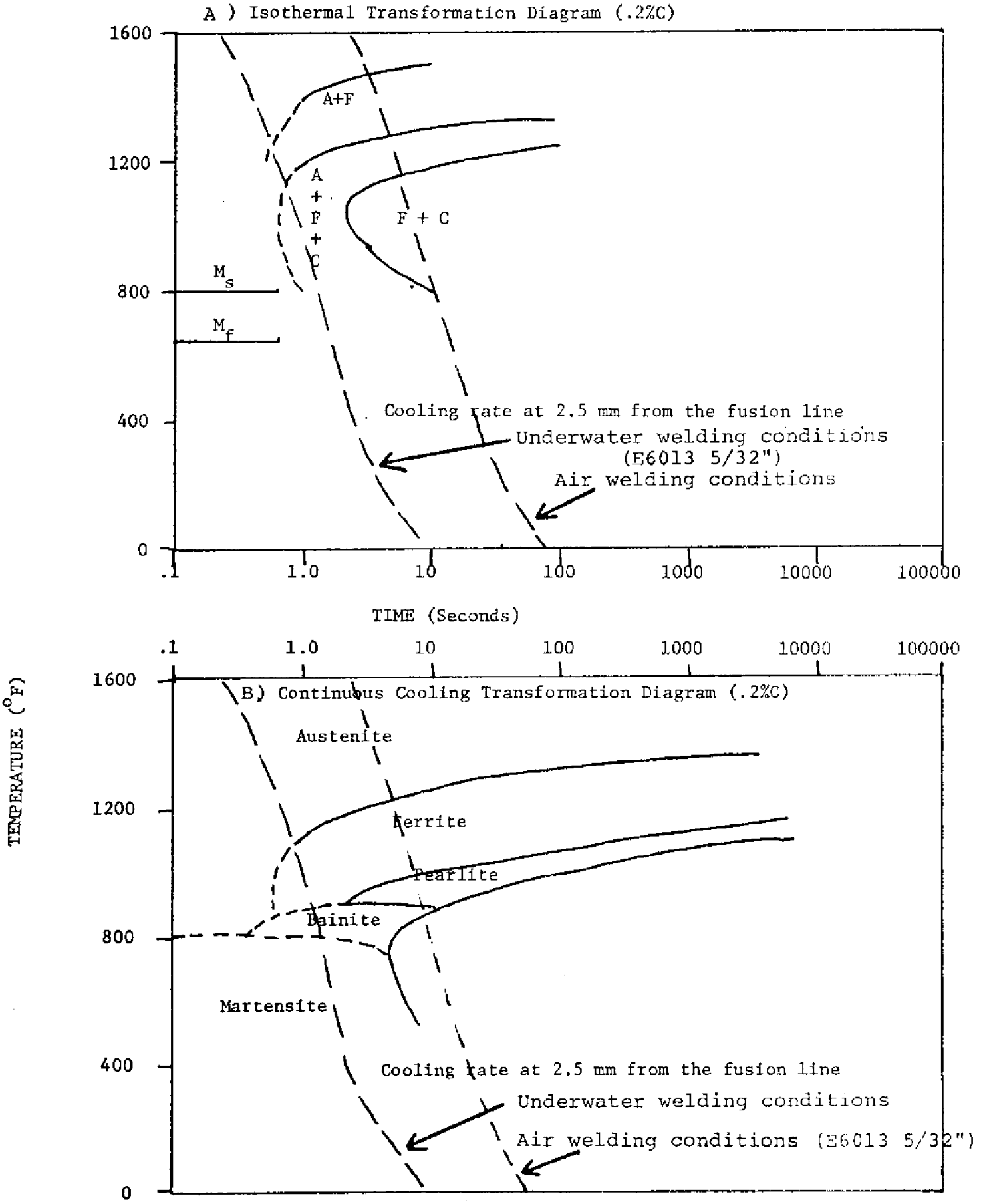

Figure 6-6B shows the similarity between the two types of diagrams for low-carbon steel. More care must be exercised in distinguishing between them for other steels. The Continuous Cooling Transformation (CCT) curves are specific to the austenitized temperature. Since this is varying in the actual weld HAZ, a completely accurate prediction becomes almost impossible. However, by observing the relative amounts of these various recrystallization, grain growth, and phase transformation product structures across the HAZ of air and underwater welds, the basic differences in their thermal histories can be determined and studied.

6.3 MICROHARDNESS IN UNDERWATER WELDING

An investigation of the time-temperature histories of different portions of a weld HAZ will show that various heat treatments occur at these locations and will produce crystal structures that are characteristic of the particular heating and cooling conditions to which the regions were subjected. It then becomes desirable to differentiate between these various crystal transformation structures. One method is of course to view the microstructure using microscopy and noting regions of different grain size and different crystal phases (pearlite, ferrite, martensite). However, it is also possible to indirectly differentiate between these microstructural regions by testing the hardness of each zone, and plotting these values along a cross section of an underwater weld. The hardness values can often be directly correlated with the crystal transformation structures present, and can also be used to indicate what some of the physical properties of the welded joint are likely to be. Figure 6-7 shows an underwater weld microstructure and its corresponding microhardness survey. It will now be explained why hardness can

FIGURE 6-7

MICROSTRUCTURE AND MICROHARDNESS OF #7014 UNDERWATER WELD KHN (100 GM)

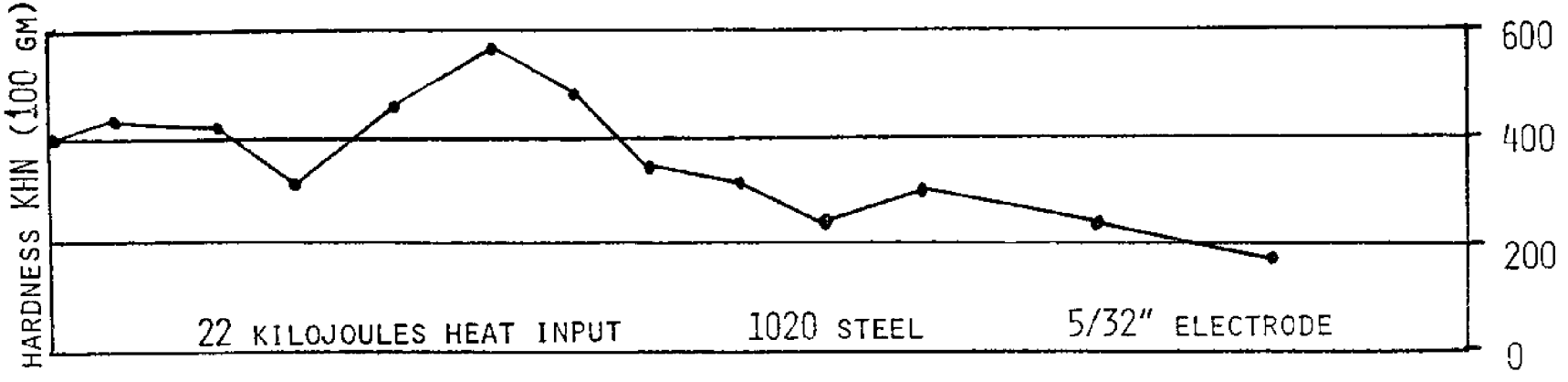

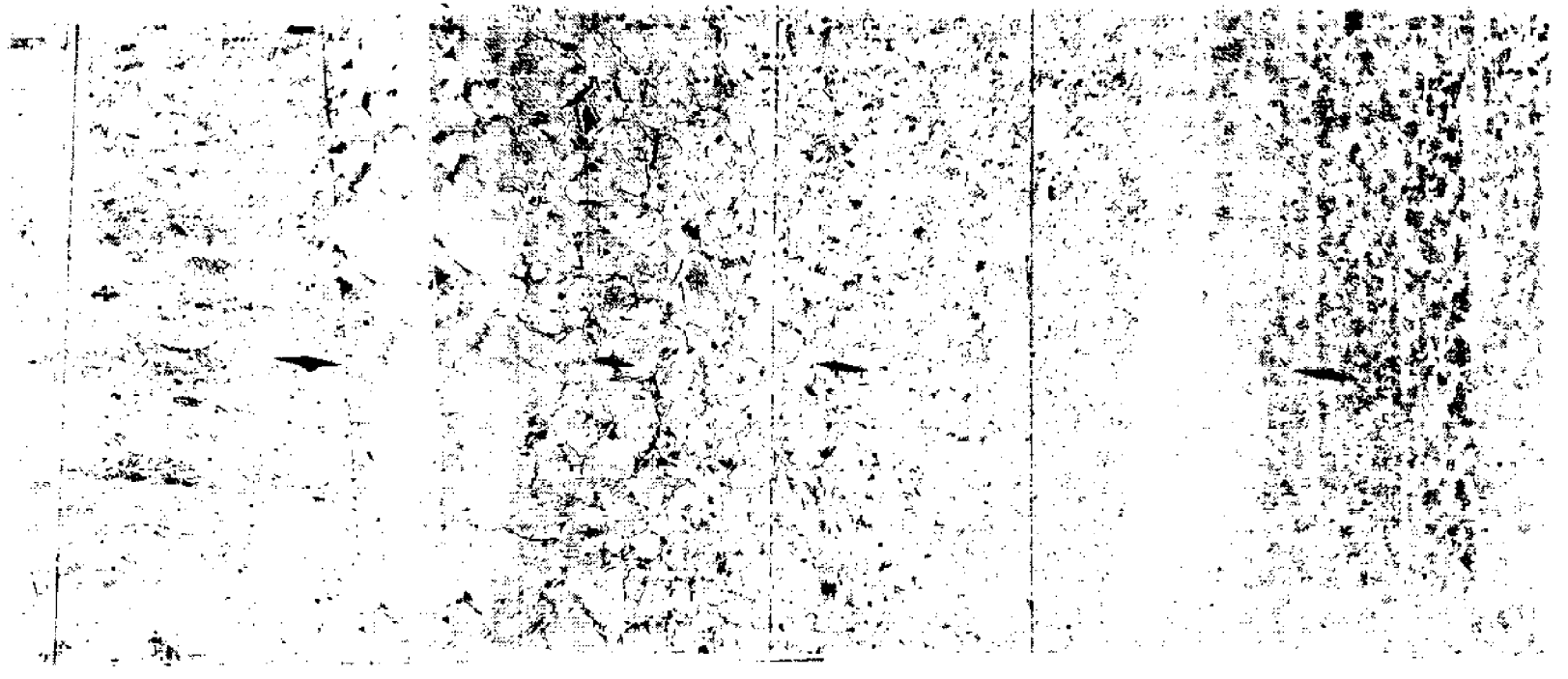

be associated with a weld microstructure.

Martensite is the hardest crystal structure in steels. If a steel is formed with a 100% martensitic structure, that steel will be the hardest steel possible with that particular carbon content. Higher carbon contents will result in harder martensite. The element in martensite that makes it so hard is the carbon. The pure iron, or ferrite, is a very soft element. So, the more carbon, the harder the steel will be in any heat treated condition, and the harder will be its martensitic structures. Figure 6-8 shows the relationship between carbon content and the maximum hardness possible, which would correspond to a fully martensitic structure in the given carbon content steel.

Steel normally contains (in place of martensite) a crystal structure called pearlite, which is a lamellar layering of ferrite and cementite. Because pearlite contains cementite (Fe_3), it is much harder than pure ferrite crystals yet still much softer than martensite. Pearlite is the equilibrium structure, whereas martensite requires conditions of very fast cooling (non-equilibrium) or quenching for its formation. How severe, or fast, this quench must be in order to produce a fully martensitic structure will depend on the steels' chemical composition (mostly the carbon content). Measuring the cooling rate to form 50% pearlite and 50% martensite has been taken as one way of determining the "hardenability" of the steel. This cooling rate is called the critical cooling rate. A steel that forms pearlite very quickly is not as likely to end up with martensite and is less hardenable.

To determine if a region will become pearlite or martensite during quenching, the "severity of the quench" must be known. A more severe quench will result in a larger or deeper-hardened zone in a cooling plate. Because of the many unknown

FIGURE 6-8

RELATION OF HARDNESS VALUES TO CARBON CONTENT AND PERCENTAGE MARTENSITE

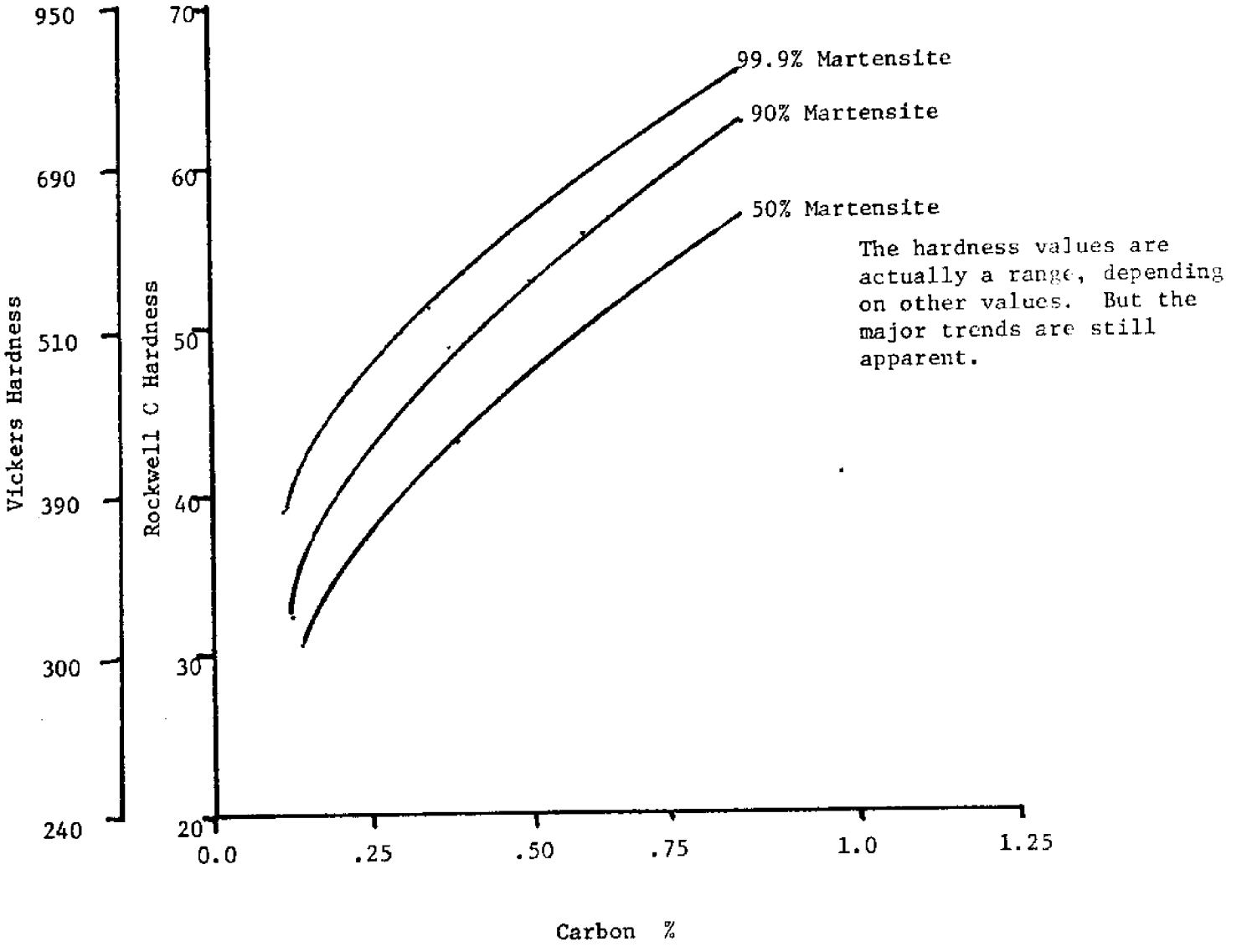

From: Metal Handbook, Vol. 2, ASM, 1964

factors influencing underwater welding, theoretical predictions of the hardness of the weld metal and HAZ are very difficult to make. But, the correlation remains valid, if we know the quench conditions, and thus the cooling rates for every point in the weld joint. As an example of quenching rates, we consider brine quenching (a fairly severe type) during which the austenite is supercooled during the quench and forms martensite. In the transforming range of temperatures (800-1200°F), the metal may be cooling as quickly as 900°F/sec. So, it remains in this region for only a fraction of a second and thus, illustrates the rapidness of the martensite forming process.

Because of the difficulty in determining the quench rates for underwater welding, it is often necessary to work backwards, determining what the quench rate must have been for a resulting hardness. For a known carbon content, a particular hardness value then corresponds to a specific microstructure composition. Thus, the microstructure is eventually linked through the hardness readings to the cooling rate. Faster cooling, or quench rate, will result in a higher hardness value. Cooling rates faster than the critical cooling rate for a particular steel will produce more than 50% martensite, with a high hardness reading. Cooling rates which are slower than this critical cooling rate will produce decreasing amounts of martensite and increasing amounts of bainite and pearlite, giving lower hardness values. Fastest cooling occurs from the highest temperatures.

The reason the HAZ is often more affected by hardening than the weld metal itself is because of their slightly differing carbon contents. Because the weld metal is at a higher maximum temperature, it will cool more rapidly. But, it has a lower carbon content because of solidification segregation, and so is less hardenable. From the standpoint

of determining the cooling rate, the heat input to the weld is the most important factor in welding. Even for different processes (SMA, GMA), the cooling rates will be similar for the same heat input. Higher heat input results in slower cooling rates. And the hardness values that result will be a good indicator of the microstructure that is present as a result of the cooling history.

6.4 POTENTIAL UNDERWATER WELDING DEFECTS

Very seldom are welds found with absolutely no defects. Depending on how hard someone looks at a weld, there will always be at least some minor imperfection or discontinuity. But, slight discontinuities in the structure or appearance of a weld do not necessarily mean that the weld should be rejected. Defects should be distinguished from discontinuities as being imperfections that are judged to be damaging or detrimental to the proper function and safety of a weldment. As we move towards the utilization of growing numbers of welds in underwater situations, we should remember that because of the increased difficulty in procedures to inspect welds once completed, only those imperfections which will actually be a danger to the integrity of the structure should be repaired.

Several of the defects found in underwater welds are common to air welds. Others are more unique to underwater welding and will be dealt with in more complete detail. Actually, almost all the problems associated with obtaining perfect air welds are present in underwater welding situations as well. Arc strike embrittlement, lack of penetration, non-homogeneity of the weld bead metal, problems with gases in the weld metal, slag inclusions and hot and cold cracking are all significant areas of difficulty in underwater welding. Two basic factors in underwater welding increase the problems with defects: rapid quenching and hydrogen.

6.41 Quenching-Induced Defects

At an arc strike area, the steel has been heated above the lower critical temperature and cooled extremely rapidly. Underwater welding situations only worsen the problem because the arc may be a little more difficult to strike underwater and because the water will induce even faster cooling rates. This produces a martensitic structure that is worse still because it has not been properly protected from the atmosphere (water) by a slag covering. If the arc happens to occur at a region of high stress intensity, failure may result from this small defect. Thus, arc strikes ought to be avoided and should be repaired by covering it with a smooth weld bead or else, grinding the arc strike down flush with the base plate.

Lack of penetration or fusion is always a serious defect. This is the failure of the weld bead to properly connect the two workpieces. Often this condition will result in hairline cracks between the two pieces giving rise to high stress intensity fields. In underwater welding, the problems of shallow penetration are increased because the cooling effect of the water tends to cause a definite decrease in the penetration of the weld. It may be necessary to design the joints used in underwater welding to provide for this inherent lack of penetration and fusion.

Dilution is the process of mixing that occurs during welding when the parent metal is melted by the welding arc and mixed with the weld rod metal. A low lever of dilution represents a weld bead that is most similar to the base metal, containing only a small amount of welding rod metal. The problem of dilution is most serious when a non-homogeneity in the final weld bead results. In most cases, this is not a serious problem.

Slag inclusions occur with increasing frequency as the rate of solidification of the weld puddle increases. As the welding are melts the electrode, much of the slag is injected into the weld puddle by the force of the arc and melting metal droplets. The slag is designed to quickly rise to the surface of the weld bead and provide a protective covering for the weld. However, if the weld puddle solidifies before the slag has a chance to float to the surface, it will be caught in the weld metal. The likeliness of slag becoming submerged in the weld puddle increases as the turbulence of the welding arc and puddle increases. Thus, a more stable arc will provide for less slag entrapment. In underwater welding, the extremely rapidly growing dendrites in the weld metal very often overtake escaping slag particles. And because the turbulence of an underwater welding arc region is often increased by the bubble and the rapid quenching of the water, uneven weld beads with more slag are sometimes observed. The slag will be found slightly below the top of the weld bead in underwater welds. Observing where these inclusions are found, in conjunction with observing the dendritic structures will provide much information regarding the solidification of underwater welds.

Undercutting can be a very serious defect because it creates a notch effect and thus, a stress concentration and possible crack initiation point. Undercutting occurs when the solidification process takes place too rapidly to allow the weld puddle to completely fill back into the toe of the melted puddle region. In air welding, it indicates that the welding speed is too fast. Underwater, it occurs very frequently as the result of the rapid cooling induced by the surrounding water. The solution to undercutting remains unclear. Certainly this is a problem that needs to be dealt with more fully.

Porosity is the problem of small gas bubbles becoming trapped in the weld metal. The presence of these gases can be harmful as in the case of O_2 and N_2 because the oxides and nitrides formed from these gases will cause embrittlement of the metal. The mechanical defect of having a small hole in the welded joint is not as critical as the associated chemical problems. The presence of O_2 will reduce the strength, hardness, and notch toughness of the metal, especially when it is dissolved in quantities greater than .1%. But in underwater welding, when the high temperature of the welding arc dissociates water into hydrogen and oxygen, the possibility of oxygen being present in the welding atmosphere is quite good. Thus, the oxidizing functions of the electrode coating are still necessary and critical in underwater welding situations. Nitrogen is not a problem underwater. Hydrogen will be dealt with separately in the next section. Porosity has been found to increase with welding current in underwater welding, regardless of the type of electrode or the waterproofing method, and the composition of the gas enclosed in the porosity is reported to be mostly hydrogen (Masumoto, et al., 1971). Porosity can also be the result of gases coming out of solution as the temperature of the metal is lowered. These gases may also have reacted with the metal to produce oxides and nitrides that are then released from porosity. The porosity is often concentrated along the dendritic branches where the bubbles have become trapped and have been unable to reach the surface.

Problems of porosity are increased in underwater welding by the rapid weld metal solidification. Gases can, however, be present in the weld metal and remain soluable and so, not form detectable porosity. The embrittlement problem from the gases will still persist. Hydrogen is the worst offender as a dissolved gas within the weld microstructure. That portion of the hydrogen which evolves as porosity or escapes

the weld microstructure completely does not pose the same threat.

6.42 Hydrogen-Induced Defects

Much recent investigation has been conducted on hydrogen embrittlement and hydrogen-induced cracking.[62] Because underwater welding induces an arc atmosphere that is high in water vapor content and in dissociated oxygen and hydrogen, it is thought that hydrogen may be especially critical.[48,49] Hardening in the HAZ and residual stresses which may also develop are precursors for hydrogen cracking. Hydrogen will not induce cracking unless the region is hardened and contains residual stresses. Higher hardness and faster cooling rates will give the weld zone a higher susceptibility to hydrogen cracking.

Hydrogen is picked up during heating and dissolves into the austenite. As the temperature cools down, the solubility of hydrogen goes down and so, the hydrogen attempts to diffuse out of the weld metal into the air and into the HAZ. This zone of hydrogen diffusion is about 1mm for average welding conditions and so, in an underwater welding HAZ of width 1-2mm, the hydrogen will be present. Hydrogen coming out of solution may go to form or enlarge porosity.

Hydrogen in porosity holes has been determined to be harmless. Hydrogen may result in cracking through the following mechanism involving the hydrogen that has supersaturated the metal:

(1) The hydrogen diffuses to areas of stress concentration such as an area of martensite structure.

(2) This stress area causes a crack initiation, either prior to, or after the introduction of hydrogen.

(3) The hydrogen now precipitates and forms a small void or crack and induces further stress on the crack tip,

causing it to propagate.

(4) The crack grows in steps to the critical size and may then fail catastrophically.

Undercutting and excessive reinforcement in underwater welds present additional areas of stress concentration. Using austenitic electrodes may help because diffusion out of gamma iron is much slower than from alpha iron and the diffusion into the HAZ is limited by the rate out of the weld metal.[22] Thus, the tendency is for the hydrogen to diffuse into the air rather than into the HAZ. The solubility of the hydrogen is higher in the austenite and this further discourages hydrogen diffusing into the HAZ. There is no easy solution to hydrogen problems in underwater welding except to suggest eliminating the hardened zone and stress concentration areas.

PART SIX

EXPERIMENTATION AND RESULTS IN METALLURGY, MICROSTRUCTURE, AND METAL TRANSFER

Contents

7.0 INTRODUCTION

This portion of the report details the original experimentation and investigation that were conducted on the metallurgy and microstructure of underwater shielded metal-arc welding.

(1) The discussion begins with some general considerations concerning underwater welding research explaining the reasoning behind choosing a comparative study between air and underwater welds.

(2) The discussion then proceeds with the identification of the relevant welding process parameters, which are found to be:

   a. welding current
   b. welding speed
   c. electrode size and type
   d. polarity
   e. air or underwater environment

(3) Descriptions of the equipment and the procedure used to obtain the data and also the method of analysis are presented. A short discussion of safety follows.

(4) The bulk of material relates to the analysis and documentation of the information obtained in this study. The types of data included are:

   a. welding current and voltage recordings for all welds
   b. welded bead appearance and regularity
   c. geometrical measurements and comparisons
   d. micorhardness profiles and comparisons
   e. microstructural studies of the weld HAZ
   f. general observations and remarks on assorted details not included in a previous subject division

Although much of the data follows certain trends and makes analysis straightforward, other portions of the accumulated data appears contradictory or nebulous. Conclusion and recommendations are based on the author's best attempts to correlate and make sense out of the results. Readers are reminded that, because more than one explanation will often explain the facts, new information may lead to new conclusions. All data is included in this report to allow for reevaluation and continued analysis by future workers.

7.1 EXPERIMENTAL RATIONALE FOR COMPARING AIR AND WATER WELDS

The complexities of a totally theoretical analysis of underwater welding make simplifying assumptions necessary and lead to uncertainty and error. Even if the temperature histories could be completely described, the resulting structural transformations would still require experimental investigation. Although the basic mechanisms of structural change are known and understood, the highly transient and nonuniform nature of welding makes accurate microstructural prediction impossible. And even if the weld microstructure were completely determined, it is doubtful that the resulting mechanical properties could be accurately predicted. Thus, once again, experimental investigation and verification would be necessary. Similar variables in the physical manipulation of the welding arc make a precise estimation of the welding heat input from specified welding conditions impossible. It is clear that the specific nature of the links from the optimum welding conditions to the heat input and temperature histories to the microstructural formations to the mechanical joint properties are not fully understood. However, it does not appear profitable or justifiable to ignore these metallurgical links and proceed with a hit-and-miss mentality.

One simple approach to the problem of determining how the heat transfer phenomena and microstructural transformations affect underwater welding is to study the differences between air welding and underwater welding. Since the basic welding metallurgy in air has been well-studied,[52,73,74] much understanding of underwater welding metallurgy can be gained by examining the dissimilarity between air and water welds. Because most underwater welding has been performed under emergency conditions for salvage or temporary repair to ships and offshore structures, each situation has been somewhat unique and therefore, is not easily compared with other underwater welding efforts or with air welding results. Although some workers have provided comparisons between air and water welds,[24,49,62] the research reported here attempts to provide more fundamental material upon which to base general conclusions and insights into underwater welding metallurgy.

7.2 IDENTIFICATION OF UNDERWATER WELDING PROCESS VARIABLES

After examining air and underwater weld beads produced under similar conditions, an attempt has been made to explain the differences by invoking knowledge of the bisic mechanisms of the welding arc, metal transfer, heat transfer, solidification, and microstructural transformations. The differences which are observed between air and underwater welds can then provide insight into the fundamental changes in the basic welding mechanisms. In an extensive review of the literature, it has been established that no such fundamental network of differences and modificational trends between air and underwater welding has been determined.

Several potentially important variables have been neglected in this report. It is probable that they do influence the underwater weld quality in a manner which is similar to their

effect in air welding. Further work is recommended to assess the magnitude and nature of these factors. The thickness of the welded plate is not a variable in the present investigation. In air, the effect of increasing the plate thickness is to increase the cooling rate in the weld metal and HAZ. However, a saturation phenomenon is observed in which the cooling rate reaches a maximum value, limited by the thermal conductivity of the plate; past a certain value, thicker plates will not result in a faster cooling rate. In underwater welding, the surrounding water will make the plate seem thicker to the weld bead and thus, result in faster cooling (compared to the same thickness in air) and a narrower limiting thickness. The effect of water depth (or pressure) was not involved in this study.

Pressure has been shown to exert some influence on GMA air welding.[10,54] Its effects on underwater metal-arc welding are not well-studied. The angle of the electrode with the workpiece was constant in this study (70-80°). Some variations might result from different lead angles in the degree of undercut experienced, but they were not investigated. The arc length is normally an important variable in welding. However, because the drag technique is employed in underwater welding due to the limitations on visibility, the arc length becomes a function of the welding current, voltage, and electrode type. Welding machines have a specific relationship between the current and voltage, with the current being the independent variable. Thus, the arc length and voltage are both dependent properties of the current, welding machine, and the electrode. Figure 7-1 illustrates these relationships.

Using the drag technique, the welding arc "digs" out the weld crater at a very specific rate. This speed is a function of the electrode and the current setting. Forcing the electrode to go faster will usually result in an uneven,

FIGURE 7-1

VOLTAGE AND ARC LENGTH AS FUNCTIONALLY DEPENDENT PROPERTIES OF THE WELDING POWER SOURCE CHARACTERISTICS AND THE WELDING CURRENT SETTING

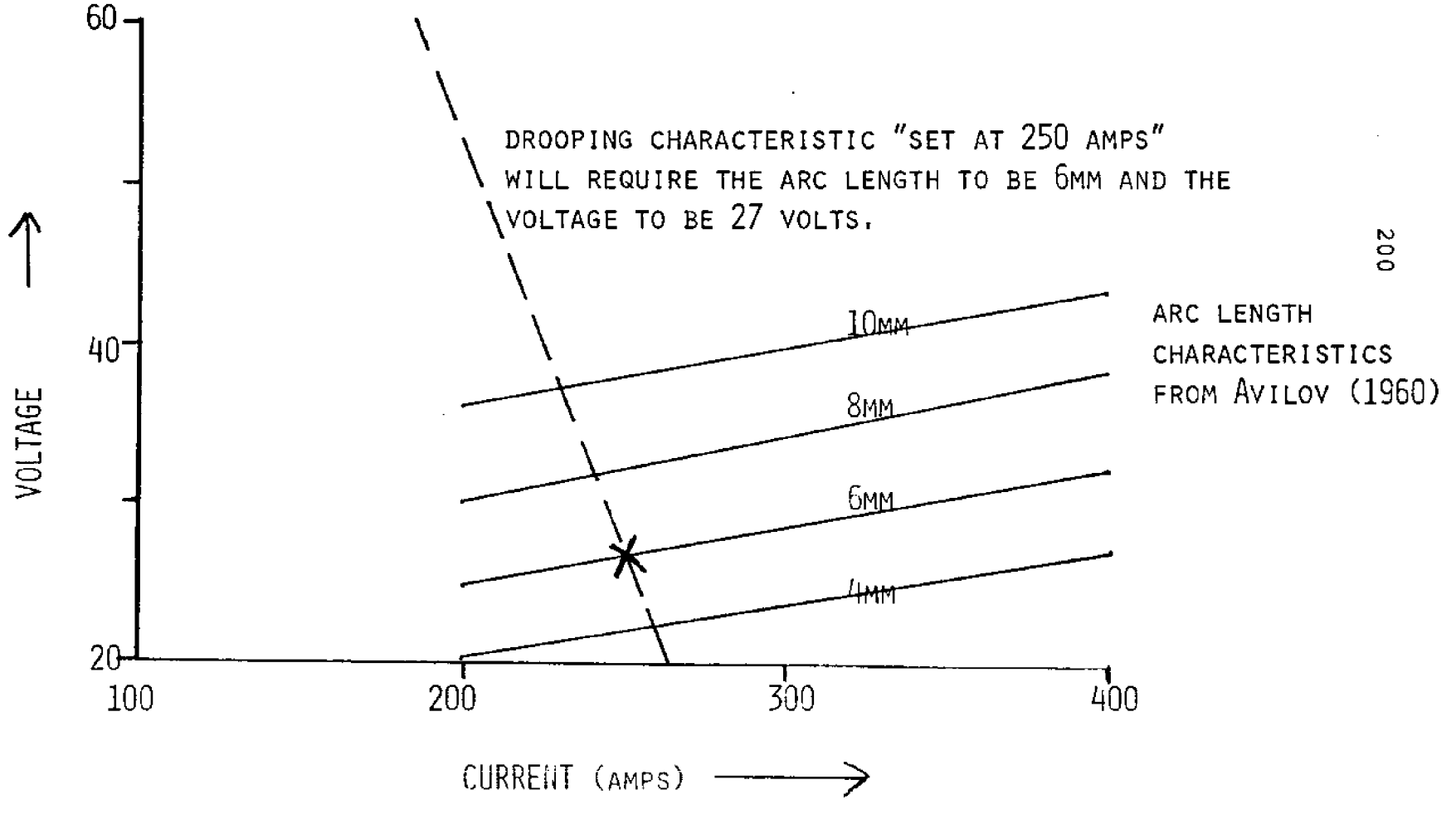

sporadic weld bead, while retarding the electrode will cause the weld bead to spread out without an improvement in the penetration. Thus, the drag technique leads to a natural, characteristic welding speed. However, some welds were produced by increasing or decreasing this natural speed and sotthe speed is treated as a welding parameter variable. The type of coating used on the different electrodes influences the speed, the arc length, and the voltage, so it is an important factor. The size of the electrode has major effects on the size of the weld bead, the bead shape, the cooling rates, and thus, the hardness profiles. Thus, the electrode size, the flux coating material, the current, the polarity, and the speed are the process variables which were chosen to be investigated in this study.

The electrode types and sizes were those which had been recommended or considered by previous investigators.[12,22,62] The following electrodes were used in this study:

E6013: Medium thick titania coating. Medium penetration. Smooth and flat bead with good wetting and appearance. It is designed for a medium-long arc and not for the drag technique, although it will operate satisfactorily in this mode.

E7014: Thick titania with iron powder coating. Medium penetration, good wetting. Designed to do the work of the E6013 with similar speed, but with increased deposition rate, improved appearance, and increased ease of welding using the drag technique.

E7024: Very thick titania with iron powder coating. Light penetration. Designed for drag welding with increases in deposition rate and speed. Good mechanical and X-ray quality.

E6027: Very thick mineral with iron powder coating. Deep penetration. Drag with slower speed than E7024,

TABLE 7-1

SUMMARY OF RECOMMENDED WELDING PARAMETERS

		Air Welding			Underwater Welding		
		Current (amps)		Speed (ipm)	Current (amps)		Speed (ipm)
1/8"	E6011	---		---	160	(Burkes, 1950)	-- ---
	E6013	50-120	(Airco)	---	---	---	---
		95-125	(R. T. Brown, 1974)	11-16 ipm	115-150	(R. T. Brown, 1974)	17-24 ipm
	E7014	115-150	(Westinghouse)	---	---	---	---
		150-170	(R. T. Brown, 1974)	13-15 ipm	150-170	(R. T. Brown, 1974)	11-15 ipm
	E7024	140-180	(Westinghouse)	---	---	---	---
		130-170	(R. T. Brown, 1974)	12-14 ipm	170+	(R. T. Brown, 1974)	15-16+ ipm
General 1/8"					140-150	(Levin, Kirkley, 1972)	---
5/32"	E6011	---		---	200	(Burkes, 1950)	---
	E6013	120-190	(Westinghouse)	---	170-190	(Navy, 1968)	13-16 ipm
		---	---	---	200-260	(Silva, 1971)	---
		---	---	---	200-250	(Brown, 1973)	---
		---	---	---	190-210	(Meloney, 1973)	12-15 ipm
		150-170	(R. T. Brown, 1974)	15-19 ipm	160-190	(R. T. Brown, 1974)	14-23 ipm
	E7014	120-190	(Airco)	---	200-250	(Brown, 1973)	---
		170-190	(R. T. Brown, 1974)	12-13 ipm	170-210	(R. T. Brown, 1974)	11-17 ipm
	E7024	180-250	(Westinghouse)	---	---	---	---
		240-280	(Silva, 1971)	---	200-260	(Silva, 1971)	---
		170-210	(R. T. Brown, 1974)	11-15 ipm	170+	(R. T. Brown, 1974)	11-13+ ipm
	E6027	180-250	(Westinghouse)	---	---	---	---
		250-300	(Silva, 1971)	---	240-280	(Silva, 1971)	---
		130+	(R. T. Brown, 1974)	10-11+ ipm	140+	(R. T. Brown, 1974)	---
					180-200	(Levin, Kirkley, 1972)	---
General 5/32"		---	---	---	200-220	(Avilov, 1955)	---
3/16"	E6013	100-210	(Westinghouse)	---	220-260	(Navy, 1968)	12-14 ipm
		180-200	(R. T. Brown, 1974)	15-17 ipm	200-240	(R. T. Brown, 1974)	15-16 ipm
	E7014	190-260	(Westinghouse)	---	---	---	---
		220-260	(R. T. Brown, 1974)	11-13 ipm	220+	(R. T. Brown, 1974)	7-8+ ipm
	E6027	250-325	(Westinghouse)	---	---	---	---
		190-210+	(R. T. Brown, 1974)	10-13 ipm	180+	(R. T. Brown, 1974)	8-10+ ipm
					250-270	(Avilov, 1955)	---
General 3/16"		---	---	---	225-280	(Craftweld)	---

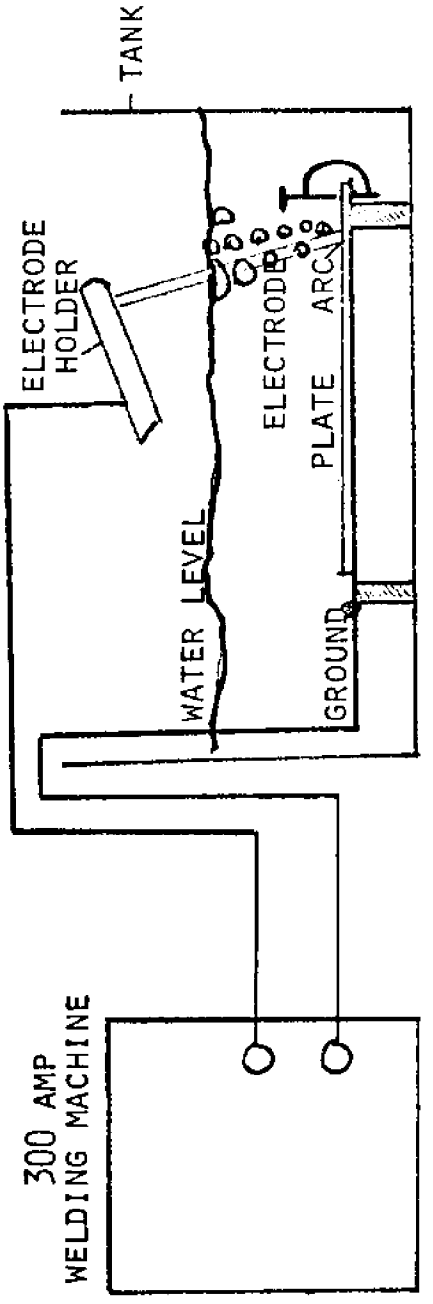

FIGURE 7-2
WELDING ARRANGEMENT

but with superior mechanical properties.

Some of the differences between these electrodes are indicated by the weld beads obtained in this study, although the electrodes behave somewhat differently in air and underwater conditions. The size of the electrodes chosen were 1/8-inch, 5/32-inch, and 3/16-inch. The welding current ranges for the various electrodes were estimated by using the recommendations of previous workers. Table 7-1 is a compilation of previous data on recommended underwater welding conditions compared with those of similar recommendations for air welding.

7.21 Description of Research Equipment

Several basic pieces of equipment were involved in initially welding the specimens, recording the welding current and voltage, cutting and polishing and etching the weld bead cross sections, obtaining microhardness profiles, photographing the weld cross sections for geometrical measurements, and photographing the microstructure of the weld metal and HAZ for analysis.

The actual welding was performed using a 300 amp AC-DC gas metal-arc welding machine that was connected to a normal shielded metal-arc electrode holder and workpiece ground. The experimental welding set-up is shown in Figure 7-2. The welding machine's voltage-current characteristics are assumed to be similar enough to a normal shielded metal-arc machine to avoid problems with substituting it. Based on some of the experimental difficulties in obtaining a high enough current with the arc lengths which are formed in underwater drag welding, it is thought that a machine with an adjustable slope characteristic might work better. Also, because underwater welding requires more current than air welding, a 400amp machine is recommended for further work.

The welding machine was connected to a strip chart recorder that measured the voltage directly between the welding electrode and the ground, and measured the voltage across a known resistance to give a reading for the welding current. The recordings were made at a chart speed of 2.5mm./sec. This speed is not fast compared to the metal transfer mechanisms and does not provide data on the metal transfer phenomena. The speed is sufficient to indicate the average current and voltage and the changes that occurred as a result of elongating arc length and other welding irregularities and discontinuities. The recordings also give an accurate measure of the elapsed welding time and thus aid in determining the average welding speed. Because the recordings are considered relevant for possible future reference, yet are not individually significant, they are not included in this report.

The specimen plates were photographed using a Polaroid camera. These photographs were used to record and document the weld bead appearance. The specimens were cut on a horizontal band saw and mounted. Grinding and polishing was done on a seried of grit wheels. Macrophotographs were taken with the Polaroid camera, using a close-up lens to give a magnification of 7.5X.

A Wilson Tukon Microhardness Tester was used to perform the microhardness profile surveys. A 100 gram load was used to insure the measurement of the local hardness value. Microstructural photography was performed using an American Optical Metallograph at a magnification of 100X and Polaroid film was employed to record pertinent microstructural formations.

7.22 Description of Experimental Procedure

All welding was done in a 4' x 2' x 2' plexiglass tank with an aluminum frame under 6" of water. For each of the ten electrodes picked to be used in the study, a set of four or five weld beads were welded with a range of currents on a

single plate specimen. A specimen plate was 4" x 6" x 1/4" and the weld beads were made across the 4" dimension of the plate. Each weld bead was thus about one-inch from the edge or from other beads. One specimen was prepared for air welding with straight polarity, one was made underwater using straight polarity, and a third was made underwater with reverse polarity. Thus, three complete sets of plates were prepared with each of ten electrodes, giving a total of 30 plates. Each plate contained four weld beads so that a total of 120 cross-sectional specimens were prepared, polished, etched, photographed and analyzed. This was an immense job, which with only one worker, took several months. Hopefully, the results are worth the agony. The ten electrodes used were:

E6013	(1/8", 5/32", 3/16")
E7014	(1/8", 5/32", 3/16")
E7024	(1/8", 5/32", ---)
E6027	(--- , 5/32", 3/16")

Once the weld bead specimens had been welded and photographed, they were cut in preparation for making the cross-sectional specimens. A 3/8" strip was cut from the plate perpendicular to the weld beads. This strip was then cut so that each weld bead cross section could be mounted individually in plastic resin. The mountings were allowed to dry overnight, and then the weld cross sections were ground and polished. The grinding was accomplished by using a series of gradually decreasing grit size grinding wheels. The grit wheels used were sizes 80, 120, 240, 320, and 600. After grinding on the finest wheel, the sample is washed in soap and water, rinsed with alcohol, and dried. At this stage, the specimens have very fine scratches in the metal surface, and these must be polished smooth on a cloth polishing wheel with a polishing compound of distilled water and .3 micron alumina. Once the specimen has been polished so that the scratches are removed and the surface is microscopically clean, the weld cross sections are etched with 1% Nital solution for

8-10 seconds, then washed, dried, and placed in a dessicator to protect the polished and etched surfaces.

A hardness profile was then run vertically through the weld HAZ and weld metal. Indentations were made at 500 micron (.5mm) intervals and the grain size and microstructure were visually observed and recorded along the transverse. Macrophotographs of the weld bead cross section were made and from these enlarged photographs, the width, penetration depth, reinforcement height, total area, HAZ width and the percentage of weld metal were measured. These parameters and the effects of underwater welding on them comprise the geometrical analysis. Finally, for a few selected weld beads, a microphotograph transverse of the HAZ and weld metal were made to more explicitly analyze the microstructural formations.

7.23 Description of Analytical Procedure

The strip chart recordings were analyzed to give the average current range and the average voltage range. The variation in the current was also measured and recorded as the arc stability, K ($K = \frac{I\ max}{I\ min}$). This gives an idea of the regularity and smoothness of the resulting weld bead. The chart recordings gave the true current through the arc. By looking at the weld bead appearance record on the weld plates, and by comparing arc stability values and weld bead shape factors, the optimum (or at least the best obtained) welding conditions were determined for each electrode type. Table 7-1 also presents those currents and speeds considered optimum from this study. These comparative observations between the optimum welding conditions in air and underwater comprise the first major group of investigative conclusions. The geometrical characteristics of the various welds were further analyzed to show the effects of current, electrode size and type, and welding medium on the weld shape.

The analysis then switched to involve the hardness profiles and microstructural formations of the various weld

FIGURE 7-3

VOLTAGE AND CURRENT RECORDINGS DURING AIR AND UNDERWATER WELDING
E7014 1/8" ELECTRODE

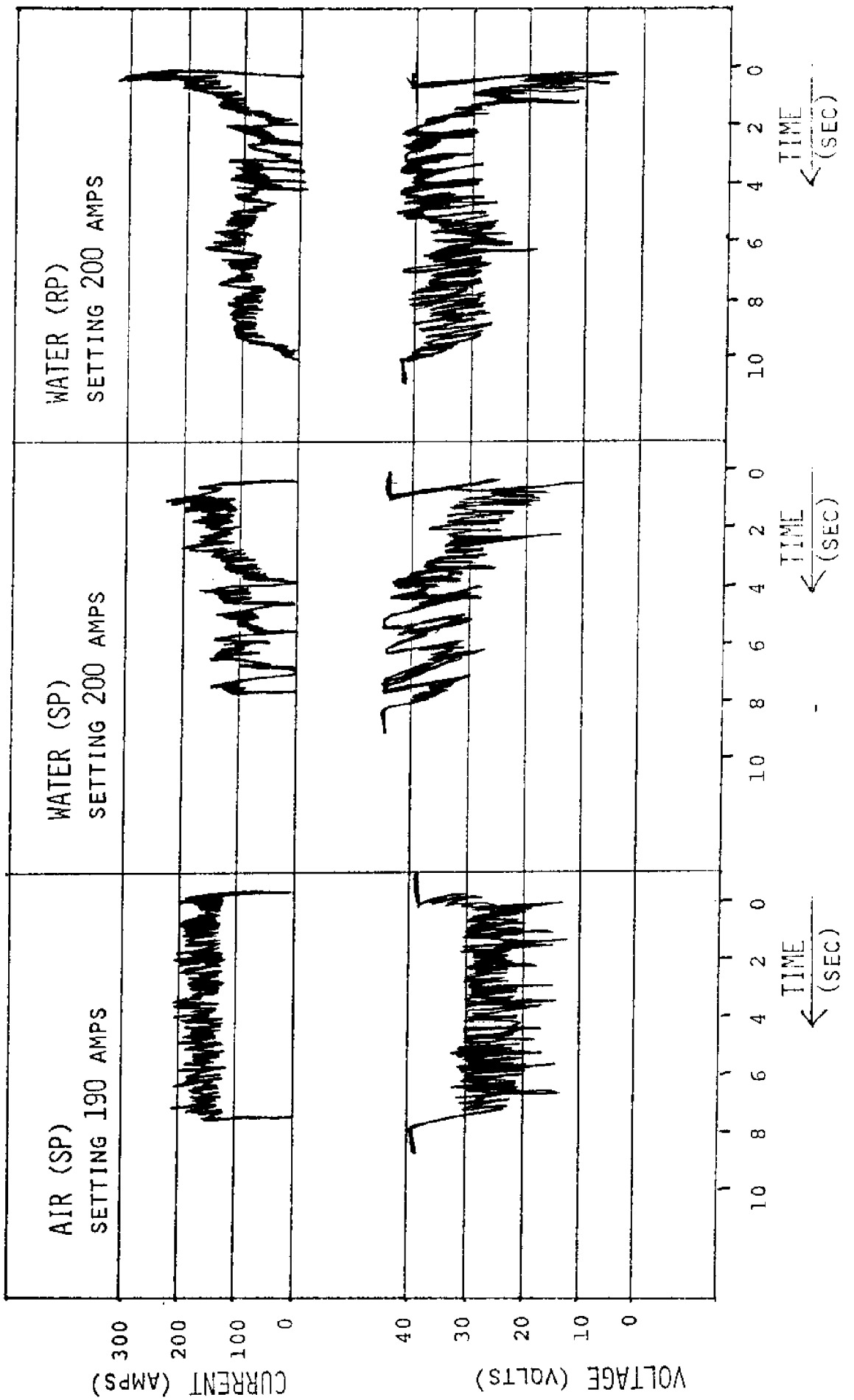

HAZ's. These crystal and grain structures were linked back to the cooling rates that produced them. Comparing the HAZ of air welds with the HAZ of similar water welds gave the second series of basic conclusions concerning the effect of underwater welding on the cooling rates and microstructural transformations of the weld metal and HAZ. An attempt has been made to explain the observed changes from air welding in terms of the fundamental processes that are modified or affected by underwater welding.

7.24 Welding Current Voltage Recordings

The comparative portion of these experiments depends on the completeness and accuracy of the voltage and current recordings. They provide information concerning the total heat input to the weld. This is the factor which is used to compare and relate the weld beads to one another. They also provide limited information concerning the metal transfer mode of the underwater welding arc. In this case, the mode is determined to be drop transfer, which is identical to that found in normal air welding arcs. This observation is in agreement with earlier work by Silva (1971), who also determined that the metal transfer mode of an underwater SMA welding arc was drop transfer. This section will examine only a couple of voltage-current recordings in detail and summarize the others. Figure 7-3 shows the results of recordings from E7014 - 1/8" welds in air and underwater. For the air weld, the minimum welding current is fairly constant at 125 amps. The spikes jumping up to 175-200 amps represent drops of metal transferring between the electrode and the weld puddle. The voltage goes down because the effective arc gap (resistance) is decreased by the presence of the droplet. This also causes the current to increase because the arc resistance is reduced. So, the average arc current is the lower limit of the current range and the average arc voltage is the upper limit of the voltage range.

The air weld shows an arc that is well-behaved. However, the underwater arc shows quite an irregular behavior. Both the water (SP) and water (RP) welds have current recordings that drop to zero current (arc broken) several times in the course of 10 seconds. This is caused by an elongation of the welding arc underwater. This elongation is the result of the water cooling the outside of the electrode flux covering and causing an arc barrel to form around the electrode core metal. As this arc barrel becomes longer and forces the arc length to become longer, the voltage climbs because of more resistance and the current drops for the same reason. It is seen that even when the arc becomes more consistent, the welding current is lower and the voltage is higher than in air. This implies that a longer arc with lower current will result in underwater welding. The extent of this effect becomes very important in determining the quality of the resulting underwater weld bead. Figure 7-4 shows that this arc length may vary in an oscillatory manner during welding, even in air. This produces variations in the heat input, penetration, and other weld bead parameters.

In general, the E6013 and E7014 electrodes gave the most consistent recordings, showing that the arc barrels of these electrodes were less affected by the underwater cooling effects. This is indicated by the fact that the current settings on the welding machine corresponded well with the actual measured current. The differences between the setting current and the actual current were small for E6013 electrodes of all three sizes. The underwater current appears limited to an actual 225 amps at a setting of 300 amps on the machine. This may have prevented the optimum welding current from being obtained. Because of this effect, a higher current range of 400 amps is recommended for an underwater welding machine unless the flux coatings can be redesigned to give a more suitable arc barrel length and thus, a shorter arc length.

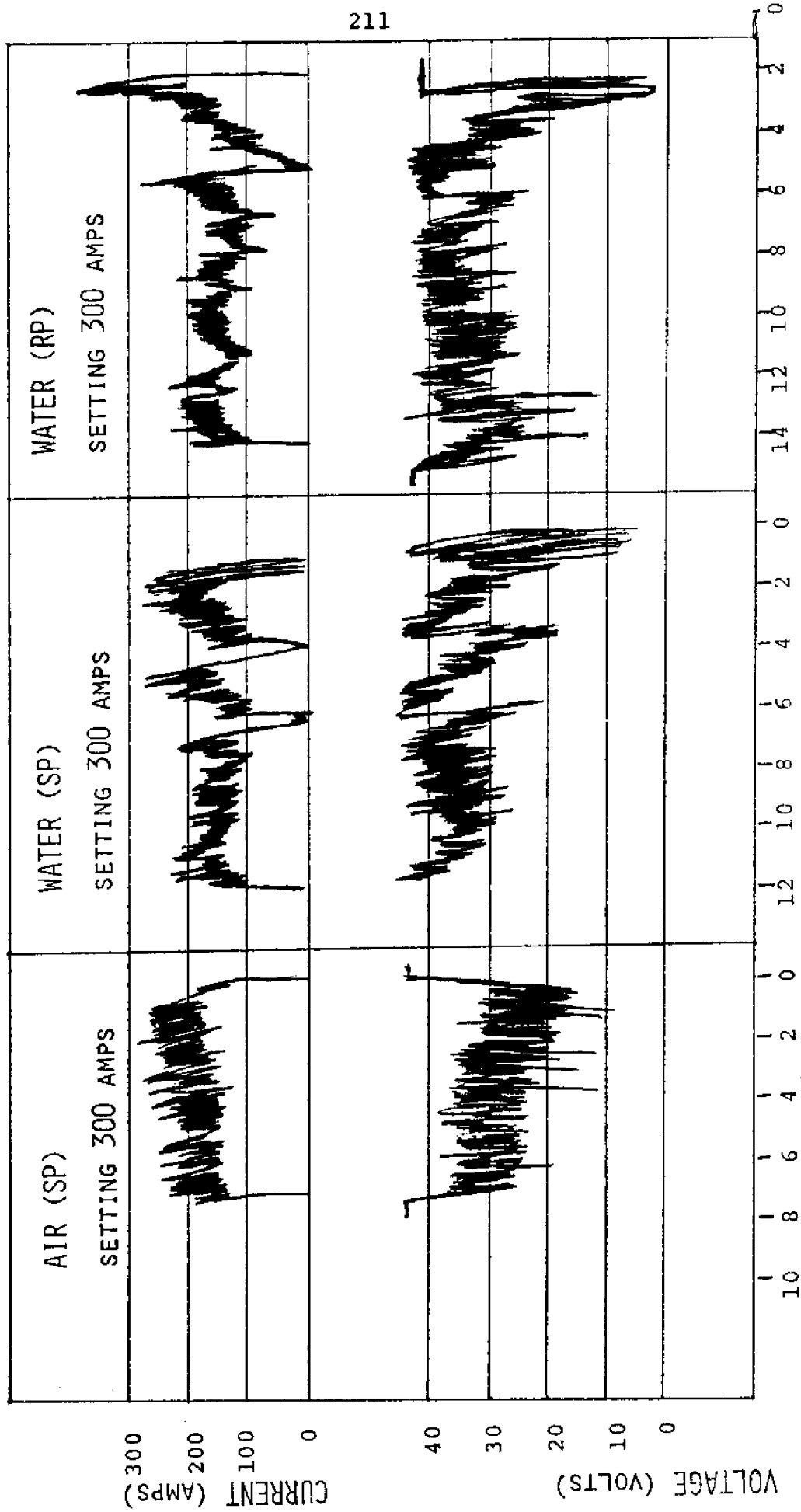

FIGURE 7-4
VOLTAGE AND CURRENT RECORDINGS DURING AIR AND UNDERWATER WELDING
E6027 3/16" ELECTRODE

For the E7024 and E6027 electrodes, the underwater welding current is limited to 175 amps regardless of the machine setting. Even with air welding, the current appears limited to 200 amps. This low current gave weld beads that were very sporadic and uneven and therefore, unsatisfactory. Optimumly high welding currents were not obtained.

E6013 - 1/8" recordings show that the air welding arcs were fairly constant, so that very consistent welds resulted. The variation in length tending towards an unstable arc is most critical with a low welding current. As the welding current approaches the optimum values of 150-170 amps, the current variation decreases and becomes stable to within $\pm$5 amps. This reflects an observation that underwater welding arcs, when welded at the optimal welding current are more stable or consistent than air welding arcs. But, the threshold current for obtaining stable arcs and consistent and regular weld beads is higher in underwater welding than in air welding.

E6013 - 3/16" air welding arcs show good stability at all welding currents in the range of 125-225 amps. The stability at 175 and 200 amps are the best ($\pm$5 amps), and this stability is a good indication that these are the optimum welding currents. The best underwater (SP) welding are stability results at 250 amps. Underwater (RP) arcs were most stable at 200 and 225 amps, but the variabiiity at 225 amps is moderately high ($\pm$20 amps). Thus, two observations can be made from E6013 data:

(1) The optimum welding current for underwater welds is higher than that for similar air welds;

(2) The arc stability for smaller electrodes is higher than that for larger electrodes and is apparently a function of the mechanical process of "chipping" the outside of the flux coating during welding. Better designed underwater coatings are recommended.

The E7014 - 1/8" air weld arcs show good stability in the range of 125-150 amps of ±15 amps. Underwater (SP) arcs are most stable at currents of 150-200 amps. Underwater (RP) arcs are similarly stable above 150 amps, and are very stable (±5 amps) at 175 and 200 amps. Again, the optimum welding currents for underwater arcs are higher than for air arcs.

The E7014 - 3/16" air welding arcs were stable for 200-275 amps (Actual current 175-225 amps). The underwater (SP) arcs were unstable at 200-275 amps and resulted in broken arcs. But the actual currents were only 200-225 amps. Here is a case where the optimum water welding current could not be achieved due to the elongated underwater arc lengths. Underwater (RP) arcs show similar instability except at 275 amps (175 actual). Again, the optimum welding current was not obtained.

The E7024 - 1/8" air welding arcs were stable in the range of 150-190 amps. The underwater (SP) welding arcs were unstable at 175 and 200 amps, but they were stable at 225 and 250 amps (±15 amps). The underwater (RP) arcs were unstable at all current settings, but this was probably due to the fact that the elongated arc length limited the actual currents to below 150 amps. Thus, for both underwater series, the optimum welding current was probably not achieved.

E6027 - 5/32" air welding arcs were relatively stable (±20 amps) with no arc breaks, even though the current was limited to 125 amps. Underwater (SP) arcs were not satisfactory at any of the current settings of 225-275 amps. Underwater (RP) arcs were marginally stable (no arc breaks) at settings of 250 and 275 amps, although the actual welding current was only 100-125 amps. The optimum welding current was probably not obtained for either underwater weld series.

E6027 - 3/16" air weld arcs are less stable than other air arcs with a variation in current of 40 amps. The current is limited by the elongated arc length to values below 200 amps, although the settings went as high as 300 amps. The optimum welding current must be above the 200 amps which were achieved. The underwater (RP) arcs behaved similarly to the underwater (SP) arcs. The maximum attained current was 150 amps and again, the optimum welding current must lie above this range.

Figure 7-5 shows that, although the arc length may be slightly increased in underwater welding, the basic arc characteristics are almost identical between air and underwater welding. The current and voltage are fairly constant except that 80-100 times per second, a small droplet of metal is projected across the arc, lowering the voltage and increasing the current. This recording also shows that the metal transfer mode in underwater SMA welding remains similar to that of air SMA welding with a drop transfer frequency of 80-100 small drops/second.

7.25 Summary of Voltage-Current Observations

(1) The basic metal transfer and arc characteristics of air welding arcs and underwater welding arcs are identical.

(2) A major limitation in underwater welding results from the elongation of the arc barrel length due to the cooling effect of the water.

(3) The optimum welding current for underwater arcs is higher than the corresponding optimum air welding current for the same electrode.

(4) At the optimal welding current, underwater arcs appear to be more stable than air welding arcs at their corresponding lower optimum current values.

FIGURE 7-5

HIGH SPEED VOLTAGE AND CURRENT RECORDINGS FOR AIR AND UNDERWATER WELDING

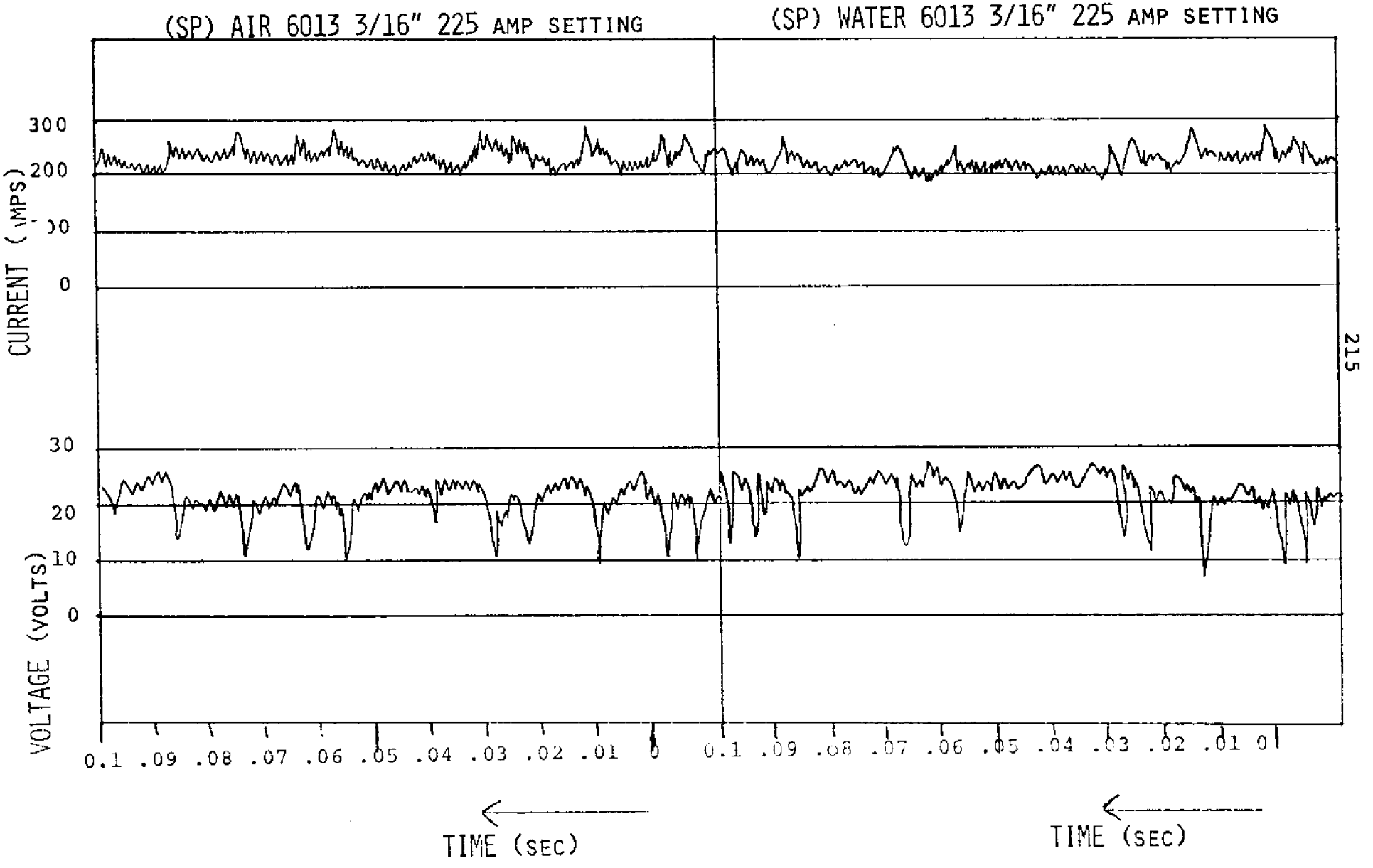

(5) For several of the underwater welding arcs, the optimum current was not obtained because of the elongated arc length limitation.

(6) The optimum current range increases with electrode size and may be different for each particular electrode type.

(7) The arc stability for smaller electrodes is higher than that for larger electrodes.

(8) Table 7-2 contains a summary of the optimum obtained voltage and current characteristics for air welds and underwater welds.

7.26 Underwater Weld Bead Appearance

The variability in the welding arc induces inconsistencies in the final weld bead deposit. The size of the weld bead changes with the instaneous heat input. Thus, the weld bead width and the penetration vary irregularly with an irregular welding arc. So, the appearance reflects the stability of the welding arc. Irregular penetration is undesirable because it can result in incomplete fusion in actual welded joints. This effect of weld shape variability due to arc instability is easily observable by comparing various electrode deposits from both air welding and underwater welding conditions, and measuring the weld deposit widths. Table 7-3 summarizes these results from the best obtained weld beads. E6013 - 1/8" air weld widths vary between 3.2mm and 4mm. The minimum width is 80% of the maximum width. This is a smooth weld bead. The comparable underwater weld bead widths vary between 1.6mm and 4.8mm for water (SP) and between 3.2mm and 6.4mm for water (RP). The minimum widths are now only 33% and 50% of the maximum width. These weld beads thus show more variability. E6013 - 5/32" and 3/16" air weld beads show a variability of 80% while the underwater variation of the minimum from the maximum is increased to 60-70%. E7014 - 1/8" electrodes show identical variability for air and

TABLE 7-2

WELDING SPEED, CURRENT, AND POWER INPUT

ELECTRODE	CURRENT (AMP)	VOLTAGE (VOLT)	POWER (KILOWATTS)	SPEED (IPM)	HEAT INPUT (KJ/IN)
6013 AIR	90-110	20-23	2-2.5	12-16	9-10
1/8" SP	130-150	25-27	3.4-4	24-25	9-10
RP	130-140	26-27	3.4	17-22	9
6013 AIR	130-170	23-27	3.5-4.2	17-19	11-13
5/32" SP	160-190	25-29	4-5	20-25	11-12
RP	150-180	21-24	3.6-4	19-23	10-11
6013 AIR	160-180	20-23	3.4-3.8	15-17	14-17
3/16" SP	180-210	23-30	4.6-5.4	16-18	13-18
RP	160-180	27-28	4.6-4.8	22-23	15-24
7014 AIR	130-150	24-26	3.5	13-15	14-15
1/8" SP	150-160	27-28	4-4.5	19-21	11-12
RP	140-150	27-28	4.3-4.7	22-25	13-15
7014 AIR	160-180	23-26	4-4.3	12-13	17-19
5/32" SP	170-190	27	4.6-5	12-17	18-23
RP	130-170	27-30	4-4.8	11-13	20-23
7014 AIR	200-240	23-26	4.8-5.8	11-13	23-26
3/16" SP	160-190	28-35	5.8	12	34-36
RP	120-180	30-45	4.5-5.5	7-8	38-48
6027 AIR	120-180	32-42	4.3-5.4	10-11	28-32
5/32" SP	----	----	4.5-5.5	----	----
RP	80-130	38-42	5-5.5	7	28-42
6027 AIR	140-170	34-39	5-5.5	10	29-36
3/16" SP	150-190	35-45	4-5.5	9	36-44
RP	100-160	34-40	4-5.5	8	36-52
7024 AIR	120-150	26-31	3.5-4.3	12-14	18-30
1/8" SP	150-160	30-35	3.5-5.5	15-16	21-22
RP	50-100	37-43	3.7	7-9	23-32
7024 AIR	140-160	30-35	5-5.2	13-15	24-27
5/32" SP	130-180	35-45	3.6-6.3	13	33-36
RP	80-200	35-45	4-5.3	7	35-44

TABLE 7-3

WELD BEAD WIDTH VARIATIONS FOR OPTIMUM OR BEST CONDITIONS

ELECTRODE TYPE	AIR (SP) WIDTH VARIATION	MIN / MAX %	WATER (SP) WIDTH VARIATION	MIN / MAX %	WATER (RP) WIDTH VARIATION	MIN / MAX %
E6013 1/8"	3.2-4	80	1.6-4.8	33	3.2-6.4	50
E6013 5/32"	6.3-8	80	4-6.4	62	5.6-8	70
E6013 3/16"	6.3-8	80	6.4-9.6	66	5.6-8.6	64
E7014 1/8"	8-9.6	83	6.4-8	80	6.4-8	80
E7014 5/32"	8-9.6	83	4.8-8	60	6.4-9.6	67
E7014 3/16"	11.2-14.4	78	9.6-12.8(0)	75	6.4-12.8	50
E7024 1/8"	12.8-14.4	89	4.8-12.8	37	6.4-9.6	67
E7024 5/32"	9.6-12.8	86	8-11.2(0)	72	6.4-11.2	57
E6027 5/32"	9.6-12.8	75	6.4-9.6(0)	67	9.6-14.4	66
E6027 3/16"	12.8-17.6	73	3.2-11.2(0)	29	6.4-11.2	57

water welding, but the rest of the electrodes are more variable in underwater Welding. E7024 and E6027 electrodes underwater (SP) were so variable that even the best weld beads were interrupted and skipped. This is a very severe effect. It is, again, probably caused by the elongation of the arc due to the water cooling of the outside of the flux coating forming the arc barrel.

7.27 Underwater Weld Shape Variables

One of the most easily investigated aspects of underwater weld bead characteristics is the weld shape. The shape is directly or indirectly a result of the various welding parameters, although direct influences are not always clear. Good penetration is a very important quality. Better penetration will allow deeper and more narrow joints to be welded with less joint preparation. Penetration will also affect the soundness of the fusion achieved by a weld. The larger an electrode, the more metal will be deposited during a weld. Penetration is, therefore, expected to deepen proportionally, but this does not really indicate if the electrode had good penetration or if it was just so large that deep penetration was unavoidable. A better measure of an electrode's penetration qualities under a particular set of welding parameters is called the weld-penetration-shape factor. This factor gives an indication of the penetration relative to the size or width of the weld bead. It is designated by the symbol S.

$$S \equiv \frac{\text{(Width of weld bead)}}{\text{(Penetration of the weld bead)}}$$

In air welding, the optimum value of this penetration-shape factor is reported to be 1.2 to 1.3. Depending on the welding conditions, though, this factor can range between .8 and 20. Madatov (1969) found that with iron powder electrodes and the drag method of welding, the shape factor in underwater welding was more likely to be between 3 and 5. This indicates a bead

shape which is more spread out and less penetrating, due in part to the rapid cooling rates in underwater welding. The present experiments provide more data for evaluating this property under varying conditions. Comparisons can therefore be made between the values for air welding and underwater welding for the same welding conditions.

Another indicator used in describing weld beads has to do with the relative amounts of parent metal and weld metal present in a weld. This indicator is called the "percentage of weld metal." A higher "percentage of weld metal" indicates that more of the weld was just laid onto the metal plate or joint from the electrode and that less penetration and fusion took place. Madatov (1962) reports that in underwater arc welding using a normal manual method of holding an arc gap, the weld consists of eighty percent (80%) filler metal with only twenty percent (20%) parent metal incorporated or fused into the final weld. This represents a value of the "percentage of weld metal" of 80%. This value improves significantly when using the drag technique of welding to produce a weld with only fourty to sixty percent (40-60%) of the weld being filler weld metal. This indicates a "percentage of weld metal" of only 40-60%. More parent metal (a lower "percentage of weld metal") points to more favorable penetration and fusion. These values are all easily measured by comparing the cross-sectional areas of different portions of a weld. The percentage of reinforcement versus the total weld area is the "percentage of weld metal." For this reason, photographs of the welded cross sections are used to evaluate various shape relationships. Madatov (1969) found that as the current increases, the reinforcement remains fairly constant in height, but the width increases more quickly than the penetration, causing a higher shape factor and a higher percentage of weld metal as the bead spreads out on top of the plate. Increasing the current is consequently not always a technique which yields benefits.

Another interesting geometrical shape characteristic is the relative height of the reinforcement and the penetration. Deep penetration with low reinforcement is desired. Thus, by measuring the penetration and dividing by the total weld bead height, penetration plus reinforcement, a factor relating the percentage of the total bead that is fused down into the base metal is obtained. Values of these parameters are summarized in Tables 7-4 to 7-7 as well as indicated on the weld bead profiles of all the weld bead profiles of all the weld bead series obtained. Variations from non-optimum welding conditions as well as from variations with size and type of electrode make a determination of underwater welding differences difficult.

7.28 Underwater Weld Bead Shape Controlling Factors

A possible factor contributing to some of the differences between weld bead shapes is the polarity of the electrode. Figure 2-2 illustrates the ideal differences between straight polarity and reverse polarity for shielded metal-arc welding. Straight polarity may result in a deeper penetration and a narrower bead because the electrons move towards the plate and impinge on it, releasing their heat of ionization to the plate. Most of the heat is used to melt the base plate, and a smaller fraction heats the electrode without fusion into the base plate can occur. Reverse polarity may result in wider, shallower beads with more weld reinforcement. Because reverse polarity may increase the melting rate of the electrode, the resulting weld bead may be larger. With straight polarity, the problem of undercutting can be more severe because the are is cutting deeply into the base plate and the weld metal may not have enough time to flow back into the sides of the weld crater. However, undercut is also a problem in reverse polarity. The water may exert a narrowing effect on an underwater straight polarity weld, but otherwise the air and underwater beads are surprisingly similar. The underwater reverse polarity bead is quite similar in shape as well. More distinction

TABLE 7-4

WELDING PARAMETERS AND WELD BEAD SUMMARY FOR E6013 ELECTRODE

ELECTRODE SIZE, MEDIUM, POLARITY	ARC CHARACTERISTICS				WELD APPEARANCE			SHAPE		SIZE		MAXIMUM HARDNESS (KHN) (100 g)
	AMPS.	STABILITY	SPEED	HEAT INPUT	UNDERCUT	SMOOTHNESS	REGULARITY	W/P	P/(R+P)	TOTAL AREA	%REINFORCEMENT	
1/8" AIR SP	80	1.7	15	6	No	Good	Good	5.5	.21	8	.83	395
	95	1.6	11	10	No	Good	Good	6.1	.32	12	.69	590
	115	1.6	16	10	No	Good*	Good	4.6	.44	9	.55	306
	125	1.5	12	9	No	Good	Good*	5.0	.41	11	.57	253
1/8" WATER SP	100	3.1	20	6	Slight	Poor	Poor	3.9	.45	5	.44	560
	115	1.6	20	8	Severe	Poor	Fair	5.8	.31	4	.54	485
	140	1.8	24	9	Severe	Poor	Fair*	3.4	.48	8	.48	540
	165	1.3	25	10	Severe	Poor	Poor	2.2	.53	10	.36	560
1/8" WATER RP	125	1.4	17	7	Severe	Poor	Poor	2.3	.51	14	.43	435
	130	1.6	21	5	Slight	Poor	Poor	2.7	.44	23	.51	405
	150	1.4	17	9	Slight	Poor	Fair*	3.4	.45	26	.52	480
	170	1.4	22	9	Slight	Poor	Poor	2.8	.54	16	.40	450
5/32" AIR SP	120	1.8	15	10	No	Good	Good	4.2	.31	16	.75	253
	150	1.7	15	12	No	Good	Good	4.6	.32	19	.63	253
	165	1.4	19	11	No	Good*	Good*	3.6	.45	21	.57	240
	175	1.3	17	13	Slight	Good	Good	3.9	.54	23	.35	225
5/32" WATER SP	130	2.2	16	12	Slight	Fair	Fair	3.7	.36	13	.7	420
	160	1.9	20	11	Severe	Fair*	Good*	3.2	.53	14	.42	540
	180	1.9	22	11	Slight	Fair	Fair	2.4	.53	21	.42	500
	190	1.5	25	12	Severe	Fair	Fair	2.2	.31	16	.37	560
5/32" WATER RP	145	1.8	15	9	Slight	Fair	Fair	3.4	.61	13	.30	600
	170	1.6	14	11	Slight	Fair	Fair	4.5	.52	15	.46	570
	175	1.7	19	11	Slight	Fair*	Fair	3.3	.49	30	.49	590
	195	1.6	23	10	Slight	Fair	Fair	2.9	.55	24	.36	470

TABLE 7-4 (Continued)

WELDING PARAMETERS AND WELD BEAD SUMMARY FOR E6013 ELECTRODE

ELECTRODE SIZE, MEDIUM, POLARITY	ARC CHARACTERISTICS				WELD APPEARANCE			SHAPE		SIZE		MAXIMUM HARDNESS (KHN) (100 g)
	AMPS.	STABILITY	SPEED	HEAT INPUT	UNDERCUT	SMOOTHNESS	REGULARITY	W/P	P/(R+P)	TOTAL AREA	%REINFORCEMENT	
3/16" AIR SP	130	1.9	12	15	No	Good	Good	9.3	.16	24	.80	265
	160	1.5	12	16	No	Good	Good	6.4	.36	28	.61	240
	180	--	15	15	No	Good*	Good*	4.0	.45	27	.52	240
	200	--	17	14	No	Good*	Good*	4.5	.46	26	.54	215
	225	1.6	16	17	No	Good	Good	--	--	--	--	--
3/16" WATER SP	160	2.5	15	16	Slight	Fair	Fair	3.0	.46	16	.56	380
	220	1.6	18	13	Slight	Fair*	Fair	2.3	.49	25	.48	450
	210	1.8	16	18	Slight	Fair	Fair	2.1	.57	28	.41	610
	240	1.5	16	18	Slight	Fair	Fair*	2.7	.57	33	.39	540
3/16" WATER RP	160	2.0	22	11	Slight	Poor	Fair	2.3	.49	26	.54	565
	190	1.8	22	15	Slight	Fair	Good	2.6	.52	30	.43	520
	200	1.8	23	24	No	Fair	Fair	4.0	.46	31	.48	465
	--	--	--	--	No	Fair	Fair	3.1	.52	40	.48	360

TABLE 7-5

WELDING PARAMETERS AND WELD BEAD SUMMARY FOR E7014 ELECTRODE

ELECTRODE SIZE, MEDIUM, POLARITY.	ARC CHARACTERISTICS				WELD APPEARANCE			SHAPE		SIZE		MAXIMUM HARDNESS (KHN) (100 g)
	AMPS.	STABILITY	SPEED	HEAT INPUT	UNDERCUT	SMOOTHNESS	REGULARITY	W/P	P/(R+P)	TOTAL AREA	%REINFORCEMENT	
1/8" AIR SP	130	1.5	14	11	No	Good	Good	6.1	.33	11	.63	270
	140	1.6	10	17	No	Fair	Good	--	--	--	--	225
	150	1.7	13	14	No	Good	Good	5	.34	15	.67	250
	155	1.8	10	18	No	Fair	Good	4.9	.52	28	.46	255
	170	1.4	15	15	No	Good*	Good*	2.3	.46	19	.47	270
1/8" WATER SP	110	3.6	15	10	Slight	Fair	Fair	3.6	.52	7	.4	500
	160	1.6	17	12	Slight	Good	Good	4.1	.48	18	.5	485
	160	1.8	19	11	No	Good*	Good*	4.3	.47	18	.5	520
	170	1.8	21	12	No	Good	Fair	3.4	.56	17	.4	560
1/8" WATER RP	90	2.3	25	10	No	Good	Poor	4.7	.57	13	.38	325
	125	1.7	25	14	No	Good	Good	4.5	.52	13	.46	240
	160	1.7	22	13	No	Good*	Good*	3.7	.61	16	.37	295
	170	1.4	25	15	No	Good	Good	5.2	.58	19	.37	315
5/32" AIR SP	150	1.6	12	15	No	Good	Good	5.2	.31	16	.64	250
	170	1.8	12	17	No	Good	Good	5.2	.35	22	.59	245
	195	1.6	12	19	No	Good*	Good*	5.0	.3	39	.44	221
	205	1.6	13	19	No	Good	Good	3.2	.36	40	.43	205
5/32" WATER SP	160	2.1	11	19	No	Fair	Fair	5.2	.34	20	.65	560
	160	1.8	13	18	No	Good	Fair	4.5	.42	20	.55	610
	180	1.7	12	23	No	Good*	Fair*	4.0	.48	24	.5	325
	210	1.6	17	18	Slight	Fair	Fair	3.7	.58	26	.34	465
5/32" WATER RP	150	2.7	10	22	No	Fair	Fair	8.1	.34	17	.65	525
	150	1.6	11	21	No	Fair	Fair	8.3	.33	33	.57	435
	170	2.0	11	23	No	Fair*	Fair*	8.7	.37	17	.58	500
	180	1.85	13	20	No	Fair	Fair	5.1	.40	27	.55	435

TABLE 7-5 (Continued)

WELDING PARAMETERS AND WELD BEAD SUMMARY FOR E7014 ELECTRODE

ELECTRODE SIZE, MEDIUM, POLARITY.	ARC CHARACTERISTICS				WELD APPEARANCE			SHAPE		SIZE		MAXIMUM HARDNESS (KHN) (100 g)
	AMPS.	STABILITY	SPEED	HEAT INPUT	UNDERCUT	SMOOTHNESS	REGULARITY	W/P	P/(R+P)	TOTAL AREA	%REINFORCEMENT	
3/16" AIR SP	220	1.7	11	23	No	Good	Good	6.4	.34	29	.58	240
	245	1.6	11	26	No	Good	Good	5.8	.41	39	.51	250
	250	1.7	13	22	No	Good	Good	7.5	.35	43	.69	225
	255	1.5	13	24	No	Good	Good	5.0	.54	43	.51	215
3/16" WATER SP	150	2.7	11	20	No	Poor	Poor	8.2	.32	38	.71	630
	180	2.5	11	25	No	Poor	Poor	4.1	.48	33	.48	485
	220	2.5	12	34	No	Poor	Poor	5.2	.51	22	.40	565
	230	2.1	12	36	No	Poor	Poor	5.9	.42	29	.52	580
3/16" WATER RP	170	2.6	9	27	No	Poor	Poor	4.3	.45	26	.50	470
	170	2.1	8	38	Slight	Poor	Poor	4.1	.49	38	.44	560
	180	2.3	8	40	No	Poor	Poor	5.9	.38	38	.63	465
	200	2.1	7	48	Severe	Poor	Fair*	3.6	.44	44	.52	610

TABLE 7-6

WELDING PARAMETERS AND WELD BEAD SUMMARY FOR E7024 ELECTRODE

ELECTRODE SIZE, MEDIUM, POLARITY.	ARC CHARACTERISTICS				WELD APPEARANCE			SHAPE		SIZE		MAXIMUM HARDNESS
	AMPS.	STABIL-ITY	SPEED	HEAT INPUT	UNDER-CUT	SMOOTH-NESS	REGULAR-ITY	W/P	P/(R+P)	TOTAL AREA	%REIN-FPRCEMENT	(KHN) (100 g)
1/8" AIR SP	130	1.8	12	16	No	Good	Good	7.8	.28	20	.75	250
	145	1.5	8	27	No	Good	Good	10	.31	35	.68	240
	150	1.7	14	16	No	Good	Good	4.6	.45	19	.52	240
	160	1.8	8	30	No	Good	Good	7	.42	38	.57	240
	170	1.6	14	18	No	Good	Good	--	--	--	--	---
1/8" WATER SP	--	--	--	--	No	Poor	Poor	6.4	.37	20	.75	420
	150	4.6	13	21	No	Poor	Poor	6.2	.35	25	.6	560
	170	1.9	16	21	No	Poor	Poor	5.3	.48	18	.44	580
	180	2.1	15	22	No	Poor*	Poor*	5.3	.45	30	.46	540
1/8" WATER RP	--	--	--	--	--	Poor	Poor	--	--	--	--	--
	--	--	--	--	--	Poor	Poor	--	--	--	--	--
	100	2.8	9	23	No	Fair*	Fair*	7.7	.29	18	.67	560
	100	2.8	7	32	No	Poor	Fair	6.1	.27	14	.71	465
5/32" AIR SP	160	1.7	10	24	No	Good	Good	8.8	.31	24	.7	256
	170	1.9	11	22	No	Good	Good	5.7	.41	28	.6	210
	195	1.6	15	23	No	Good	Good	4.7	.50	30	.53	230
	195	1.6	13	27	No	Good	Good	4.3	.55	38	.6	182
5/32" WATER SP	140	6	9	33	No	Poor	Poor	5.7	.44	16	.62	435
	170	2.3	11	28	Slight	Poor	Poor	4.5	.5	41	.53	390
	170	5.8	13	36	No	Fair*	Fair*	5.9	.38	30	.63	360
	--	--	--	--	No	Poor	Poor	4.8	.51	39	.61	435
5/32" WATER RP	--	--	--	--	--	Poor	Poor	--	--	--	--	--
	--	--	--	--	--	Poor	Poor	--	--	--	--	--
	100	--	7	35	No	Poor	Poor	9	.32	21	.71	520
	140	2.6	7	44	No	Fair*	Fair*	6.2	.30	27	.70	385

TABLE 7-7

WELDING PARAMETERS AND WELD BEAD SUMMARY FOR E6027 ELECTRODE

ELECTRODE SIZE, MEDIUM, POLARITY.	ARC CHARACTERISTICS				WELD APPEARANCE			SHAPE		SIZE		MAXIMUM HARDNESS (KHN) (100 g)
	AMPS.	STABILITY	SPEED	HEAT INPUT	UNDERCUT	SMOOTHNESS	REGULARITY	W/P	P/(R+P)	TOTAL AREA	%REINFORCEMENT	
5/32" AIR SP	70	3.2	10	12	No	Fair	Good	7.7	.26	21	.76	209
	90	2.4	10	16	No	Fair	Good	6.9	.23	15	.73	230
	130	1.7	10	28	No	Good*	Good*	5.7	.42	33	.51	200
	160	1.7	11	32	No	Fair	Fair	6.2	.47	53	.53	200
5/32" WATER SP	--	--	--	--	--	Poor	Poor	--	--	--	--	--
	--	--	--	--	--	Poor	Poor	--	--	--	--	--
	--	--	--	--	No	Fair	Poor	6.2	.36	34	.62	630
	--	--	--	--	No	Fair	Poor	5.5	.38	24	.62	485
5/32" WATER RP	--	--	--	--	No	Poor	Poor	--	--	--	--	--
	100	2.1	9	28	No	Poor	Poor	--	--	--	--	--
	130	--	--	--	No	Poor	Poor	8.4	.24	54	.74	690
	140	1.7	7	42	Severe	Fair	Fair	5.1	.27	52	.77	405
3/16" AIR SP	185	2.0	10	29	No	Good	Good	5.7	.41	39	.64	305
	190	2.1	10	28	No	Good	Good	6.5	.43	48	.58	255
	190	2.2	10	36	No	Fair	Good	5.2	.46	69	.54	220
	205	1.9	13	28	No	Fair	Good	5.9	.45	51	.51	245
3/16" WATER SP	180	2.5	10	32	No	Fair	Poor	6.3	.37	36	.58	500
	180	2.8	9	36	No	Fair*	Poor*	5.4	.36	57	.79	520
	180	3.6	9	42	No	Poor	Poor	8.8	.22	44	.79	420
	160	2.8	8	44	No	Poor	Poor	5.7	.32	40	.70	525
3/16" WATER RP	170	2.0	8	37	No	Fair	Fair	5.3	.39	42	.62	485
	130	2.4	8	36	No	Fair	Fair	4.7	.41	26	.74	435
	150	2.3	9	34	No	Fair*	Fair*	7.6	.30	39	.69	485
	150	2.7	6	52	Severe	Fair	Fair	4.9	.37	46	.61	485

is noted between various sizes and differently coated electrodes than between air and underwater conditions (Figure 7-5).

Thus, a possible conclusion is that the water environment does not directly change the metal transfer or electrode melting processes, but rather, after the weld bead is laid down, the water influences the solidification and cooling mechanisms. Reverse polarity may accentuate the flux barrel length problem by causing the electrode to melt, without simultaneously melting the flux coating. Straight polarity may give a more even burnoff of the flux coating and melting of the electrode.

The other welding factor, besides the current, which is influencing the weld bead shape is the welding speed. The natural drag speed seems to be determined by the electrode size and type, and current. In water, the natural drag speed decreases by 2-4 inches/minute, using E6027 - 5/32" and 3/16", apparently due to the slower rate of flux burnoff. However, for 1/8" E6013 and E7014, the underwater speed is faster than in air. This implies that another force is acting to increase the speed underwater. If the water is constricting the arc, then the arc may be digging out the crater faster because of its concentrated current density, or power, and this would cause the speed to increase. The effect of longer arc decreases the current density and thus, lowers the digging power of the arc. If the welding speed is hindered artificially in hopes of improving the weld shape, it is found that almost no improvement in penetration is achieved and that the weld bead just becomes wider. So, the electrode should be allowed to proceed at its natural drag speed. The penetration is limited by the current density of the arc and this is often controlled by the maximum attainable current because of the long barrel length. Consistent with the idea that the water environment may be modifying the current density of the arc is the observation that underwater weld beads are slightly

FIGURE 7-5

WELD BEAD SHAPE FACTORS

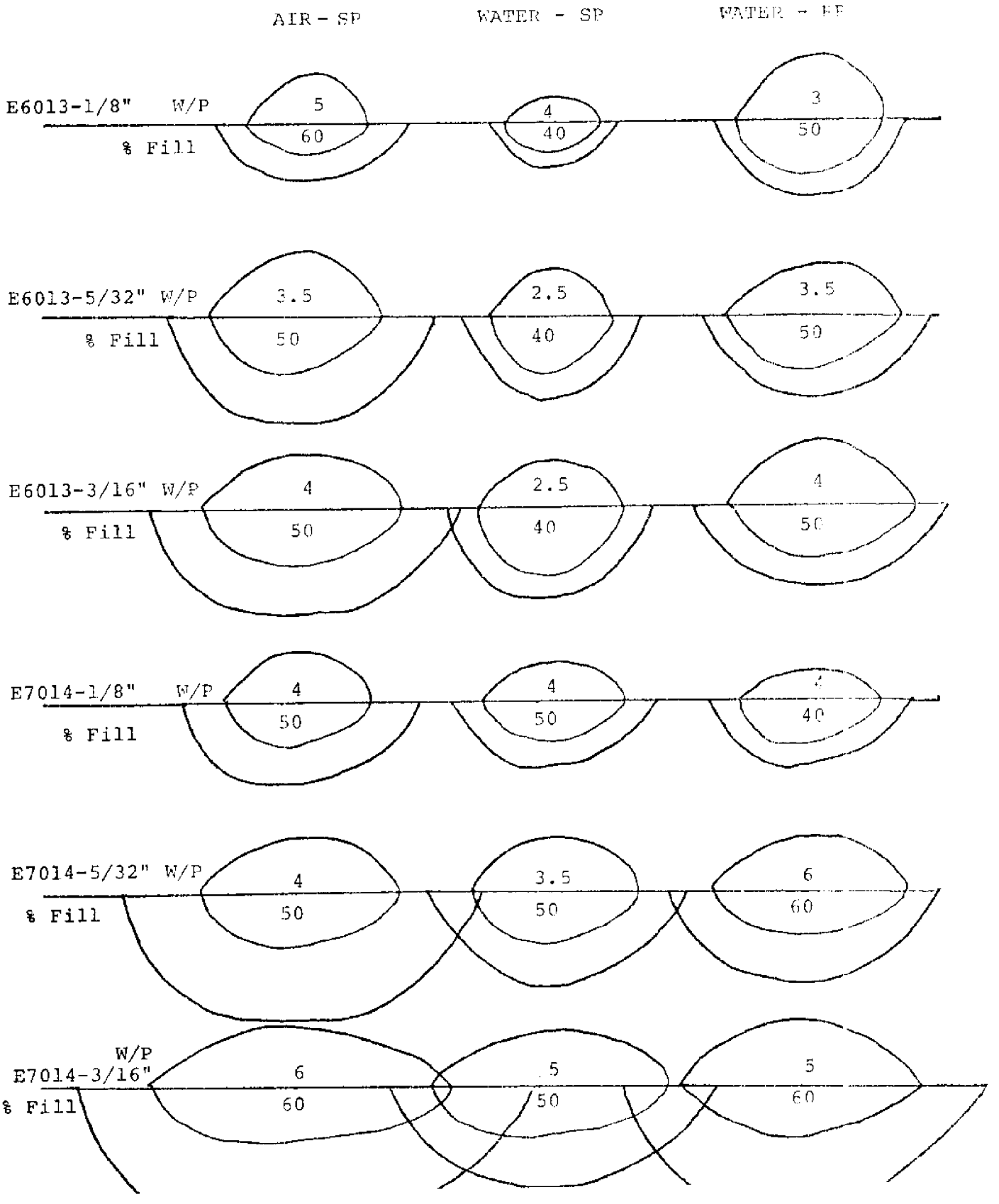

more narrow than air weld beads. This effect is more noticeable with the smaller electrode sizes since the larger electrode coverings provide insulation between the arc column and the water column.

7.29 Underwater Weld Geometrical Characteristics

Figures 7-6 through 7-9 contain a representative sample of macrophotograph profiles magnified 7.5 times which were used to determine the weld bead geometrical characteristics. There are three separate factors giving rise to changes in the weld bead shapes:

(1) The weld bead shapes are changing as a result of moving from non-optimum welding conditions (current) to the optimum or best obtained welding conditions.

(2) The weld bead shapes change due to varying electrode size and coating type.

(3) There are various changes which result in switching from air welding conditions to underwater welding conditions.

The effects from underwater welding conditions are masked behind these other two factors. The most significant weld beads are those which were produced with near the optimum welding current. The following discussion will be observations on the actual weld beads and will attempt to characterize general trends as they emerge.

E6013 - 1/8" air weld beads were 7-11mm^2 in size with penetrations of between .5 and 1.2mm. The widths were between 3mm and 6mm, giving shape factors (W/P) of 6.1 to 4.6 and percent reinforcement values of 57-83. The idealized optimum weld bead is shown in Figure 7-10. The penetration of 1mm is not very satisfactory, which is one of the problems of 1/8" electrodes. Underwater straight polarity welds and reverse polarity welds appear to be very different in shape. This is not explained. Other electrodes do not produce

FIGURE 7-6

WELD BEAD SHAPE CHARACTERISTICS
E6013 5/32"
Magnification 7.5 X

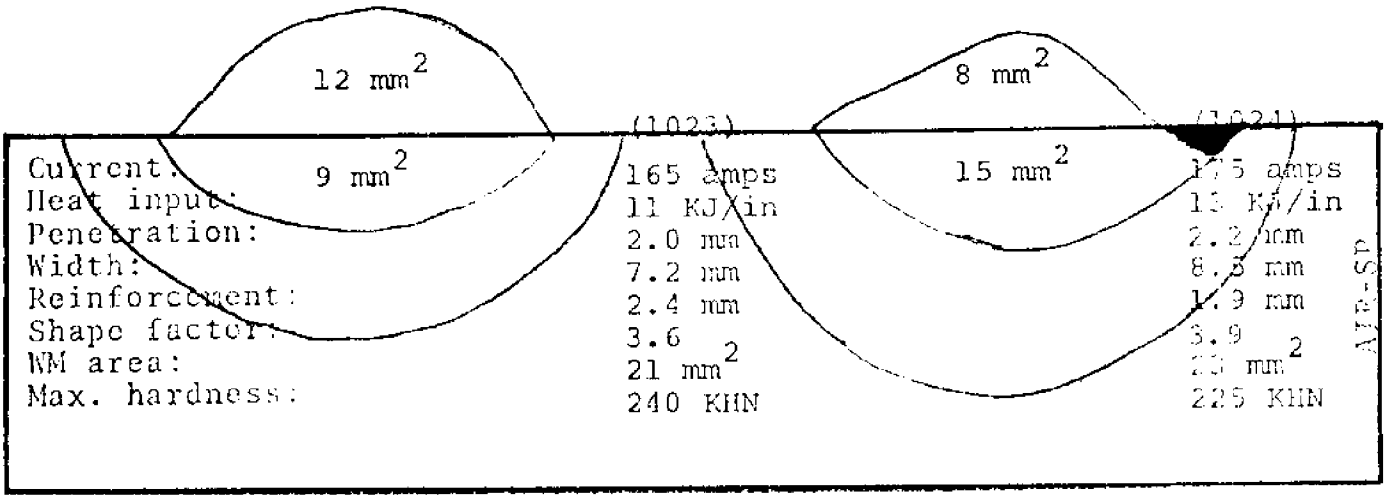

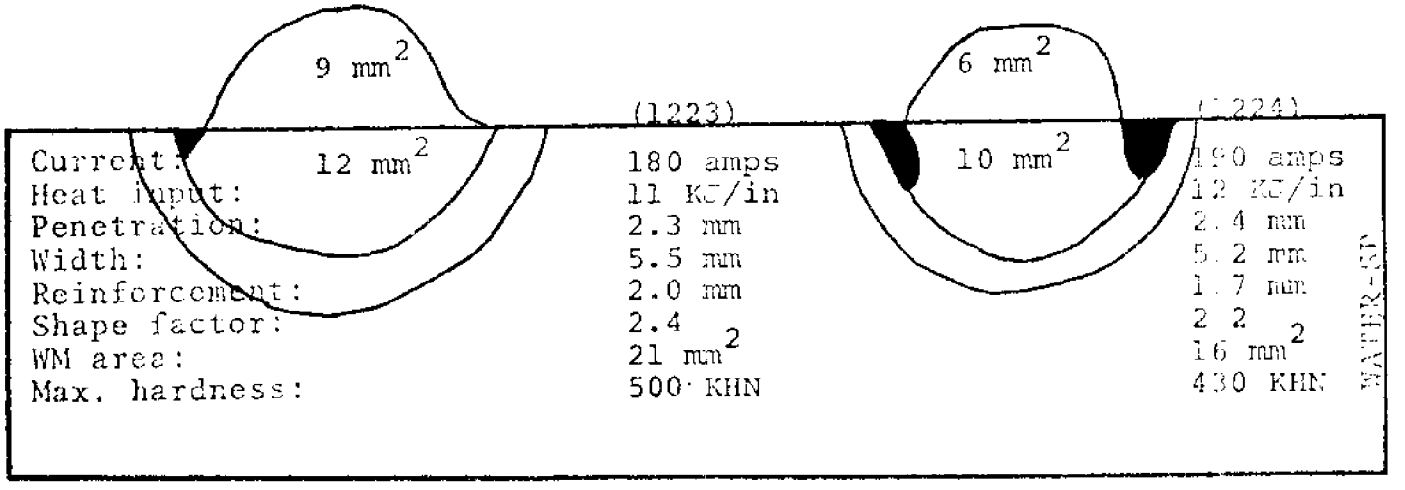

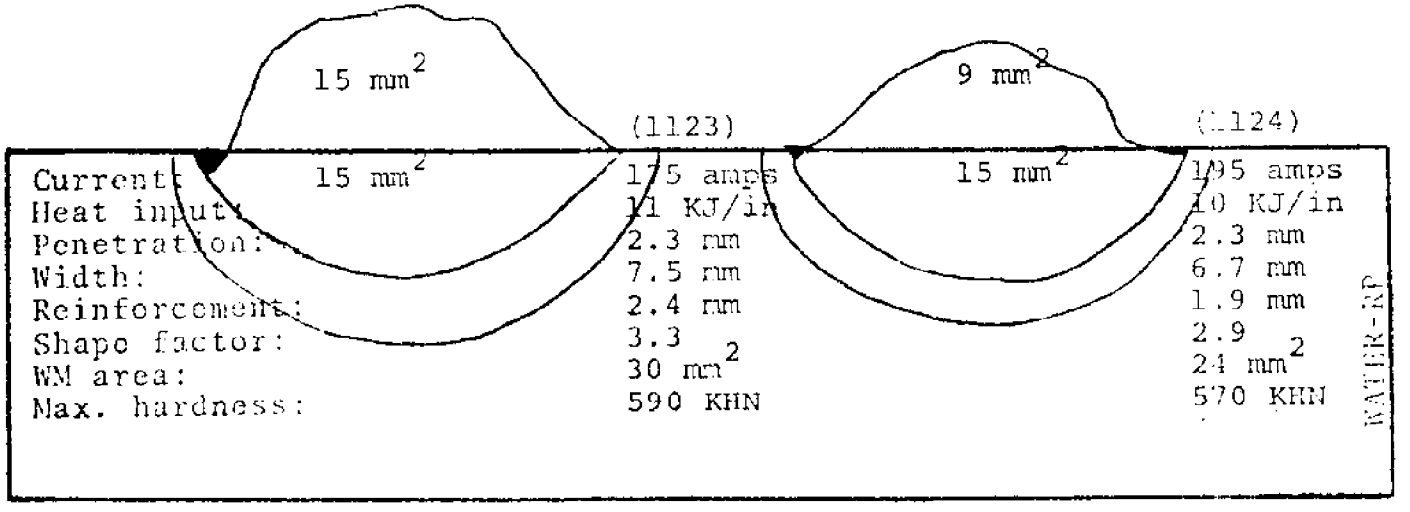

FIGURE 7-7

WELD BEAD SHAPE CHARACTERISTICS
E7014 5/32"
Magnification 7.5 X

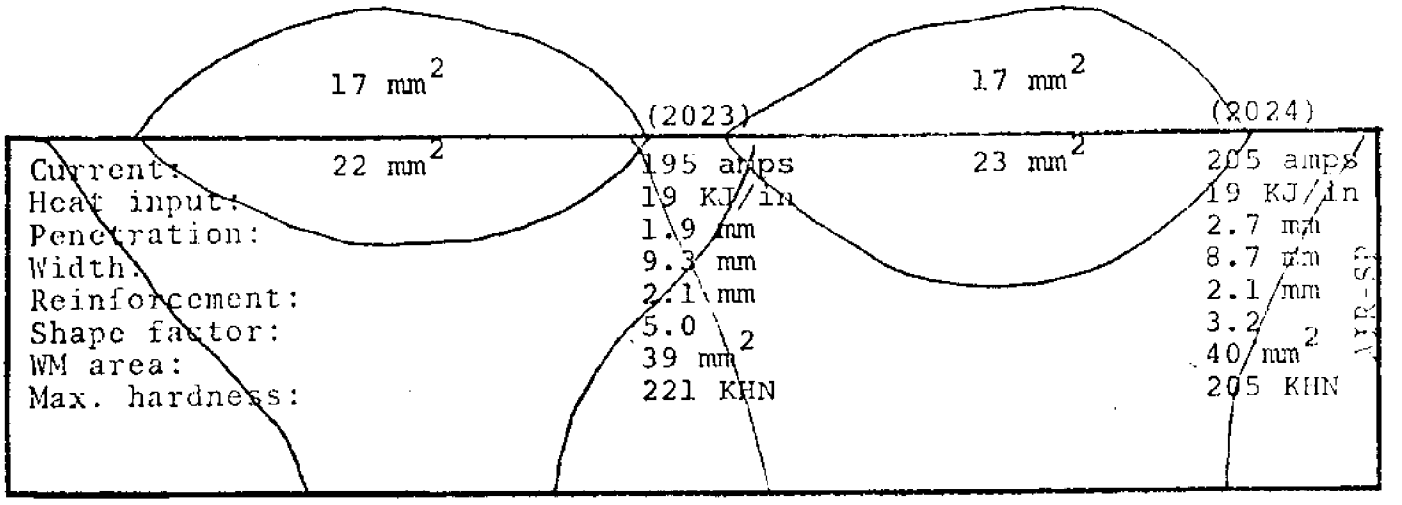

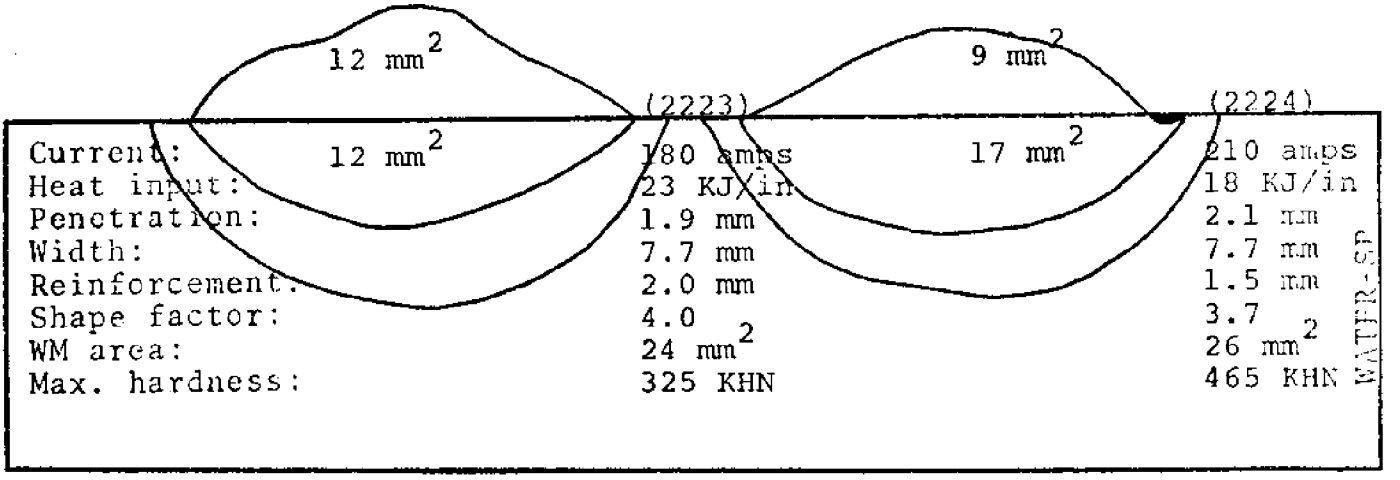

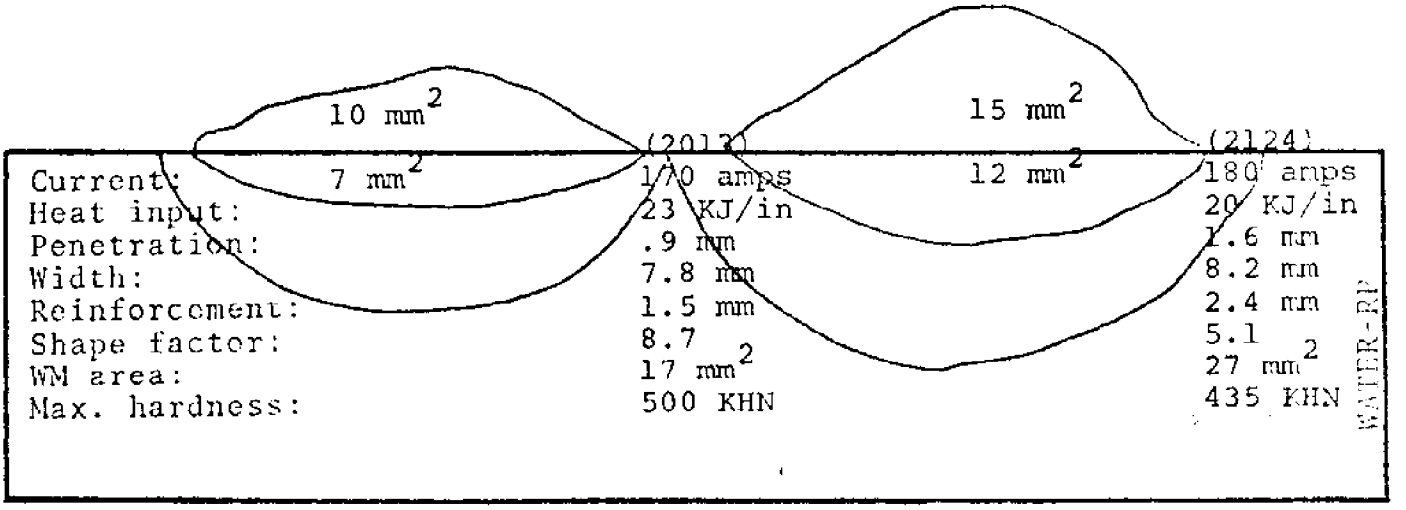

FIGURE 7-8

WELD BEAD SHAPE CHARACTERISTICS
E7024 5/32"
Magnification 7.5 X

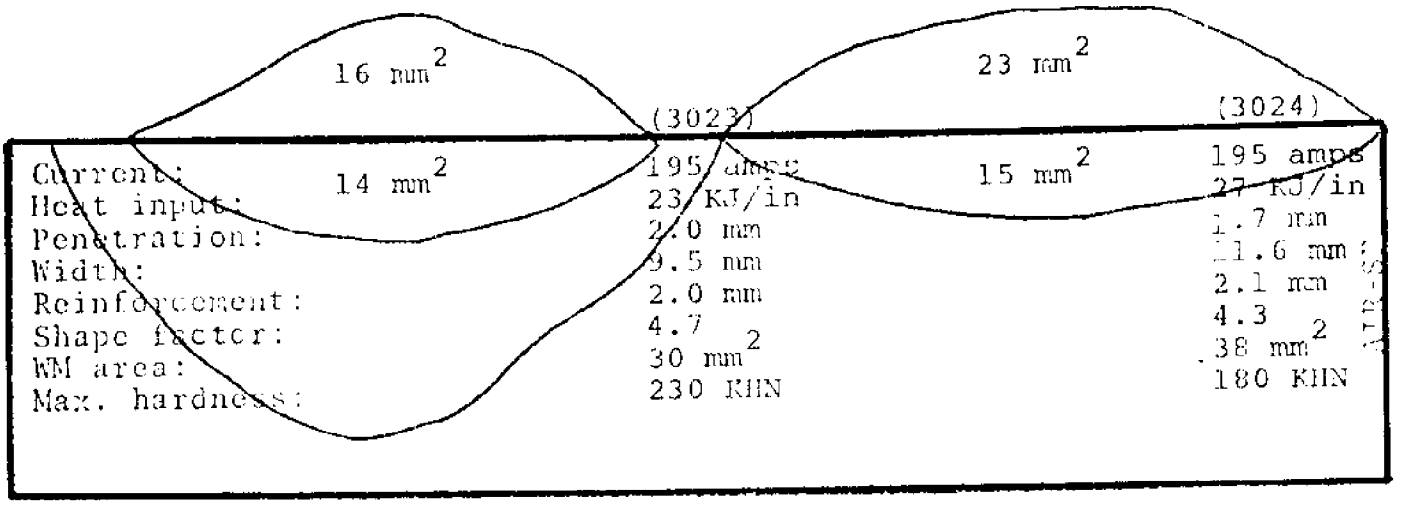

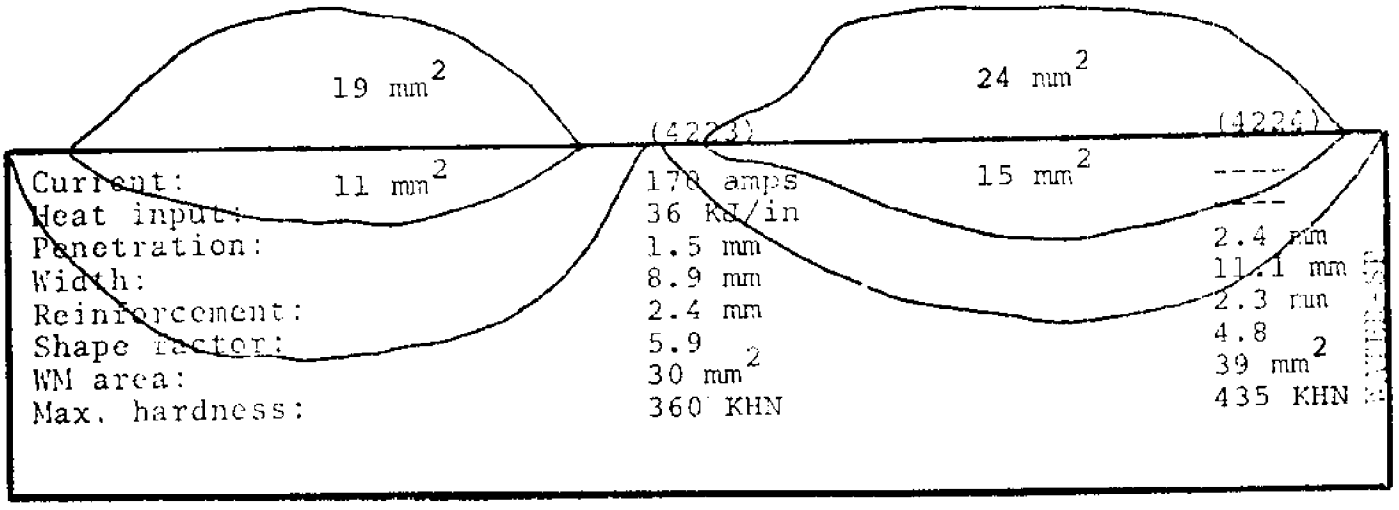

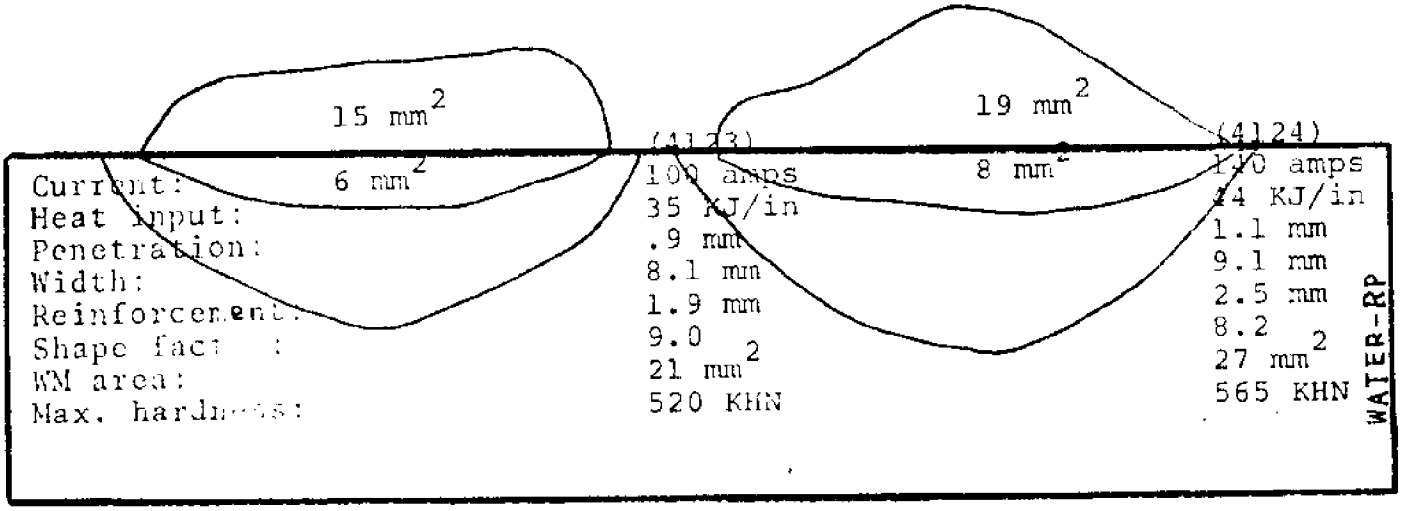

FIGURE 7-9

WELD BEAD SHAPE CHARACTERISTICS
E6027 5/32"
Magnification 7.5 X

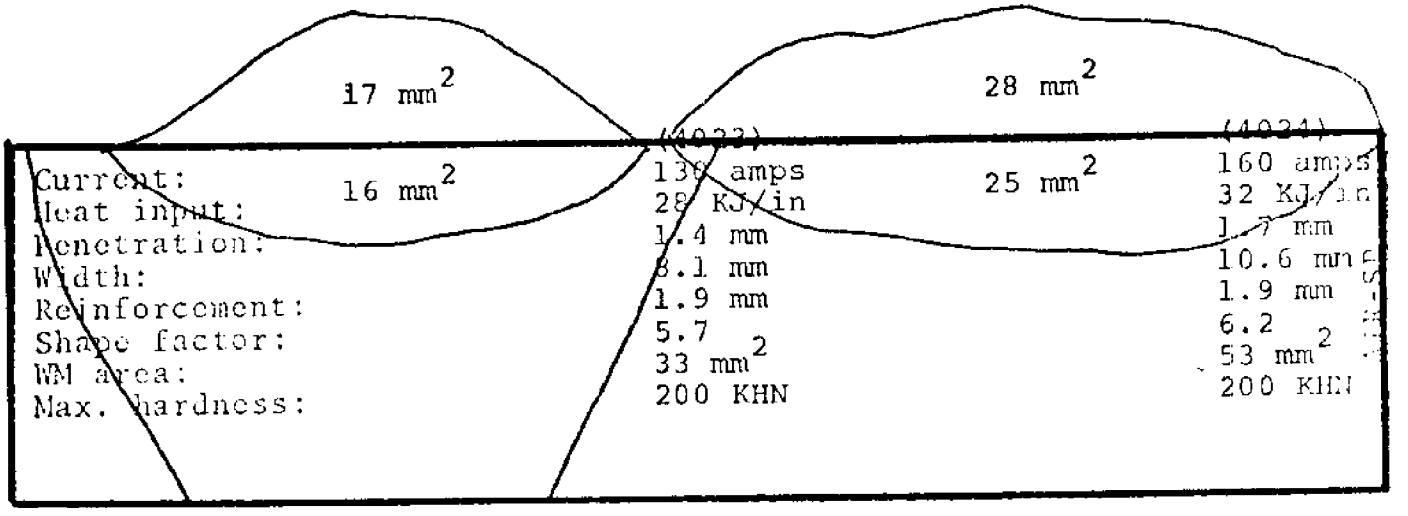

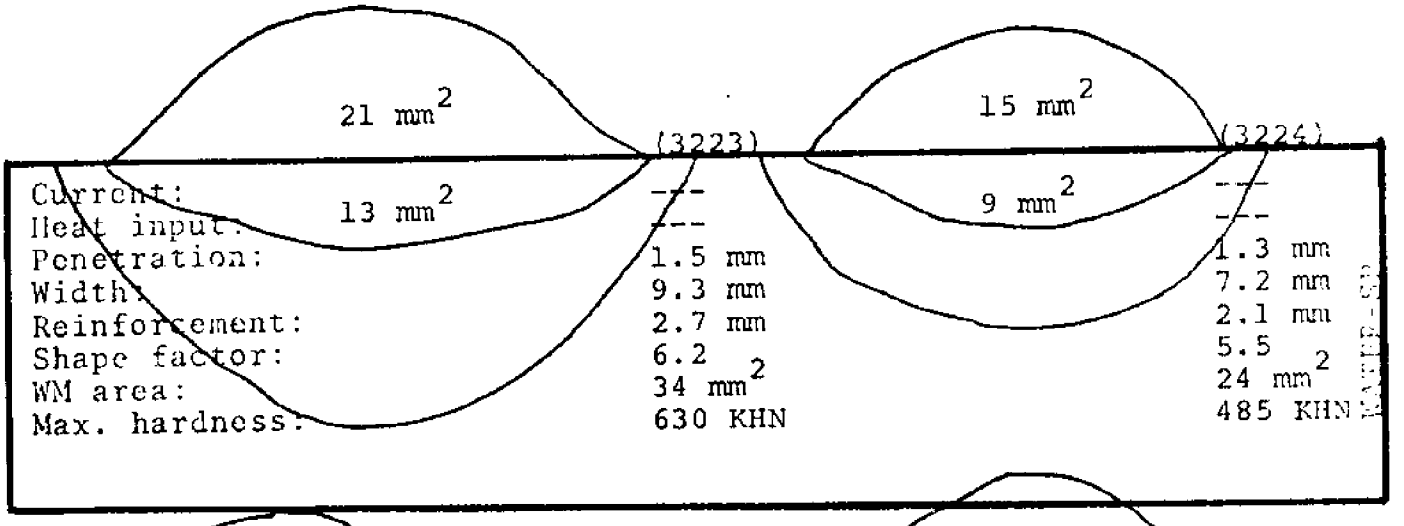

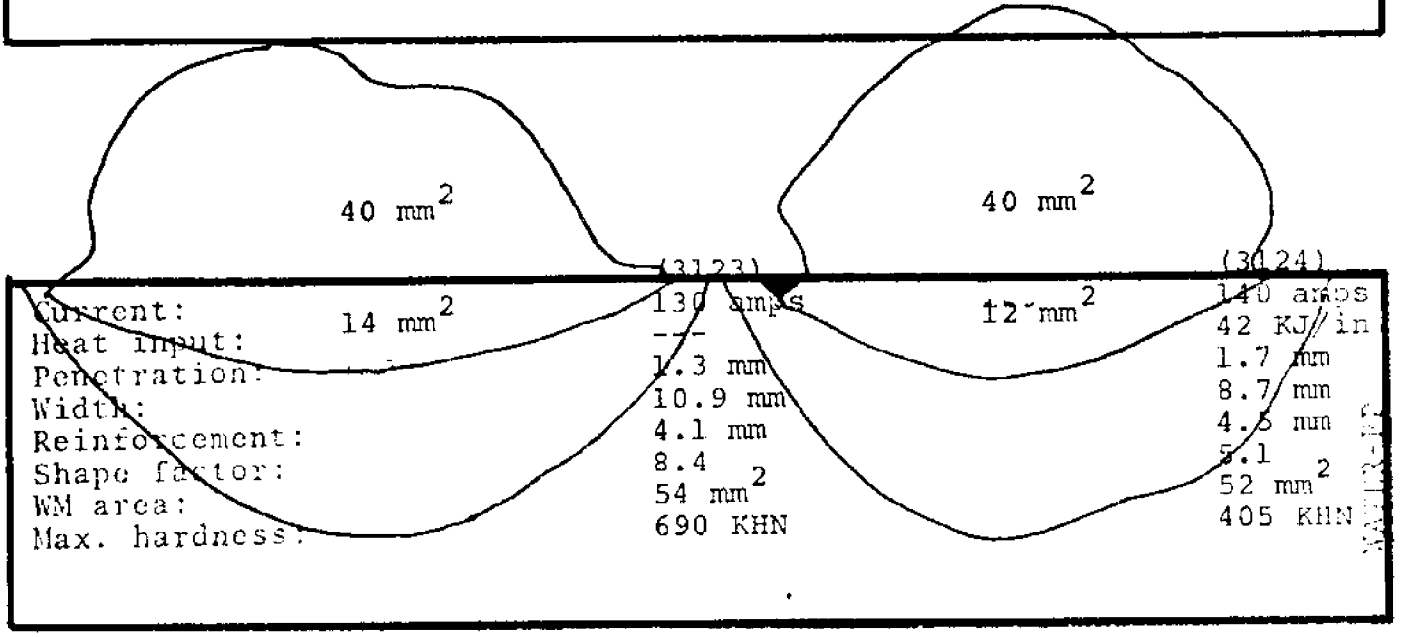

such contrasting shapes between the two polarities. The straight polarity welds are much smaller than the reverse polarity having a size of 4-10mm^2 compared to 14-26mm^2 for reverse polarity. Straight polarity penetration was .5mm to 1.7mm. This is deeper than the air welds. Reverse polarity penetration was 1.9mm-2.1mm which is better than the air welds, but the welding current was higher also. This is the beginning of evidence that the penetration depends on the welding current. The straight polarity width is 2.9-4.1mm, giving weld shape factors of 5.8 to 2.2. Reverse polarity welds were 4.4-6.9mm wide with shape factors of 3.4 to 2.3. Seven out of the eight underwater weld cross sections show undercutting. Air reinforcements vary between 1.5mm and 2.0mm. Underwater reinforcements were 1.1-1.5mm for straight polarity and 1.6-2.7mm for reverse polarity. The percentage reinforcement for straight polarity varies from 36 to 54, and for reverse polarity from 40 to 52. Thus, from E6013 - 1/8" data, it appears that underwater welds produce better shaped welds with more penetration, less width, and less reinforcement. The undercut is a problem.

E6013 - 5/32" weld beads are larger than the 1/8" beads. Air weld sizes are between 16mm^2 and 23mm^2. Underwater straight polarity size was 13mm^2-30mm^2. Thus, the size is surprisingly similar for welding currents that were only slightly different. Heat inputs to the air welds were 10-13kJ/in while that to the underwater welds was 9-12kJ/in. Thus, these series of welds are very similar and comparable. Penetration was 1.2-2.1mm for air, 1.2-2.4mm for underwater straight polarity, and 1.6-2.3mm for underwater reverse polarity. Air weld widths were 5-8.5mm. Underwater (WP) widths were 4.4-5.5mm and underwater (RP) widths were 6.4-7.5mm. For the same arc current, the narrowing effect in the underwater welds seems important. At 175 amps, the air weld has a penetration of 2.2mm and a width of 8.5mm giving a shape factor of 3.9. The underwater (SP) weld bead with 180 amps is 2.3mm deep, 5.5mm wide, resulting in a shape factor of 2.4. Underwater (RP) at 175 amps gives a penetration of 2.3mm

and a width of 7.5mm, and a shape factor of 3.3. The height of reinforcement is 1.9-2.5mm for the air welds, 1.5-2.1mm for the SP welds, and 1.2-2.4 for the RP welds. The percentage reinforcement in the air was 35-75%; in SP welds it was 37-70%; and in RP welds it was 30-49%. These data show that the underwater welds resulted in more of the weld bead penetrating or fusing into the base metal, giving better shaped welds with better fusion. However, undercutting was observed in all of the underwater welds. The depth of the undercutting (.1 - .8mm) may not be as significant as the notch effect which results regardless of depth.

E6013 - 3/16" air weld beads show about the same penetration as the previous weld beads. This seems to again indicate that the penetration only increases with welding current, regardless of the electrode size. Thus, at 125 amps, the 1/8" electrode gave a penetration of 1.2mm while the 5/32" electrode at 120 amps gave a penetration of 1.2mm and the 3/16" electrode at 160 amps gave a penetration of 12.mm. The 3/16" air penetration ranges from .6mm to 1.9mm. Underwater penetration values are deeper giving 1.7-2.8mm for straight polarity and 2.0-2.7mm for reverse polarity. It appears that the water may constrict the arc and give a higher current density and thus, a deeper penetration and a narrower bead. Air widths were between 5.6mm and 7.7mm. Water (SP) widths were 5.2-7.6 and water (RP) widths were 5.3-8.3mm. But the W/P shape factors in underwater welds were better than the air values (Air: 4.0-9.3, Water (SP): 2.1-3.0, Water (RP): 2.3-4.0). Reinforcement heights were similar in air and underwater. Table 7-4 summarizes these parameters for #6013 weld beads. Figures 7-10 to 7-12 show idealized optimum weld beads with all three sizes of #6013 electrodes. From the E6013 data, it continues to appear that underwater welds with slightly higher currents produce better shaped weld beads. But the overall impression, especially for the 3/16" electrodes, is that the shapes are almost identical between air and underwater for the same optimum current.

FIGURE 7-10

TYPICAL WELD BEAD SHAPES AND MICROHARDNESS PROFILES OF E6013 1/8" FOR COMPARABLE AIR AND UNDERWATER WELDS

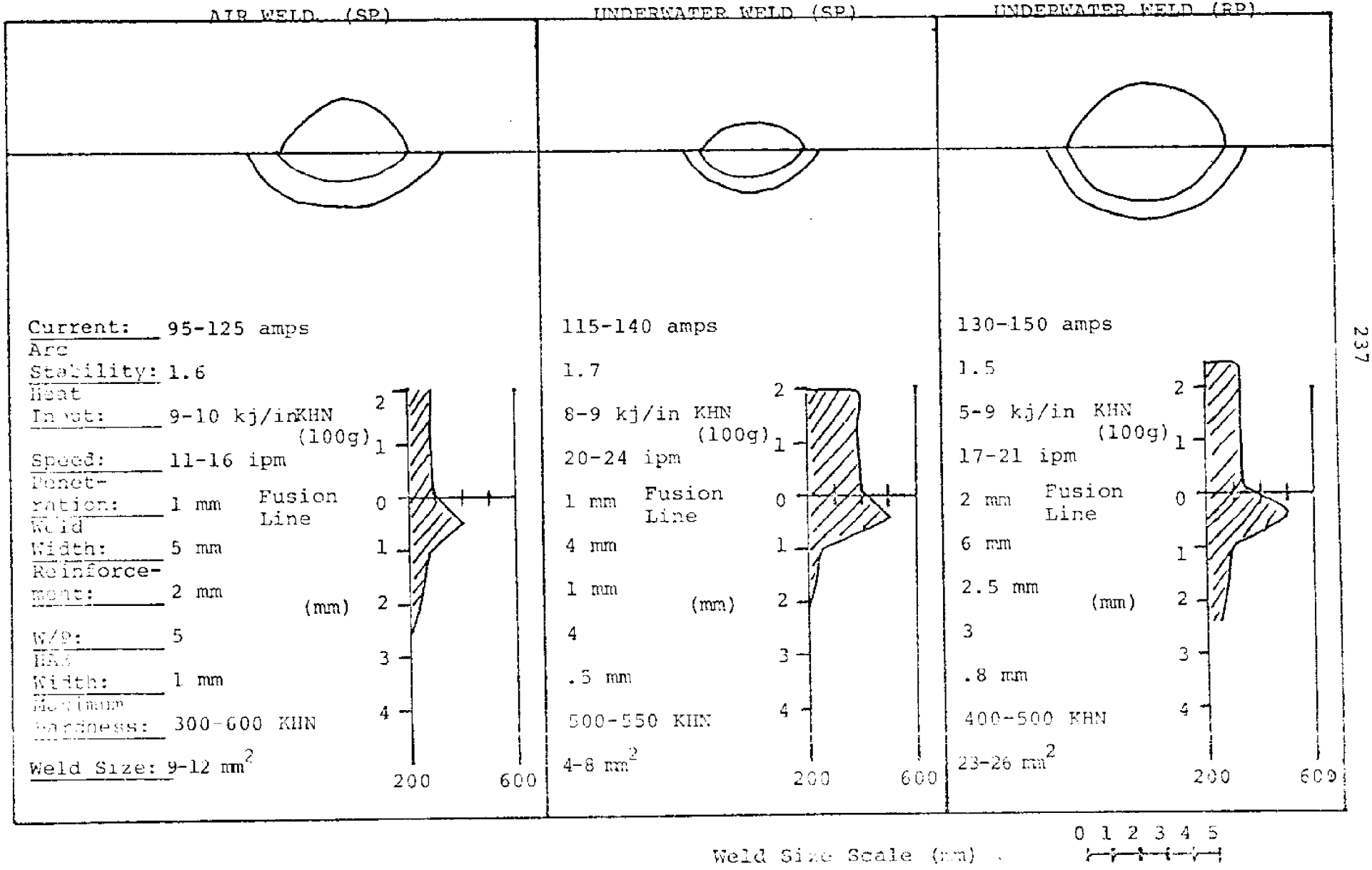

FIGURE 7-11

TYPICAL WELD BEAD SHAPES AND MICROHARDNESS PROFILES OF E6013 5/32" FOR COMPARABLE AIR AND UNDERWATER WELDS

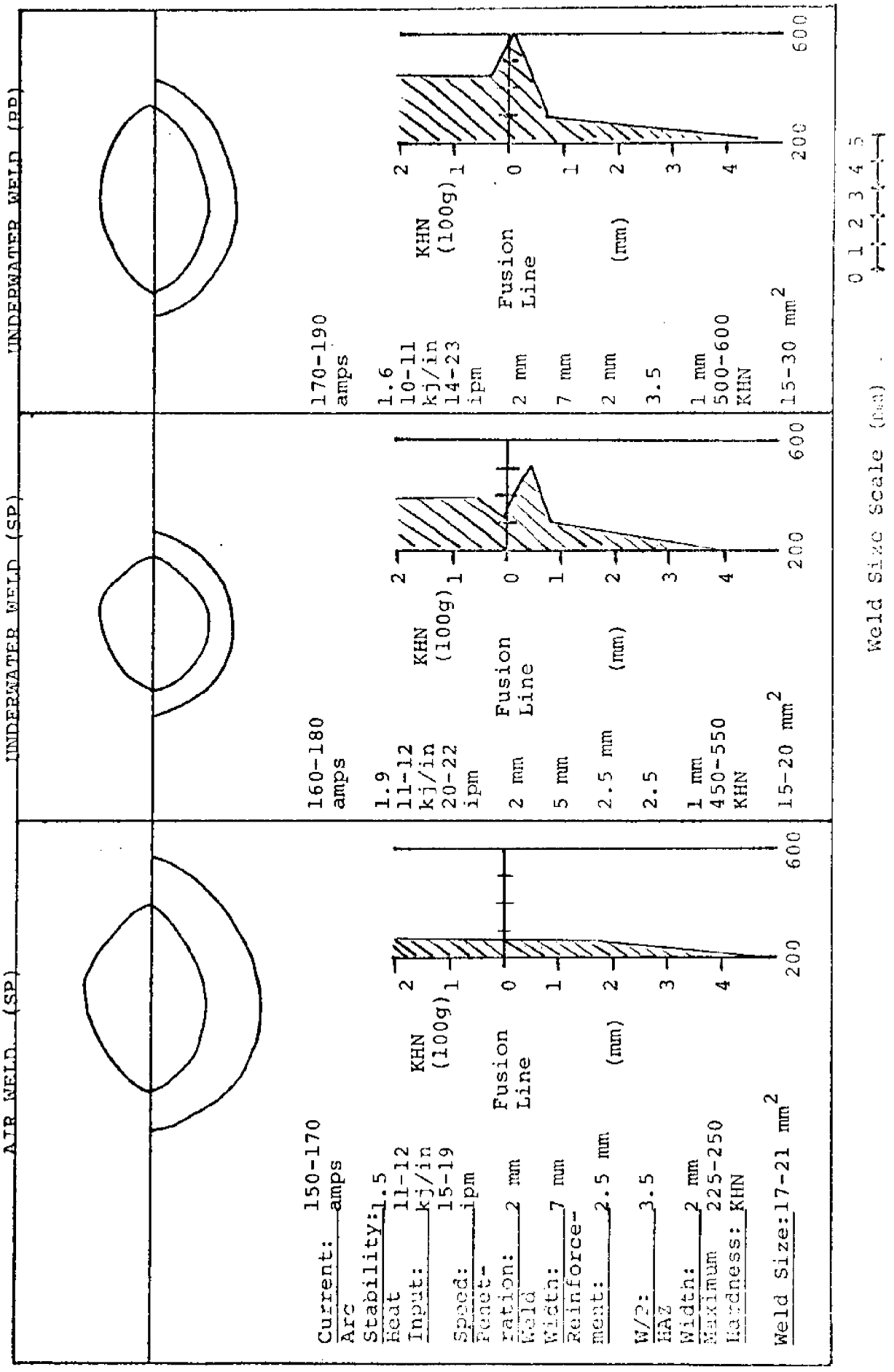

FIGURE 7-12

TYPICAL WELD BEAD SHAPES AND MICROHARDNESS PROFILES OF E6013 3/16" FOR COMPARABLE AIR AND UNDERWATER WELDS

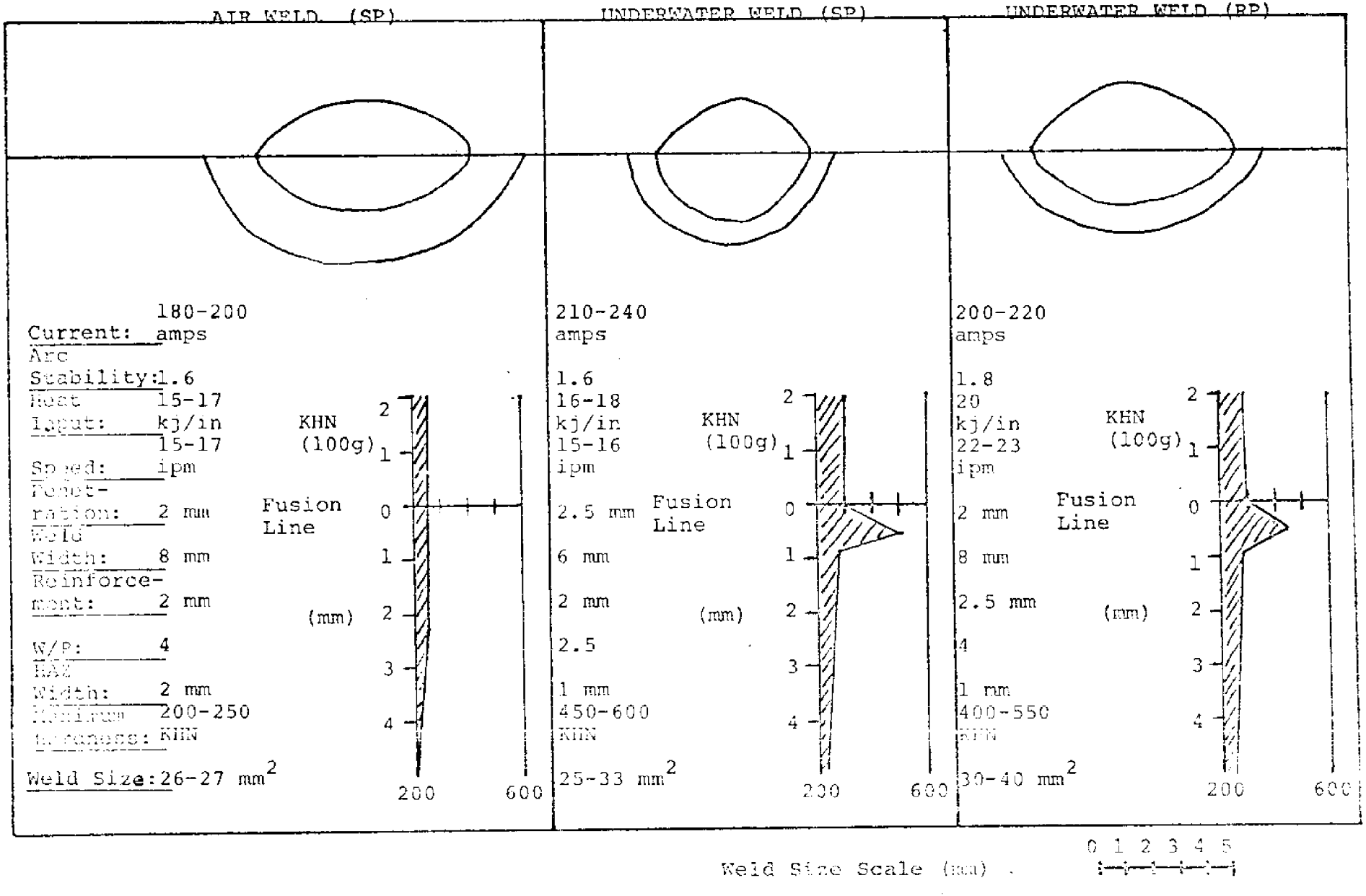

For #7014 - 1/8" electrodes, the air weld shape is almost identical to the water weld shape for the best weld beads. Figure 7-13 shows the idealized weld beads and shows that they result at the same optimum currents.

For E7014 - 5/32" electrodes, the underwater welds have less penetration, but this is only due to the current limitation. In air, 170 amps gives a 1.3mm penetration. This is matched by a 1.9mm penetration underwater (SP) at 180 amps and by a 1.6mm penetration underwater (RP) at 180 amps. The shape factors for air are 3.2-5.2 and those of underwater welds are 3.7-5.2 (SP) and 5.1-8.7 (RP). Because the optimum welding currents were not obtained underwater, the weld shapes are not as good as the air shapes. Figure 7-14 summarizes these variables for the best obtained welds from each series.

E7014 - 3/16" weld beads are ideally summarized in Figure 7-15. The welds are all quite large (Air: 20-43mm^2, Water (SP): 22-38mm^2, Water (RP): 26-44mm^2). The weld beads are very similar in size. The air welds are very spread out with shape factors of only 5-6.4. The air penetration is 1.3-2.4mm. The underwater welds are very similar with shape factors of 4.1-3.2 (SP) and 1.6-2.4mm (RP). The positive arc constriction effects are being counteracted by the elongated arc length current limitation.

Because the E7024and E6027 electrodes were so inhibited by the elongated arc effect, they will not be reviewed. The weld beads obtained and the summary of their shapes and characteristics are shown in Figures 7-16 to 7-19. Table 7-8 contains a summary of the penetrations since this is such an important parameter.

7.291 Summary of Weld Shape Observations

(1) The largest variations in weld bead shape resulted from going from non-optimum to optimum current values.

(2) Penetration is a function of the current input and is not strictly dependent on the electrode size.

FIGURE 7-13

TYPICAL WELD BEAD SHAPES AND MICROHARDNESS PROFILES OF E7014 1/8" FOR COMPARABLE AIR AND UNDERWATER WELDS

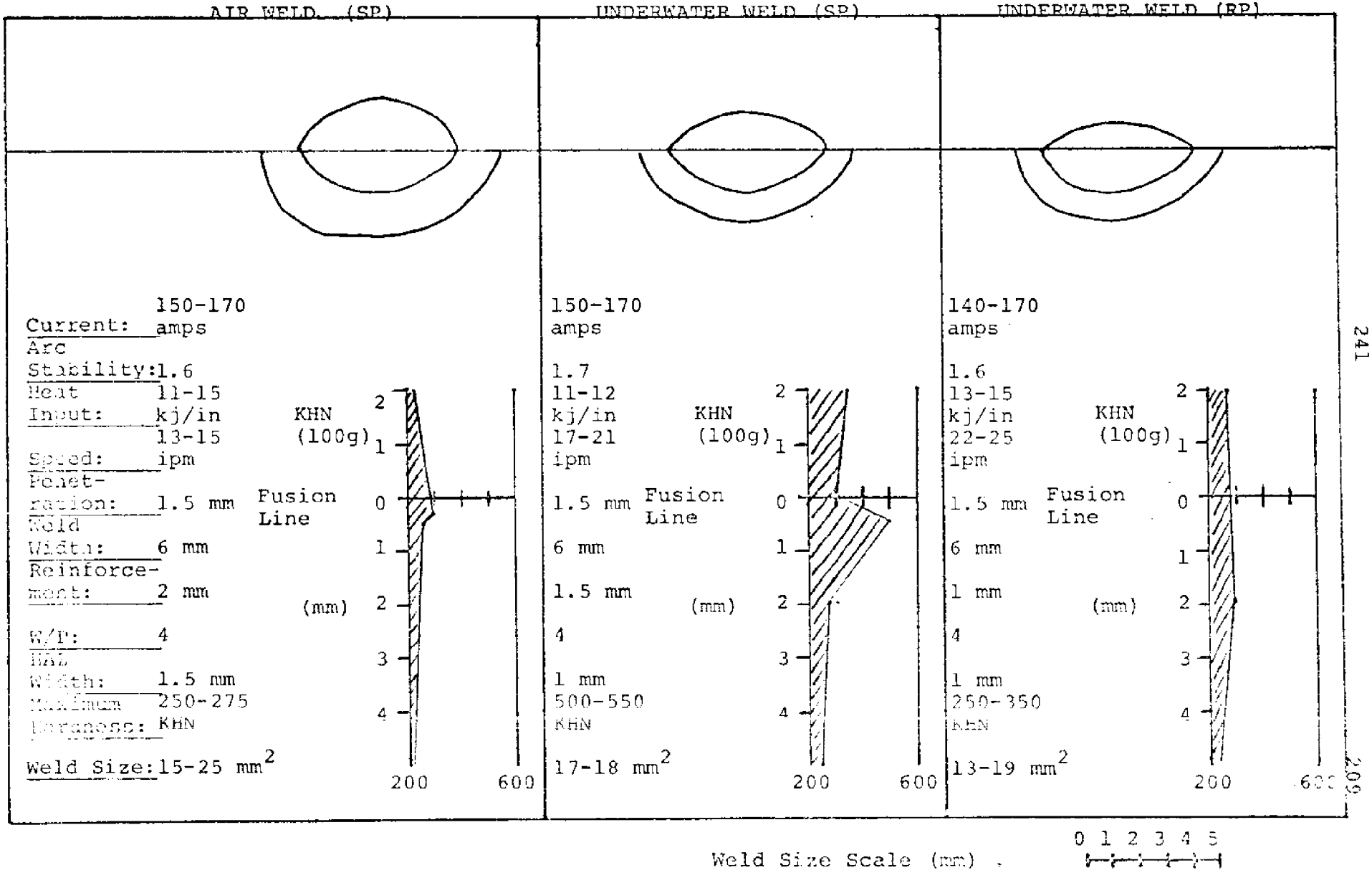

FIGURE 7-14

TYPICAL WELD BEAD SHAPES AND MICROHARDNESS PROFILES OF E7014 5/32" FOR COMPARABLE AIR AND UNDERWATER WELDS

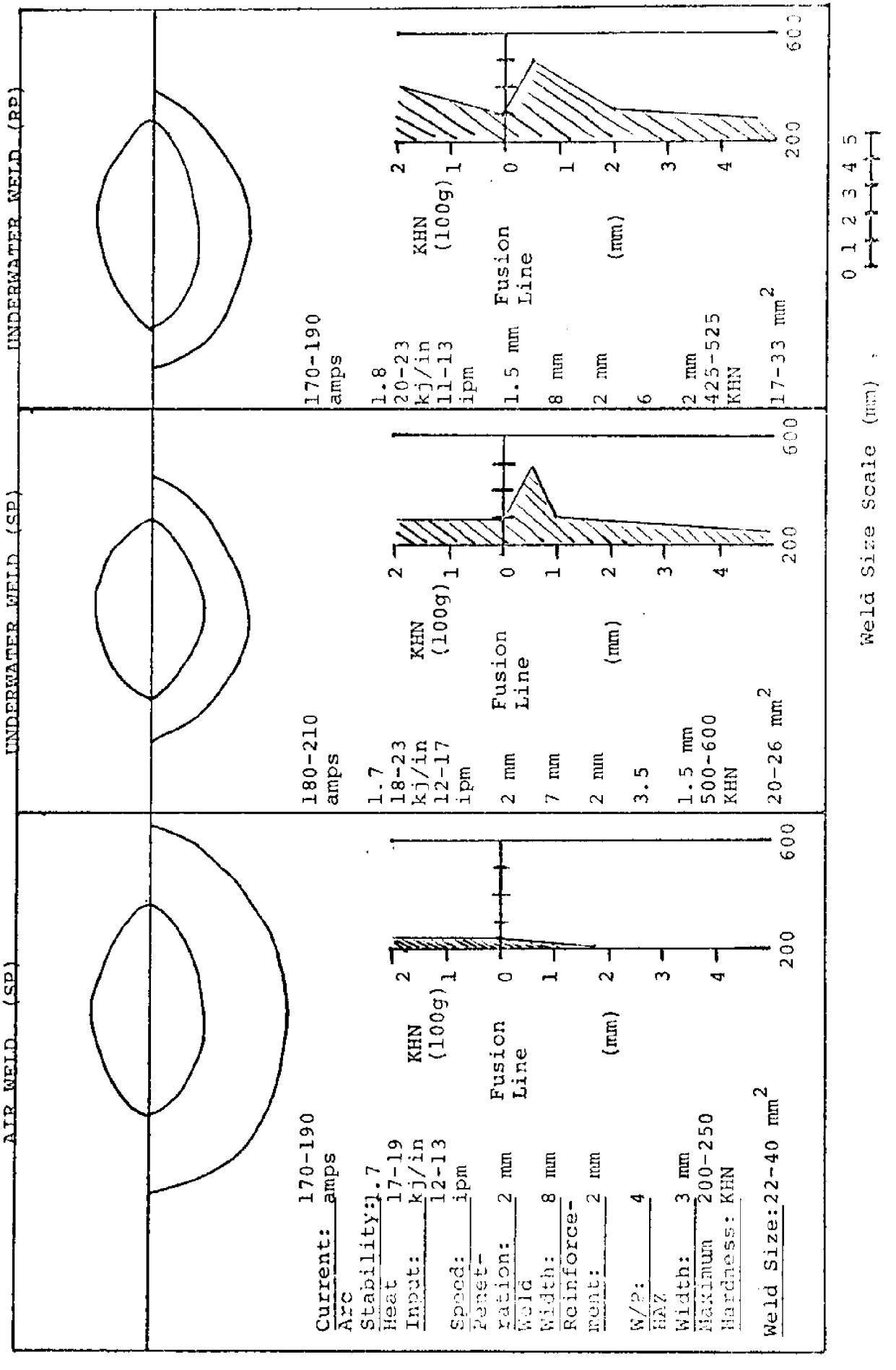

FIGURE 7-15

TYPICAL WELD BEAD SHAPES AND MICROHARDNESS PROFILES OF E7014 3/16" FOR COMPARABLE AIR AND UNDERWATER WELDS

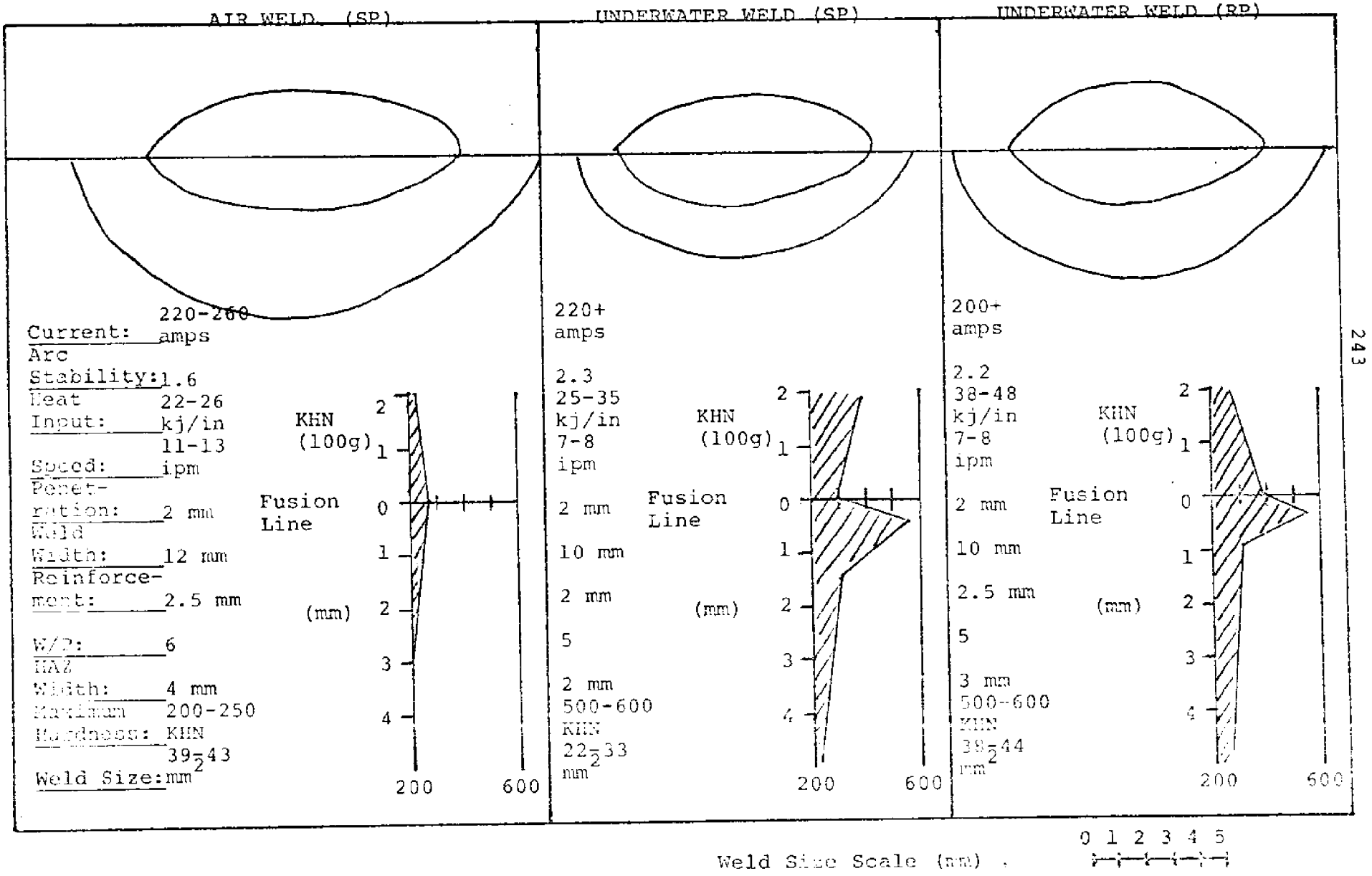

FIGURE 7-16

TYPICAL WELD BEAD SHAPES AND MICROHARDNESS PROFILES OF E7024 1/8" FOR COMPARABLE AIR AND UNDERWATER WELDS

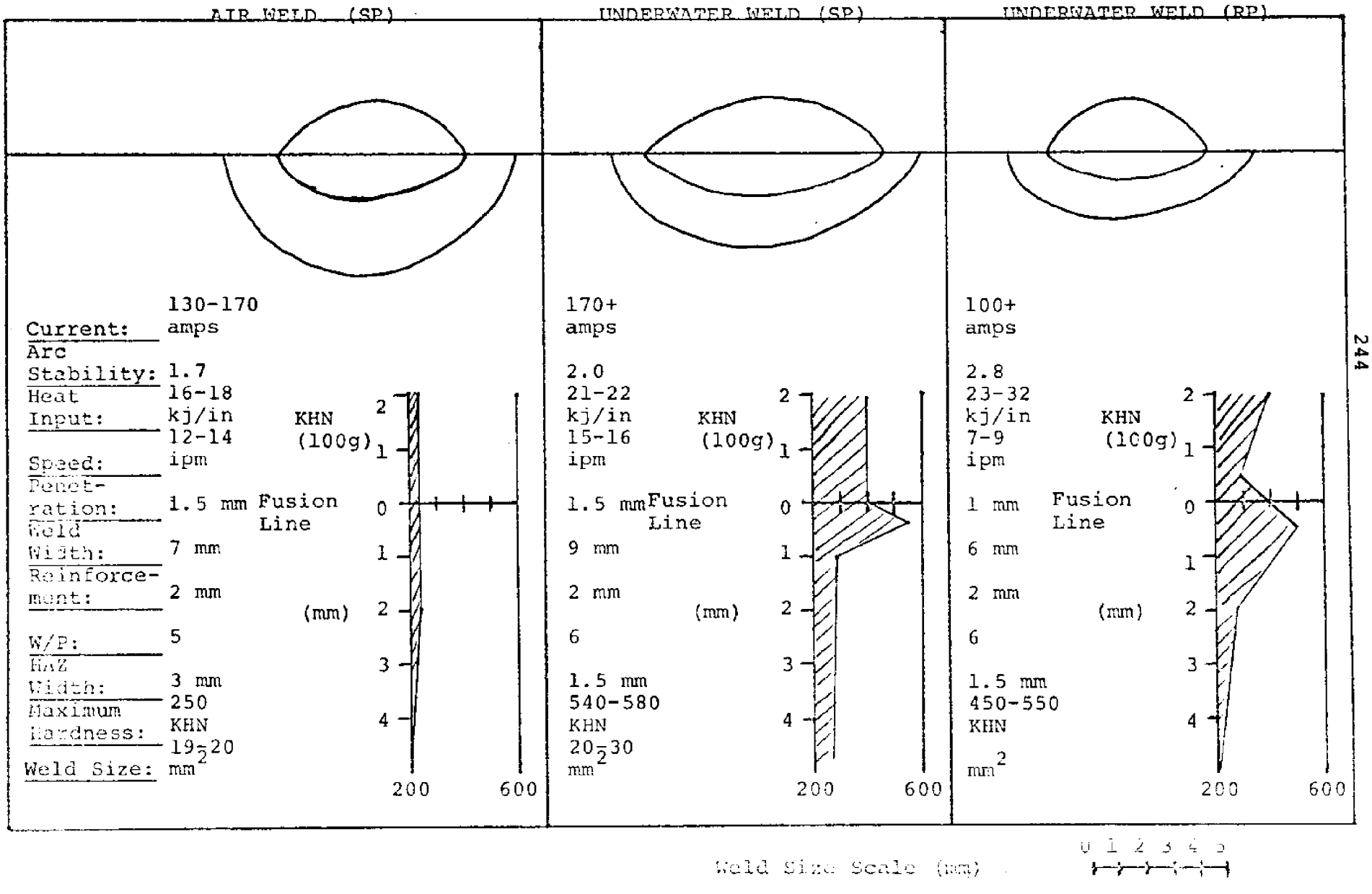

FIGURE 7-17

TYPICAL WELD BEAD SHAPES AND MICROHARDNESS PROFILES OF E7024 5/32" FOR COMPARABLE AIR AND UNDERWATER WELDS

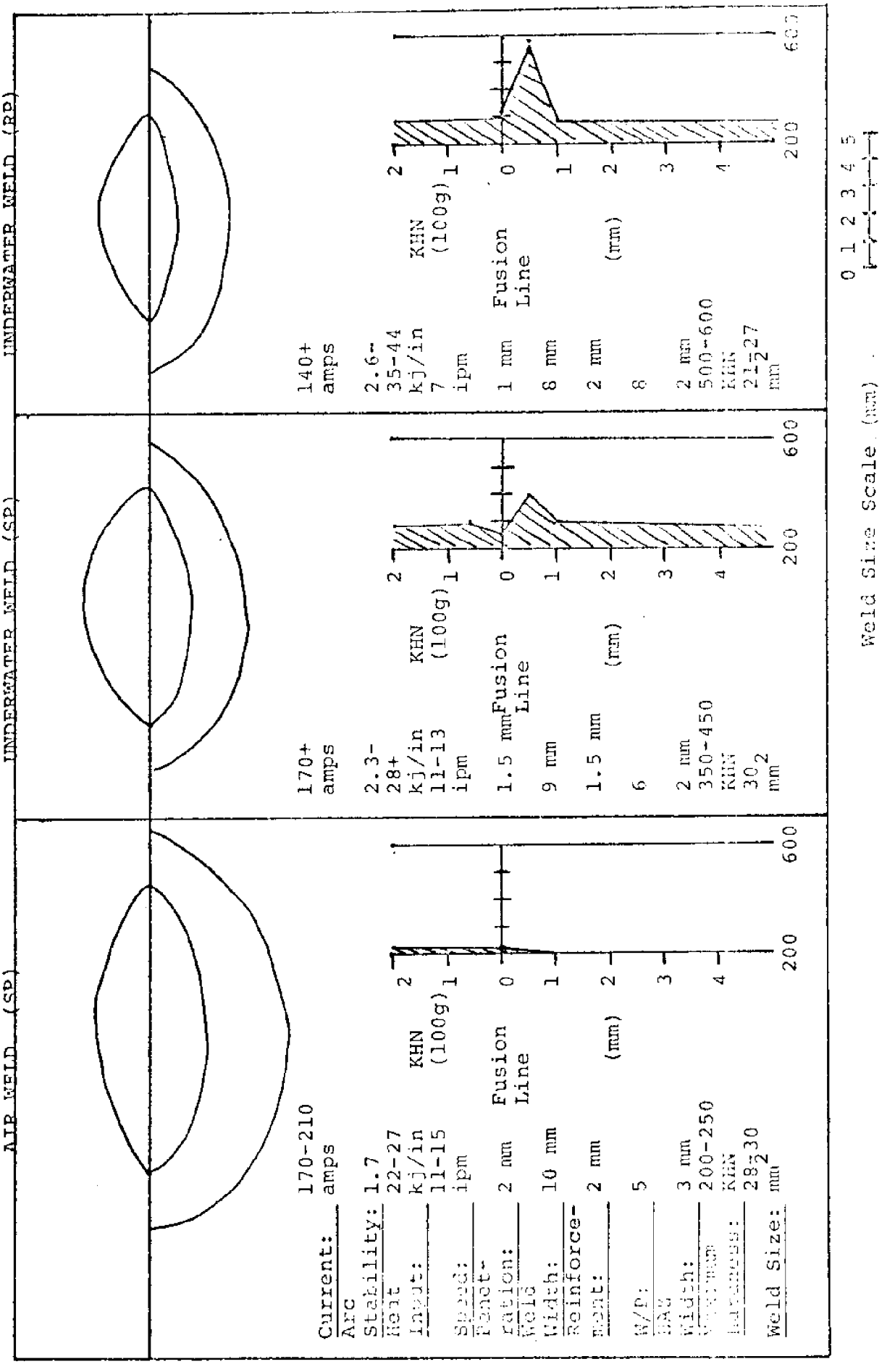

FIGURE 7-18

TYPICAL WELD BEAD SHAPES AND MICROHARDNESS PROFILES OF E6027 5/32" FOR COMPARABLE AIR AND UNDERWATER WELDS

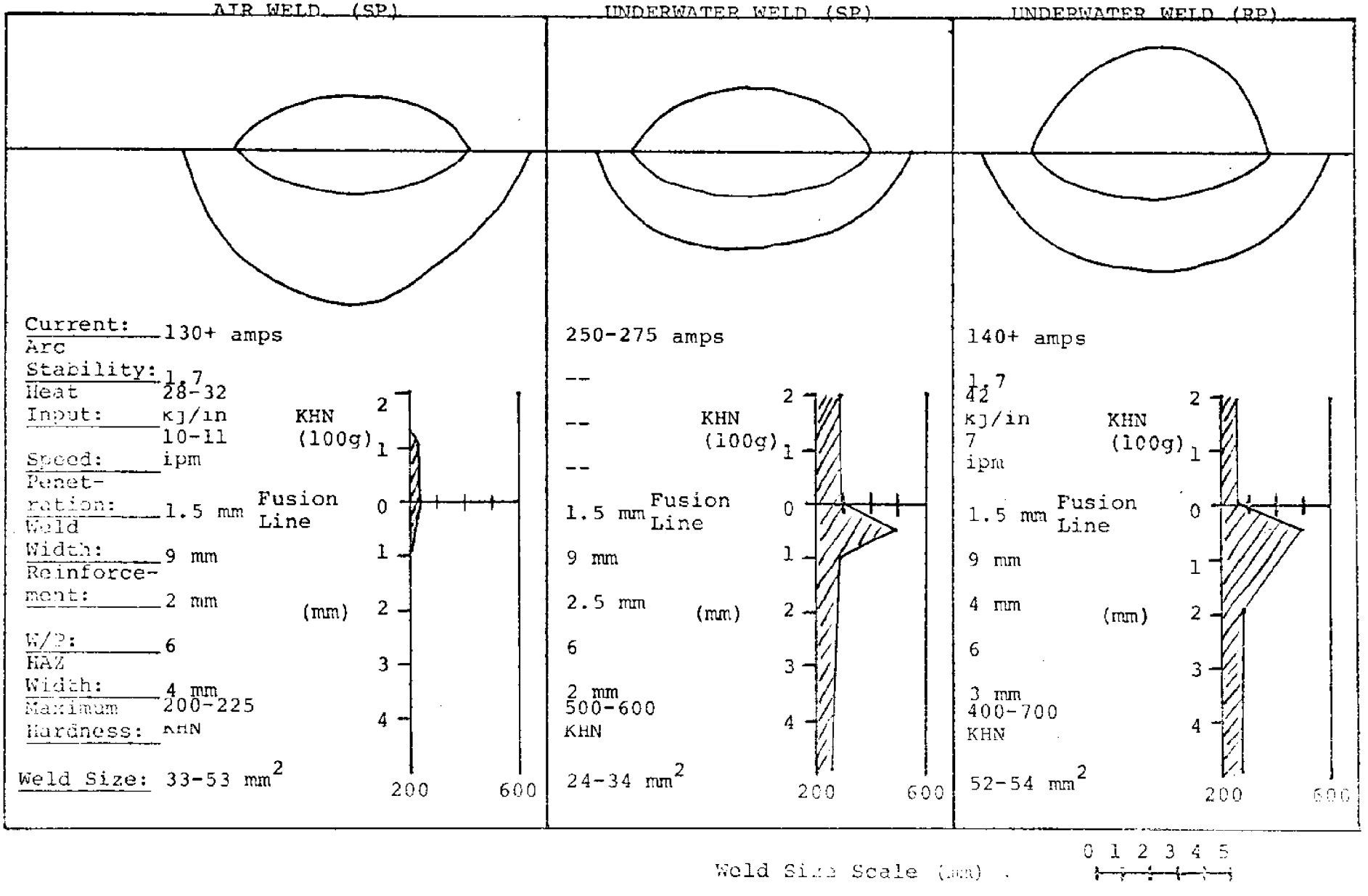

FIGURE 7-19

TYPICAL WELD BEAD SHAPES AND MICROHARDNESS PROFILES OF E6027 3/16" FOR COMPARABLE AIR AND UNDERWATER WELDS

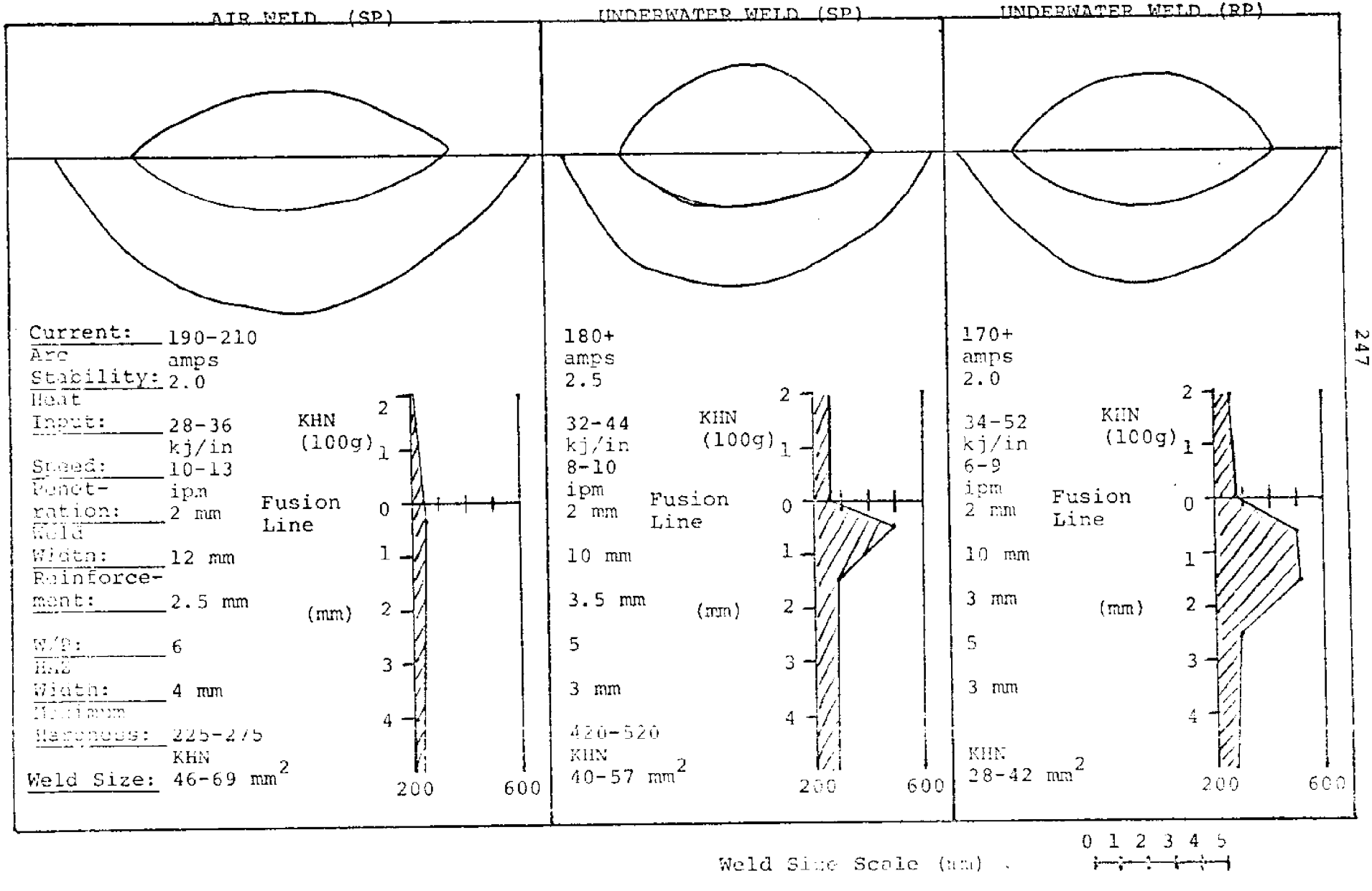

TABLE 7-8

PENETRATION COMPARISON

		1/8"	5/32"	3/16"
E6013	AIR	.5-1.2MM	1.2-3MM	.6-1.9MM
	SP	.5-1.7	1.2-2.4	1.7-2.8
	WATER RP	1.9-2.1	1.6-2.3	2.0-2.7
E7014	AIR	.8-1.9	1.1-2.7	1.3-2.4
	WATER SP	1.2-1.9	1.2-2.1	1.3-2.0
	WATER RP	1.2-1.8	.9-1.6	1.8-2.4
E7024	AIR	.9-1.6	.9-2.0	----
	WATER SP	1.2-1.9	1.2-2.4	----
	WATER RP	.9	.9-1.1	----
E6027	AIR	----	.6-1.7	1.7-2.4
	WATER SP	----	1.3-1.5	1.1-2.0
	WATER RP	----	1.3-1.7	1.3-2.1

(3) E6013 water welds had deeper penetration and a better shape than the air welds. For #7014, this effect was neutralized by the inability to achieve optimum underwater welding currents.

(4) Undercutting is a problem with many of the underwater welds. The depth is not as important as there just being a notch.

(5) The weld bead size increases with the size of the electrode since the current is increasing as well. The increase is the same for air and underwater welds.

(6) Underwater welds give the same penetration as air welds for the same current or heat input. But water welds will be narrower and so the underwater bead shape factors will be better.

(7) Underwater welds, at their optimum current which is higher than for air, give better penetration and a higher percentage of fused metal. But both effects may only be a result of the higher optimum current.

(8) Taken as a whole, the weld shape parameters indicate that there is not very much of a difference between air welds and water welds made at their respective optimum currents. This suggests that the most critical effects of the water do not begin until the weld puddle has formed and begins to solidify.

(9) Undercutting results from rapid solidification of the weld puddle, hindering the metal from flowing back into the edges of the crater. This is the most severe shape effect from underwater welding.

7.292 Microhardness Profiles and Comparisons

Microhardness profiles were made across all of the weld bead samples. The results were recorded in a series of charts, each chart corresponding to a particular electrode. Some of these figures will be discussed separately to identify observations and results which are based on individual electrode data.

Then, the trends which appear to prevail throughout several of the charts will be repeated and generalized to form the basis of the conclusions from this portion of the study.

E6013 - 1/8" Profiles

Figure 7-20 shows the Knopp microhardness surveys from the air (SP), water (SP), and water (RP) welding series. The base metal hardness appears to be 200Hk (100 gram). But values as low as 160Hk were recorded. For practical purposes of comparing hardness profiles, 200Hk (100g) is considered to be the base metal hardness, and higher values are reported as hardened areas. Of all the air weld samples, E6013 - 1/8" welds produced the highest hardness values over the largest range. This is a very simple effect to explain because the values of the heat input are the lowest and the size of the weld beads are small. Low heat input and small welds lead to conditions of fairly rapid cooling rates. Cooling rates are quantified by relating them to the resulting hardness values. The heat inputs were between 6.4 and 10kJ/in and the resulting hardness values were in all cases above 274Hk (100g). This indicates that transformation structures other than pearlite are present. The hardened HAZ region extends for approximately 1.5mm. The underwater straight polarity welds were extremely hardened. The weld metal was hardened as well as the HAZ to hardness values above 400Hk (100g). The HAZ grains adjacent to the fusion line were most severely hardened, giving hardness values of 600Hk (100g). This hardening that occurs in the weld metal itself is quite serious and results in an entire weld bead that is extremely hard and brittle. The HAZ widths appeared to be less in water welds than in air and were between 1mm and 2mm. The heat input values were very similar to the air welds; being between 6kJ/in and 10kJ/in. The hardness gradient is very rapid; going from 600Hk to 200Hk in less than 2mm.

The underwater reverse polarity welds appeared to be less severely hardened and the weld metal hardness was between 300 and 400Hk. The maximum hardness values in the HAZ grain coarsened region were all less than 500Hk. The heat input to these

E6013-1/8"

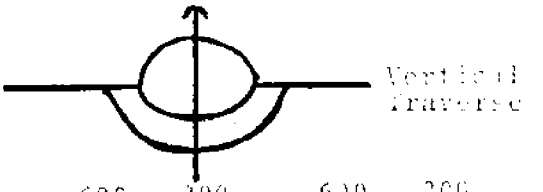

VICKERS
MICROHARDNESS
(100 grams)

FIGURE 7-20

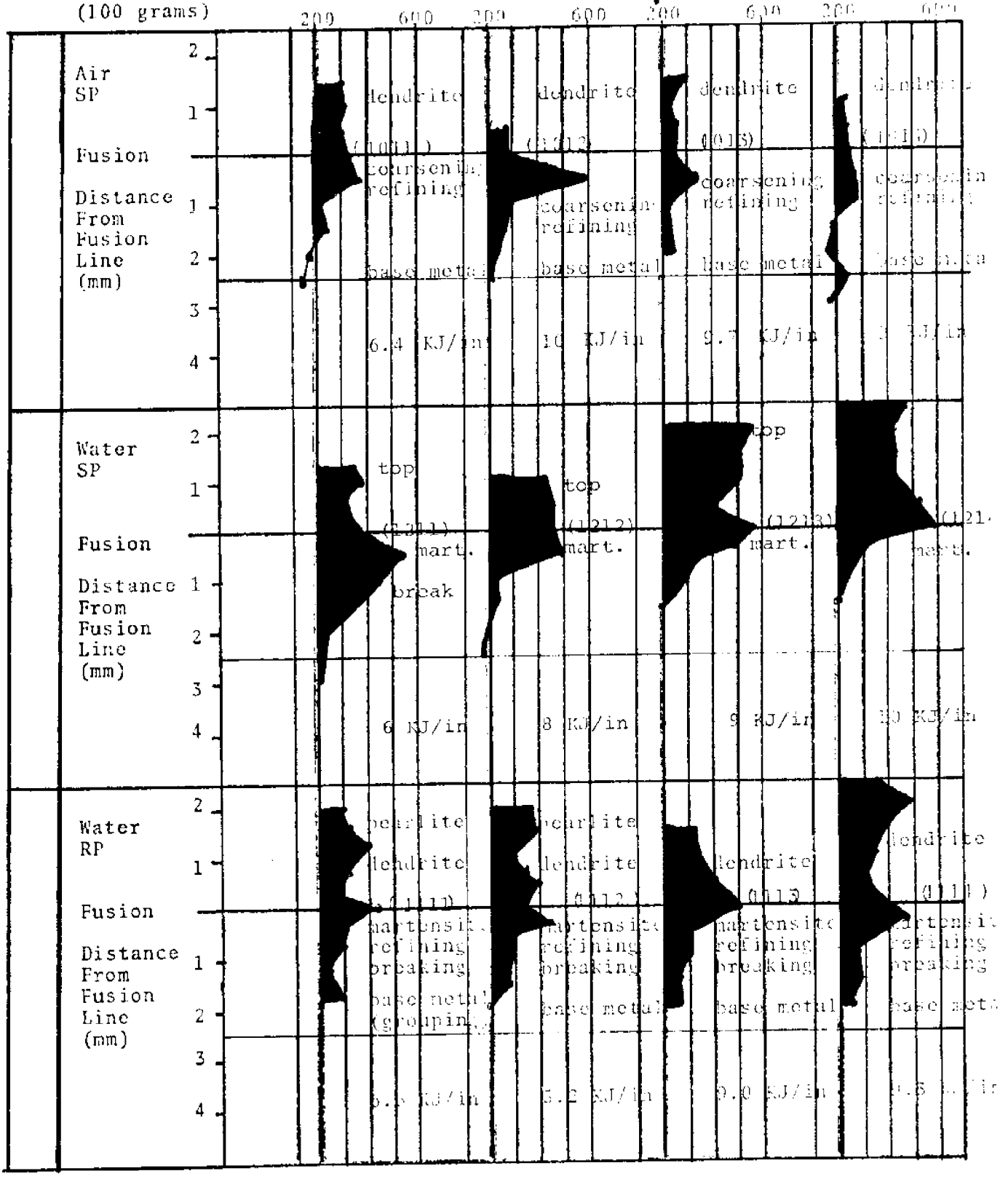

weld beads was the same as the other two series, 5-9kJ/in, so that this does not explain the occurrence of less severe hardening with reverse polarity.

Another factor may provide a partial explanation. Reverse polarity supplies most of the arc heat to the electrode, and thus, tends to melt more electrode than plate. This clearly occurred in this case, since the size of the weld bead is much larger than in either straight polarity case. Another explanation might be that the heat input was larger than the average heat input indicates. This is an argument in favor of using the weld bead size rather than the average calculated heat input as a comparative indication of heat to the weld. Because the weld bead size is larger, it is postulated that more heat was available to slow the cooling rates in the HAZ and weld metal (WM) and resulted in the reduced hardness profiles. However, in both the underwater situations, the resulting hardness readings are unacceptably high.

E6013 - 5/32" Profiles

Figure 7-21 shows the hardness profiles for the three welding series involving E6013 - 5/32" electrodes. In the air profiles, the size of the weld deposits and the heat inputs are large enough to reduce the hardening to values below 250Hk. The size of the HAZ can still be determined by looking for the grain refinement region or the partially refined region which marks the edge of the HAZ. This also marks the A_1 temperature isotherm of 1330°F. The HAZ width was 1mm to 1.5mm. Underwater straight polarity welds resulted in WM hardening of 400Hk (100g). The entire weld bead was hardened. The HAZ region adjacent to the fusion line must contain martensitic formations because the hardness reached values of 500Hk. But the hardening drops to the base metal hardness levels within .5mm-1mm showing the extremely localized deposits of martensite. The entire HAZ widths were more narrow than the air weld HAZ's because of the steepness of the isothermal field lines in underwater welds.

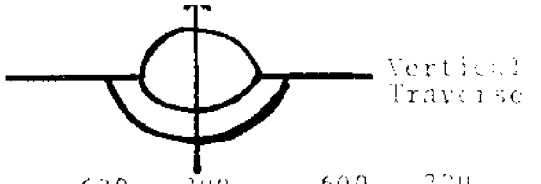

E6013-5/32"

FIGURE 7-21

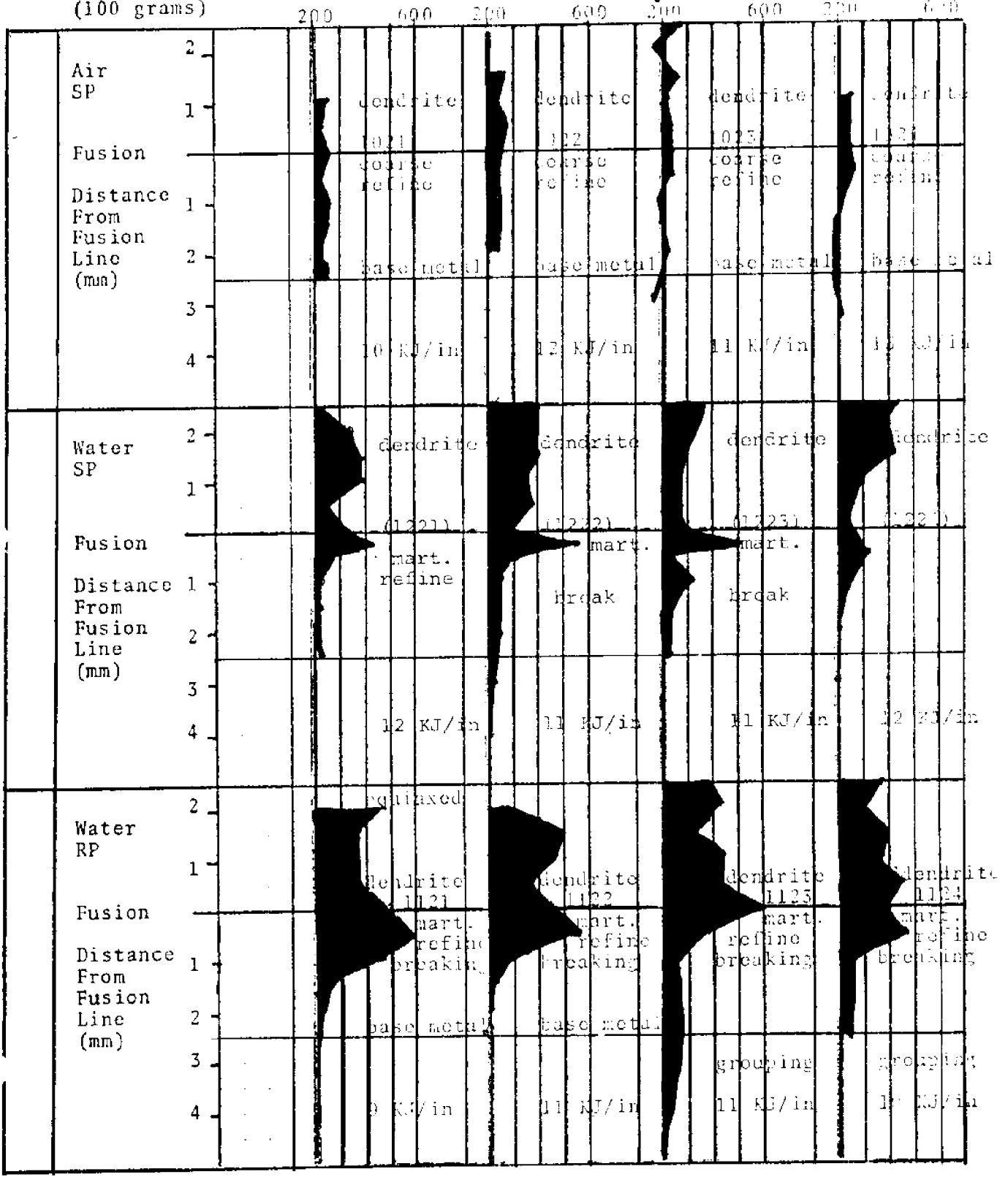

The width to the edge of the HAZ varies between .5mm and 1mm. Although the heat inputs to both the air (SP) welds and underwater (SP) welds were between 10kJ/in and 13kJ/in, the extent of heat spreading in the water welds was only 50%-70% of the spatial extent in air. The underwater reverse polarity welds also show a severe hardening of the WM to 400Hk. This shows a higher hardening than the underwater straight polarity and also a higher hardness than the previous 1/8" weld beads. Two explanations might apply. The heat inputs of 9-11kJ/in are below those of the underwater (SP) 5/32" welds and also the weld bead sizes are smaller than the underwater (RP) 1/8". Thus, two trends seem to begin to emerge:

(1) Larger weld beads will give less hardening. This implies that the cooling rates are less. This would follow because the larger weld bead area represents a larger heat source and so, the heat will dissipate more slowly.

(2) Higher heat inputs to weld beads of the same size will cause less hardening. Again, this implies that the cooling rates were less. This again follows from the idea that more heat in the weld bead will dissipate less rapidly.

It is very possible that these two effects are identical. Unless the weld puddle is heated above the melting point, heat input will be exactly proportional to the size of the weld bead. The underwater (RP) 5/32" weld HAZ regions appear very similar to the previous underwater HAZ's. The maximum hardness values are 500-600Hk (100g), but the hardening deops to 250Hk within 1mm. Thus, the HAZ widths defining the 1330°F isotherm lines are between .75mm and 1mm, again showing that the areas of extent of maximum temperatures in underwater welding are less by 20% to 50% than those in air.

E6013 - 3/16" Profiles (Figure 7-22)

The air weld profiles are very similar to the previous 5/32" welds except that the extent of the HAZ is larger,

255

E6013-3/16"

Vertical Traverse

VICKERS MICROHARDNESS (100 grams)

FIGURE 7-22

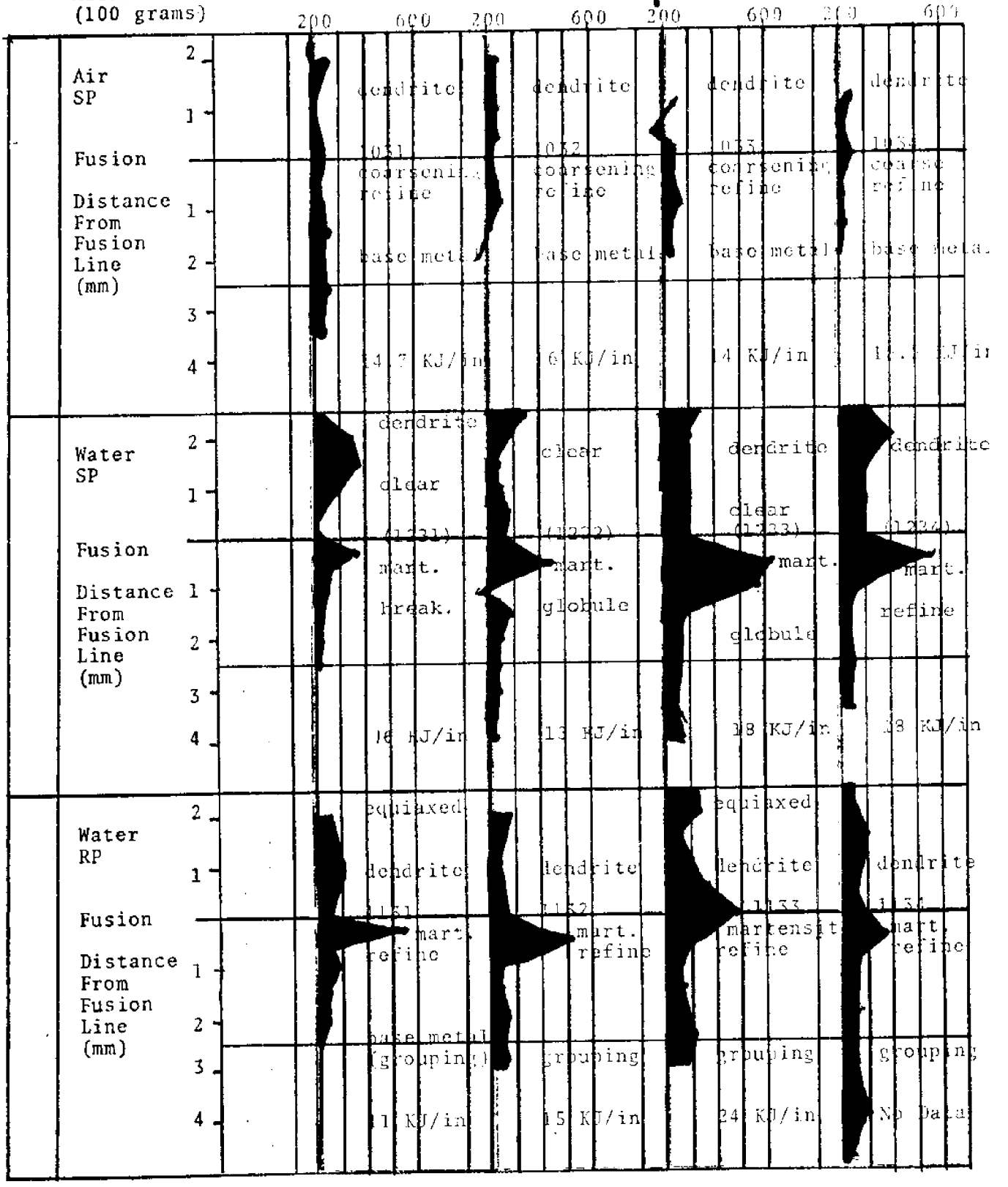

corresponding to the higher heat inputs of 14-17kJ/in. The HAZ widths were 1.5mm to 2mm. The underwater weld profiles show a striking decrease in hardening from the previous 1/8" and 5/32" electrode series. Underwater straight polarity heat inputs were 13-18kJ/in and gave only moderate hardening in the WM of 200-300Hk (100g). Although a very hard region (600Hk) was found near the fusion line, this hardening is only locally present and decreases to 250Hk within .5mm. Underwater reverse polarity welds had heat inputs of 11-24kJ/in and gave even less hardening than the straight polarity series. The WM was hardened slightly to 300Hk and the martensitic spike was between 400Hk and 500Hk. The HAZ widths of both underwater weld series were between 1mm and 1.5 mm. A peculiarity was noticed with an underwater weld bead with a heat input of 24kJ/in. The HAZ is elongated from a "U" shape to a "V" shape. This appears to be a result of the head conduction vertically through the plate being limited and constrained to change direction and move horizontally. This is beginning evidence that the primary heat flow is conduction through the base plate, in spite of the surrounding water. In comparing the #6013 series welds, the trend of decreasing hardness profiles with increasing size or heat input is obvious. Possible differences between straight polarity and reverse polarity are not as clear. The remaining hardness profiles indicate similar trends and will not be individually discussed.

7.293 Restatement of General Microhardness Trends and Conclusions

Too much information can be as useless as too little, so the main points of the preceding discussion are summarized here for clarity.

(1) One of the most basic observations was that the larger heat inputs normally produced larger weld beads. Although this is not necessarily a linear function, the trend is obviously towards increasing the weld bead size with increasing heat inputs. Figure 7-23 shows the basic trend to produce, both in air and underwater, a weld bead size (mm^2) that

FIGURE 7-23

RELATION BETWEEN HEAT INPUT AND WELD BEAD AREA

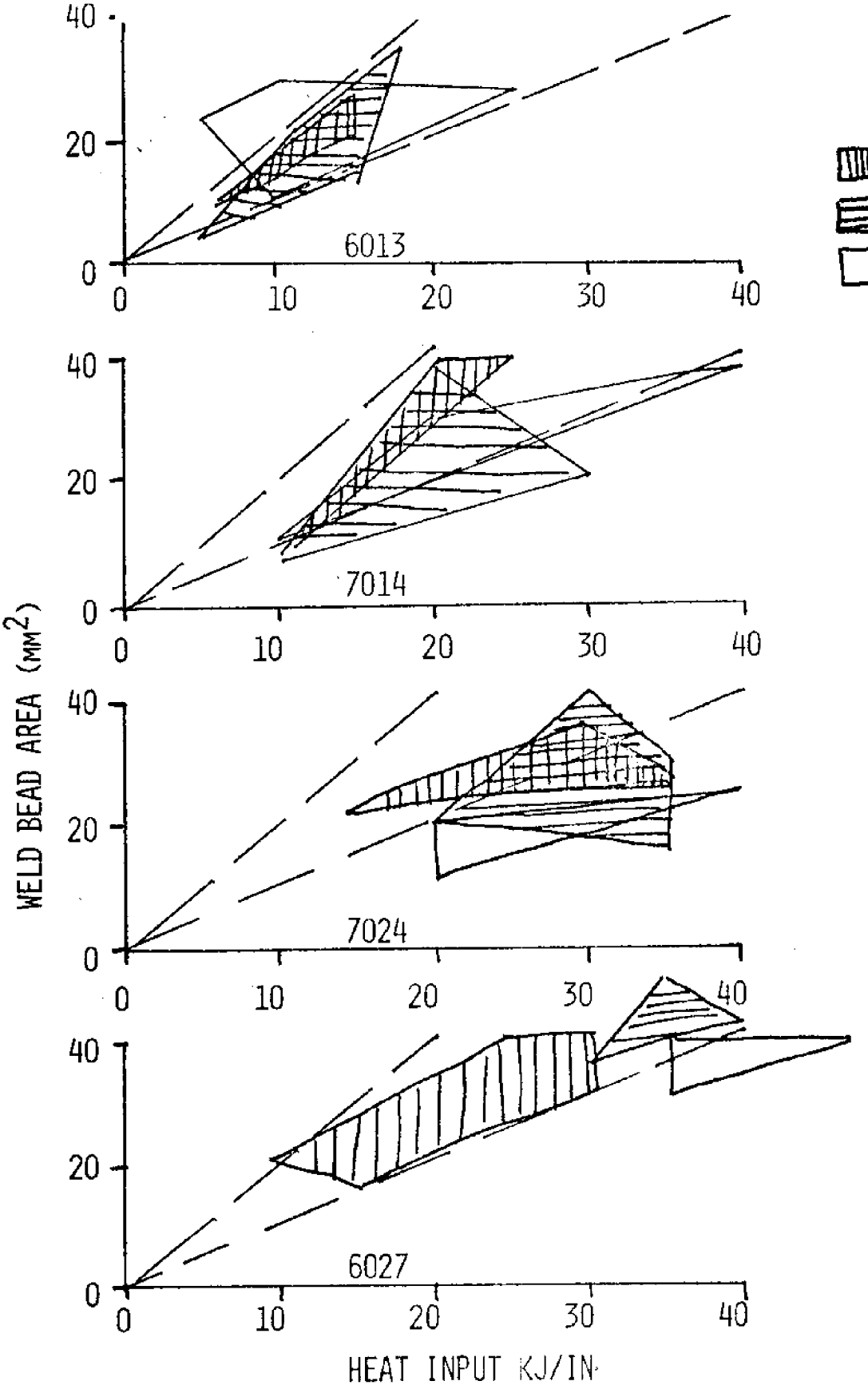

is 1 to 2 times the heat input (kJ/in). This trend remains unchanged between air and underwater welding.

(2) HAZ widths in air welds are 20% to 50% wider than the corresponding weld bead HAZ width from an underwater weld. This shows that the temperature gradients across the underwater HAZ are steeper.

(3) Differences between straight polarity and reverse polarity were not easily recognized. Some effects may be present from the fact that reverse polarity results in a more direct heating to the electrode, and less to the plate.

(4) The average heat input value calculated from the average current, voltage, and speed may be less indicative of the actual instantaneous heat input than the weld bead size.

(5) Localized martensite transformations appear in almost all underwater welds immediately adjacent to the fusion line, but extending for less than .5mm.

(6) Larger weld beads produce less hardening.

(7) Higher heat inputs will cause less hardening as well. This effect seems to dominate the effects from size. These two effects would be identical if the weld puddle were only heated to exactly the melting temperature (no superheating).

(8) The primary mechanism of heat dissipation from the weld bead appears to be conduction through the base plate rather than directly into the surrounding water.

(9) E6013 electrodes appear to result in the lowest heat inputs. E7014 electrodes are slightly "hotter" than E6013. E7024 and E6027 both have much higher heat inputs and are approximately equal to each other in heat input.

(10) Heat input that is not accounted for in the weld bead size may be going to heat the liquid above melting, or else it may be serving as preheat for the weld plate. Either effect will serve to reduce the cooling rates and thus reduce the hardening.

(11) The critical heat input that results in an HAZ that extends to the bottom of the 1/4" plate for air welds is 25kJ/in. For water welding, it takes 40kJ/in to saturate the plate. This shows that air welding requires less heating to extend the maximum temperature profiles a given distance (heat is dissipated 60% faster in underwater welds).

(12) The best comparative measure for predicting cooling rate comes from measuring the heat input per unit weld bead size.

7.3 MICROSTRUCTURAL STUDIES OF UNDERWATER WELDING

This section simply contains a number of partially-illustrated microphotographs taken at 50X and 100X magnification of both air and underwater weld HAZ regions and weld beads. Many of the structures described in section III on underwater metallurgy and microstructure are shown. Further interpretations are left to the reader.

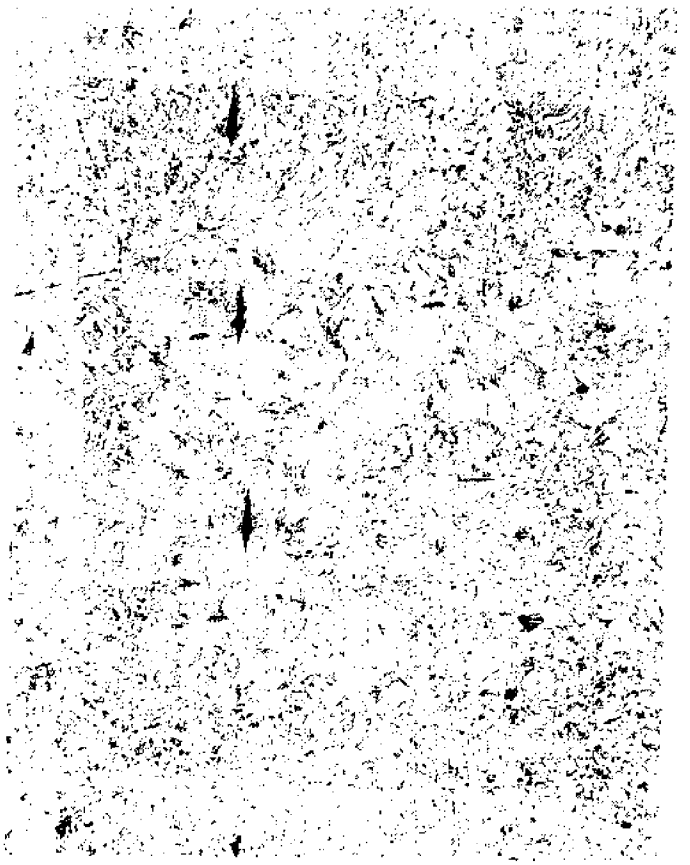

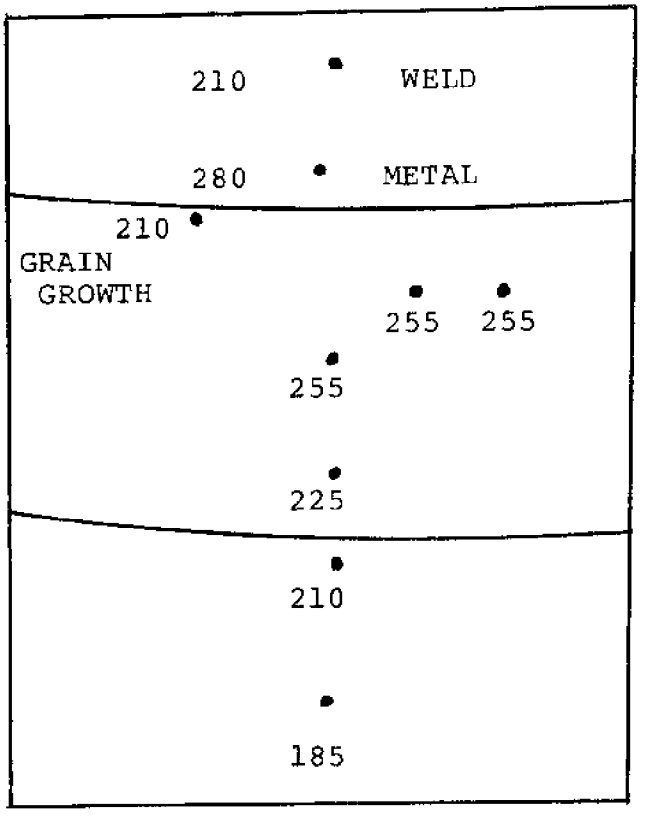

FIGURE 7-24

MICROSTRUCTURE AND MICROHARDNESS OF SINGLE PASS AIR WELD

FIGURE 7-25

MICROSTRUCTURE AND MICROHARDNESS OF OVERLAPPING HAZ REGIONS
KHN (100 GM)

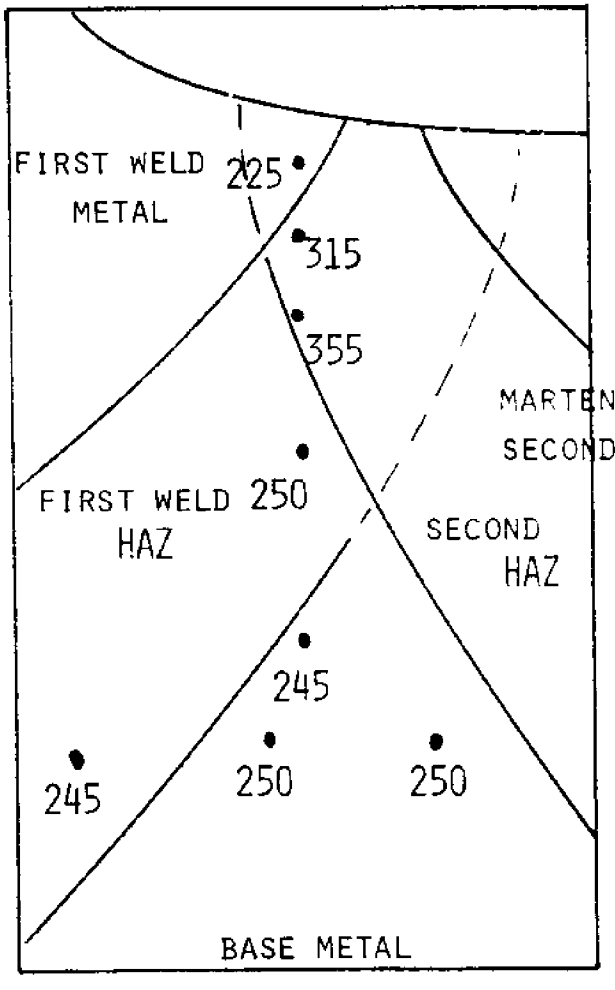

1020 1/4" PLATE STEEL 50X

E7014 ELECTRODE (5/32") (UNDERWATER)

FIGURE 7-26

MICROSTRUCTURE AND MICROHARDNESS OF UNDERWATER WELDS WITH OVERLAPPING HAZ
KHN (100 GM)

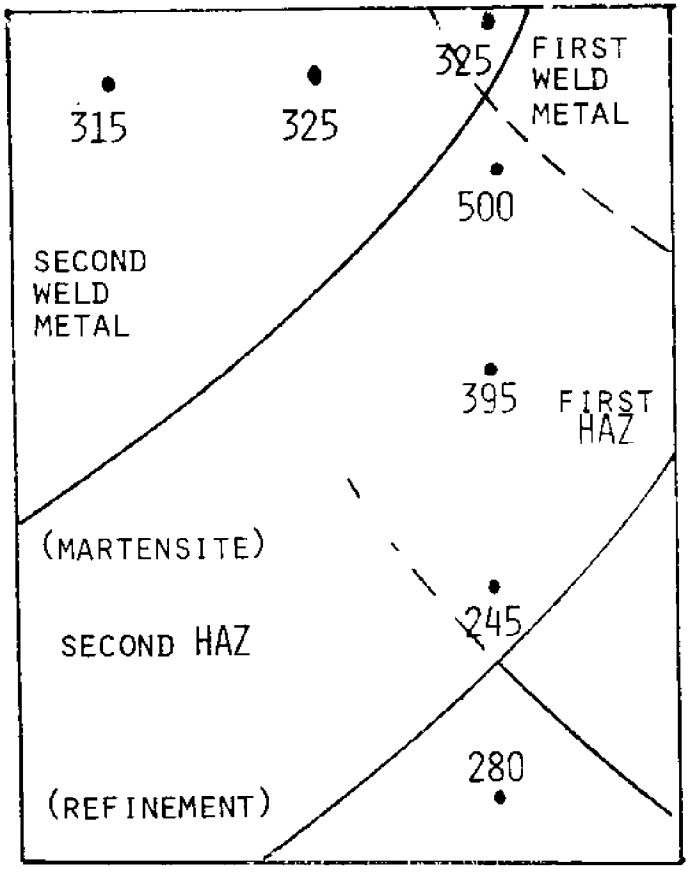

1020 1/4" PLATE 50X

5/32" E7014 ELECTRODE (UNDERWATER)

FIGURE 7-27

MICROSTRUCTURE OF E7014 5/32 WATER RP 21 KJ/IN

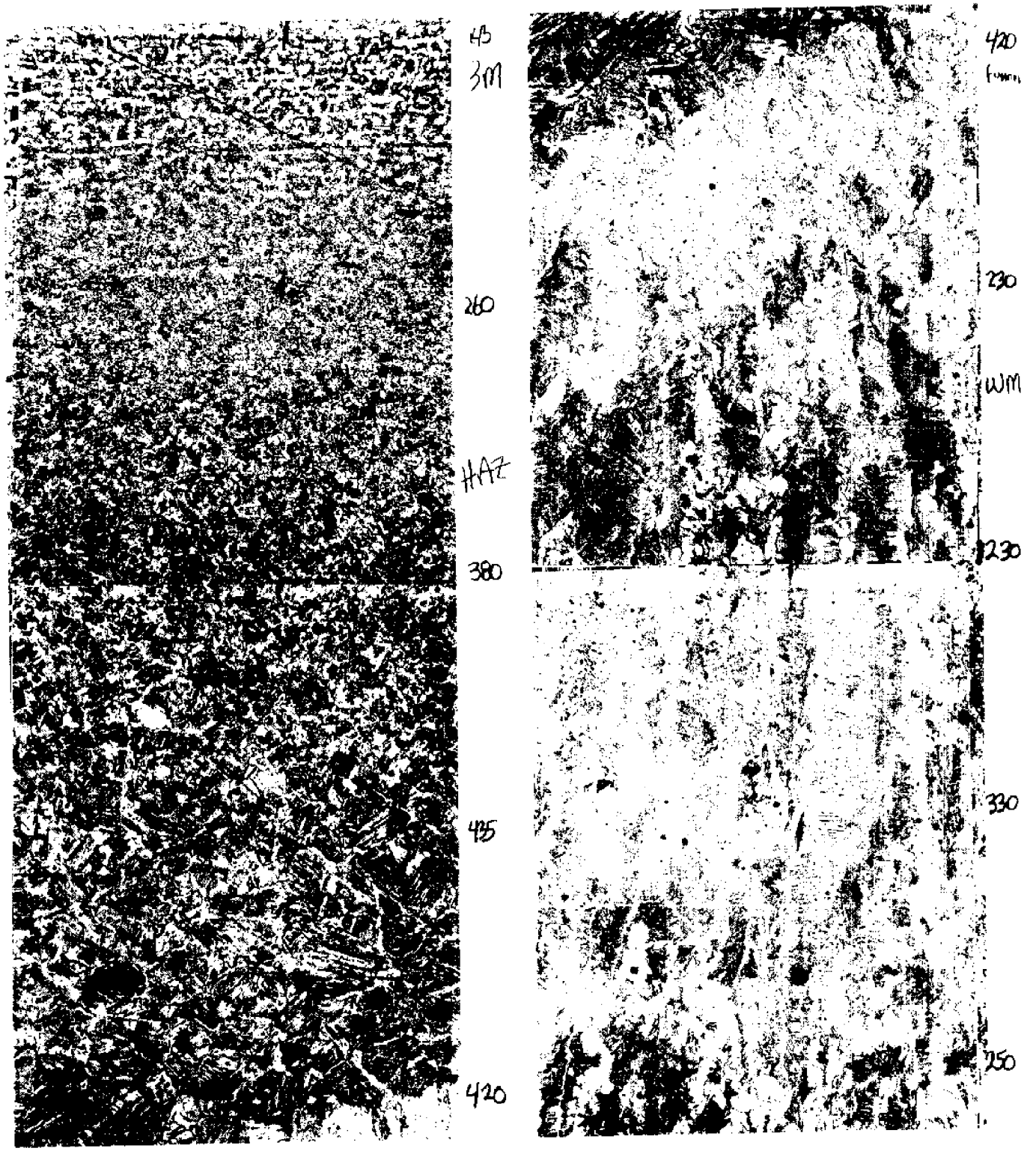

FIGURE 7-28

MICROSTRUCTURE OF E7014 WATER SP 5/32 18 KJ/IN

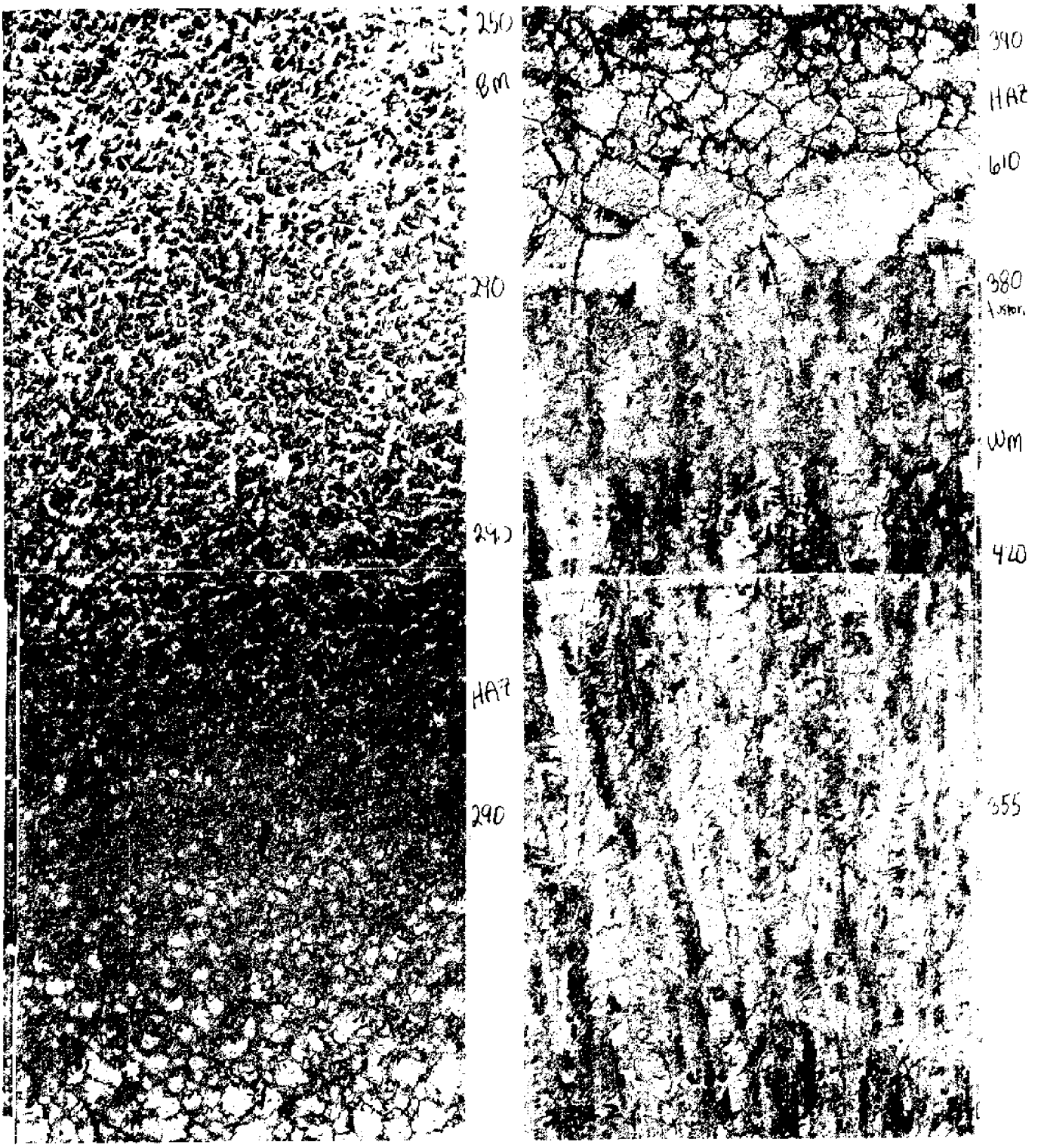

FIGURE 7-29

MICROSTRUCTURE OF E6013 5/32" WATER SP 11 KJ/IN

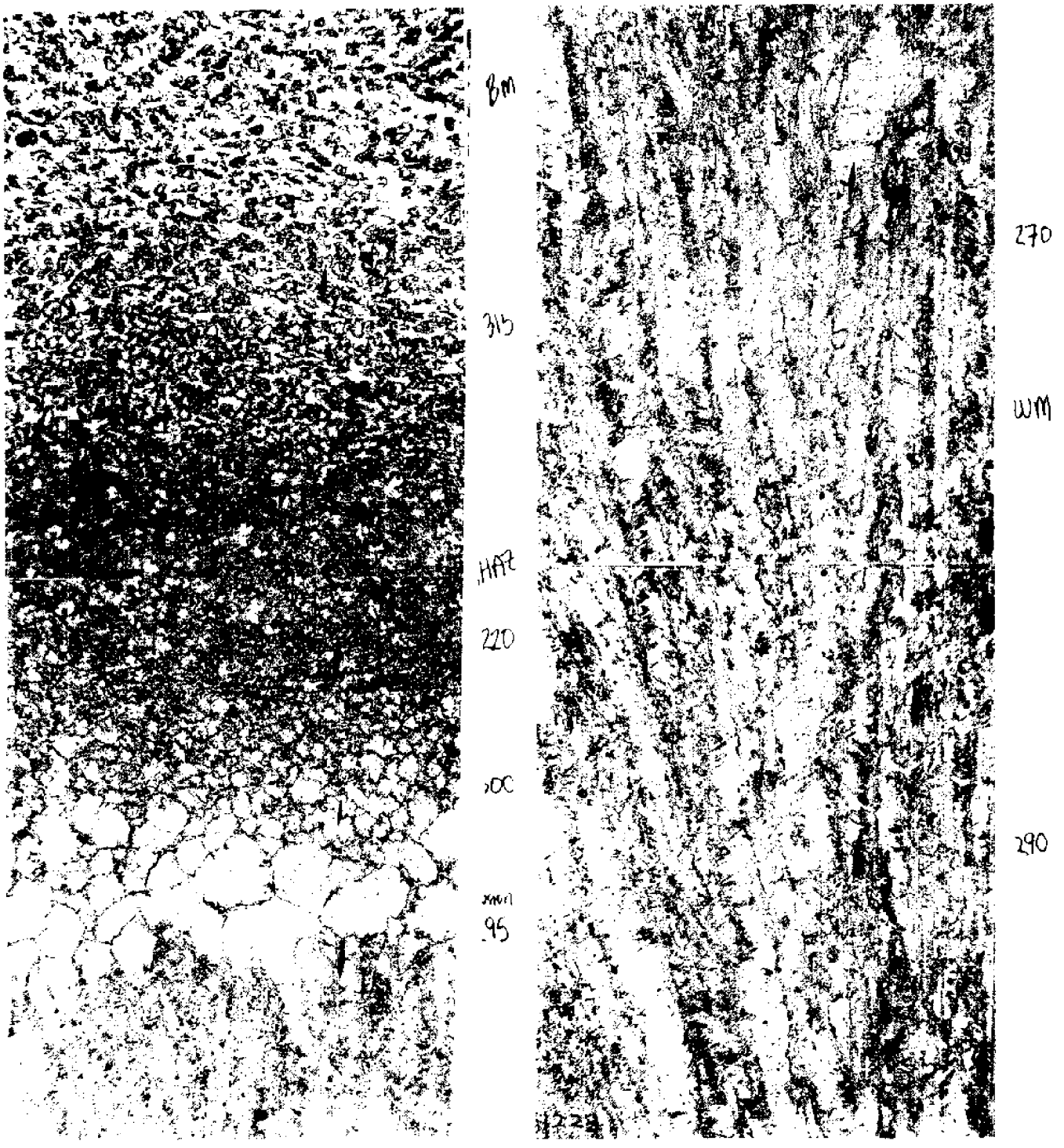

7.4 CONCLUSIONS AND RECOMMENDATIONS FOR ADDITIONAL EXPERIMENTAL INVESTIGATION

If the previous sections have succeeded in tracing the development of underwater welding technologies, and in compiling and summarizing past experimentation in underwater welding, and in clearly presenting the additional experimental data and observations, then it is now time to restate the most relevant ideas that have developed and suggest directions and goals for underwater welding experimentation.

(1) Temperature histories from air welds and water welds show that the cooling rates in an underwater weld HAZ are 10-15 times faster than the cooling rates in a similar air weld.

(2) Although the cooling effects are accentuated underwater, the mechanism of heat flow in underwater welding remains the same as in air; no significant portion of the heat is dissipated directly from the weld puddle into the water. The cooling rate is faster around a small weld bead, and this size dependent cooling is especially critical underwater where the rapid cooling will lead to hardened structures. It is therefore recommended that a larger size electrode be used in underwater welding.

(3) The rapid cooling rates in an underwater weld HAZ produce non-equilibrium structures which are not usually encountered in air welding.

(4) However, the underwater metal transfer and fusion processes are basically similar to those in air. Thus, the weld bead shape of underwater welds are only slightly different form corresponding air welds.

(5) Continuous Cooling Transformation diagrams (CCT) are the most useful metallurgical charts for use in underwater welding microstructural prediction. However, because the austenitization temperatures vary across the weld HAZ, even these predictive diagrams are not completely accurate.

(6) The HAZ of an underwater weld is not as wide as a similar air weld HAZ. While the air weld HAZ will consist almost entirely of a grain refined structure, much of the underwater weld HAZ remains an enlarged grain structure. This is because the large grains of austenite do not have the necessary time to recrystallize to ferrite and pearlite and remain as large grains of semi-quenched transformation products such as bainite, martensite, and Widmanstätten structures.

(7) The speed of an electrode, when employing the underwater drag method, is a function of the current density of the arc. The water may tend to slow down the electrode by cooling the flux coating and thereby inducing a longer arc barrel and thus, a lower current density. However, if the arc length is not elongated, the cooling effect of the water directly on the arc column may cause a constriction of the arc and thus, increase the arc current density and hence, the speed. The welding arc should be allowed to proceed along the weld seam at its natural speed, and should not be artifically controlled. Variations in the instantaneous welding speed will occur and will result in variable heat input, penetration, and bead size. Thus, all welding parameters must be identified as ranges of values.

(8) The current settings between optimum air welds and corresponding optimum underwater welds changes for two distinct reasons. Because of the rapid heat dissipation in underwater welding, the welding current should be increased by 10 to 30 amps above the recommended air welding values. In addition, because the arc length is longer in underwater drag welding, there is a discrepancy between the machine current setting and the actual measured value. This difference was 15-25 amps for E7013 and E7014 electrodes, but became an unworkably high 50-150 amps for E7024 and E6027.

BLANK

PART SEVEN

RECOMMENDATIONS FOR FURTHER EXPERIMENTAL INVESTIGATIONS AND DEVELOPMENTS IN UNDERWATER WELDING

Contents

8.0 INTRODUCTION

This report summarizes a program of experimental and analytical investigation and information compilation involving three years work at M.I.T. During this same three year period the interest and enthusiasm in the industry is underwater welding rechnologies have increased significantlv. At the present time more experimental investigation is planned by M.I.T. continuing development of equipment, materials and techniques, and processes is taking place in the underwater welding and diving firms, and more offshore industries are showing an interest in underwater welding capabilities. In many respects underwater welding technologies are in a critically important period of development. It seems wise to pause and evaluate what has developed to the present point and project the needs and present capabilities into the future in order to recommend some fruitful areas of future endeavor.

8.1 FUTURE EXPERIMENTATION

Several areas of needed experimental work emerge.

(1) Workers in Russia have briefly mentioned that the underwater arc may result in the burnoff of several oxidizing agents from the flux coating in underwater welding. This would be a critical effect from the standpoint of producing a good match between the weld metal and base metal. Such questions point to the continuing need for basic metallurgical investigations.

(2) Weld defects such as porosity need to be linked back with a fundamental mechanism. Wet electrode coverings has been suggested as the cause of porosity. Other defects such as lack of fusion, lack of penetration, and undercutting need to be understood as the results of a more fundamental process. Once the basic causes of these defects are known, procedural suggestions for

methods of avoiding or minimizing their impact or the welded joint integrity could be suggested.

(3) A better understanding is needed in the area of matching weld metal to parent metal. Metallurgical reasons for a metal's weldability need to be investigated. Underwater welding feasibility for metals other than mild carbon steels ought to be obtained. This may involve new developments in the area of welding electrodes. Possible cooperation between electrode manufacturers and academic research groups is called for. Increased use of medium carbon and low alloy structural steels in the underwater environment makes investigation of the underwater weldability of these steels critical. Because these metals are more hardenable than low-carbon steel, underwater welding is expected to be more difficult using them. This investigation has considered only low-carbon steel. Other investigators have begun underwater welding of these higher grade materials (Meloney, 1973).

(4) Basic research ought to be continued to evaluate hydrogen-induced failures, corrosion-stress failures, and other poorly understood failure mechanisms that are particularly critical in the underwater environment. There is presently a discrepancy between laboratory investigation techniques and actual field case work. Laboratory test specimens tend to be unrefined welding situations. More thought ought to be given to more accurate simulation of the underwater welding situations.

(5) A more thorough knowledge of actual joint mechanical properties for various underwater welding processes, joint design, and materials is needed. This would allow a design engineer to determine more accurately the applicability of underwater welded work to a particular job situation.

(6) For this work to become of practical value to the ocean engineer, the correlations between microstructure and weld joint properties must be developed. It will also be important to realize that more is involved in underwater welding than just the weld. Problems of visibility and electrode guidance, joint preparation and fit-up, diver comfort and maneuverability, and related difficulties will have to be minimized from an operational viewpoint. Simple extrapolations from lab work to actual application is especially tenuous when dealing with the ocean environment.

(7) Some thought and effort should be given to the effect of depth (or increasing pressure) on the underwater welding processes. Gas evolution rates, voltage and current relationships, metal transfer, etc., should all be considered as possible functions of depth.

(8) The effect of natural and induced turbidity in the underwater environment remains a problem in any underwater welding attempt. The mechanism behind, as well as the composition of covered-arc electrode induced turbidity ought to be determined.

(9) More accurate and more flexible computer modelling of the HAZ thermal histories will prove valuable in explaining the basic heat flow mechanisms and focusing on the critical parameters controlling the cooling rates. In particular, the alternate modelling technique discussed in section 5.7 ought to be pursued to give a more accurate modelling potential. However it must be stressed that only as the model is able to predict some definite effects will it prove to be of any value to underwater welding process development.

(10) Clear advantages and disadvantages of straight polarity and reverse polarity have not been determined. If no

major difference is found, this ought to be stated. In general there remain many "loose ends" which should be more precisely defined in terms of causes, effects and mechanisms involved.

8.2 POSSIBILITIES FOR FUTURE DEVELOPMENTS

At the present time it appears that the basic need for fundamental information about underwater welding has been met. Many of the basic mechanisms have been adequately described. The research reported in this project has done much to explain the mechanisms behind the major difficulties with underwater welding. Describing the problems is only half of the job, and suggesting realistic solutions is a necessary task as well. The following items suggest directions or trends that might be followed in obtaining solutions to the basic difficulties encountered in underwater welding.

(1) Some thought might be given to a power supply that has both a variable current and an independently varying voltage. Also, because of the current leak between machine setting and actual arc conditions, an underwater current meter would be ideally situated with the welder-diver.

(2) There ought to be a continuing exchange of information between the various research groups and universities, the industrial and commercial developers, and government facilities concerning advances and developments in underwater welding.

(3) Now that the rapid cooling rates in underwater welding have been documented, some suggestions towards solutions are appropriate. Perhaps the most obvious solution is to transform an underwater welding situation into an air welding job by constructing a temporary enclosure of some type around the weld area. Various devices have

been applied towards this goal. The next general idea is to reduce the cooling rates in the HAZ by some type of preheating or insulation. The heat from flame preheating is dissipated too rapidly to be of value; strip heaters might work. Insulating the plate from the cooling effect of the water everywhere adjacent to the weld joint might substantially reduce the cooling rate. A third idea is to perform some sort of post-weld heat treatment to recrystallize and soften the hardened HAZ regions. Multipass welding or some form of flame post-heating might prove effective. Still another idea is to increase the heat input to the weld bead area without increasing the weld size. This sort of effect may explain the success of underwater, exposed GMA processes. Other ideas will certainly occur to those interested in improved underwater welds.

(4) Various combinations of shielding, shrouds, multipass techniques, etc., ought to be investigated, keeping in mind that when working in the underwater environment, the simplest tools are the best. The general area of underwater welding equipment appears underdeveloped.

(5) Because of the elongated arc barrels of E7024 and E6027, these two electrodes are not recommended for underwater welding. Further investigation might be directed at the design of electrode flux and waterproof coatings to be used specifically in underwater welding. These coatings should provide for drag welding, but must still melt properly when surrounded by the water.

(6) Turbidity remains an operational problem in many underwater welding situations. Continued improvement in visual aids for underwater welding is encouraged. In addition, some work might be done towards adapting the semi-automatic robot-type welding equipment that is being developed for other applications to underwater GMA welding.

(7) An underwater welding code is encouraged. The current effort by the American Welding Society, Marine Construction Committee is commended.

8.3 FUTURE EFFORTS AT M.I.T.

Efforts at M.I.T. in underwater welding will continue for a short time towards the development of some simple engineering solutions to the major underwater welding problems. Now that the basic supporting information for underwater welding mechanisms has been documented, it appears time to suggest by example some remedial measures. Although the development of elaborate gadgetry is not thought to be appropriate, some simple devices to air in underwater SMA may be developed and tested. It is hoped that a few simple modifications to the basic process or technique will serve as an encouragement to the underwater welding industry to pursue the development of these modifications with the end result being the advancement of underwater welding technologies and thus the furthering of underwater structural maintenance, repair and construction methods and capabilities.

8.4 CONCLUDING REMARKS

This report has attempted to provide scientific and technical explanations for the basic problems in underwater welding. It has not attempted to suggest remedial modifications to the welding process. However, now that the basic problems are thoroughly understood, their subsequent solutions ought to be more easily developed. It is hoped that the scope of these specific suggestions will not limit thoughts in the area of underwater welding. A proper solution to the varied problems that face this area of fabrication will not come from any one source at any one time. It is hoped that this report of the state of affairs in the practical

technology and the technical research in underwater welding will prove helpful in understanding underwater welding phenomena and developing more successful welding methods.

8.5 BIBLIOGRAPHY & REFERENCES FOR ENTIRE REPORT

(1) Adams, C., (1958), "Cooling Rates and Peak Temperatures in Fusion Welding," Welding Journal, p. 210s.

(2) Anderssen, A. H., (1972), "The Underwater Application of Exothermic Welding," M.I.T. Engineer's Thesis.

(3) Avilov, T. I., (1955), "Electrodes for U.W. Welding and Cutting Steel," Welding Production, Vol. 3, No. 6.

(4) Avilov, T. I., (1959), "The Static Characteristics of the Welding Arc Under Water," Svarochnoe Proizvodstvo, No. 5, pp. 16-17.

(5) Avilov, T. I., (1960), "Properties of Underwater Arcs," Welding Production, Vol. 7, No. 2, pp. 30-33.

(6) Avilov, T. I., (1962), "Reply to N.M. Madatov's Paper on the Peculiarities of an Underwater Arc," Welding Production, (BWRA Trans.), Vol. 9, No. 3, pp. 76-79.

(7) Billy, A. F., (1971), "Investigation of Underwater Semi-Automatic Arc Welding for Naval Salvage and Seafloor Construction," NCEL Preliminary.

(8) Billy, A. F., (1971), "The Effects of Gas Metal-Arc Parameters in Seawater on Welding Current, Arc Voltage, Bead Geometry, and Soundness," NCEL Preliminary.

(9) Bodger, J. F., (1971), "Underwater Welding: A Review of the Literature," Welding Institute Bulletin, Vol. 12, No. 2.

(10) Brandon, (1970), "Parameters for Pressurized Inert Gas Metal-Arc Welding of Aluminum," Welding Journal, Vol. 49, No. 11, pp. 510s-520s.

(11) Brown, A. J., (1971), "Methods of Research in Underwater Welding," B.S. Thesis, M.I.T.

(12) Brown, A. J., (1973), "Mechanisms of Heat Transfer During Underwater Welding," M.S. Thesis, Department of Ocean Engineering, M.I.T.

(13) Brown, A. J., Brown, R. T. and Masubuchi, K., (1973), "Interim Report on Fundamental Research on Underwater Welding," from M.I.T.

(14) Brown, A., Staub, J. A., and Masubuchi, K., (1972), "Fundamental Study of Underwater Welding," Paper No. OTC 1621, 1972 Offshore Technology Conference, Houston, Texas.

(15) Burks, R. H. (1950), "Underwater Welding Aids Ship Salvage," Welding Engineer, Vol. 35, No. 4, pp. 20-22.

(16) DeSaw, Caudy, Mishler, (1969), "Determination of the Feasibility of Shielded Metal-Arc Welding and Oxygen Cutting at Depth of 600-feet," U.S. Navy Contract N00014-66-C-0199, Battelle, Columbus, Ohio.

(17) Digges, T. G., Rosenberg, S. J., Geil, G. W., (1966), Heat Treatment and Properties of Iron and Steel, National Bureau of Standards, Monograph 88.

(18) Elliss, J. B., (1969), "Arc Welding in the Ocean: A Diver-Welder Shares His Experience," Metal Construction and Bridge Welding Journal, March, pp. 151-154.

(19) Emerson, H., Angel, T., and Cox, L., (1967), "Saturation Diving - A Tool for Underwater Welding and Cutting," Presented at the Symposium on Underwater Welding, Cutting, and Hand Tools, Battelle Memorial Institute, Columbus, Ohio, pp. 1-5.

(20) Gilman, (1970), "The Application of Hyperbaric Welding for the Offshore Pipeline Industry," OTC 1970, Vol. 2, No. 1252, pp. 243-248.

(21) Grossman and Bain, (1935), Principles of Heat Treatment, American Society for Metals.

(22) Grubbs, C. E., Seth, O. W., (1970), "Multipass All-Position 'Wet' Welding--A New Underwater Tool," OTC #1620, pp. 41-54.

(23) Hasui, I., (1971), "Plasma Underwater Welding," Journal of Japan Welding Society, Vol. 40, No. 7, pp. 622-631.

(24) Hasui, Fukushima, Kinugawa, (1972), "Development of Underwater Plasma Welding Process," Second International Ocean Development Conference, Vol. 2, October 5-7, Tokyo, Japan, pp. 1005-1036.

(25) Hibshman, M. S., Jensen, C. D., and Harvey, W. E., (1933), "Electric Arc Welding Under Water," Journal of the American Welding Society, Vol. 12, No. 10, pp. 4-9.

(26) Hipperson, A. J., (1943), "Underwater Arc Welding," Welding Journal, Vol. 22, No. 8, pp. 329s-332s.

(27) Hydro Tech International, Inc., (1973), Hydroweld, Houston, Texas, (Company Literature).

(28) Kemp, W. N., (1945), "Under Water Arc Welding," Transactions of the Institute of Welding, Vol. 8, No. 4, pp. 152-156.

(29) Kumose, F., K. Yamada and H. Onone, (1968), "Underwater Welding Method for the Construction of Outsized Ships," Welding Journal, March, pp. 194-206.

(30) Levin, Kirkley, (1972), "Welding Underwater," Metal Construction and British Welding Journal, May, Vol. 4, No. 5, pp. 167-170.

(31) Lynch, Pilia, (1969), "Pipeline Hot-tap Welding under 110 Feet of Sea Water," Welding Journal, March, Vol. 48, No. 3, pp. 183-190.

(32) Madatov, (1961), "Concerning the Effect of the Salinity of Sea Water on the Process of Underwater Welding by Consumable Electrode," Welding Production, Vol. 8, No. 4, April, pp. 36-41.

(33) Madatov, N. M., (1962), "Underwater Welding Electrodes with Coatings Containing Iron Powder," Welding Production, No. 8, p. 25.

(34) Madatov, N. M., (1962), "Some Peculiarities of an Underwater Arc," Welding Production, Vol. 9, No. 3, pp. 72-76.

(35) Madatov, N. M., (1962), "Special Features of Underwater Touch Welding," Automatic Welding, Vol. 15, No. 9, pp. 52-55.

(36) Madatov, N. M., (1965), "The Properties of the Bubble of Steam and Gas Around the Arc in Underwater Welding," Automatic Welding, Vol. 18, No. 12, pp. 25-29.

(37) Madatov, N. M., (1966), "Energy Characteristics of the Underwater Welding Arc," Welding Production, Vol. 13, No. 3.

(38) Madatov, N. M., (1966), "The Static Volt-Ampere Characteristics of Underwater Arcs," Automatic Welding, Vol. 19, No. 4, pp. 49-53.

(39) Madatov, N. M., (1969), "Shape Relationships for Underwater Welding," Welding Production, March, Vol. 16, No. 3, pp. 18-23.

(40) Madatov, N. M., (1970), "Underwater Ship Repair," Naval Ship Systems Command, Washington, D. C.

(41) Madatov, N. M., (1972), "Influence of the Parameters of the Underwater Welding Process on the Intensity of Metallurgical Reactions," Welding Research Abroad, March, p. 63.

(42) Madatov, Pokhodnya, Kostenko, (1965), "High Speed X-ray Cinematography of the Underwater Welding Arc," Welding Production, September, Vol. 12, No. 9, pp. 72-73.

(43) Madatov, Potapevskii, (1967), "Features of Underwater Thin Wire Welding," Welding Production, Vol. 14, No. 2, February, pp. 51-55.

(44) Masubuchi, K., (1970), Materials for Ocean Engineering, M.I.T. Press, M.I.T.

(45) Masubuchi, K., (1971), "Underwater Thermit Welding of 50-ton Padeye," Final Report under Contract N00-111-71-C-0188 to the Boston Naval Shipyard and Office of the Navy Supervisor of Diving, Salvage, and Ocean Engineering, Naval Ship Systems Command from M.I.T.

(46) Masubuchi, K. and Anderssen, A. H., (1973), "The Underwater Application of Exothermic Welding," OTC #1910

(47) Masumoto, Nakashima, Kondo, Matsuda, (1971a), "Study on Underwater Welding," July, Report 1, Journal of Japan Welding Society, Vol. 40, No. 7, pp. 683-693.

(48) Masumoto, et al., (1971b), "Study on Underwater Welding," August, Report 2, Journal of Japan Welding Society, Vol. 40, No. 8, pp. 748-754.

(49) Meloney, M., (1973), "The Properties of Underwater Welded Mild Steel and High-Strength Steel Joints," M.S. and Engineer's Thesis, Department of Ocean Engineering, M.I.T.

(50) Mishler, Randall, (1970), "Underwater Joining and Cutting--- Present and Future," OTC, Vol. 2, pp. 235.

(51) Mohr, Kluttz, White, (1973), "Hydroweld Underwater Welding Process," OTC #1782.

(52) Nippes, E., (1959), "The Weld Heat Affected Zone," Welding Journal, January, p. 1s.

(53) Pavelec, V., (1968), "Temperature Histories in Thin Steel Plate Welded with TIG," Ph.D. Thesis, University of Wisconsin.

(54) Perlman, Pense, Stout, (1969), "Ambient Pressure Effects on Gas Metal-Arc Welding of Mild Steel," Welding Journal, June, Vol. 48, No. 6, pp. 2315.

(55) Pilia, (1967), "Underwater Pipeline Welding, 110-Feet Down," Symposium on Underwater Welding, Cutting and Hard Tools, Battelle Memorial Institute, pp. 33-40.

(56) Robinson, (1967), "Underwater Welding in a Dry Environment," Symposium on Underwater Welding, Cutting and Hard Tools, Battelle Memorial Institute, pp. 21-29.

(57) Rosenthal, D., (1941), "Mathematical Theory of Heat Distribution during Welding and Cutting," Welding Journal, Vol. 20, pp. 220s-234s.

(58) Savich, I. M., (1969), "Underwater Welding with Cored Electrode Wire," Welding Production, October, Vol. 22, No. 4, pp. 70.

(59) Sheinkin, Krenov, (1962), "Certain Features of Arc Burning and Metal Transfer when Welding using a Consumable Electrode with the Arc Shielded by Steam," Automatic Welding, No. 9, Vol. 15, September, pp. 34-39.

(60) Shlyamin, A. I., Dubova, T. N., (1961), "Semi-Automatic Underwater Welding," Welding Production, No. 7, July, pp. 49-55.

(61) Silva, E. A., (1968), "Welding Processes in Deep Ocean," Naval Engineer's Journal, Vol. 80, No. 4, August, pp. 561-568.

(62) Silva, E. A., (1971a), "An Investigation of Fusion Controlled Metallurgical Bonding in the Marine Environment," Ph.D., University of California at Berkeley.

(63) Silva, E. A., Hazlett, (1971b), "Shielded Metal-Arc Welding Underwater with Iron Powder Electrodes," Welding Journal, June, pp. 406.

(64) Silva, E. A., (1971c), "Gas Production and Turbidity During Underwater Shielded Metal-arc Welding with Iron Powder Electrodes," Naval Engineer's Journal, December, p. 59.

(65) Staub, J. A., (1971), "Temperature Distribution in Thin Plates Welded Underwater," Naval Engineer's Thesis, Department of Ocean Engineering, M.I.T.

(66) Tanbakuchi, R., (1967), "Measured Metal Temperatures During Arc Welding," Ph.D. Thesis, University of Wisconsin Madison.

(67) "Underwater Cutting and Welding," U.S. Navy Technical Manual, U.S.N. Supervisor of Diving, Naval Ship Systems Command.

(68) Vagi, J. J., Mishler, H. W., Randall, M. D., (1968), "Underwater Cutting and Welding State-of-the-Art," a report to the Naval Ship Systems Command from Battelle Memorial Institute, Columbus Laboratories, Ohio.

(69) Wallace, K. W., Morrissey, G., (1968), "Dry-Weld Modes in an Underwater Habitat," Offshore, Vol. 28, No. 10, p. 67.

(70) Warren, Angel, Gray, (1971), "Saturation Diving, A Tool for Offshore Pipelining," OTC #1436.

(71) Waugh, R. C., Eberlein, O. P., (1954), "Underwater Metallic Arc Welding," Welding Journal, Vol. 33, No. 10, pp. 531s-534s, October.

(72) Brown, R. T., Masubuchi, K., (1973), "Latest Developments in Underwater Welding Technologies," Underwater Journal, Vol. 5, No. 5.

(73) Lancaster, J. F., (1965), The Metallurgy of Welding Brazing and Soldering, American Elsevier Pub. Co. Inc., New York.

(74) Linnert, G. E., (1967), Welding Metallurgy, Vols. I and II, American Welding Society.

(75) Seferian, (1962), The Metallurgy of Welding, Chapman & Hall, London.

(76) Kihara, Suzuki, Tamura, (1957), "Researches on Weldable High-Strength Steels," Society of Naval Architects of Japan, Tokyo, Cap. 4: Weld Hardening.

APPENDIX A

UNDERWATER WELDING OF LOW-CARBON AND HIGH-STRENGTH (HY-80) STEEL

Preprint of a Paper Presented at the
1974 Offshore Technology Conference

by

K. Masubuchi and M.B. Meloney

OFFSHORE TECHNOLOGY CONFERENCE
6200 North Central Expressway
Dallas, Texas 75206

PAPER NUMBER OTC 1951

Underwater Welding of Low-Carbon and High-Strength (HY-80) Steel

By

Koichi Masubuchi, Massachusetts Institute of Technology, and
Michael B. Melonay, U.S. Navy

This paper was prepared for presentation at the Sixth Annual Offshore Technology Conference to be held in Houston, Tex., May 6-8, 1974. Permission to copy is restricted to an abstract of not more than 300 words. Illustrations may not be copied. Such use of an abstract should contain conspicuous acknowledgment of where and by whom the paper is presented.

ABSTRACT

This paper covers two subjects, the first being multipass welding of low-carbon steel, and the second, a feasibility study of underwater welding of HY-80, a quenched-and-tempered steel with a minimum yield strength of 80,000 psi. Shielded metal-arc process was used for welding these metals.

An experimental study was made of properties of multipass underwater weldments of low-carbon steel.

A study also was made into the feasibility of welding HY-80 steel underwater. Lap and tee joints were fabricated, and tests were conducted to determine joint strength, ductility, and overall weld quality.

INTRODUCTION AND BACKGROUND

Shielded metal-arc underwater welding has been the most studied underwater welding process to date; however, the depth of knowledge of this process has proven satisfactory for the underwater repair and salvage of ships since World War II. With the expansion of various ocean engineering activities, industry now needs the capability to fabricate steel structures underwater, as well as maintain them.

Tremendous savings could be made if undersea pipelines, offshore oil towers and other ocean structures could be fabricated in place by a wet welding process. This current commercial need has spurred great interest, not only in developing such a wet welding process, but in understanding the physical processes and phenomena of underwater welding in general.

During the last several years, a series of studies have been conducted on underwater welding at the Department of Ocean Engineering of the Massachusetts Institute of Technology (1). For example, the National Sea Grant Office of the National Oceanic and Atmospheric Administration has sponsored a three-year program since July 1, 1971 entitled "Fundamental Research on Underwater Welding and Cutting" (2,3). This program covers the following phases:

Phase 1: Survey of fundamental information on underwater welding and cutting

Phase 2: Study of heat flow during underwater welding and cutting

References and illustrations at end of paper.

Phase 3: Mechanisms of metal transfer in underwater arc welding

Phase 4: Effects of water environment on metallurgical structures and properties of welds

Phase 5: Development of improved underwater welding methods

A final report of this program will be published in the summer of 1974.

As a part of Phase 4 of the above program, a thesis study was conducted during the 1972/73 academic year by Lt. M. B. Meloney, U.S. Navy, who was then a graduate student at M.I.T. This paper briefly summarizes results obtained in this thesis study (4).

Part 1 of this study evaluated some of the properties of multipass shielded metal-arc underwater welds. Multipass welds are very often recommended or required during underwater repair welding due to poor joint fit-up, thick plating, etc., and are therefore commonly employed in underwater repair and salvaging operations (5). However, the physics, and even the basic properties of multipass welds are not well-known. Grubbs (6) in 1972 reported success by the Chicago Bridge and Iron Company in producing sound multipass underwater SMA welds, but this was the only reference found which investigated any aspect of multipass welding.

Part 2 of this study was an iniital investigation into the feasibility of welding HY-80 steel joints underwater. The U.S. Navy has almost two decades of experience in the air welding of HY-80 plate for submarine hulls (7,8). Its large strength-to-weight ratio, plus good weldability under controlled conditions makes HY-80 steel an obvious choice as a surface ship hull material as well. There is presently a substantial number of naval vessels afloat with all or part of their hull structure fabricated with HY-80 steel.

A literature survey revealed no published record of any experimental or theoretical work done on underwater welding of any high-strength steel. Verbal conversations with some engineers at the Department of the Navy indicated that no study has been made on underwater welding of HY-80 steel. In fact, the consensus of opinion was that a high-strength quenched-and-tempered steel such as HY-80 could not be satisfactorily welded underwater. The major reason appears to be sensitivity of HY-80 steel to hydrogen embrittlement. Even in air welding, delayed cracking due to hydrogen often occurs, especially when a weld is made with electrodes which have absorbed moisture. When a weld is made underwater, hydrogen which exists in water would cause delayed cracking.

However, no one, to the best of our knowledge, has ever tried to weld HY-80 steel underwater. We are fully aware that high-quality welds in HY-80 steel would not be obtained in underwater wet welding. We felt that it is worth a while to find out whether it is possible to perform emergency underwater repair or temporary welding for salvaging operations. The major objective of this study was to determine the practical limits of joint strength and ductility, as well as the overall quality which is achievable in the underwater welding of HY-80 steel.

PART 1 - UNDERWATER WELDING OF LOW-CARBON STEEL

Objective

The objective of Part 1 investigation was two-fold. First, to gain practical experience in the "art" of underwater welding under controlled laboratory conditions in order to fabricate actual fillet-weld lap and tee joints underwater from HY-80 steel plates. Second, to determine the tensile strength and notch toughness of multipass underwater welded butt joints and compare these values to bead-on-plate specimens and base plate properties. All welds were made by one of the authors, Lt. M. B. Meloney, who is not a qualified welder.

Procedures

Water Tank. The welding experiments were conducted in a steel tank measuring 4 feet long, 3 feet high, and 2 feet wide. The tank was filled with ordinary tap water (Boston, Mass).

Power Source. A Lincoln Ideal-arc Model R3M 400 amp D.C. welding machine was used as the power source. DCRP was used in all experiments because of the ease in all experiments in initiating and maintaining an arc, and the less dense flux cloud produced during welding, with no apparent loss in weld penetration.

Welding Criteria. MIL-STD-00418B

(SHIPS) - Mechanical Tests for Welded Joints (9) was used as a standard in the preparation, welding, cutting, and testing of tensile and Charpy impact specimens.

Welding Materials. Cold rolled mild steel (ASTM 242) plates in 3/16" and 3/4" thick were used. These plates were welded with E6013 electrodes 5/32" in diameter. Electrodes were coated with paraffin prior to welding.

Welding of 1/4" Specimens for Tensile Tests. Plates 10 inches long and 6 inches wide were received in a cleaned and surface-primed condition. For transverse bead-on-plate welds, the weld was made across the width of the plate. For longitudinal bead-on-plate welds, three 10" x 2" strips were machine cut from each 10" x 6" plate prior to welding. For transverse butt joints, each 10" x 6" plate was cut in half across the width so that two 5" x 6" plates could be butt welded to the original 10" x 6" size, and then cut to proper specimen sizes.

The regions to be welded on each plate was sanded and wire-brushed to remove primer paint and expose clean metal along the desired weld line. The plates were clamped to a tray placed in the water tank and manually welded in fresh water 8 inches deep.

Bead-on-plate welds were made in single pass. Ungrooved butt joints were multipass, with two full passes made on both sides of the plates. Due to the excessive turbidity which evolves during underwater welding, it was necessary to use a wooden straight edge as an electrode guide in order to lay down a straight weld bead along the desired weld line.

After completing the transverse welds, one inch was cut off each long side of the plate and discarded in order to eliminate any edge effects in the test specimens. The remaining 10" x 4" welded plate was cut into two 10" x 2" pieces and machined as shown in Figure 1.

The longitudinal welded plates also were machined to the same size as the transverse tensile specimen. The weld reinforcement was ground off, but care was taken not to eliminate weld undercut.

Welding of 3/4" Specimens for Charpy Tests. Two 4" x 4" x 3/4" plates were butt welded in the same manner as the 1/4" transverse butt joints. Many multipass welds were made in the ungrooved joint in order to completely fill the joint. All passes were made on one side with hand clamps preventing angular distortion of the plates. The joint gap was approximately two electrode diameters wide, so two full passes could be made side-by-side without resulting in slag entrapment. Five Charpy specimens (10mm x 10mm and 55mm long) were prepared from the welded butt joint. The specimens were cut perpendicular to the weld bead with the center of the metal coinciding the center of the Charpy specimen.

Welding Parameters. The Navy Underwater Cutting and Welding Manual (5) gives a recommended current range for welding underwater with E6013 electrodes. This was used as a guideline in initial bead-on-plate test runs. Then the range of current settings for given travel speeds was optimized as follows:

1/4" mild steel plate

Current	190-205 Amps (DCRP)
Voltage	28-33 Volts
Travel speed	11.7-14.5 in./min.
Ambient temp.	39.6°F

3/4" mild steel plate

Current	210-230 Amps (DCRP)
Voltage	21-27 Volts
Travel speed	9.5-11.4 in./min.
Ambient temp.	41°F

Experimental Results. Results of tensile tests are shown in Table 1.

Charpy impact tests were conducted at three temperatures, 68°F, 32°F, and -60°F. Test results are shown in Table 2.

Discussion of Results

Bead-on-Plate Tensile Tests. Weld penetration in the longitudinal and transverse bead-on-plate specimens extended down to about two-thirds the plate thickness. However, even with this deep penetration, specimen behavior during the testing approached that of unwelded base plate rather than that of welded butt joints.

Transverse bead-on-plate specimens showed the best strength and ductility of the three specimens tested. This is rather surprising in view of the fact that these specimens were loaded in a direction perpendicular to weld undercut. Instead these specimens performed significantly better than the longitudinal bead-on-plate welds which were loaded in parallel to weld undercut notches,

and thus failed by a means other than root crack initiation and propagation.

In the longitudinal weld specimens, all zones of the weld strain equally and simultaneously. The region with the poorest ductility will therefore initiate fracture below the ultimate tensile strength of the surrounding base metal. All fractures in these specimens initiated in the weld metal bead. The conclusion then is that for underwater welded mild steel, weld metal embrittlement rather than weld undercut will initiate premature failure.

Butt Joint Tensile Tests. Comparison of butt weld test results to bead-on-plate test results indicates that bead-on-plate specimens do not simulate actual butt joint behavior very well. No matter how deep the bead-on-plate weld penetration may be, there will still be some base metal below the weld bead which will significantly alter test results.

Transverse multipass butt joints had 68% the tensile strength and only 42% the ductility of the transverse bead-on-plate specimens, whereas the bead-on-plate specimens had 93.2% the tensile strength and 74% the ductility of ASTM 242 base plate. In addition, the butt joints all failed through the weld metal, as predicted by the longitudinal specimen test results, while the transverse bead-on-plate specimens failed in all three regions without preference.

Series 3 results correlate very well with the work of Grubbs (6) who also tested the tensile and impact properties of multipass underwater welded mild steel. This leads to the conclusion that the extensive bead-on-plate underwater welding investigation carried out by Silva (10) does not give a good indication of actual underwater welded joint performance.

Charpy Impact Tests. Results of impact tests show that the multipass underwater welds met the minimum impact values for marine steels (i.e., 10 to 15 ft-lb. minimum at 32°F) (7). The brittle fracture transition temperature is just about at 32°F which makes the welds barely satisfactory for use in the coldest ocean water regions.

Again, Charpy impact test results correlate well with the work of Grubbs* except for the higher value at 30°F which indicates a significantly lower transition temperature (about 0°F) for his welds (6).

* Multipass underwater weld Charpy impact values were: 24 ft-lb. at 70°F; 22 ft-lb. at 30°F; 10 ft-lb. at -30°F.

Conclusions

a. Satisfactory multipass underwater welded butt joints can be fabricated. However, joint strength could be significantly improved by increasing weld metal and heat affected zone ductility, and decreasing weld undercut. Weld zone ductility can be increased by reducing the severe quenching effect of the aqueous environment and thereby improving weld zone microstructure. Undercut can be reduced through improved welding technique and optimization of welding parameters.

   Improving weld zone grain structure will also increase joint notch toughness.

b. Porosity was not a significant problem either in single pass bead-on-plate welds or in multipass butt joints.

c. Bead-on-plate tensile specimens indicated the weakest regions in the underwater weld zone (i.e., weld metal, and undercut notch root) where premature fracture is most likely to occur. However, bead-on-plate specimens did not give a valid indication of actual butt joint performance.

d. Excessive turbidity created in the water during welding made proper placing of the bead extremely difficult, especially in the welding of thin plate butt joints where a close fit up leaves no groove to guide the electrode along the desired weld line. In multipass welding, a wider joint gap may be used which provides better guidance for the welder.

PART 2 - UNDERWATER WELDING OF HY-80 STEEL

Objective

The objective of Part 2 investigation was to determine the feasibility of welding HY-80 steel plate underwater in order to fabricate joints of reasonable quality and strength for temporary repairs such as interim (voyage) repairs or for use during

salvage operations. The general approach taken was to compare specific properties of simple underwater welded joints with the same joint configuration welded in air. Joints were fabricated and specimens prepared and tested in accordance with Department of Defense MIL-STD-00418B Mechanical Tests for Welded Joints (9) and with MIL-S-16216H Fabrication, Welding and Inspection of HY-80 Submarine Hulls (8).

Fillet-weld lap joints, tee-bend joints and tee-tensile joints were fabricated with 1/4" HY-80 plate in air and underwater, and the specimens tested and compared. Also, 3/4" tee-bend joints and tee-tensile joints were fabricated underwater, with specimens cut and tested. Fillet-weld lap joints and tee joints were selected, because these joints are more suitable for repair work than butt joints which require accurate joint fit-up. Most welds were made by Lt. Meloney, while some air welds were made by a qualified Navy welder for HY-80 construction.

Since the major objective of this study was to obtain practical evidence, only limited investigations were made of metallurgical structures of welds. Detailed metallurgical studies of underwater HY-80 weldments are being made at M.I.T.

Procedures

The same welding equipment and set-up used for the underwater welding of low-carbon steel was used for the underwater welding of HY-80 steel plates, 1/4" and 3/4" thick. E11018 and E310-16 electrodes 1/8" in diameter, heated in holding ovens for a minimum of four hours, were used. Both electrodes were hand-coated with paraffin after cooling and prior to welding.

Welding of 1/4" HY-80 Fillet-Weld Shear Specimens. Transverse fillet shear specimens were cut from welded plates as shown in Figure 2. Specimens were welded with E11018 electrodes 1/8-inch in diameter.

Specimens also were welded with E310-16 electrodes. This was based on results obtained by Grubbs (6) who reported success in reducing hydrogen trapping and cracking problems through the use of austenitic stainless steel electrodes in the underwater multi-pass welding of structural grade steels with high carbon equivalent.

The range of welding parameters used in the underwater welding of fillet weld shear specimens were as follows:

E11018 electrode

current	180-210 Amps (DCRP)
voltage	28-36 Volts
travel speed	9.8-12.1 in/min.
heat input	32,132-36,030 Joules/in.
ambient temp.	43.6°f

E310-16 electrode

current	160-180 Amps (DCRP)
voltage	35-39 Volts
travel speed	10.6-13.7 in/min.
heat input	27,328-35,660 Joules/sec
ambient temp.	44.1°F

Immediately after welding, the plates were carefully visually examined for surface cracking (i.e., longitudinal, transverse, crater cracking) under a 5X viewing glass. The welded plate was then stored on a laboratory shelf for a minimum of 7 days, then visually examined again and cut into 1-1/4" specimens on a heavy-duty hydraulic band saw. No case of surface cracking (immediate or delayed) was found through visual observation. In addition, a dye penetrant test was conducted on a randomly selected plate prior to cutting into specimens. All four E11018 beads showed no case of surface cracking. Substructure characteristics will be discussed later.

Air-Welded Specimens. For comparison with the underwater welded specimens, identical shear fillet weld specimens were air welded using the following parameters:

E11018 electrode

current	120-135 Amps (DCRP)
voltage	43-48 Volts
travel speed	8.0-13.3 in/min.
heat input	25,985-43,537 Joules/in.
ambient temp.	72.5°F

Some specimens were welded by Lt. Meloney, while other specimens were welded by a qualified Navy welder for HY-80 construction.

Welding of 1/4" HY-80 Tee Joints. Tee joint specimens used for tee-bend tests and tee-tensile tests were cut from welded plates as shown in Figure 3. Six specimens were cut from each plate, with three being used as tee-bend specimens and three as tee-tensile specimens. The plate assembly was placed in the water tank tray, with the base plate positioned at a 45 degree angle to the horizontal plane. Both single

and multipass welds were made, using 1/8" E11018 electrodes.

Single and multipass welds also were made in air, using 1/8" E11018 electrodes.

Experimental Results

Fillet-weld shear tests and tee-bend tests were conducted in accordance with the procedures and specifications of MIL-STD 00418B (9). Results are listed in Tables 3 through 7. Figure 4 shows a cross-section of a single pass underwater welded tee joint using E11018 electrodes.

Discussion of Test Results

1/4" HY-80 Fillet-Weld Shear Tests. It is first apparent that the single pass underwater fillet weld (Series 5) had extremely poor shear strength. There were a number of reasons for this, including inadequate penetration, off-center weld bead positioning, and excessive undercut.

More encouraging was the performance of the multipass shear specimens in which penetration was adequate, the wider bead positioned correctly, and the effects of undercut lessened. The average shear strength of these specimens was 69,056 psi, which is 79.7% of comparable single pass air-weld specimens also welded by Meloney (Series 7).

Air-welded specimens made by an qualified Navy welder (Series 8) showed the highest average shear strength of 104,614 psi, while that of Series 7 was 86,632 psi. The reason multipass underwater welds are compared to single pass air welds in this case is that with the air-welded specimens an adequate and acceptable joint was made with a single pass. The use of the drag technique, which is required in low visibility underwater welding, inhibits the welder from weaving the electrode along an ungrooved joint fit-up, as is frequently done in air welding.

Shear strengths of multipass underwater welds using E310-16 electrodes (Series 9) were lower than those of multipass underwater welds using E11018 electrodes (Series 6) but higher than those of single pass welds (Series 5).

1/4" HY-80 Tee-Bend Tests. The significant characteristic of the tee-bend test is that it measures primarily weld surface quality. Table 4 shows that the base metal bend strength is greater than that of any welded specimen. Thus, in no case was 100% joint efficiency attained, and welded tee joints will degrade bend strength to a degree proportional to weld surface quality. MIL-STD-00418B does not take into account weld bead size in bend strength calculations. However, it can be seen from Table 4 that weld bead size is not significant since, for air welds (no undercut) single pass bend strength (13,230 psi) is 96.3% of multipass bend strength (13,733 psi), even though the average multipass throat dimension was 21% larger than that of the single pass series. The overall loss in bend strength for single pass and multipass underwater welds was 32.1% and 29.9% respectively compared to air welds. Therefore, weld degradation due to surface defects is significant, i.e., an average of 31% for single and multipass welds. The multipass underwater welds had somewhat higher bend strength than single pass underwater welds due partly to the larger fillet size and partly to the less significant, further removed undercut notch.

1/4" HY-80 Tee Tensile Tests. Tee-tensile tests were conducted in order to determine relative tee joint strength in the absence of bending. As shown in Figure 4, a tee joint has two undercut notches, one at each fillet toe. However, it was found that fracture did not initiate from these notches and fracture occurred in a shear mode in the weld metal. In other words, even though the weld had undercuts, the "weakest link" in the joint was the weld metal. Results are shown in Table 5.

Since specimens in Series 14 showed poor results, an additional weld was prepared underwater (Series 15). Shear strength of Series 15 (67,185 psi) was 88% of that of Series 17. By comparing results of Series 16 and 17, one finds that the maximum loads increases approximately proportionally to the throat dimension because the shear strength remains about the same.

3/4" HY-80 Tee Joints. The minimum preheat temperature for 3/4" HY-80 plate is 125°F versus 75°F for 1/4" plate (8), therefore, the adverse effect of ambient water temperature on the underwater weldability of 3/4" HY-80 was expected to be considerable. Experimental results and metallographic examination

of 3/4" welded joints confirmed this expectation.

Bend tests of 3/4" underwater welded multipass tee joints were conducted for the purpose of comparing tee-bend performance to base plate performance. However, the bend strength of the unwelded 3/4" plate greatly exceeded the rated capacity of the bend testing machine resulting in an incomplete set of data. Even so, some tentative conclusions on the relative bend strength of 3/4" tee joints can be drawn. Firstly, as shown in Table 6, the bend strength of these joints is well below 58% of base plate bend strength compared to 68.4% for 1/4" tee joints. Secondly, the ratio of total bend angle at failure for 3/4" tee joints is 24.5% the total bend angle of 1/4" tee joints (Table 4). Assuming 3/4" base plate has the ductility of 1/4" base plate (i.e., 180° total bend angle without failure), the percentage of 3/4" tee joint to base plate ductility is only about 5%.

Tee-tensile test results were equally disappointing (as shown in Table 7). The shear strength of 3/4" underwater welded multipass tee joints was only 31.4% the shear strength of 1/4" underwater welded multipass tee joints. The loss in weldability of thick HY-80 plate (>1/2") is extraordinary.

Tee Joints Welded in Salt Water. At a last step in this investigation, 1/4" and 3/4" tee joints were welded in salt water, to see if there was any difference in joint weldability between fresh and salt water. "Dayno Synthetic Sea Salt" was used to make the artificial sea water used in this test. Since time did not permit the cutting and testing of test specimens, it was decided to weld the two sets of tee joints under the identical conditions used in making the fresh water welds and then make a qualitative comparison of weld quality obtained in the two aqueous media. No reference was found which investigated the difference in the hydrogen cracking potential of a salt water media compared to fresh water; however, since no case of hydrogen-induced macrocracking was observed in any fresh water weld, none was anticipated in salt water welding. The rationale here was that fresh water welding produced an ample supply of dissociated hydrogen in the arc, and quenched the weld bead just as fast as salt water would. Thus, the conditions for hydrogen cracking were present, and the fact that none occurred in fresh water was quite surprising. Salt water welding would be expected to cause some changes in the rate of hydrogen dissociation, and possibly in the amount entrapped in the weld zone, but these would be minor perturbations from fresh water welding conditions, and therefore, no major changes from fresh water results would be expected.

Metallurgical Studies

Limited studies also were made of metallurgical structures of underwater welds of HY-80 steel plates. However, results are not discussed here because of the limited length of this paper.

The most interesting result was that no extensive crack was observed in any of the HY-80 welds made underwater. Masubuchi and Martin (11) reported the occurrence of microcracks in the heat-affected zone close to the fusion line even in HY-80 welds made in air. Similar microcracks also were found in HY-80 underwater welds made in this study. However, none of these microcracks extended to a macrocrack which indicates that HY-80 steel is rather insensitive to hydrogen cracking. A further study is being conducted on this subject.

CONCLUSIONS

a. Experimental results showed that fairly efficient joints, comparable to underwater welded mild steel joint efficiency, could be fabricated underwater with thin HY-80 steel plate. (Thin plate here means ≤1/2", i.e., where minimum preheat temperature increases above 75°F). For thicknesses greater than 1/2" underwater weldability decreases dramatically.
These findings may appear restrictive however, due to the higher strength to weight ratio of HY-80 steel compared to mild steel, most unarmored naval ship hulls will require relatively thin plate when fabricated from HY-80 steel. Therefore, the 1/2" maximum thickness restriction may in fact encompass the large majority of future naval ships.

b. Loss in underwater welded joint strength and ductility, when compared to similar air welded joints, resulted from two main causes: weld undercut, and weld zone microstructural changes and defects caused by severe quenching. It was found that for 1/4" HY-80 steel plate undercut accounts for almost 75% of the total underwater weld degradation, and weld zone structural changes and effects for the other 25%.

c. In 3/4" HY-80 underwater welded joints, internal weld defects, especially heavy slag inclusion, prevented adequate fusion of weld metal and base metal. This accounts for the major portion of total weld degradation when compared to 3/4" HY-80 base plate.

d. In general, multipass underwater welding of HY-80 steel is preferred to single pass welding. Multipass welds were much more porous than single pass welds, but the effect of porosity was secondary compared to single pass weld undercut caused by the severe quenching of the aqueous environment. Porosity will reduce effective weld crossectional area, but undercut will cause severe stress intensities at the notch roots which, in turn, cause premature, catastrophic fracture, especially in the presence of bend stresses. Multipass welds not only decrease the degree of undercut, but increase fillet size and in so doing, "push" the undercut further away from the joint intersection. Therefore, a crack which initiates at an undercut notch root must propagate through a greater portion of the fracture tough HY-80 base plate rather than through the more notch sensitive weld metal and heat affected zone.

e. It was demonstrated in the underwater welding of thin HY-80 plate that weld undercut could be greatly reduced (but not eliminated) through the optimization of welding parameters and proper welding technique. This is where the largest payoff per dollar invested will result.

f. Underwater weld quality and overall joint strength could be significantly increased through the use of post-weld surface treatment. After both single and multipass welding, weld beads should mechanically be peened or ground down in order to eliminate surface cavities, and reduce or eliminate undercut.

Unlike weld undercut, surface cavities will not significantly reduce joint strength per se; however, it will allow the water environment access deep into the weld metal. This will result in accelerated corrosion through the formation of differential aeration cells which would eventually cause extensive local corrosion through the heat affected zone and into the base metal.

REFERENCES

(1) Brown, T., Masubuchi, K.,"Latest Developments in Underwater Welding Techniques," Underwater Journal, October 1973, 202-212.

(2) Brown, A. J., Staub, J. A., Masubuchi, K.,"Fundamental Study of Underwater Welding," OTC 1621, Offshore Technology Conference, May 1972.

(3) Brown, A. J., Brown, R. T., Masubuchi, K."Fundamental Research on Underwater Welding," Interim Report from Department of Ocean Engineering, M.I.T., February 1973.

(4) Meloney, M. B."The Properties of Underwater Welded Mild Steel and High Strength Steel Joints," M.S. Thesis at M.I.T., June 1973.

(5) "Underwater Cutting and Welding Technical Manual," NAVSHIPS 0929-000-8010, Naval Ships System Command, Washington, D.C., 1969.

(6) Grubbs, Seth,"Multipass All Position 'Wet' Welding--A New Underwater Tool," OTC 1620, Offshore Technology Conference, 1972.

(7) Masubuchi, K., Materials for Ocean Engineering, M.I.T. Press, Cambridge, Mass., 1970.

(8) "Fabrication, Welding and Inspection of HY-80 Submarine Hulls," MIL-S-16216H, Naval Ships System Command, Washington, D.C.

(9) "Mechanical Tests for Welded Joints," MILSTD 00418B(SHIPS), Naval Ships

System Command, Washington, D.C., 1967.

(10) Silva, E. A.,"Welding Processes in Deep Ocean," Naval Engineers Journal, Vol. 80, No. 4, August, 1968.

(11) Masubuchi, K., Martin, J. C., "Mechanisms of Cracking in HY-80 Steel Weldments," Welding Journal Research Supplement, August, 1962.

TABLE 1 - RESULTS OF LOW-CARBON STEEL TENSILE TESTS

SPECIMEN	TENSILE STRENGTH (PSI)	% ELONG. IN 2 IN.	% REDUCTION IN AREA	FRACTURE LOCATION*
SERIES 1: SINGLE PASS LONGITUDINAL BEAD-ON-PLATE				
1A	65,610	9.4	12.0	W.M.
1B	60,370	7.8	11.1	W.M.
1C	64,000	9.3	12.0	W.M.
1D	66,200	9.3	11.9	W.M.
1E	54,825	12.5	11.0	W.M.
AVERAGE SERIES 1	62,200	9.7	11.6	---
SERIES 2: SINGLE PASS TRANSVERSE BEAD-ON-PLATE				
2A	72,210	26.9	19.3	B.M.
2B	68,925	24.2	23.4	B.M.
2C	64,710	15.9	24.5	HAZ
2D	52,840	11.9	16.3	W.M.
2E	55,140	13.0	14.6	W.M.
AVERAGE SERIES 2	62,765	18.4	19.6	---
SERIES 3: MULTIPASS TRANSVERSE BUTT WELD				
3A	49,333	6.3	9.7	W.M.
3B	51,200	9.7	11.3	W.M.
3C	27,570	3.6	6.1	W.M.
3D	43,285	7.4	9.2	W.M.
AVERAGE SERIES 3	42,847	6.8	9.1	---

*NOTES ON FRACTURE LOCATION:

W.M. = WELD METAL
HAZ = HEAT AFFECTED ZONE
B.M. = BASE METAL

TABLE 2 - RESULTS OF MULTIPASS LOW-CARBON STEEL CHARPY IMPACT TESTS (SERIES 4)

SPECIMEN	TEST TEMPERATURE (°F)	IMPACT ENERGY (FT-LBS.)
4A	68°F	28.0
4B	68°F	28.2
4C	68°F	26.1
AVERAGE	68°F	27.4
4D	32°F	20.0
4E	32°F	13.5
4F	32°F	11.7
AVERAGE	32°F	15.1
4G	-60°F	7.6
4H	-60°F	6.4
4I	-60°F	8.0
AVERAGE	-60°F	7.3

TABLE 3 - RESULTS OF FILLET WELD SHEAR TESTS

SPECIMEN	MAX. LOAD TO FAILURE(LBS.)	SHEAR STRENGTH $\frac{\text{LBS}}{\text{LINEAR INCH}}$ $(\frac{\text{LBS}}{\text{IN.}})$	AVE. THROAT DIMENSION(IN)	SHEAR STRENGTH (PSI)
SERIES 5: SINGLE PASS UNDERWATER WELDS USING E11018 ELECTRODES				
5A	17,500	7,000	0.1435	48,800
5B	11,800	4,720	0.1172	40,280
5C	20,300	8,120	0.1570	51,720
AVERAGE SERIES 5	16,533	6,613	0.1392	46,933
SERIES 6: MULTIPASS UNDERWATER WELDS USING E11018 ELECTRODES				
6A	33,600	13,440	0.1758	76,472
6B	36,100	14,444	0.2120	68,132
6C	25,175	10,069	0.1609	62,562
AVERAGE SERIES 6	31,625	12,651	0.1829	69,055
SERIES 7: SINGLE PASS AIR WELDS BY MELONEY USING E11018 ELECTRODES				
7A	32,100	12,840	0.1461	87,916
7B	31,600	12,640	0.1589	79,522
7C	37,945	15,179	0.1642	92,470
AVERAGE SERIES 7	33,881	13,553	0.1564	86,637
SERIES 8: SINGLE PASS AIR WELDS BY QUALIFIED HY-80 WELDER USING E11018 ELECTRODES				
8A	41,460	16,584	0.1561	106,204
8B	39,280	15,713	0.1523	102,156
8C	38,770	15,508	0.1484	104,484
AVERAGE SERIES 8	39,837	15,935	0.1523	104,281
SERIES 9: MULTIPASS UNDERWATER WELDS USING E310-16 ELECTRODES				
9A	22,565	9,026	0.1856	48,644
9B	26,842	10,736	0.1894	56,674
AVERAGE SERIES 9	24,703	9,881	0.1875	52,660

* Note: All welds except those in Series 8 were welded by Lt. Meloney

TABLE 4 - RESULTS OF TEE-BEND TESTS*

SPECIMEN	FRACTURE LOAD (LBS)	TOTAL BEND ANGLE AT FAILURE	TYPE FRACTURE**
SERIES 10: SINGLE PASS UNDERWATER WELDS USING E11018 ELECTRODES			
10A	9,894	43°	2
10B	8,590	29.5°	2
10C	8,934	32°	2
10D	8,514	30°	2
AVERAGE SERIES 10	8,983	33.6°	---
SERIES 11: MULTIPASS UNDERWATER WELDS USING E11018 ELECTRODES			
11A	9,254	31°	2
11B	9,365	33°	2
11C	9,548	33.5°	2
11D	10,341	46°	2
AVERAGE SERIES 11	9,627	35.9°	---
SERIES 12: SINGLE PASS AIR WELDS USING E11018 ELECTRODES			
12A	13,418	71.5°	2
12B	12,897	69°	2
12C	13,376	72°	2
AVERAGE SERIES 12	13,230	70.8°	---
SERIES 13: MULTIPASS AIR WELDS USING E11018 ELECTRODES			
13A	13,952	76.5°	2
13B	13,362	72°	2
13C	13,957	81°	2
13D	13,662	71°	2
AVERAGE SERIES 13	13,733	75°	---
SERIES 14: 1/4" HY-80 BASE PLATE (UNWELDED)			
B.P.A.	14,170	180°	No Fracture
B.P.B.	13,978	180°	No Fracture
AVERAGE SERIES B.P.	14,074	180°	---

* All welds were made by Lt. Meloney
**Refer to Figure 5 for fracture types

TABLE 5 - RESULTS OF TEE-TENSILE TESTS

SERIES 14 & 15: MULTIPASS UNDERWATER WELDS BY MELONEY USING E11018 ELECTRODES

SPECIMEN	MAX. LOAD TO FAILURE (LBS.)	SHEAR STRENGTH $\left(\frac{LBS}{LINEAR\ INCH\ IN.}\right)$	AVE. THROAT DIMENSION (IN)	SHEAR STRENGTH (PSI)
14A*	15,520	6,207	0.1579	39,300
14B**	12,542	5,017	0.1356	36,996
14C***	16,500	6,600	0.1445	45,658
AVERAGE SERIES 14	14,854	5,941	0.1460	40,651
15A	25,520	10,208	0.1563	65,310
15B	27,356	10,942	0.1602	68,326
15C	27,060	10,823	0.1594	67,920
AVERAGE SERIES 15	26,645	10,657	0.1586	67,185
SERIES 16: SINGLE PASS AIR WELDS BY QUALIFIED HY-80 WELDER USING E11018 ELECTRODES				
16A	24,620	9,848	0.1269	77,604
16B	23,925	9,570	0.1285	74,464
16C	21,775	8,711	0.1241	70,193
AVERAGE SERIES 16	23,440	9,376	0.1265	74,087
SERIES 17: MULTIPASS AIR WELDS BY QUALIFIED HY-80 WELDER USING E11018 ELECTRODES				
17A	30,670	12,266	0.1567	78,276
17B	28,200	11,280	0.1523	74,064
17C	29,120	11,774	0.1556	75,668
AVERAGE SERIES 17	29,330	11,773	0.1547	76,003

* 13.5° Total Bend

** 28° Total Bend

*** 9° Total Bend

TABLE 6 - RESULTS OF TEE-BEND TESTS IN 3/4" HY-80 PLATES

SERIES 18: MULTIPASS UNDERWATER WELD BY MELONEY USING E11018 ELECTRODE

SPECIMEN	FRACTURE LOAD (LBS)	TOTAL BEND ANGLE AT FAILURE	TYPE FRACTURE
18A	37,858	9°	3
18B	38,550	9.5°	3
18C	36,519	8°	3
AVERAGE SERIES 18	37,642	8.8°	---
SERIES B.P.: 3/4" HY-80 BASE PLATE (UNWELDED)			
B.P.A.	64,275*	42°	No Fracture
B.P.B.	64,275*	39°	No Fracture
AVERAGE BASE PLATE	64,275*	40.5°	---

* Rated capacity of bend testing machine

TABLE 7 - RESULTS OF TEE-TENSILE TESTS IN 3/4" HY-80 PLATES

SERIES 19: MULTIPASS UNDERWATER WELD BY MELONEY USING E11018 ELECTRODES

SPECIMEN	MAX. LOAD TO FAILURE (LBS)	SHEAR STRENGTH $\left(\frac{LBS}{LINEAR\ INCH}\right)$ $\left(\frac{LBS}{IN.}\right)$	AVE. THROAT DIMENSION (IN)	SHEAR STRENGTH (PSI)
19A	28,730	11,493	0.5078	22,632
19B	21,910	8,762	0.4296	20,395
19C	18,915	7,566	0.3711	20,388
AVERAGE SERIES 19	23,185	9,273	0.4361	21,138

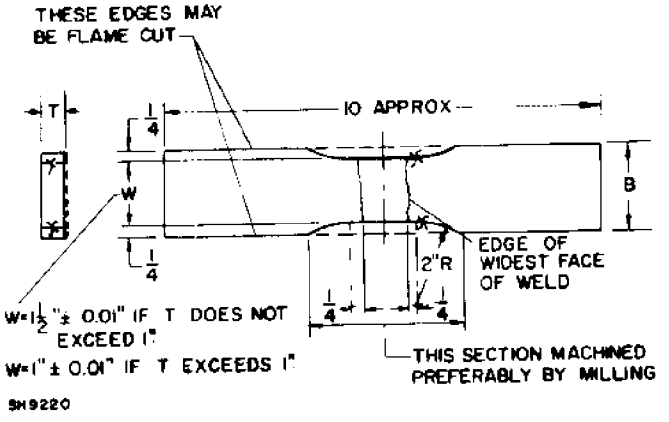

Fig. 1 - Transverse tensile specimen.

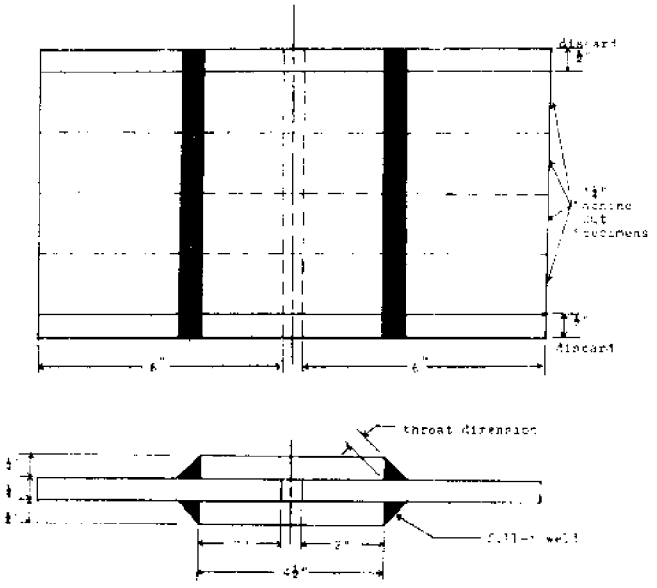

Fig. 2 - Transverse fillet-weld specimen.

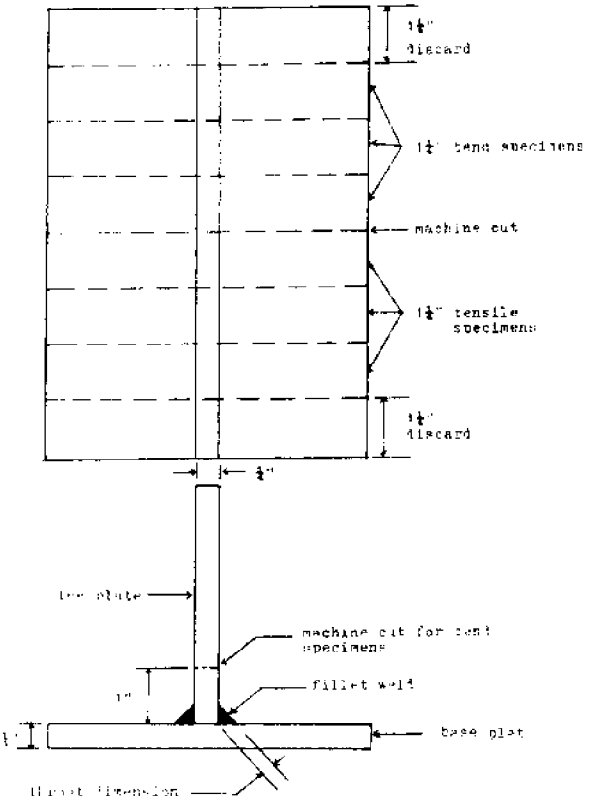

Fig. 3 - Tee-bend and tee-tensi e specimens.

Fig. 4 - Single pass underwater welded tee joint using E11018 electrode. (3x, 3% NITAL ETCH)

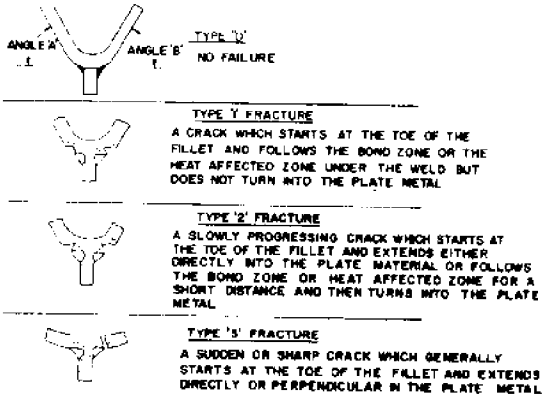

Fig. 5 - Types of fracture in tee-bend specimens.

APPENDIX B

UNDERWATER WELDING OF HY-80 STEEL

Summary of "An Investigation of Underwater Welded HY-80 Steel" - Masters Thesis by Stanley Leon Renneker

by

Chon-Liang Tsai

Objective

The objective of this report was two fold; first was the desire to extend previous laboratory work and to evaluate the ability to fabricate acceptable underwater welded HY-80 steel joints, under working conditions, within the guidelines of the United States Navy governing underwater welding operation. Secondly was the desire to investigate the occurrence of the hydrogen embrittlement phenomena in the underwater welded HY-80 steel joints.

Three separate experiments were conducted and the findings are discussed. Subsequently, the general conclusions and recommendations for underwater welding of HY-80 steel are presented.

The Experimentations

The Microscopic Investigation - The specimens used for the microscopic investigation were prepared as shown in Figure 1. Each specimen was finished on a series of finishing wheels, ranging from a #80 through #120, #240, and #320. Next, each specimen was polished on a #600 finishing wheel, using a 0.3 alumina/distilled water solution. Finally, each specimen was etched using a 2% Nital Solution.

Porosity has been observed extensively throughout the weld metal from the microscopic investigation. A greater degree of porosity, and a greater number of cracks, were found in the overhead welds than in the vertical welds or the down-hand welds. The cracks which occurred were found to be in the weld metal in the form of "fusion" cracks or "transverse" cracks, which initiated in the weld metal and extended into the heat affected zone. Underbead cracking in the heat affected zone, which normally occurred in air welds, was not observed. The type of cracks which occurred in welded HY-80 steel joints are not dependent on hydrogen embrittlement.

The Microhardness Test - The microhardness tests of the underwater welded HY-80 steel lap joints were conducted on a Wilson Model LL Tukon Microhardness Tester. A load of 500 grams was used for the tests. The resulting diamond imprint was microscopically measured in mm, converted to a Knoop Hardness in Kg/mm^2, and then approximated to a Rockwell C value. The microhardness test specimens were prepared from the underwater welded HY-80 steel doubler plate, shown in Figure 2. The test specimen has been micro-polished with a 0.3 alumina/distilled water solution on a #600 polishing wheel and then etched with a 2% Nital solution.

The hardness of the weld metal is greatest near the heat affected zone and decreases near the water. However, the hardness of the heat affected zone appears to increase nearer the water.

The Mechanical Bend Test - The mechanical bend tests of the underwater welded HY-80 steel lap joints were conducted on an Instrum test machine. A guided bend test jig was used in conducting thest tests. The HY-80 steel lap joint bend specimens were prepared from the underwater welded HY-80 steel doubler plates as shown in Figure 3 and 3b. The arrows on the doubler plates indicate the "north" direction of the plate during the underwater welding process.

The failure characteristic curve indicates the time to failure with a crosshead speed of 0.02 inches per minute, and the load necessary to cause the failure to occur. The load increases sharply with time, reaches the point of fracture initiation, than drops fast and later on slower. In the case of the two overhead welded HY-80 steel lap joint specimens, the test specimen OH-1 experienced failure of the weld metal and complete fracture of the specimen before any failure was initiated in the base metal, but the weld area of specimen OH-2 was uneffected by the load. In all the other cases of the HY-80 steel lap joint specimens, failure occurred at the toe of the weld and was of the Type "2" fracture as described in MIL-STD-00418B(SHIPS).

The surface of the Type "2" fractures and the OH-1 specimen appeared gray and silky with fibrous dimples indicating a ductile shear type fracture.

Conclusions

Underwater welded HY-80 steel may not experience hydrogen embrittlement as does air welded HY-80 steel. This is true despite the fact that the weld metal of an underwater welded HY-80 steel joint contains pores of entrapped gas, where source is the bubble resulting from the dissociation of the water environment. The rapid cooling rate and steep temperature distribution during underwater welding process gives insufficient energy for the molecular hydrogen entrapped in the pores of the weld metal, to be dissociated to atomic hydrogen and adsorbed by the atoms which form the surface layer of the pore, without adsorption, absorption cannot occur. Even though some atomic hydrogen is present and adsorbed, absorption and diffusion to the critical areas of tri-axial stresses are unlikely to occur due to the low temperature of the environment. In addition, the rapid strain rate prevents what little hydrogen which may diffuse into the lattice structure from traveling to the critical areas of tri-axial stresses.

The microscopic investigation revealed extensive porosity and "fusion" and "transverse" cracks in the weld metal, which occurred as a result of high tensile shrinkage stresses and hard martensite microstructure. Porosity is a less critical weld defect compared to "fusion" cracks and the "transverse" cracks.

The water quench temperature of the welded joints for HY-80 steel doubler plates was around 71°F which was sufficiently below "room temperature" to prevent the completion of diffusion of hydrogen. The quench was severe enough to cause shrinkage tensile stresses high enough so that when combined with the hard microstructure, "fusion" and "transverse"

cracks occurred. The underbead cracking in the heat affected zone would have occurred as a result of the high shrinkage tensile stresses and microstructure, as well as complete hydrogen diffusion. But the underbead cracking has not been observed during the underwater welding of the HY-80 steel doubler plates.

Kobayashi and Aoshimo[3] observed that at water quench temperatures above 122°F, hydrogen diffusion is advanced to a degree that it is able to overcome the affinity of hydrogen for areas of high stress concentration. This upper limit for hydrogen embrittlement phenomena is supported by the minimum preheat and interpass temperature requirement for the welding of HY-80 steel, which is set at 125°F.

The lower bound for hydrogen embrittlement phenomena can also be applied to other low alloy steels.

In the multi-pass technique during underwater welding process, the heat affected zone of subsequent passes does not appear to temper the weld metal or heat affected zone of previous passes. In fact, the microhardness tests results seem to indicate that regions of heat affected zone and weld metal which fall within the heat affected zone of subsequent passes are actually hardened. This is not in agreement with Meloney[4], who concluded that the "multi-pass regions" experienced less hardness.

The regions of greatest microhardness should be the most susceptable to microcracking in the presence of tri-axial tensile stresses and hydrogen embrittlement.

Recommendations

Since the underwater welded HY-80 steel joints can be fabricated, under working conditions, without hydrogen embrittlement, work should be undertaken to optimize the underwater welding process for HY-80 steel and other low alloy steels. Underwater welding should be performed for various

HY-80 steel and other low alloy steel joints with the help of MKX hard hat diving system and hydraulic tool package. Included in the joints to be welded should be butt joints, as well as tee joints and lap joints. All of these joints should be welded in all positions using the multi-pass technique. These working dives should explore various joint configurations for each type of joint and various weld pass preparation techniques. This may enable the underwater welding of HY-80 steel and other low alloy steel joints to be expanded from the realm of repair into that of fabrication.

The effects of preheat and interpass heat on the rapid cooling rate and thermal stresses in the region of the weld zone should be investigated. This investigation should be conducted in the light of the possible effect of preheat and interpass heat on the hydrogen embrittlement phenomena. The study should be conducted to determine if it is also possible to elevate the temperature of the weld zone above the region of critical hydrogen embrittlement, while attempting to overcome the effects of the rapid cooling rate, or whether a possibly non-critical condition will be corrected, only to create a critical one.

An investigation of the thermal stresses occurring during the underwater welding process should be conducted, in order to determine their contribution to the mechanical characteristics of the cracking of the underwater welded joint. By utilizing the information techniques developed by Ueda and Yamakawa[5], Fujita and Nomoto[6], and Brown et. al.,[7], a thermal elastic-plastic analysis of the underwater welded joint could be conducted. As a result of this investigation, it should be possible to make a definitive statement as to the effect of the temperature change rate and the resultant thermal stresses, on an underwater welded joint, with regard to specific joint service life requirements.

FIGURE 1

THE MICROSCOPIC INVESTIGATION

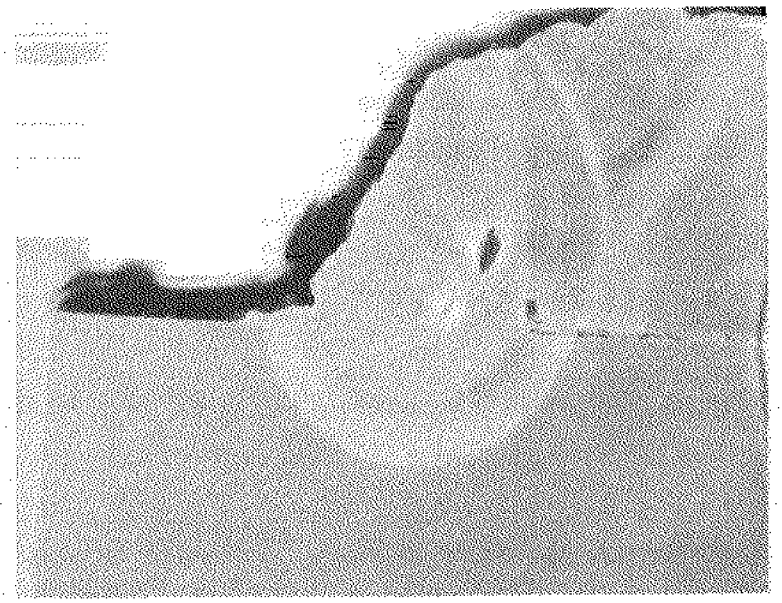

Multipass Downhand Underwater Welded Lap Joint #1 Using E11018 Electrode (5x, 2% Nital)

Lap Joint #1 Showing Extensive Porosity Throughout Weld Metal (100x, 2% Nital)

FIGURE 2

DOWNHAND WELDED MICROHARDNESS TEST SPECIMEN

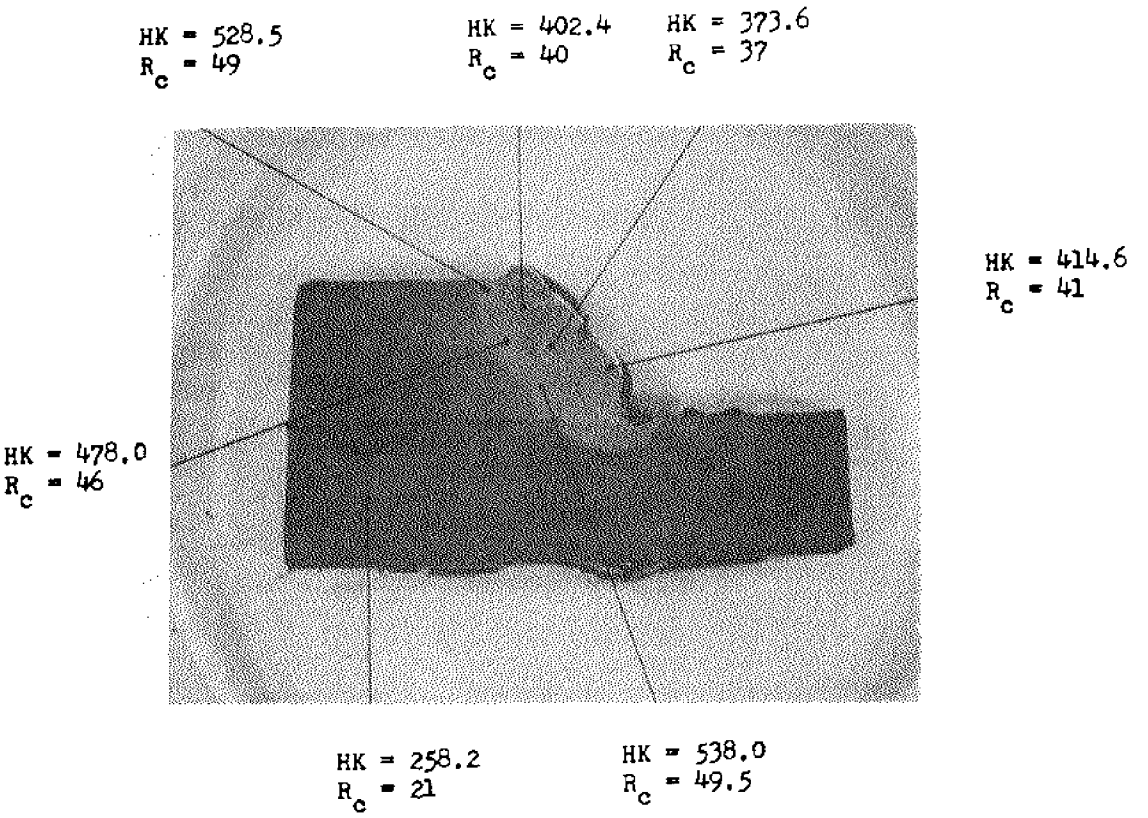

FIGURE 3-a

PREPARATION OF LAP JOINT BEND SPECIMENS

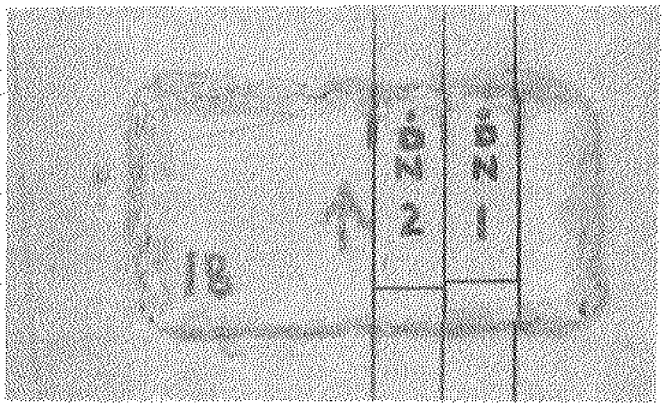

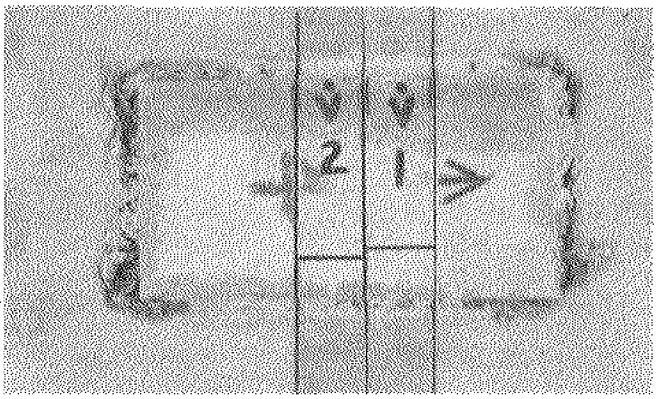

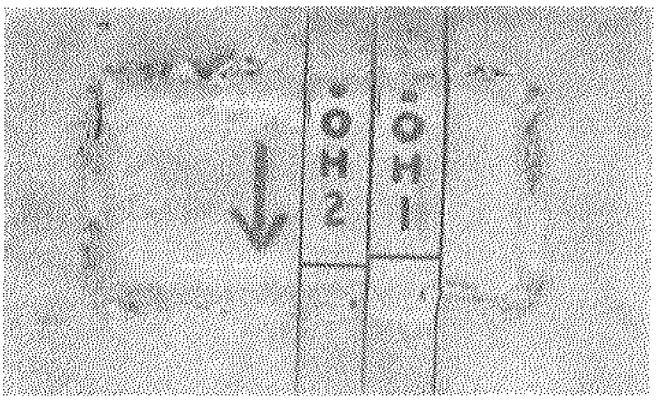

FIGURE 3-b

RESULTS OF BEND TEST ON DOWNHAND WELDED LAP JOINT
BEND TEST SPECIMEN DN-1

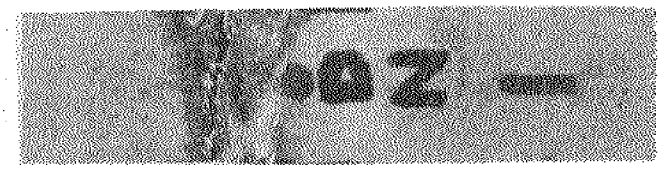

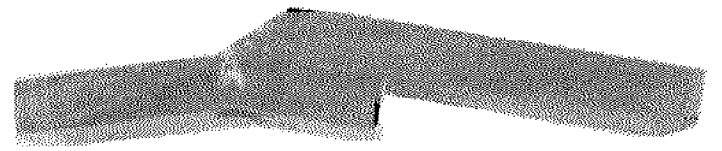

References

(1) Cabelka, J., "Delayed Cracks in Welded Joint," Proceedings of the First International Symposium: Cracking and Fracture in Welds, November, 1971, Tokyo, Japan.

(2) Masubuchi, K., and Martin, D.C., "Mechanisms of Cracking in HY-80 Steel Weldments," AWS 43rd Annual Meeting, Cleveland, Ohio, April 9-13, 1962.

(3) Kobayashi, T. and Aoshima, T., "Welding Cracks in Low Alloy Steels," Proceedings of the First International Symposium: Cracking and Fracture in Welds, November, 1971, Tokyo, Japan.

(4) Meloney, M.B., "The Properties of Underwater Welded Mild Steel and High Strength Steel and High Strength Steel Joints," OE and SM Thesis, M.I.T., June, 1973.

(5) Ueda, Y., and Yamakawa, F., "Mechanical Characteristics of Cracking of Welded Joints," Proceedings of the First International Symposium: Cracking and Fracture in Welds. November, 1971, Tokyo, Japan.

(6) Fujita, Y. and Nomoto, F., "Studies of Thermal Stresses in Welding with Special Reference to Weld Cracking," Proceedings of the First International Symposium: Cracking and Fracture in Welds, November, 1971, Tokyo, Japan.

(7) Brown, A.J., Brown, R.T., and Masubuchi, K., "Interim Report on Fundamental Research of Underwater Welding," M.I.T., February 1973.